Dissertation zur Erlangung des Doktorgrades der Technischen Fakultät der Albert-Ludwigs-Universität Freiburg im Breisgau

Energy-Efficient Collaborative Beamforming in Wireless Ad Hoc Networks

Institut für Informatik
Technische Fakultät
Albert-Ludwigs-Universität Freiburg

Thomas Janson

July 2015

Energy-Efficient Collaborative Beamforming in Wireless Ad Hoc Networks

Thomas Janson

Dissertation zur Erlangung des Doktorgrades der Technischen Fakultät der Albert-Ludwigs-Universität Freiburg im Breisgau

Dekan:	Prof. Dr. Georg Lausen
Erstgutachter:	Prof. Dr. Christian Schindelhauer (Universität Freiburg)
Zweitgutachter:	Prof. Zvi Lotker (Ben-Gurion University of the Negev)

Datum der Disputation: 3.6.2015

Zusammenfassung (deutsch)

Die Effizienz von Routing-Algorithmen in Ad-Hoc Netzwerken kann anhand von Latenzzeit (Delay), Datendurchsatz und Energieverbrauch bewertet werden. In dieser Dissertation analysieren wir die Verwendung von Collaborative Beamforming in Ad-Hoc Netzwerken und entwerfen Routing-Algorithmen, die die Latenzzeit sowie den Energieverbrauch einer Multi-Hop Übertragung verbessern. Die Technik Beamforming nutzt mehrere ungerichtete Antennen um eine Richtcharakteristik zu erzeugen. Entsprechend werden bei Collaborative Beamforming die Antennen von mehreren verteilten Geräten genutzt um Beamforming zu betreiben.

Wir betrachten den Fall, dass jeder Knoten eine omnidirektionale Antenne für die drahtlose Kommunikation hat. Da das SINR-Modell den Effekt von Beamforming nicht berücksichtigt, basiert unser Kommunikationsmodell auf dem Ausbreitungsmodell von elektromagnetischen Wellen im Vakuum. Wir untersuchen Netzwerke, bei denen die Knoten auf einer eindimensionalen Line, in der zweidimensionalen Fläche, und im dreidimensionalen Raum mit einheitlichen Abständen platziert sind. Zusätzlich betrachten wir eine zufällige Knotenplatzierung in der Ebene.

Wir stellen einen Broadcast Algorithmus für den Fall vor, dass das Netzwerk aus n Knoten auf einer Linie besteht. Eine Nachricht kann in Zeit $\Theta(\log n)$ im gesamten Netzwerk verbreitet werden. Die Gesamtenergie beträgt $\Theta(n)$ und ist nur um einen konstanten Faktor größer als beim Standardansatz, wo die Nachricht sequentiell zum Nachbar auf der Line weitergeschickt wird. Für ein Netzwerk mit Knoten auf einer quadratischen Fläche präsentieren wir einen Unicast Algorithmus, der eine Nachricht über Distanz d von Start- zu Zielknoten mit Latenzzeit $\Theta(\log\log d)$ und Energieverbrauch $\Theta(d)$ überträgt.

Direktes Senden zu einem Empänger in Entfernung d benötigt die Sendeleistung $\Theta(d^2)$, und ein Multi-Hop Verfahren kann den Energiebedarf auf $\Theta(d)$ zum Preis einer erhöhten Latenzzeit von $\Theta(d)$ reduzieren. Im Vergleich können wir die Sendeleistung auf $\Theta(\sqrt{d})$ oder $\Theta(\log d)$ je nach Geometrie der Knotenplatzierung reduzieren. Wir stellen drei Algorithmen mit verschiedenen Stärken (Trade-offs) vor. Der erste Algorithmus ist für Knoten in einem Gitter entworfen und hat für eine Punkt-zu-Punkt Übertragung die Latenzzeit $\Theta(\log d)$ und den Energieverbrauch $\Theta(\sqrt{d})$. Der zweite Algorithmus reduziert ebenfalls für Knoten im Gitter die Latenzzeit auf $\Theta((\log\log d)/\varepsilon)$ mit Energie $\Theta((\sqrt{d})^{1+\varepsilon})$ für $\varepsilon > 0$. Der dritte Algorithmus ist für ein Netzwerk in einem 3-dimensionalen Gitter konzipiert. Er benötigt Zeit $\Theta(\log d)$ und reduziert die Übertragungsenergie auf $\Theta(\log d)$.

Collaborative Beamforming erfordert eine phasengenaue Synchronisation der Knoten mit einer Genauigkeit weniger als einer Periode $1/f$ der Trägerfrequenz f (etwa $f = 2,4\,\mathrm{GHz}$). Andere Arbeiten setzen die Synchronisation der Knoten als gegeben voraus, z.B. durch Kenntnis der kompletten Charakteristik des Übertragungskanals (full-CSI). Wir hingegen können für unsere Algorithmen Selbst-Synchronisation zeigen, wobei die Synchronisation während des Routings und ohne weitere Schritte hergestellt wird.

Zuletzt präsentieren wir ein verteiltes Protokoll für den Medienzugriff (MAC). Dabei werden die grundlegenden Mechanismen von Beamforming dazu genutzt, dass mehrere Geräte in einem Funknetz auf der selben Frequenz und zur gleichen Zeit kommunizieren können, ohne sich gegenseitig zu stören. Das Verfahren erhöht den Signal-Rausch-Abstand (SNR) eines Übertragungskanals mit gleichzeitiger Verringerung der Datenrate. Eine andere mögliche Anwendung dieses Verfahrens ist die Herstellung einer Verbindung zu weit entfernten Knoten, wo das Signal sonst zu schwach ist (z.B. in Netzwerken mit heterogenen Knotenverteilungen).

Abstract

The efficiency of routing algorithms in ad hoc networks is measured by delay, throughput, and energy. In this thesis, we analyze the usage of collaborative beamforming in ad hoc networks and design routing algorithms to enhance the transmission delay and decrease energy consumption of multi-hop communication. Beamforming is a technique to achieve directional radio by using multiple antennas with an omnidirectional characteristic. Accordingly, collaborative beamforming uses multiple antennas of distributed nodes to perform beamforming.

In our setting, each node has one omnidirectional antenna for wireless communication. Since the SINR-model does not cover the effects of beamforming, our communication model is based on the propagation model of electromagnetic waves in free space and we consider line-of-sight communication. We study nodes placed on a one-dimensional line, in a two-dimensional plane, and in three-dimensional space with uniform node distances. For the plane, we also study random node placements.

For n nodes placed on a line, we present a broadcasting algorithm, which broadcasts a message in time $\Theta(\log n)$. The total energy is $\Theta(n)$, which is only a constant factor larger than for the standard approach, where nodes sequentially transmit the broadcast message to their nearest neighbors. For nodes placed in an area in the plane, we present a unicast operation, which can transmit a message over distance d between source and target with delay $\Theta(\log\log d)$ and energy consumption $\Theta(d)$.

While direct point-to-point communication over distance d needs transmission power $\Theta(d^2)$, and multi-hop needs power $\Theta(d)$ and delay $\Theta(d)$, we can reduce the power to $\Theta(\sqrt{d})$ or $\Theta(\log d)$ depending on the geometry of node placement. We present three algorithms with different trade-offs. The first algorithm is designed for grid nodes in the plane and has a point-to-point delay of $\Theta(\log d)$ and energy consumption of $\Theta(\sqrt{d})$. The second algorithm for the same geometry decreases the delay to $\Theta((\log\log d)/\varepsilon)$ with energy $\Theta((\sqrt{d})^{1+\varepsilon})$ for $\varepsilon > 0$. The third algorithm requires a three-dimensional grid network, achieves a delay of $\Theta(\log d)$, and reduces the total energy to $\Theta(\log d)$.

One necessary requirement for collaborative beamforming is phase-synchronization of the nodes collaborating for beamforming. Phase-synchronization means a precision error less than a period $1/f$ of the carrier frequency f (e.g. $f = 2.4\,\mathrm{GHz}$). While similar works assume synchronization is already given for instance by full channel state information (full-CSI), we can proof that our algorithms are self-synchronizing, i.e. synchronization is established during routing hops with no further steps necessary.

Finally, we present a distributed medium access control (MAC) protocol that uses the basic concepts of beamforming and allows several devices in a wireless network to communicate on the same carrier frequency, at the same time, and without interfering each other. The scheme increases the signal-to-noise ratio of a communication channel while decreasing the data rate. Another possible application is establishing connectivity to remote nodes where regular transmission power is insufficient, e.g. in wireless networks with inhomogeneous node densities.

Acknowledgments

First of all, I like to thank my supervisor Christian Schindelhauer for the opportunity to do my doctorate at his chair in Freiburg. He gave me the chance to work in many different research fields and doing everything from low-level implementations to pure theory. I am very grateful for the close teamwork in research and wonderful discussions. I particularly appreciated his enthusiasm and interest to gain a deeper understanding in topics such as wireless networks, which motivated me to learn a lot about physics and electrical engineering.

My thanks goes to my other coauthors Liaquat Ali, Amir Alsbih, Alexander Ens, Peter Mahlmann, Leonhard M. Reindl, and Johannes Wendeberg for giving me insight in the other topics peer-to-peer networks, databases, localization, and signal processing. Some of the methods used in these research fields could be applied in this thesis as well. The joint work with Alexander and Johannes, in which we implemented a low-level wireless data transmission, was a helpful addition to create the model used in this thesis.

I also wish to thank my workmates Christian Ortolf and Johannes Wendeberg being always open-minded and interested in each others ideas and current work; I am also very grateful to them reading parts of this work and giving feedback. All members of the chair 'Computer Networks and Telematics' (also including Kerstin Pfeiffer and Norbert Küchlin) created a wonderful working atmosphere.

Special thanks go to my father Manfred Janson who as a communication engineer drew early my attention to computer science and electrical engineering, which led in the long run to this work.

Contents

1 Introduction

Today's digital world appears for the end-user wireless with smartphones and laptops equipped with GSM/UMTS and WLAN. From a technical point of view, only the last connection from the mobile device to a mobile phone tower or a WLAN-router is wireless and the interconnection in the backbone is mostly established via wires. Having a wired backbone decreases the flexibility of the mobile network. The demands of the network infrastructure has to be planned and installed in advance which might fail for example with traffic peaks at new years eve or checking emails in the wilderness, where the infrastructure is limited. This unsatisfactory situation motivates the research of ad hoc networks, which are wireless networks without a wired backbone and the mobile devices establish the routing themselves. The transmission range between mobile devices is limited due to limited transmission power. So, data might be passed in a chain of mobile devices from the sender to the target.

Basic performance metrics of networking are connectivity, throughput, delay, and power consumption. Connectivity to a network is the minimum requirement for a device to have a wireless service and is still unresolved even for cellular networks which do not have a hundred percent network coverage. With given connectivity, the data rate reflects the quality of service where some services like audio/video transmission have a minimum requirement for continuous transmission. Moreover, the overall data throughput of the network is also of interest and users have to share network resources, e.g. available wireless channels. Delay is important when it comes to processing of real time sensor data or audio/video chat where only short delays are acceptable. Specially, energy consumption puts a strong constraint on mobile networking. Mobile devices are mostly battery driven which has two implications: to have a long battery life and mobile service, devices cannot be permanently active, and when being active, power consumption is limited. Here, power for wireless transmission has a great share besides power for computations or input/output (e.g. displays). Secondly, design goals of mobile devices are small-sized and light-weighted, which does not favor the use of high-capacity batteries, large antennas, or a wireless hardware that can output strong signals like a radio mast. While a wireless infrastructure can be adopted to local conditions and the expected users' behavior and thus provide a homogeneous service everywhere (and mostly only costs are the barrier), ad hoc networks have to cope with heterogeneous conditions and spatial distributions of devices themselves.

Different models have been proposed to represent wireless networks in order to optimize wireless systems and algorithms on a higher layer to the specific properties of wireless networks. In the process, more and more physical properties have been

included and utilized.

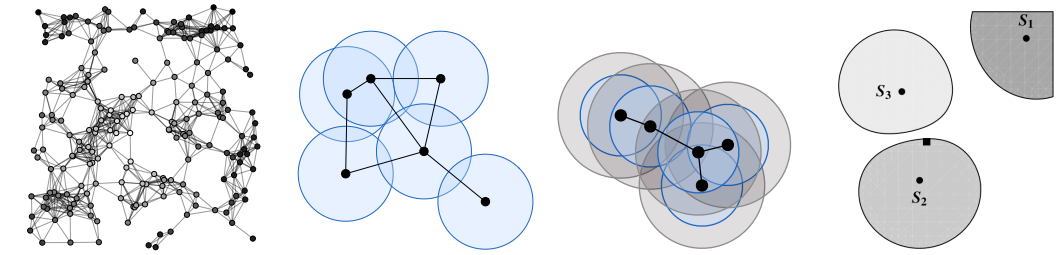

(a) graph-oriented model [CK85] (b) unit disk graph [CCJ90] (c) quasi unit disk graph [KMW04] (d) SINR diagram [AEK+12]

Figure 1.1: Models of wireless ad hoc networks

A starting point are graph-oriented models [CK85] in 1985, where edges reflect communication links between devices (here denoted as nodes) able to communicate. Unit-disc graphs [CCJ90] include the placement of nodes and limit the communication distance of nodes to a fixed radius. Hence, a node can receive a message if one sender within a unit range transmits and no other transmitter in unit range interferes. This model was extended to quasi unit-disk graphs [KMW04], where the deterministic boolean property of receiving was weakened. Here, a message transmission without interference always succeeds in range $p \leq 1$, in a longer range $(1 - p)$ a message might be received, and over unit range transmission is not possible (range p blue and range 1 grey in Figure 1.1(c)). This reflects a signal attenuation arising from the distance between sender and receiver and possible errors due to a low signal.

The combined interference power of multiple nodes can have an effect over long distances. This is not modeled by interferences in the local area of a unit disk. By contrast, Gupta and Kumar [GK00] use the SINR-model for the analysis of the capacity of ad hoc networks. The signal-to-noise-and-interference (SINR) model directly reflects the quality of a received signal and how strong the signal is disrupted by interferences. Depending on the magnitude of error, the data rate decreases or the transmission even fails. However, it is shown in [LL09] that a unit disk graph can be emulated in the SINR model. The emulation decreases the throughput with a polylogarithmic factor in the network size but ensures valid transmissions in the SINR-model of algorithms designed in the unit disk model. The possibility of emulating unit disk graphs into SINR-models shows that interferences only have local effects (with appropriate restrictions in the path loss model) and it is possible to visualize for each transmitting device s_i a reception zone (see Figure 1.1(d)), where receivers can receive successfully without interference [AEK+12].

The SINR model assumes that the signals of multiple transmitters are uncorrelated and computes the expected signal power of the superposed signal. However, if the signals of n transmitters are correlated, the signal power can be factor n higher than

the expected uncorrelated signal power. Multi-antenna techniques coordinate the signals of multiple antennas to exploit this effect. This is known under multiple-input multiple-output (MIMO), where multiple-input denotes the coordinated input at multiple transmitting antennas and multiple-output denotes the output signals at multiple receiving antennas which are jointly processed. The result is a directed radiation pattern. In Figure 1.2, we can see in (a) a single transmitting antenna (black dot) with

(a) single sending antenna (b) 3 multiple sending antennas

Figure 1.2: Radiation pattern of omnidirectional transmitting antennas

omnidirectional radiation pattern and in (b) multiple antennas producing a directed pattern with only a beam towards a receiver (black box). This produces less interferences in other directions illustrated by the encircling grey line. Since transmission power is concentrated on a main beam, the technique is called beamforming.

The physical effect of beamforming cannot be explained in the SINR-model covering only signal power and signal attenuation with the distance. Thus, we will use a more detailed model in this work to describe the effect and apply beamforming in ad hoc networks. The model is derived from the propagation model of electromagnetic waves, which are used for wireless transmissions. We restrict our model to free space and analyze the line-of sight signal which travels from sender to receiver on the shortest path. This excludes effects of multi-path propagation like shadowing, where an obstacle is between sender and receiver, or scattering, where a signal is reflected at obstacles, walls and traverses on multiple paths from sender to receiver.

Beamforming enhances the signal strength in a beam towards the receiver which improves the signal-to-noise ratio at the receiver and in result increases the data rate. Besides, multiple antennas can also be used for spatial multiplexing. Here, multiple parallel channels are established between a sender with multiple antennas and a receiver with multiple antennas. In each channel an independent and parallel data stream can be transferred, and thus the overall data rate increases. The ability of spatial multiplexing requires a rich environment with much scattering and multi-path propagation. If such an environment is not given[1], beamforming dominates the data rate improvement of multiple antennas. We consider in this work the case where beamforming is the best choice. For comparison of beamforming and spatial multiplexing, the related work section will contain relevant works for both techniques.

[1]Beamforming outperforms the capacity improvements of spatial multiplexing, if the angular spread between communication partners is too small and the channel matrix $\mathbf{H}$ has a low rank [GA02].

In this thesis, we analyze the application of beamforming in ad hoc networks. We consider the case where each device in the network is equipped with one antenna. Multiple devices have to collaborate and jointly use their antennas for beamforming, which is called collaborative beamforming. The main achievement of this work are multi-hop routing schemes with collaborative beamforming that can transmit a message from a sender to a receiver with improved transmission delay and reduced energy consumption (compared to a multi-hop protocol, which forwards a message to a neighboring node towards the target until the target is reached). In detail, we can improve the transmission delay for transmission distance d from $\Theta(d)$ up to $\Theta(\log \log d)$ and reduce the transmission power from $\Theta(d)$ up to $\Theta(\log d)$. We can achieve one important secondary aim: self-synchronization between devices collaborating for beamforming. The accuracy of synchronization has to be less than one period $1/f$ of the carrier frequency f (e.g. 0.2 ns for 2.4 GHz) to achieve distributed beamforming. Comparable works assume that synchronization is already given, e.g. by full channel state information (full-CSI). In addition, we present a distributed medium access control (MAC) protocol that utilizes the basic concepts of beamforming and allows several devices in a wireless network to communicate on the same carrier frequency, at the same time, and without interfering each other. Another possible application of the protocol is establishing connectivity to remote nodes where regular transmission power is insufficient, e.g. in wireless networks with inhomogeneous node densities.

1.1 Outline

The thesis is structured into six parts.

Chapter 1 - Introduction We motivate the utility of beamforming for ad hoc networks and describe relevant related work in this field.

Chapter 2 - Communication Model We define our setting of wireless ad hoc networks and describe all relevant characteristics and parameters for wireless data transmission between nodes in the network. The chapter begins with a short introduction of the propagation model of electromagnetic waves to describe the characteristics of beamforming.

Chapter 3 - Analysis of Beamforming with Multiple Antennas First, we analyze how we can improve communication with beamforming, i.e. reduction of interference, increase of the data rate, and extension of the transmission range. Given multiple senders (see Figure 1.2(b)), we study how to allocate transmission power to the senders to maximize the power transferred to a receiver. We characterize the directional radio pattern of multiple sending antennas in the plane [JS12].

Chapter 4 - Transmission Schemes with Collaborative Beamforming We present transmission schemes which combine multi-hop routing with collaborative transmit beamforming. We begin with a simple example of two-hop relaying. Then we present successive transmission schemes for nodes placed on a one-dimensional line, in a two-dimensional plane, and in three dimensional space [JS13, JS14a, JS14b, JS14c]. For the last two cases, we investigate different trade-offs of transmission delay and energy consumption.

Chapter 5 - A Distributed MAC Protocol Turning Interferences into Noise We use the mechanisms of beamforming to create a medium access control (MAC) protocol enabling multiple nodes to communicate simultaneously on the same frequency. The protocol does not need a central control and communication partners can turn interferences into power reduced noise by applying filters similar to beamforming [JES15].

Chapter 6 - Conclusions We sum up what we have achieved in this work and outline open problems.

1.2 Publications

Parts of this work have been peer-reviewed and published in the following conference and workshop proceedings.

- Thomas Janson and Christian Schindelhauer. Analyzing Randomly Placed Multiple Antennas for MIMO Wireless Communication. In *Fifth International Workshop on Selected Topics in Mobile and Wireless Computing (IEEE STWiMob'12)*, pages 745-752, Barcelona, Spain, October 2012 (Section 3.4)
- Thomas Janson and Christian Schindelhauer. Broadcasting in Logarithmic Time for Ad Hoc Network Nodes on a Line using MIMO. In *Proceedings of the 25th ACM Symposium on Parallelism in Algorithms and Architectures, SPAA'13*, pages 63-72, Montreal, Canada, July 2013 (Section 3.0, 4.2)
- Thomas Janson and Christian Schindelhauer. Self-Synchronized Cooperative Beamforming in Ad-Hoc Networks. In *Proceedings of the 16th International Symposium on Stabilization, Safety, and Security of Distributed Systems (SSS'14)*, LNCS 8756, pages 135-149, Paderborn, Germany, September 2014 (Section 4.3)
- Thomas Janson and Christian Schindelhauer. Cooperative Beamforming in Ad-Hoc Networks with Sublinear Transmission Power. In *2nd International Workshop on GReen Optimized Wireless Networks (GROWN'14)*, Larnaca, Cyprus, October 2014 (Section 4.4)
- Thomas Janson, Alexander Ens, and Christian Schindelhauer. Turning Interferences into Noise in Ad Hoc Networks. In *Telecommunication Systems*, accepted in June 2015 (Section 5)

We also published the following peer-reviewed papers (grouped by topic) during my time as doctoral candidate, which are not part of this thesis.

Signal Processing:

- Alexander Ens, Thomas Janson, Leonhard M. Reindl, Christian Schindelhauer. Low-Power Simplex Ultrasound Communication for Indoor Localization. In the *22nd European Signal Processing Conference (EUSIPCO 2014)*, Lisbon, Portugal, 2014
- Alexander Ens, Thomas Janson, Leonhard M. Reindl, Christian Schindelhauer. Robust Multi-Carrier Frame Synchronization for Localization Systems with Ultrasound. In *Proceedings of the 18th International OFDM Workshop 2014 (InOWo'14)*, Germany, 2014

Peer-to-Peer Networks:

- Thomas Janson, Peter Mahlmann, and Christian Schindelhauer. A self-stabilizing locality-aware peer-to-peer network combining random networks, search trees, and DHTs. In *Proceedings of the 16th International Conference on Parallel and Distributed Systems (ICPADS'10)*, pages 123-130. IEEE, December 2010

- Amir Alsbih, Thomas Janson, and Christian Schindelhauer. Analysis of Peer-to-Peer Traffic and User Behaviour. In *Fourth International Conference on Internet Technologies & Applications (ITA 2011)*, Wrexham, Wales, September 2011

Databases:

- Liaquat Ali, Thomas Janson, and Georg Lausen. 3rdf: Storing and Querying RDF Data on top of the 3nuts Overlay Network. In *10th International Workshop on Web Semantics (WebS 2011)*, pages 257-261, Toulouse, France, August 2011
- Liaquat Ali, Thomas Janson, Georg Lausen, and Christian Schindelhauer. Effects of Network Structure Improvement on Distributed RDF Querying. In *6th International Conference on Data Management in Cloud, Grid and P2P Systems (Globe 2013)*), volume 8059 of *Lecture Notes in Computer Science*, pages 63-74. Springer, Prague, Czech Republic, August 2013
- Liaquat Ali, Thomas Janson, Georg Lausen, and Christian Schindelhauer. Towards Load Balancing and Parallelizing of RDF Query Processing in P2P Based Distributed RDF Data Stores. In *22nd Euromicro International Conference on Parallel, Distributed and Network-Based Processing (PDP 2014)*, pages 307-311, Turin, Italy, February 2014

Indoor Localization:

- Thomas Janson, Christian Schindelhauer, and Johannes Wendeberg. Self-Localization based on ambient signals. In *6th International Workshop on Algorithms for Sensor Systems, Wireless Ad Hoc Networks, and Autonomous Mobile Entities (ALGOSENSORS 2010)*, volume 6451 of *Lecture Notes in Computer Science*, pages 176-188, Bordeaux, France, 5 July 2010
- Thomas Janson, Christian Schindelhauer, and Johannes Wendeberg. Self-Localization Application for iPhone using only Ambient Sound Signals. In *International Conference on Indoor Positioning and Indoor Navigation (IPIN) Proceedings*, pages 259-268. IEEE, September 2010
- Johannes Wendeberg, Thomas Janson, and Christian Schindelhauer. Self-Localization based on Ambient Signals. *Theoretical Computer Science*, volume 453, pages 98-109, 2012

1.3 Notation

Units

m	meter	
s	second	
Hz	hertz $= \mathrm{s}^{-1}$	(frequency)
F	farad	(electrical capacitance)
H	henry	(inductance)
V	volt	(electric potential)
A	ampere	(electric current)
Ω	ohm	(electrical resistance)
W	watt	(power)
J	joule $= \mathrm{W} \cdot \mathrm{s}$	(energy)
dB	decibel $= 10 \log_{10}(r)$	(logarithmic power ratio r)

Constants/Variables

c	$\approx$	3.0×10^{8}	m/s	speed of light
ε_0	$\approx$	8.854×10^{-12}	F/m	permittivity of free space (electric constant)
f_c	e.g.	2.4×10^{9}	s^{-1}	carrier frequency
λ	e.g.	0.125	m	carrier wavelength $= c/f_c$
v	e.g.	(10,1)	m	Euclidean vector (node position in the plane)

Operations

$\Re(x)$	real part of complex value $x \in \mathbb{C}$
$\Im(x)$	imaginary part of complex value $x \in \mathbb{C}$
$\lvert x \rvert$	absolute value of a scalar or length of vector x e.g. distance $\lvert u - v \rvert$ between position u and v
$\mathcal{N}(0, \sigma^2)$	normal distribution with expected value 0 and variance σ^2
$\mathrm{Prob}[X = x]$	probability that a random variable X has the value x
$\mathbb{E}[X]$	the expectation of X of random variable X
$\mathrm{Var}[X]$	the variance of random variable X
$\sqrt{\mathrm{Var}[X]}$	the standard deviation of random variable X
$\mathcal{O}(\cdot)$, $o(\cdot)$, $\Omega(\cdot)$, $\omega(\cdot)$, $\Theta(\cdot)$	Landau notation describing asymptotic behavior

1.4 Related Work

The related work section is subdivided into the topics beamforming and collaborative beamforming. For classification of beamforming, we also cite relevant research papers for spatial multiplexing with multiple antennas. Some technical terms might be first properly introduced in the following Chapter 2 where we present the communication model used in this work. Just in case, explanations about most technical terms can be found in the glossary on page 178.

Beamforming with Multiple Antennas Krim and Viberg summarize in [KV96] the development in signal processing and consider uniform linear and circular array geometries. Indeed they focus on sensor arrays but the geometric derivations can be applied to antenna arrays in the same way.

The authors of [OMPT05] analyze in 2005 the beam-pattern of n sensor nodes placed in a disk with radius r with a uniform distribution (which is comparable to our analysis [JS12] presented in Section 3.4 [2]). For the theoretical analysis of the pattern they make similar assumptions with perfectly synchronized nodes, all nodes have the same transmission power, and a channel only containing the line-of-sight path. In their model, nodes are equipped with isotropic antennas and at first they consider an elevation angle relative to the plane containing the disk, but the subsequent analysis is reduced to the signal strength in the plane with elevation angle 0. We instead assume dipole antennas in our model and for the analysis of the beamforming pattern in the plane both model will have the same result. An approximation function for the average signal power for a given emission angle α is derived from mathematical textbooks including Bessel-functions expressing similar to our result the main beam and side lobes. A third case, which we called random noise, is not defined or analyzed here. Instead, the authors are able to approximate the cumulative distribution of signal powers that can occur in all emission angles α. They additionally address the problem of imperfect phases for beamforming due to errors in synchronization. They differentiate between a closed-loop initialization where the senders synchronize to a beacon of the receiver or an open-loop initialization, where the senders in a cluster synchronize to a nearby reference point and together with known sender positions and the target position they can set up the phases for beamforming. For the closed-loop, they assume that phase jitter follows a Tikhonov distribution. In the open-loop case, the localization of the senders can be error-prone and the position errors are modeled uniformly distributed in a given range.

Spatial filtering with beamforming is not perfect and the beamforming pattern also shows strong side lobes besides the desired main beam. If a device is receiving a signal arriving from the direction of the main beam and a side lobe points towards an interfering sender, the interference will be strong. Thus, it might be beneficial to not only maximize the signal strength towards the receiving direction but also

[2] [OMPT05] is an independent work to ours and we were unaware of it when writing [JS12].

strongly attenuate or even null the signal in known directions with strong interference. Optimizations have been presented for linear antenna arrays (antennas are placed on a line) [EKKG05] and a circular array geometry (antennas are placed on several circles around a reference point in the center) [RXS11]. A Kalman filter is used to update the beamforming pattern to changes in the environment.

However, beamforming is already a standard in use in IEEE WLAN 802.11n/ac and offers (with higher SNR) maximum data rate for short distances or improved signal reception over long distances. According to the white paper [Net13], the increased SNR with beamforming makes 256-QAM (modulation with 8 bit per symbol) possible in Wi-Fi networks in the first place. Before, this was only possible in wireless networks using parabolic antennas in point-to-point connections. Additionally, beamforming allows multiple channels to different users at the same time, with a single channel to each user with multi-user beamforming or even multiple spatial streams to each user with MU-MIMO (multiple user-multiple-input multiple-output) [LBB+13].

Phase shifts of beamforming can be implemented at many stages of the hardware chain: A digital delay in baseband of unmodulated data at the processor can be produced; the baseband signal is modulated on an intermediate frequency (IF) that can be delayed; the IF signal is mixed with the local oscillator (LO) signal to the radio frequency (RF) signal and it is possible to produce a phase shift at the local oscillator or delay the RF signal. Both [NKH05, PCLM12] give an overview of the different solutions and present a solution for phase shifting at the local oscillator with a phase error less than 10°. In [PCLM12], the authors also provide variable amplitude with 2-bit resolution for better side-lobe suppression. Arguments pro LO beamforming in comparison to RF beamforming is less influence on the signal linearity [PCLM12]. In comparison, a beamforming implementation in the RF chain can reach a 2.5% gain error and phase error less than 10° for the 2.4 GHz frequency band (used in the 802.11 standard) [HCP11]. This is reached by using a vector modulator-based active phase shifter structure according to the principle that the signal is first split into real and imaginary part with a quadrature filter and and both signals are multiplied with a voltage value according to the phase angle. An example for a vector modulator is the AD8341 of Analog Devices [Ana14] with the frequency range 1.5 GHz to 2.4 GHz, continuous phase control of 360° and magnitude control of −4.5 to −34.5 dB at a price of 7.59 $ (in November 2014). In this work, we will assume only beamforming in the radio frequency (RF) part and only analyze beamforming on the carrier of the radio frequency.

Spatial Multiplexing with Multiple Antennas Beamforming with multiple antennas enhances the SNR of a single transmission channel but the channel capacity (maximum achievable data rate) only increases with $\Theta(\log(1 + \mathrm{SNR}))$. It is also possible to establish multiple parallel transmission channels with multiple antennas, which is called *spatial beamforming*. Tse and Viswanath describe in [TV05] multiple antenna arrays limited to uniform linear arrays and derive the channel capacity under the the

Rayleigh fading model. The capacity in $\Theta(n_{\min})$ where $n_{\min}$ is the minimum of sending antennas and receiving antennas is possible when using the V-BLAST architecture [WFGV98] and $n_{\min}$ parallel and independent channels are established. This is possible by generating a singular value decomposition $\mathbf{H} = \mathbf{U} \cdot \mathbf{\Lambda} \cdot \mathbf{V}^*$ of the channel matrix $\mathbf{H}$ and perform an operation at the sender and receiver. The sender performs a preprocessing operation and multiplies the input vector $\mathbf{x}$ (where entry x_i is the input for the i-th antenna and contains an independent stream) with the unitary rotation matrix $\mathbf{V}$. The receiver multiplies the output vector $\mathbf{y}$ (where y_i is the received signal of the i-th antenna) in a postprocessing step with the unitary rotation matrix $\mathbf{U}^*$. In result, the transmission through the wireless channel will only affect a signal attenuation on the parallel and independent channels and the signals of the parallel channels won't get mixed up. The i-th channel will be attenuated by the signal value λ_i which is contained in the diagonal matrix of singular values $\mathbf{\Lambda}$. However, the requirements for a high capacity are fast fading, a high SNR, and large singular values reflecting a rich environment. In this work, we investigate the opposite case with low SNR and small singular values in the free space scenario.

Pollock et al. [PAK03] extend the MIMO channel capacity calculation with parameters of the antenna positioning and the angular spread. In theory, the capacity grows linearly with the number of antennas for Rayleigh fading channels. But they show for realistic scenarios that the capacity is significant lower because of insufficient antenna spacing and angular spread.

Foschini and Driesen [DF99] investigate the impact of the array geometry of multiple antennas on the channel matrix. They consider line-of-sight propagation for linear arrays, arrays with antennas spread along an arc, and uniform circular arrays. Additionally, they analyze linear arrays located on a street with two reflecting building walls alongside the street. They also compute the capacity for Ricean channels.

The authors of [OTA+07] categorize placing the transmit and receive antennas of a MIMO system for highest capacity as fundamental design issue (This is related to our analysis of beamforming [JS12] depending on the antenna array geometry, see Chapter 3.4). With Particle Swarm Optimization, they search for the antenna placement with highest channel capacity, which they derive from the properties of the channel matrix $\mathbf{H}$. Their model includes scattering objects as isotropic radiators which are uniformly distributed. Olgun et al. present numerical results for the placement of antennas in two-dimensional plane and three-dimensional space where each antenna can be placed at 100^2 respectively 100^3 discrete points. They compare the capacity of arrays created with Particle Swarm Optimization (PSO) with the capacity of uniform linear arrays (ULA) and uniform circular arrays (UCA). For up to six antennas per array, PSO outperforms UCA and UCA outperforms ULA. For more than six antennas per array, PSO barley improves the capacity level of UCA and the authors conclude that uniform circular arrays are a good design option.

For spatial multiplexing, it is necessary to have linear independent phases between each pair of sender and receiver antennas. This results in many large eigenvalues in

the channel matrix H and spatial multiplexing can be applied. If Rayleigh fading with independent at random phases holds here, we can assume large eigenvalues. In contrast, small eigenvalues indicate dependencies between antennas and it is only beneficial to perform beamforming with these dependent antennas. The dependencies arise from the environment and positioning of antennas. In most cases, we are not able to change the environment or the positions of the antennas to improve the channel matrix H. Another approach here is having an oversupply of antennas at each device and only using a subset of these antennas, which has the desired properties. The article [MW04] gives an overview of works in the field of MIMO systems with antenna selection. The goal is to reduce hardware complexity and consequently costs while retaining almost the same channel capacity (data rate). For each radio channel, a RF chain (which operates in the radio frequency band) and an antenna is needed. Since RF chains have a much higher price compared to the the price of antennas [BWK05], the solution is to have more antennas than RF chains and only operate with a subset of antennas.

Collaborative Beamforming A single device like a router might only have a small constant number of antennas attached to it. The corresponding beamforming gain is then also limited by a small constant. In contrast, multiple devices can collaborate to use their antennas together for collaborative beamforming and thus the beamforming gain can be up to the number of collaborating nodes. At most, this can be in the order of the the network size n and we will see in the following that the network throughput can increase in $\mathcal{O}(n)$ when applying collaborative beamforming.

In a recent work [MLÖ12], Özgür et al. present a hierarchical broadcasting scheme for n nodes in a one-dimensional network (This is related to our broadcasting algorithm [JS13] presented in Section 4.2). The basic scheme distributes information in clusters of size M and the beamforming gain of the the M nodes is used to transmit the messages to the target. This recursion step is repeated in a hierarchical strategy. Their analysis assumes a path-loss exponent $1 \leq \alpha < 2$ in the line-of-sight case. At the same time, they demand low SNR $\ll 0$ dB and for small-range communication between neighboring nodes a $\text{SNR}_s \leq n^{\alpha-2}$. In our algorithm presented in Section 4.2, we assume a path-loss exponent $\alpha = 2$.

The authors of [MÖL13] use a similar approach to ours in [JS14a] (see Section 4.3) by using beamforming of rectangular areas. Their algorithm spreads the information to a telescope-like region with increasing adjacent rectangles. Then, a mirrored construction is appended in order to reach the target node. They conclude that the beamforming gain is maximized up to a constant factor at each receiver as long as the area size of beamforming nodes is much smaller than $\sqrt{n}$ for n nodes in the network. The authors cannot give a closed form for the dimensions of the rectangles and refer to a Matlab program computing optimal sizes. They use an amplify-and-relay scheme, i.e. relay nodes between source and target forward the noisy signal. An important difference to our approach is that they allow additional transmission power $a > 1$ for a short period $1/a$. Interestingly, their choice is $a = \Theta(1/n^{2/3})$ which results in

throughput $T = \mathcal{O}(n^{2/3})$. We show that the choice of adjacent rectangles might be problematic, since our simulation results indicate that some receivers in the adjacent rectangle might not be reached. In this thesis, we emphasize the large influence of the carrier wavelength and present a closed-form solution for the placement and dimensions of rectangular beam-forming areas. Furthermore, we present a solution which does not need the full channel state information. It is not addressed in [MÖL13], but if the synchronization problem of the scheme can be solved (in an energy-efficient way), the scheme can transmit data with a transmission energy being sublinear to the transmission distance[3]. This is reached by the combination of transmit and receive beamforming, which multiplies the beamforming gain and decreases the necessary transmission power. But the relay nodes forward a signal with such low SNR ($\text{SNR}_s = n^{-\gamma}$ with $\gamma > 1$) that they might not notice the signal in noise, and it might be challenging to control an operation at the relay nodes. Another difference to our scheme is that telescopic beamforming only considers a fixed number of rectangular clusters between source and target, which does not depend on the transmission distance. And so, the number of nodes performing collaborative beamforming is also not proportional to the distance. By contrast, we use $\Theta(\log\log n)$ clusters and retransmissions to achieve necessary beamforming gain. The implication for the scheme in [MÖL13] is that they only have a constant number of retransmissions during routing of one message, and the throughput is only throttled by this constant (Due to interference, the source might have to wait for a new message transmission until the preceding transmission has been delivered to the target).

Gupta and Kumar [GK00] analyze the throughput capacity of wireless networks. The throughput capacity of a network node specifies the average data rate to a communication partner multiplied by the communication distance. For the case of nodes positioned independently at random in the plane and random communication pairings, they show that the capacity is $\Theta(\frac{1}{\sqrt{n\log n}})$ in the best case. Here, multiple-hop routes using nearest neighbors turn out to be the best choice. It turns out that the communication bottleneck is a cut through the middle of the network, on which each node has to uphold $\mathcal{O}(\sqrt{n})$ connections throttling the throughput by a factor of $\mathcal{O}(\frac{1}{\sqrt{n}})$, because nodes have to share their channel with $\mathcal{O}(\sqrt{n})$ communications being routed through them in the multi-hop scheme. It is necessary to increase the sending power by $\mathcal{O}(\log n)$ to guarantee network connectivity with high probability when nodes are placed independently at random. By this, the throughput is further reduced by a factor of $\mathcal{O}(\frac{1}{\sqrt{\log n}})$. In [JS14a] (see Section 4.3), we use a similar argument when nodes are randomly distributed in the plane.

In [NGS09], Niesen, Gupta, and Shah present a communication scheme called hierarchical relaying that achieves order-optimal throughput for path loss exponent $\alpha \in [2, 3)$ by exploiting collaborative beamforming. Here, nodes in designated areas cooperate for beamforming in order to increase the transmission radius and the cooperating nodes

[3] In Appendix A is an approximate computation of the transmission energy of [MÖL13].

act as relay between source and target of a message. Receiving and decoding a message with collaborative beamforming makes it necessary that the signals, which are received by all nodes in the area, are exchanged and combined for spatial filtering. The signals are exchanged as quantized observation, e.g. digitized samples, which is larger than the original message size. For exchanging the signals, the authors suggest a hierarchical approach, where areas in a smaller scale inside the area of relaying act again as relay areas. The number of these recursive steps is $\log^{1/2-\delta}(n)$ for $\delta \in (0, 1/2)$ and n nodes in the network. When the recursion terminates for a small area of the network, TDMA is used for exchanging the signal observations. They assume uniform distributed phases between all pairs of nodes in the network and full-CSI, i.e. phase-shift between each sender-receiver pair is known.

Collaborative MIMO Özgür, Leveque, and Tse show in [ÖLT07] that linear capacity in the number of nodes n is possible. To achieve linear scaling they use collaborative MIMO where the number of parallel spatial streams is in the order of collaborating nodes. Similar to [NGS09], they pursuit a hierarchical scheme of cooperation, where the rectangular areas of cooperating nodes are subdivided recursively to exchange data respectively received signals of data and be able demodulate the data. A requirement for linear capacity is that $\sqrt{A}/\lambda > n$ where A denotes the area A for node placing, n is the number of nodes in the network, and λ denotes the wavelength. We also arrive at the same precondition $\sqrt{A}/\lambda > m$ for our model to receive a SNR gain of $1/m$ for MIMO and nodes with m antennas in [JS12] (see Section 3.4). In [ÖJTL10] they further divide wireless networks in working regimes with the main parameters short-distance SNR, long-distance SNR, and the path loss exponent α of the environment.

Low-Power Transmissions with Beamforming Despite of high data rates using spatial multiplexing, wireless sensor networks for example focus on low energy consumption for wireless communication and sensor nodes are supposed to operate over years with only battery power supply. We will analyze to reduce transmission energy with collaborative beamforming in Chapter 4.4.

In [MBC+01] the challenges of low-power in wireless sensor networks are addressed. Sensor networks are a special case where mobile nodes are assumed to function over years without external power supply. The authors analyze in detail the energy consumption for communication consisting of software and hardware. They consider the power consumption of wireless hardware for the start-up from sleep mode and the transmission power, where the start-up energy is significantly high for short packets.

Jayaweera [Jay04] compares the energy consumption of a 2×1 MISO system, i.e. two antennas for sender beamforming and one receiver antenna to a single antennas communication (SISO). He observes that a variable data rate of M-QAM for different transmission distances can considerably improve the the performance of the system and thus reduce the energy consumption. He also analyses cooperative beamforming, where the data is distributed between nodes in a local area which then perform cooperative

beamforming. For two beamforming senders, he shows that the energy consumption is halved.

De Freitas et al. [dFdCdAM12] use MIMO techniques in wireless sensor networks to reduce the energy consumption. They differentiate between energy consumption for sending and receiving in a transmission and state in which cases multi-hop routing outperforms single-hop direct communication. They propose to use either cooperative MIMO between clusters of sensors or cooperative beamforming for receiving (SIMO) or sending (MISO). They present simulations where they compare single-hop, multi-hop, and communication with MIMO techniques and conclude that MIMO techniques are advantageous over multi-hop when data is sensitive to delay, and cooperative MIMO techniques are more energy efficient for more than four hops.

The authors of [DPP08] propose a solution for energy-efficient communication over long distances by using collaborative beamforming. Their cross layer approach coordinates several nodes on the MAC layer for cooperative beamforming on the physical layer. In a two phases protocol, they first spread the information in a local area followed by a second phase where the receivers repeat the received analog signal with adjusted phase and amplification for cooperative beamforming. Synchronization is reached by a central solution, where a selected node plays the role of a cluster head, which synchronizes the beamforming senders in the local area. Using the known positions of the collaborating nodes relatively to the cluster head, the nodes can set up collaborative beamforming in an open-loop approach. This approach also allows to send several messages at the same time using the same cooperative beamforming nodes to different directions. Communication channels are modeled with Rayleigh fading and sender beamforming is optimized in an open-loop approach to a single destination. Our approach differs here, since we assume that the signal propagation in a certain area is homogenous according the line-of-sight model, i.e. reception delay corresponds to the distance to the sending cluster and we assume that we can synchronize using the reception times and delays.

Distributed MAC protocols We present in Chapter 5 a distributed MAC protocol for ad hoc networks which is basically derived from beamforming techniques and correlating signals by phase shifts. The idea of applying pseudo-random phases is also used in MIMO channels [SL07]. Here, the case of a channel matrix with small eigenvalues is considered where spatial multiplexing is not possible. When applying different pseudo-random rotation matrices to each codeword, they can show a 22 percent reduction of the packet error ratio.

Passiatore and Camarda present in [PC14] a distributed MAC protocol for cognitive radio wireless ad-hoc networks. The performance metric is a fair channel assignment to the nodes and the quality of service. The MAC protocol is collision-free and nodes perform carrier sensing and distributed control of medium access to avoid collisions. In contrast, we expect collisions in our protocol which are resolved by a modulation scheme to increase the signal-to-noise ratio. Spread spectrum multiplexing [Gol67] also

achieves multiple parallel transmissions without central medium access control. This is achieved by repeating a baseband information in a binary sequence where a one is tantamount to sending and a zero to not sending. Each sender has a unique chosen binary sequence and the receiver can read the information by correlating the signal with the sender's sequence.

While distributed MAC protocols routing strategies are necessary for ad hoc networks without a controlling infrastructure, less cooperation between nodes for transmission (e.g. multi-hop) might be advantageous, too. The authors [WM04] address the problem of selfish nodes in ad hoc networks whose goal is to have high data rate for own traffic and participating in packet forwarding for others in the network the least possible. They analyze strategies with a trade-off between cooperating in or declining packet forwarding.

Jammers are another paradigm to cope with jamming sources of all kind which includes interferences in an ad hoc network or jamming sources in the environment. Chiang and Hu [CH11] for instance use spreading codes to cope with jammers, which can disrupt communication permanently but has limited transmission power. The basic idea is to send information with enough redundancy that it is impossible for the jammer to disrupt all information and some information can be transferred. They use FFH-CDMA or DS-CDMA to spread information in the frequency band or in time. They assume that the receivers share a set of spreading codes with the transmitter and all codes are orthogonal. We in contrast add redundancy to a transmission with pseudo random phases and share a key to generate the pseudo random phases (Chapter 5). Orthogonality of parallel communications and jammers is adjusted dynamically in our scheme which complies to the demands of ad hoc networks with heterogenous structures and conditions in the network.

2 Communication Model

The physical communication model of networks describes the connectivity between nodes specified by a boolean if two nodes can exchange data or more refined by a data rate for communication with unit bytes per second. In wired networks, the connectivity between two nodes can be obviously established by connecting them with a wire. The transmission quality depends on the physical properties of the cable with signal attenuation through cable length and (inductive) resistance, and the effects of interfering signals of the environment. Interactions between different shielded cables are not to be expected. Thus, wired networks can be nicely abstracted by graph models where nodes are the network devices and edges represent the wired connection.

In contrast if nodes communicate wirelessly, they share the same transmission medium, which is the free space. If one node emits a signal via an antenna to this same medium, all other nodes can perceive the signal. Thus, simultaneous transmissions cannot be considered in isolation from each other, which is the case for isolated wires. Instead, the parallel transmissions can disturb each other in a wireless network, which is called interference. The primary question is then if a receiving node is able to filter the interference and read the message of the intended sender without any errors. Wireless signals decay with the distance to the sender and thus signal levels highly depend on the positions of the nodes in the network and the environment, e.g. walls attenuating a signal. Hence, the following definition of the model for wireless networks will base on physical properties, i.e. positions of network nodes and characteristics of a wireless channel between sender and receiver, which maps the complete interaction between all nodes in a network.

The definition will start in a top-down view in Section 2.1 with the definition of ad hoc networks on a higher layer including the network topology and communication. In Section 2.2, we discuss the equipment of the devices for wireless communication which is focused on the antenna and its characteristics. Combining the ad hoc network topology, the environment, and the antenna characteristics we can specify a communication model in Section 2.3 if nodes are able to communicate. This model is refined in Section 2.4 for multiple-antenna beamforming, where multiple antennas cooperate to increase transmission range.

2.1 Wireless Ad Hoc Networks

An ad hoc network network is a dynamic and wireless network establishing communication between mobile devices without additional external infrastructure, i.e. WLAN

routers or mobile phone towers via a wired network. Compare Figure 2.1(a), where user device only communicates with an access point respectively radio mast, with Figure 2.1(b), where user devices directly communicate without infrastructure and only wirelessly.

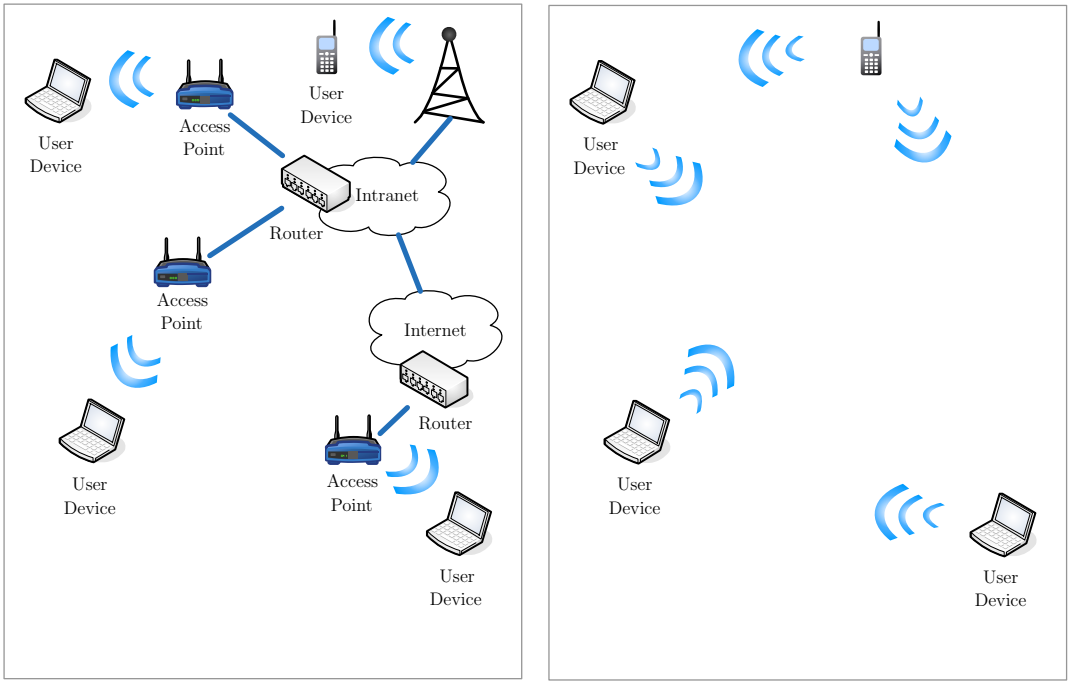

(a) Infrastructure of wireless networks (b) Ad hoc network

Figure 2.1: Illustration of wireless communication

Throughout this work we denote a device on an abstract layer as node and will not go into detail to the specifics of the hardware. Only the antenna for wireless communication will be specified. Each device in our model has exactly one antenna. To emphasize that each device including the antenna is symbolized only by the antenna symbol ⍒ (a vertical line with a triangle on top, senders are green colored and receivers red colored). In result, if we speak about multiple antennas, e.g. for MISO, SIMO, MIMO, the corresponding devices of the antennas have to cooperate.

We analyze in this work the following network setting. We have a network with n nodes placed in the plane. The nodes are stationary[1], i.e. have velocity $v = 0$. Each node is equipped with a dipole antenna for wireless communication, which is aligned perpendicular to the plane (see Fig. 2.2) resulting in an omnidirectional characteristic

[1] Other work e.g. [OMPT05] limits the nodes' movement in such a way that necessary synchronization for wireless transmission persists for the transmission time of a (short) message, which depends on the node positions.

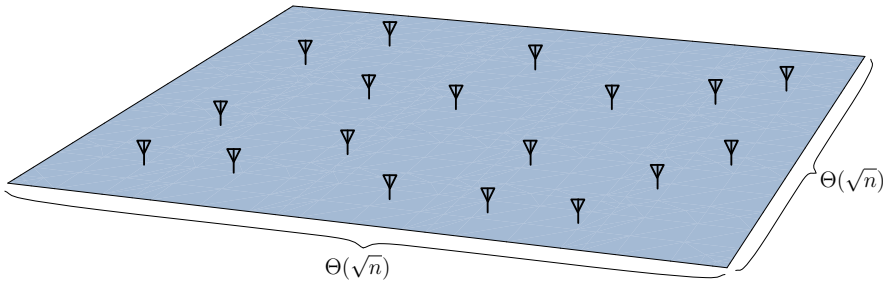

Figure 2.2: Ad hoc network in the plane where each of the n devices is illustrated only by its antenna, which is aligned perpendicular to the plane

in the plane, i.e. each antenna broadcasts in all directions alongside the plane with equal power. There, we can neglect the effect of polarization. We only consider free space, i.e. there are no obstacles, walls or floor ceiling, or atmosphere, where the radio signals are reflected or absorbed (In particular, the plane in the figures is only drawn for illustration purposes and does not reflect the signal). The antennas are used for sending and receiving signals, which essentially hold binary strings, called messages. These messages are modulated on the same carrier wave with some frequency f.

The node density in our model is constant, i.e. for node density ρ with unit nodes/m^2 the area is $\frac{n}{\rho}$ with dimensions $\frac{1}{\sqrt{\rho}}\sqrt{n} \times \frac{1}{\sqrt{\rho}}\sqrt{n}$. In result, the area of the plane grows with the number of nodes. This assumption has two effects. First, the transmission power to reach the nearest neighbors is asymptotically constant and thus we can reach with the same transmission power the same number of nodes independent from the network size. The mean distance between an arbitrary pair of source and destination for routing grows with the diameter $\Theta\left(\sqrt{n}\right)$ of the network and routing between arbitrary nodes will need more energy when the network size grows. Second and most important, beamforming characteristics when using multiple antennas depend on node distances and the radio frequency and if we keep the node density constant, these characteristics do not depend on the network size[2].

2.2 Wireless Signal Transmission

In this section, we describe how to transmit an analogous signal wirelessly from a sender antenna to a receiver antenna with an eletcromagnetic wave. We start with the specification of the antenna, followed by the electromagnetic wave which a sending antenna produces and induces a current in a receiving antenna. Then we derive the transmission power and power dissipation by the wireless devices.

[2]This is in contrast to [GK00], where all nodes are placed on an area of 1 m^2.

Dipole Antenna Each device has one dipole antenna for sending and receiving in our model. So only half duplex transmission is possible, i.e. a device can only send or receive but not send and receive at the same time. The dipole antennas are aligned perpendicular to the plane. Alongside the plane, the antennas have no directional characteristic, i.e. the reception or sending power in all directions in the plane is equal. The signal propagates on the line-of-sight path from sender to receiver with speed of light $c = 3 \cdot 10^8 \frac{\text{m}}{\text{s}}$. The signal attenuation between a sender and receiver node is only a function of the distance d between them.

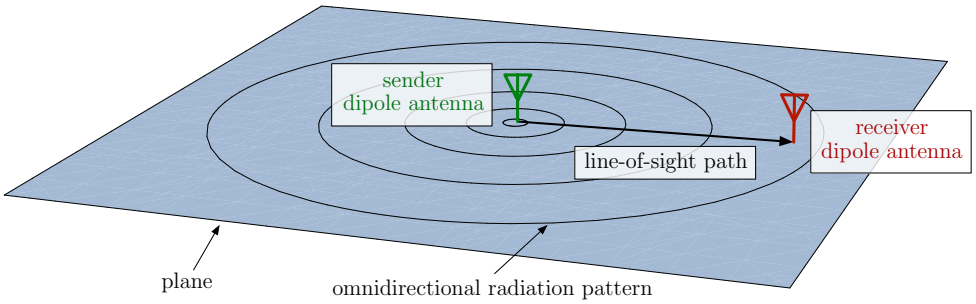

Figure 2.3: Omnidirectional radiation pattern in the horizontal plane with waves propagating in free space, i.e power density is proportional to $\frac{1}{d^2}$ for distance d to a receiver point.

Dipole antennas are vertically polarized, i.e. the Hertzian dipole has a radiation pattern where signal power is attenuated by factor $\sin^2\theta$ for elevation angle θ. Accordingly, the signal power is maximum alongside the plane with $\theta = \frac{\pi}{2}$, and zero perpendicular to the plane with $\theta = 0$. We assume (if not stated otherwise) all nodes are in the same plane, and we do not have to take polarization into account.

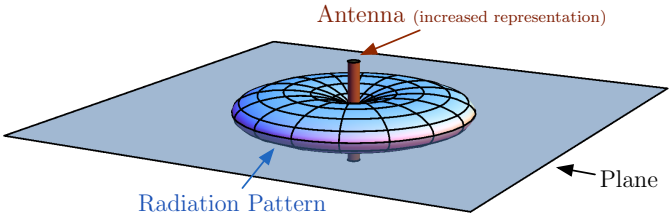

Figure 2.4: Radiation pattern of a dipole antenna (brown) with vertical polarization, where the blue-red colored surface shows all points with same radiation power.

The wavelength λ of carrier frequency f and speed of light c is

$$\lambda = \frac{c}{f} \ .$$

The wavelength for the 2.4 GHz band, which is used WLAN and bluetooth, is about 0.125 m. The length of a half-wave dipole antenna is $l = \frac{\lambda}{2}$.

Electric Fields We briefly summarize essentials for radio communication based on Maxwell's equations. You can find the following observations in much greater detail in Physics textbooks. Here, we now present a compilation of "The Feynman Lectures on Physics" Vol. I. [FLS06], chapter 28 and 29. An electric field $\mathbf{E}$ is a vector at each point describing the force on a charged particle. It is described for a single particle with charge q as

$$\mathbf{E} = \frac{-q}{4\pi\varepsilon_0}\left(\frac{e_{r'}}{r'^2} + \frac{r'}{c}\frac{d}{dt}\left(\frac{\mathbf{e}_{\mathbf{r}'}}{r'^2}\right) + \frac{1}{c^2}\frac{d^2}{dt^2}\mathbf{e}_{\mathbf{r}'}\right) \tag{2.1}$$

where $c \approx 3 \times 10^8$ m/s is the speed of light, and $\varepsilon_0 \approx 8.854 \times 10^{-12}$ F/m is the electric constant, r' is the distances to the particle where it has been considering the speed of light and the distance. $\mathbf{e}_{\mathbf{r}'}$ denotes the unit factor in the direction.

Note that this equation already combines the electric and magnetic field which is described by (the Maxwell-Faraday equation)

$$\mathbf{B} = -\mathbf{e}_{\mathbf{r}'} \times \mathbf{E}/c \ .$$

In the far-field for large distances r the last component in Equation 2.1 prevails, rendering the equation to

$$\mathbf{E} = \frac{-q}{4\pi\varepsilon_0 \cdot c^2} \cdot \frac{d^2}{dt^2}\mathbf{e}_{\mathbf{r}'} \ . \tag{2.2}$$

If a particle moves vertically along a line according, where charged particles are moved with acceleration function $a\,(t)$, the electric field has an approximated magnitude of

$$E\,(t) = \frac{-q}{4\pi\varepsilon_0 \cdot c^2 r} \cdot \sin\theta \cdot a\,(t - r/c)$$

and the orientation of the vector is as been shown in Figure 2.5.

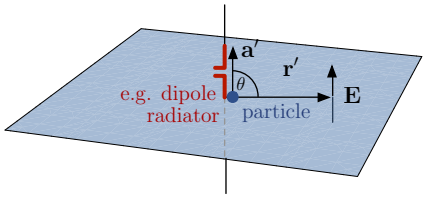

Figure 2.5: Electric field $\mathbf{E}$ in distance $\mathbf{r}'$ of a dipole radiator in the plane with a charge q accelerated with $\mathbf{a}$.

Electric fields have the superposition property. For two electric fields $\mathbf{E_1}$ and $\mathbf{E_2}$ the resulting electric field is

$$\mathbf{E} = \mathbf{E_1} + \mathbf{E_2} \ . \tag{2.3}$$

This of course applies for single charges in antennas as well as the different currents of multiple antennas.

Radio signals are modulated as sine curves with $x_0 \cos \omega t$, which leads to an acceleration of

$$a(t) = -\omega^2 x_0 \cos \omega t = a_0 \cos \omega t$$

where the angular speed $\omega = 2\pi f$ with frequency f, x_0 is the amplitude of the charged particle, and $a_0 = -\omega^2 x_0$. This results in the well-known Hertz dipole equation

$$E(t) = \frac{-q}{4\pi\varepsilon_0 \cdot c^2 r} \cdot \sin\theta \cdot a_0 \cos\omega\,(t - r/c) \ . \tag{2.4}$$

Of course the orientation of the antennas plays a major role. However, if we restrict ourselves to a two-dimensional plane with perpendicular antennas, all electric fields are oriented perpendicular to the plane. This allows us to simplify the dynamic electric field to a scalar field. The far-field approximation of Equation 2.2 holds for a distance r of a few wavelengths $\lambda = c/f$.

Transmit Power The power or energy per second of an electric wave through a unit area is

$$S \ = \ \varepsilon_0 c \cdot E^2$$

with the impedance of free space $1/(\varepsilon_0 c) \approx 376.7\,\Omega$. Thus, the power increases inversely to the square of the distance with

$$S \ = \ \frac{q^2 \cdot a(t)^2 \cdot \sin^2\theta}{16\pi^2\varepsilon_0 \cdot r^2 \cdot c^3} \ .$$

Therefore the power through the enveloping surface of radius r produced of a charge q oscillating with ω is

$$P \ = \ \frac{q^2\omega^4 x_0^2}{12\pi\varepsilon_0 c^3} \ .$$

The length of the antenna is described by x_0 which is proportional to $c/f = 2\pi c/\omega$.

At a receiver antenna parallel to the movement of the particle this causes a voltage proportional in E. Also the current is proportional according to Ohm's law, however the inductances plays a major role. Summarizing we observe that the received power P at the antenna is

$$P = kE^2 \tag{2.5}$$

where k is a suitable constant for a fixed frequency. This also holds for the combination of antennas, since the electric fields increase each voltage and each current.

This leads to two interesting observations, which has been proved useful in antenna design for a long time.

1. Two antennas in sync produce an electric field twice the size. So, four times the power arrives at the receiver antenna.

2. Two receivers can reproduce four times the power of a sender antenna if the induced current is time shifted accordingly.

This observation is only possible if one carefully considers the interplay of the locations of the antennas and the time shift to achieve the constructive interference. For this we introduce the following notations. Let $\mathbf{s_1}, \ldots, \mathbf{s_n}$ denote the locations of sender antennas in two dimensional space, likewise $\mathbf{r_1}, \ldots, \mathbf{r_n}$ denote the receiver antennas.

Power Dissipation Electric power transmission from a sender to a receiver with an electromagnetic wave causes power dissipation. On the one hand, we have a path loss from sender to receiver, on the other hand, there is a power loss at the devices in the form of heat. The overall power loss can be characterized by the damping factor a between the sender's and the receiver's amplitude, i.e.

$$V_r = \frac{a}{d} \cdot V_s$$

for the receiver's amplitude V_r, the sender's amplitude V_s, and path-loss $1/d$ for distance d between sender and receiver.

We will show the power dissipation for an example communication system (Figure 2.6) with one sender and one receiver with distance d and both are equipped with a half-wave dipole antenna. The sender produces a sinusoidal signal of the carrier with

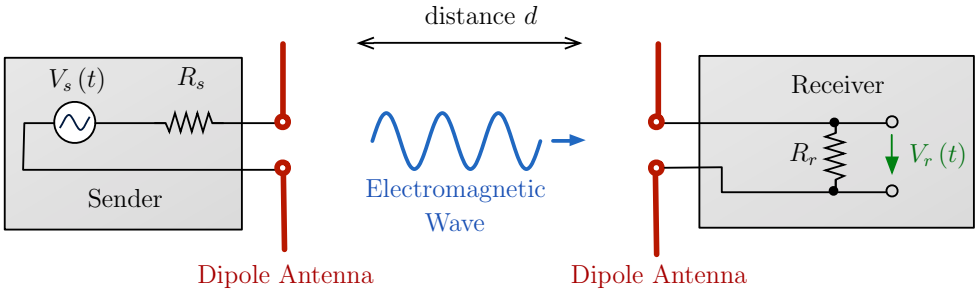

Figure 2.6: Illustration of radio transmission between sender and receiver with distance d, both equipped with a half-wave dipole antenna, internal resistances R_s, R_r, and signal voltages V_s, V_t at time t.

voltage amplitude V_s. This voltage source is in the example model in series with two impedances: the internal impedance R_s of the sender, where a part of the power is dissipated in heat, and the load of the dipole antenna, where the remainder of the power is radiated into space. The radiation resistance of a half-wave dipole antenna (see [FTU10]) is

$$R_{\text{rad}} \approx 75\,\Omega\,. \tag{2.6}$$

Let us assume a matched transmission with resistance $R_s = 75\,\Omega$ that the internal resistance is purely real. The amplitude of the current in the sender antenna is then

$$I_s = \frac{V_s}{R_{\text{rad}} + R_s} = \frac{V_s}{2 \cdot R_{\text{rad}}} \,. \qquad \text{[unit: ampere (A)]}$$

Corresponding the (RMS) power at the sender is

$$P_s = \frac{I_s \cdot V_s}{2} = I_s^2 \cdot R_{\text{rad}} = \frac{V_s^2}{4 \cdot R_{\text{rad}}} \qquad \text{[unit: watt (W)]}$$

and the radiated (RMS) power is half of it with match impedances.

$$P_{\text{rad}} = \frac{I_s \cdot V_{\text{rad}}}{2} = \frac{V_s}{R_s + R_{\text{rad}}} \cdot \frac{V_s \cdot R_{\text{rad}}}{R_{\text{rad}} + R_s} = \frac{V_s^2}{8 \cdot R_{\text{rad}}} \qquad \text{[unit: W]}$$

The power density of the wave at the receiver in distance d is

$$S = \frac{15 \cdot I_s^2}{\pi \cdot d^2} = \frac{15}{\pi \cdot R_{\text{rad}}} \cdot \frac{P_s}{d^2} \,. \qquad \left[\text{unit: } \tfrac{\text{W}}{\text{m}^2}\right]$$

The effective area broadside to a half-wave dipole antenna is (see [Pha99])

$$A = \frac{1.64\lambda^2}{4\pi}$$

which results in a power intercepted by the receiver antenna of

$$P_r = S \cdot A = \frac{15}{\pi \cdot R_{\text{r}}} \cdot \frac{P_s}{d^2} \cdot \frac{1.64\lambda^2}{4\pi} = \frac{6.15 \cdot \lambda^2}{\pi^2 \cdot R_{\text{rad}}} \cdot \frac{P_s}{d^2} \qquad \text{[unit: W]}$$

and corresponding voltage amplitude

$$V_r = \sqrt{2P_r \cdot R_r} = \frac{1.75 \cdot \lambda}{\pi \cdot \sqrt{2R_{\text{rad}}}} \cdot \frac{V_s}{d} \,. \qquad \text{[unit: volt (V)]}$$

For example, for a carrier frequency of 2.4 GHz and resulting wavelength 0.125 m this is $V_r = 0.008 \cdot \frac{V_s}{d}$. Please note, that the dependency of wavelength and the attenuation of the power during transmission results from setting the length of the antenna relatively to the wavelength, i.e. half-wave dipole antenna. In the algorithms, which we will present in the next chapters, we assume that we can reach the nearest neighbors in the network from each node[3] and thus the power to reach the nearest neighbors will increase with $\mathcal{O}(\lambda^2)$.

[3] An alternative model would be to keep the antenna length constant (or some multiple of the wavelength around a constant length) with an effective constant area of the antenna. But then, the far-field barrier also depends on the antenna length and not only on the wavelength with $d \geq 2\lambda$.

2.3 Wireless Data Transmission

To this point, we have only described the transmission of a carrier wave emitted by the antenna of the sender device and received by the antenna of the receiver device. An unchanging sinusoidal carrier wave does not contain any information and we summarize in the following how to modulate data on the carrier and what is the dependency of transmission power and the data rate.

Modulation We assume a modulation with amplitude/phase shift keying, e.g. QAM. The data is modulated on a carrier signal oscillating with frequency f over time t, i.e. the input signal of a pure carrier without any modulated data is

$$x_c(t) = \cos(2\pi f \cdot t) \ ,$$

which can be rewritten to complex numbers with

$$x_c(t) = \Re\left(\mathrm{e}^{j2\pi ft}\right) \ .$$

For amplitude modulation, we change the amplitude of the carrier signal $s_c(t)$ over time t with time-dependent amplitude $a_{\mathrm{am}}(t)$. And for phase shift keying, we change the phase of the carrier over time with phase angle $a_{\mathrm{pm}}(t)$. For simplicity we use the complex number

$$\varphi(t) = \varphi_{\mathrm{am}}(t) \cdot e^{j\varphi_{\mathrm{pm}}(t)} \ . \tag{2.7}$$

The input signal is then

$$x(t) = \Re\left(\varphi_{\mathrm{am}}(t) \cdot \mathrm{e}^{j(2\pi ft + \varphi_{\mathrm{pm}}(t))}\right) = \Re\left(\varphi(t) \cdot \mathrm{e}^{j2\pi ft}\right) \ .$$

We can only send a real-valued signal and thus taking the real part gives

$$x'(t) = \phi_{\mathrm{am}}(t) \cdot \cos(2\pi ft + \phi_{\mathrm{pm}}(t)) \ .$$

When sending this signal, we can measure the following field strength at a receiver point at distance r (see Equation 2.4)

$$\begin{aligned} E &= k_{\mathrm{phy}} \cdot \frac{\Re\left(\varphi(t) \cdot \mathrm{e}^{j2\pi f(t-r/c)}\right)}{r} + \sqrt{N_0} \\ &= k_{\mathrm{phy}} \cdot \frac{\varphi_{\mathrm{am}}(t)}{r} \cdot (\cos 2\pi f(t - r/c) + \varphi_{\mathrm{pm}}(t)) + \sqrt{N_0} \end{aligned} \tag{2.8}$$

where we combine all physical constants and basis amplification of the signal in the sender circuit to one constant

$$k_{\mathrm{phy}} = \frac{-q}{4\pi\varepsilon_0 \cdot c^2} \cdot a_0 \ .$$

The effect of polarization with factor $\sin\theta$ and elevation angle θ might be added when appropriate. Equation (2.8) also includes additive white Gaussian Noise (AWGN) with power N_0, which models environmental noise and is Gaussian distributed $N_0 \sim \mathcal{N}(0, \sigma^2)$ with variance σ^2.

The electromagnetic field induces a current in a receiving antenna that in turn can be measured as voltage signal. The magnitude of the field strength and voltage signal of a receiving antenna are proportional. Thus, we can instead analyze then input (producing an electromagnetic field at a sender) and output (which is detected at the receiver) instead, which includes no physical constants or units.

When using amplitude and phase modulation, we might first apply a frequency filter with a bandpass with the carrier frequency f as center frequency. This means for the noise with power N_0 that all noise except in the frequency band of the carrier is filtered as well. We denote the remaining noise in the frequency band of the carrier w in the following to show the difference. Both the input x and the noise w oscillate with $\mathrm{e}^{j2\pi ft}$. Besides environmental noise, noise w additionally contains noise of the receiver circuit.

The (single) input (single) output model (SISO) is the following.

Definition 1 *When a sender transmits the input signal $x = \varphi(t) \cdot \mathrm{e}^{j2\pi ft}$ with amplitude/phase modulated data $\varphi(t) = \varphi_{am}(t) \cdot e^{j\varphi_{pm}(t)}$, a receiver at distance r receives the output signal y with*

$$Y = X \cdot h + w$$

where the transfer function h models the delay an attenuation of a free-space channel with

$$h = \frac{\mathrm{e}^{-j2\pi f \cdot r/c}}{r} \ .$$

The corresponding electric field at the receiver is $E = k_{phy} \cdot \Re(X \cdot h) + \sqrt{N_0}$. While $|h|$ reflects the attenuation from the input to the output amplitude, $|h|^2$ describes the attenuation of the power, since the power of the electric field is proportional to E^2. For unit input power $|X| = 1$, we define the power equivalent of the output power as

$$P := |h|^2 \tag{2.9}$$

We assume here an appropriate pre-amplification at sender and receiver that input X and Y have the same magnitude $|X| = |Y|$ if $|h| = 1$. We will have unsynchronized clocks at sender and receiver such that the overall phase shift will be rather $\arg\left(h \cdot \mathrm{e}^{j\phi_{\mathrm{rand}}}\right)$ where we assume that unsynchronized clocks have a random phase shift ϕ_{rand}. However, the sender will start the transmission with a synchronization signal and the receiver will synchronize to that initial signal and thus compensate the delay offset that the synchronized output will be $y = x/r + w$ if we neglect synchronization errors caused by noise w.

Signal to Interference plus Noise Ratio (SINR) If a node v can receive the information of function $a(t)$ from a sender u_i, depends strongly on the the magnitude of the additionally received noise. The standard measure in literature is the Signal-to-Noise Ratio (SNR) or Signal-to-Interference+Noise Ratio (SINR). The second measure SINR (see [GK00]) also includes – besides environmental noise and noise in the receiver (e.g. amplifier stage) w – the noise produced by interfering senders u_k involved in parallel transmissions

$$\mathrm{SINR}(r) = \frac{\frac{P(u_i)}{|\mathbf{u_i}-\mathbf{v}|^\alpha}}{w + \sum_{k\neq i} \frac{P(u_k)}{|\mathbf{u_k}-\mathbf{v}|^\alpha}} . \tag{2.10}$$

The path-loss exponent α is for free space $\alpha = 2$ and a value $\alpha > 2$ typically represents scenarios with shadowing and reflection effects where obstacles absorb the energy of the signal and lead to faster attenuation. The transmission power P in Equation (2.10) does not include the path loss. Respectively, the signal power is P/d^α at distance d to the sender. Please note that we sum up the signal powers of interferences u_k and not the signal amplitude. We analyze this in Lemma 1 in the next Chapter.

The signal-to-noise ratio is independent from the absolute scale of the network, i.e. only depends on the relative distances of nodes (see Appendix A).

Data Rate in Presence of Noise The maximum possible data rate in a channel with white noise was derived by Shannon in 1949 [Sha49]. In the presence of noise with power w, each modulation scheme with power P uses a limited number of distinguishable signals. The maximum power of the received signal is then $(P + w)$. Since each transmitted signal can be perturbed by noise power w there are $K \cdot \frac{P+w}{w} = K \cdot \left(1 + \frac{P}{w}\right)$ distinguishable signals for some constant K near unity. Given a data rate R (with unit

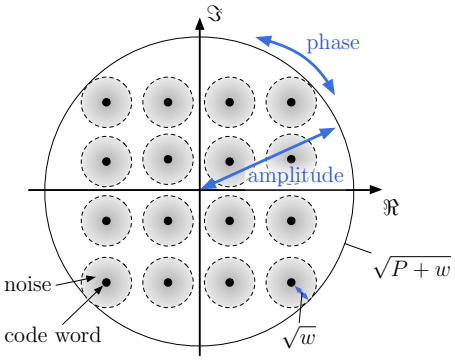

Figure 2.7: Illustration of noise 16 symbols (black dots) in 16-QAM. Disks around symbols show the error range with area w.

s^{-1}), we can transmit in a time unit up to $\left(K\left(1 + \frac{P}{w}\right)\right)^R$ distinct signals. Since we

can decode in m possible states $\log_2 m$ binary digits, this gives a maximum capacity in bits per second of the well-known Shannon-Hartley theorem

$$C = R \cdot \log_2 \left(1 + \frac{P}{w}\right) = R \cdot \log_2 (1 + \text{SINR}) \ . \tag{2.11}$$

For a low SINR ≈ 0 we can approximate

$$C \approx R \cdot \text{SINR} \cdot \log_2 (\text{e}) \ . \tag{2.12}$$

For the data rate, we follow Shannon's theorem. We also assume that a minimum SINR is necessary to establish communication.

Definition 2 *If the SINR is above a certain threshold, then communication can be established. For higher SINR values the data rate of the transmission is modeled by* $\Theta\left(f \cdot \log(1 + SINR)\right)$ *where* f *is the carrier frequency.*

The *threshold effect* [Sha49] causes the error rate to increase drastically when the noise is over a certain threshold of the system design.

There is a third source of error besides uncorrelated noise (AWGN) and interferences of parallel transmissions. When inter-symbol interference (ISI) occurs, subsequent symbols of the same transmission overlap in time. This happens in a multipath channel, where the signal is transmitted from sender to receiver over multiple paths with different delays. Of course, since we only consider the line-of-sight path, we can exclude additional paths of reflections (e.g. echoes). When we use beamforming and several antennas send simultaneously the same data signal, the signals of the antennas can be time displaced at a receive point that subsequent symbols overlap.

To prevent inter symbol interference, a guard interval [EJRS14a] can be inserted between subsequent symbols in a data transmission. In the guard interval, signal paths with longer delay fade away before the signal of the next symbol starts. This will drop the data rate depending on the factor of symbol transfer time and guard interval. The algorithms presented in Chapter 4 use send beamforming and we restrict possible time shifts of multiple super-posed data signals in a reception zone to a small constant, i.e. less than a period $1/f$ for carrier frequency f. Therefore, a small constant guard interval between symbols is sufficient to prevent ISI which decreases the data rate by a small constant factor.

Transmission Power If not stated otherwise, we assume in this work that each device has a maximum transmission power $P_{\max}$, i.e. the power is $\mathcal{O}(1)$ in the number of nodes n. This describes the use-case of a battery-driven device with guaranteed minimum lifetime. It is possible that transmitters can increase transmission power for a short period of time. E.g. step up converters can increase the supply voltage for a short period and increase output power. If a TDMA protocol with k time slots is used, each sender can send with power $k \cdot P_{\max}$ and still comply with the maximum

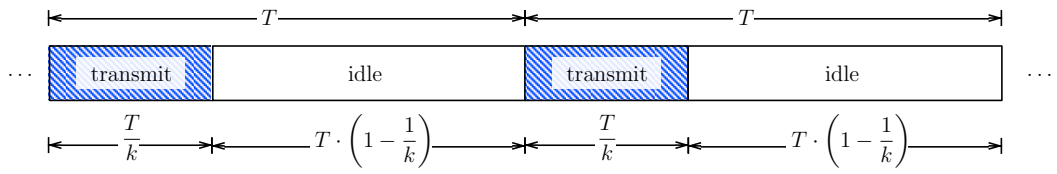

Figure 2.8: Short sending bursts in interval T and duration $\frac{T}{k}$ with power amplification $k \geq 1$

power consumption. An increased power is available during a shorter time period $\frac{1}{k}$ and increases either the reception range by factor $\sqrt{k}$ in the line-of-sight model or the data rate with a better SNR. From the Shanning-Hartley theorem we know that the information rate R is

$$R = B \cdot \frac{\log\left(1 + k \cdot \mathrm{SNR}\right)}{k} \ .$$

The signal-to-noise ratio SNR denotes here the level at the receiver when the sender transmits continuously and the improved ratio $k \cdot \mathrm{SNR}$ with $k \geq 1$ is the boosted ratio of such a short burst. Since the sender will only send $\frac{1}{k}$-th of the time, the data rate is reduced by this factor.

In the low SNR-regime for $0 \leq k \cdot \mathrm{SNR} \ll 1$, we can use the linear approximation $\log\left(1 + k \cdot \mathrm{SNR}\right) \leq k \cdot \mathrm{SNR}$ such that

$$R_{\text{low-SNR}} \quad \leq \quad B \cdot \mathrm{SNR}$$

We see that the data rate is invariant to the choice of k as long as the approximation of $\log\left(1 + x\right) \leq x$ holds for $x = k \cdot \mathrm{SNR}$. So short bursts can enable reception in the low-SNR regime without an intense reduction of the data rate. The ratio SNR includes the path loss of the signal which is in the SINR model $\frac{1}{d^\alpha}$ for transmission distance d and path loss exponent α ($\alpha = 2$ is the line-of-sight case). So the data rate will drop with $\frac{1}{d^\alpha}$ as well, which is not suitable for long distances d.

In the high SNR-regime for $k \cdot \mathrm{SNR} \gg 1$ the data rate decreases when increasing k as the following approximation shows.

$$\frac{B}{k \cdot \mathrm{SNR}} \leq R_{\text{high-SNR}} \leq \frac{B}{\sqrt{k \cdot \mathrm{SNR}}}$$

This is a reduction of data rate when only considering a single transmission. However, when using a TDMA method anyway with a schedule of k timeframes, devices are able to increase the data rate in the time frames with short bursts by factor $\Theta\left(\log k\right)$.

Assume we have a fixed modulation and adjust k according to reach a needed SNR of $\beta = k \cdot \mathrm{SNR}_0$ with $\mathrm{SNR} \geq \beta$. The data rate is then

$$R_{\beta \text{ fixed}} = B \cdot \frac{\log\left(1 + k \cdot \mathrm{SNR}_0\right)}{k} = B \cdot \frac{\log\left(1 + \beta\right)}{\beta} \cdot \mathrm{SNR}_0$$

and depends linearly to the SNR without power boost of the short bursts.

The maximum boosted supply voltage relies on physical barriers of the electronic components and is assumed to be constant. Thus, we are not able to transmit over arbitrary long distances. The duration $\frac{T}{k}$ of short bursts might be limited as well. When the necessary transmission power exceeds the maximum power output of the power supply, the energy for the short bursts has to be buffered temporarily e.g. in a capacitor (similar to a photoflash). The capacitance of the capacitor limits then the duration $\frac{T}{k}$. In return, factor k is limited as well when we assume that we need a minimum packet length to transmit, which is at least one bit.

We do not explicitly point out to use the technique of increasing the transmission power during short bursts. But we assume throughout this work that the transmission power is adjusted for the low-SNR regime and a node can reach its nearest neighbors. This technique then can be an option to establish the connection to nearest neighbors. Since the data rate is independent of k, applying this technique does not tackle the asymptotic behavior of our results.

2.4 Beamforming with Multiple Antennas

Beamforming denotes a technique for spatial filtering in wireless communications using multiple antennas. This means we can send a signal to a specific direction while attenuating the signal in other directions, or as receiver, we can receive a signal from a specific direction and filter interferences of other directions. This is similar to a directed antenna with the advantage that we can adjust the direction electronically while a directed antenna has to be rotated to change the direction.

Literature often distinguishes between three cases of single and multiple antennas at sender and receiver:

MISO (Multiple Input Single Output) a signal is emitted by multiple sender antennas and received at a single output antenna

SIMO (Single Input Multiple Output) a signal is emitted by a single sender antenna and received by multiple receiver antennas

MIMO (Multiple Input Multiple Output) multiple sender antennas emit a signal and multiple receive antennas receive the superposed signals

To apply beamforming at a sender device with multiple antennas attached to it, the device sends the same signal from all antennas at the same time. The signal contains essentially a bit string of a message which is modulated on a carrier with frequency f. The sending direction can be adjusted by delaying the signals at the individual antennas according to the direction (see Figure 2.9(a)). Vice versa, a receiver device receives a signal at multiple antennas, the signals of the individual antennas is delayed to adjust the spatial filter and finally the signals of all antennas are added to apply the spatial filter (see Figure 2.9(b)). We can determine the signal delays at the antennas to adjust beamforming by the positions of all sender and receiver antennas

in a transmission.

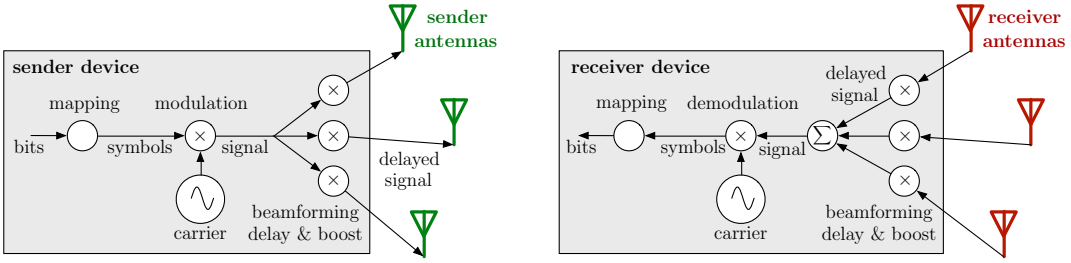

(a) sender beamforming

(b) receiver beamforming

Figure 2.9: Illustration for applying beamforming on wireless devices with multiple antennas

It is also possible to perform sender respectively receiver beamforming distributed which is called *collaborative beamforming*. Here, a set of nodes coordinates their antennas to perform collaborative beamforming. Coordination for sending includes distributing a message among all senders and synchronize all senders, that the signal delays can be adjusted as accurate as on a single device (compare Fig. 2.9(a)). For collaborative receiver beamforming, the receiver nodes also have to be synchronized and they have to exchange the received signals. Once the signals of all nodes are at one device, the device is able to add the signals (Σ-operation in Fig. 2.9(b)) and afterwards to demodulate the data. We only allow digital communication here, such that a received analog signal has to be sampled before it can be exchanged with other receivers. The sampled signal is a constant factor larger than the corresponding demodulated data, which causes an increased message size[4].

This leads to the following definition for multi-antenna beamforming, which holds for beamforming of one device with multiple antennas as well as for collaborative beamforming of multiple devices with single/multiple antenna(s).

Definition 3 *A set of sending antennas is coordinated if their locations are known at their radio stations, the carrier waves and signal encoding are synchronized and they perform the same task, e.g. send the same message. Receiving antennas are coordinated if they share these properties and the signal can be decoded without further wireless transmission. Radio stations with coordinated antennas perform collaborative beamforming.*

We assume that uncoordinated radio stations use unsynchronized clocks, which can be modeled by independently identically distributed random variables describing the relative phase shift of the carrier waves.

[4] In the seminal work of [ÖLT07] and subsequent article [ÖJTL10] this factor is expressed by a so called *observation* of a message. The increase of the message size limits multi-hop routing with uncoordinated MIMO communication because the message size grows exponentially with each hop when observations are forwarded instead of decoding them right away.

Superposition The key of understanding how beamforming enables spatial filtering is analyzing the superposition of signals of multiple antennas. On the one hand, this is the superposition of electromagnetic fields produced by multiple sender antennas in the medium, which is free space (see Equation 2.3). We assume a line-of-sight communication model without obstacles and neglect the influence of the nodes to the radio communication. On the other hand, we can add the signals of multiple receiver antennas in a receiver circuit (see Figure 2.10). The following observations likewise hold

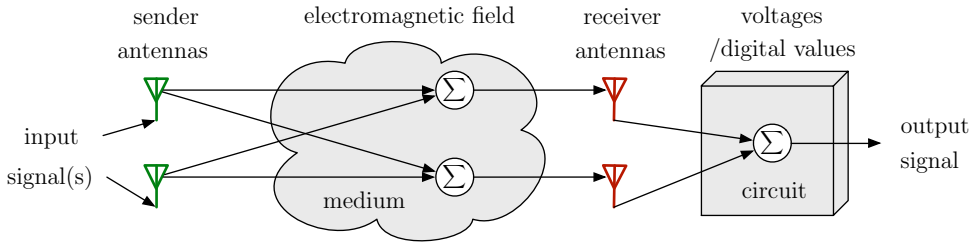

Figure 2.10: Superposition (symbol Σ) of sent electromagnetic waves in medium and signal voltages (or sampled digital values) at the receiver circuit

for planned superposition of signals of multiple sender antennas in one communication as well as for unintended superposition of signals of parallel communications, which is then called interference.

We can describe an input signal for sending at antenna u_i with

$$X_i(t) = \mathrm{e}^{j2\pi ft}$$

which oscillates with carrier frequency f over time t. This only describes the input signal of a pure carrier signal and we have to multiply it with $\varphi(t)$ (see Equation 2.7) for modulation. However, we will only consider in the following the signal of one symbol where $\varphi(t)$ is constant and we can neglect this factor. The corresponding electrical field at receiver point v for input signal $X_i(t)$ is

$$E_v = k_{\text{phy}} \cdot \Re(h_i \cdot X_i) + \sqrt{N_0}$$

where the transmission channel causes a delay and attenuation $h_i \in \mathbb{C}$ on input signal X_i and there is AWGN with power N_0. We model the channel with

$$h_i = s_i \cdot \frac{\mathrm{e}^{-j2\pi f|u_i - v|/c}}{|u_i - v|} \ .$$

The channel causes an attenuation $|u_i - v|^{-1}$ and transmission delay $|u_i - v|/c$. We add an additional artificial delay/attenuation s_i which the transmitter device adjusts[5].

$$s_i = |s_i| \cdot \mathrm{e}^{j \arg s_i}$$

[5] In this model, the RF front end gets as input the input signal X_i (containing the data) plus additional phase and amplitude values s_i to adjust phase shifts in the radio frequency signal (for beamforming), e.g. vector modulator (see Section 1.4)

This includes an attenuation of the amplitude $|s_i| \in \mathbb{R}$ and a phase shift by angle $(\arg s_i) \in [0, 2\pi)$. We will later on use s_i to adjust a beam-forming. Inserting gives

$$E_v = \frac{k_{\text{phy}} \cdot |s_i|}{|u_i - v|} \cdot \cos\left(2\pi f \left(t - |u_i - v| / c\right) + \arg s_i\right) + \sqrt{N_0} \ .$$

If multiple senders $u_1, \ldots, u_n$ emit the signals $X_1(t), \ldots, X_n(t)$, the superposition principle of Equation (2.3) holds and electric field strength at receiver v is

$$E_v = \sum_{i=1}^{n} E_{u_i} = \rho \cdot \Re\left(\sum_{i=1}^{n} h_i \cdot X_i\right) + \sqrt{N_0} \ .$$

This describes the MISO case (multiple input/single output) illustrated in Figure 2.11.

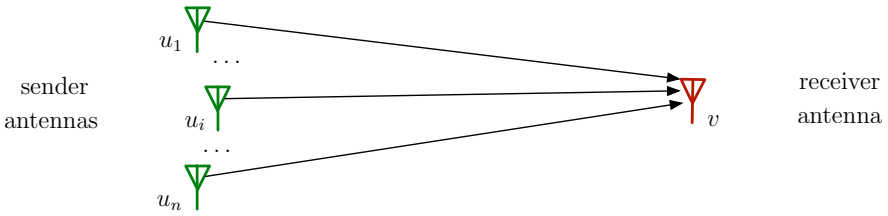

Figure 2.11: Superposition of n sender signals $u_1, \ldots, u_n$ at receiver v_k

We can derive the input-output model from that.

Definition 4 *If n multiple senders u_i with $i = 1 \ldots n$ send a signal $X_i = \mathrm{e}^{j2\pi ft}$, a receiver v will receive the output y with*

$$Y = \left(\sum_{i=1}^{n} h_i \cdot X_i\right) + w_v \tag{2.13}$$

where w_v models additive white Gaussian noise (AWGN) at receiver v. If the input signal of all senders is identical with $X = X_i$, we get

$$Y = X \cdot h + w_v \ . \tag{2.14}$$

The channel for all senders u_i to receiver point v effects $h \in \mathbb{C}$ with

$$h = \left(\sum_{i=1}^{n} h_i\right) = \left(\sum_{i=1}^{n} s_i \cdot \frac{\mathrm{e}^{-j2\pi f|u_i - v|/c}}{|u_i - v|}\right)$$

with attenuation $|u_i - v|^{-1}$ due to path loss (in the free-space model), phase shift $\mathrm{e}^{-j2\pi f|u_i - v|/c}$ due to the transmission delay, and additional sender adjusted phase shift/attenuation $s_i = |s_i| \, \mathrm{e}^{j \arg s_i}$.

We can see that the resulting output Y again oscillates with carrier frequency f over time t. The strength of Y depends on the attenuation due path loss, the amplitudes of the send signals $|s_i|$ and the phasing of the super-posed signals with transmission delays $|u_i - v|$ and chosen phases at the senders ($\arg s_i$).

For true MIMO, i.e. beamforming with multiple sending and receiving antennas, the signals of multiple antennas of a receiver are combined as well. This could be a simple addition of signals of the receiver's antennas $v_1, \ldots, v_m$ (compare Figure 2.10). However, more likely is that a phase shift ($\arg g_k$) and a dampening $|g_k| \leq 1$ is applied to the k-th signal received by the multiple antennas. These terms can be adjusted to increase the sensitivity and we combine these terms to $g_k = |g_k| \cdot e^{j \arg g_k}$. One technique to increase sensitivity is beamforming, which we consider in the next paragraph. Please note that the amplification also changes the received noise and possibly interfering messages by a factor of $|g_k|$.

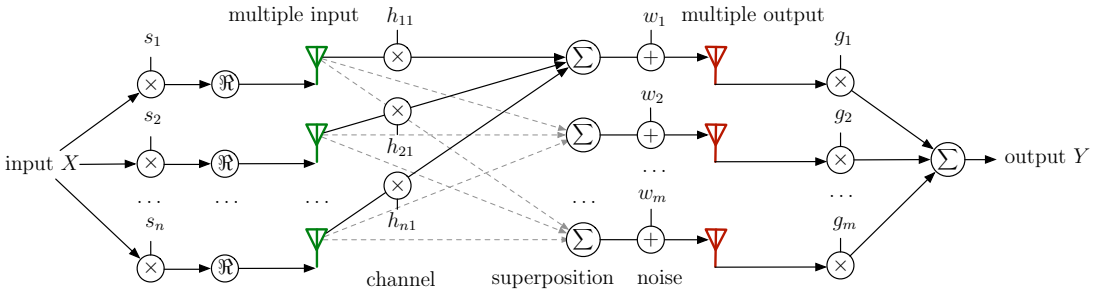

Figure 2.12: Block diagram of a signal transmission with multiple input and multiple output

Definition 5 *For (coordinated or uncoordinated) senders $u_1, \ldots, u_n$, the linear combination of output signals $Y_1, \ldots, Y_m$ received by the receiver antennas $v_1, \ldots, v_m$ is*

$$Y = \sum_{k=1}^{m} g_k \cdot Y_k = \left(\sum_{k=1}^{m} \sum_{i=1}^{n} X_i \cdot h_{ik} + g_k \cdot w_k \right)$$

where a receiver can phase-shift/attenuate each output Y_k by factor g_k. If all senders transmit the identical signal $X = X_i$, the output together with additive noise $w = \sum_{i=1}^{k} g_k \cdot w_k$ is

$$Y = X \cdot h + w \ .$$

The factor h describes the channel transfer function with

$$h = \left(\sum_{k=1}^{m} \sum_{i=1}^{n} h_{ik} \right) = \left(\sum_{k=1}^{m} \sum_{i=1}^{n} s_i \cdot \frac{\mathrm{e}^{-j2\pi f |u_i - v_k|/c}}{|u_i - v_k|} \cdot g_k \right) \tag{2.15}$$

where $s_i \in \mathbb{C}$ is chosen for each sender respectively $g_k \in \mathbb{C}$ for each receiver antenna which consists of a phase shift and an amplification. The line-of-sight path from sender u_i to receiver v_k causes an attenuation $|u_i - v_k|^{-1}$ and phase shift with $\mathrm{e}^{-j2\pi f |u_i - v_k|/c}$.

The resulting matrix $H = (h_{ik})_{i,k}$ is called the channel matrix. Figure 2.12 illustrates a multiple-input multiple output transmission with m sender and n receiver antennas.

Directional radiation pattern Besides dipole antennas with an omnidirectional radiation pattern, there also exist antennas with a directed radiation pattern, i.e. the antenna amplifies the signal of a certain direction and filters the remaining angle range. We can see in Figure 2.13 two antenna radiation patterns, where the blue line shows in

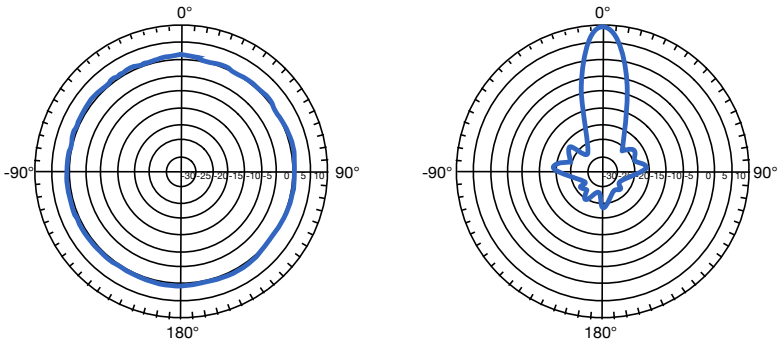

(a) omnidirectional (b) directional

Figure 2.13: Example for radiation pattern patterns

polar coordinates the radiation power (in dB) for a radiation angle in a degree range from 0° to 360°. An example are Yagi-Uda antennas [Kar10] which are also called beam antennas. Besides a (driven) dipole antenna being connected to the device, they

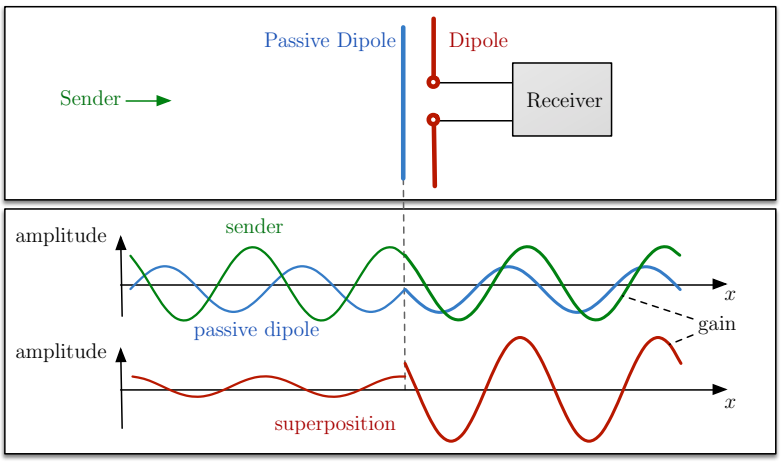

Figure 2.14: Reception with Yagi-Uda antenna with one passive dipole. The lower charts show the sender's signal, the passive dipole's signal, and the superposition of both signals

have extra passive dipoles (not connected to the device) which receive and reradiate an electromagnetic wave. If the device is in reception mode, the dipole antenna receives the super-posed field of the sender's antenna and the passive dipoles. If the sender is "in direction" of the directed antenna, the super-posed signals have approximately no phase shift at the receiving dipole, which leads to a signal gain. For other directions, there is a phase shift and the signal is attenuated. The drawback of directed antennas is that the direction can only adjusted by a mechanical rotation.

Beamforming An alternative to create a directed radiation pattern is the signal-processing technique *beamforming* that uses multiple antennas (we assume dipole antennas). Here a sender can emit the signal at multiple antennas where the signal power and a delay can be set individually at each antenna. In the opposite way, a receiver can mix the signals received at multiple antennas with individual delays and amplification. The advantage of beamforming is that the directivity can be changed with signal processing in no time and without mechanically moving the antennas.

First, we consider the case of multiple transmitting antennas and a single receiving antenna (MISO). The goal is to minimize the attenuation $|h|$ of the channel's transfer function h. We do not consider noise for the moment and all senders are coordinated and transmit $X_i = X$. From Definition 4, we get

$$\max |h| = \max \left| \sum_{i=1}^{n} h_i \right| = \max \left| \sum_{i=1}^{n} \frac{|s_i| \cdot \mathrm{e}^{j(-2\pi f |u_i - v|/c + \arg s_i)}}{|u_i - v|} \right|$$

where we already simplified $|\,\mathrm{e}^{j2\pi ft}\,| = 1$ for the signal oscillating with carrier frequency f. The sum of complex vectors is maximum if all complex values have the same argument, i.e. $\sum_i X_i \cdot \mathrm{e}^{j\phi_i} = \sum_i X_i$ if it holds $\phi_i = \phi_k$ for each i, k. If we choose[6] $(\arg s_i) := 2\pi f \,|u_i - v|\,/c$, the signals of all senders have the same phase at v.

$$\max |h| = \max \sum_{i=1}^{n} \frac{|s_i|}{|u_i - v|}$$

Here, the output only depends on the input amplitudes $|s_i|$ and the attenuation due to path loss $|u_i - v|^{-1}$. If we have a total power limit $P \leq \sum_i |s_i|^2$, we analyze in Section 3.3 how to optimally assign power $|s_i|$ to the sender antennas.

Definition 6 *Beamforming gain is the boost of a signal of multiple sending antennas $u_1, \ldots, u_n$ compared to a single antenna u with the same sending power, i.e. $|s|^2 = \sum_i |s_i|^2$.*

$$g_{beam} = \frac{(\sum_{i=1}^{n} h_i)^2}{h^2} = \frac{\left(\sum_{i=1}^{n} s_i \cdot \frac{\mathrm{e}^{-j2\pi f |u_i - v|/c}}{|u_i - v|} \right)^2}{\left(s \cdot \frac{\mathrm{e}^{-j2\pi f |u_i - v|/c}}{|u - v|} \right)^2} \tag{2.16}$$

[6] As already noted in related work (Section 1.4), there are several approaches to set up the phasing even for a complex multi-path environment, e.g. closed-loop or open-loop approach [OMPT05]. Since we assume free space in this work, we can derive the phasing from the antenna positions.

Figures 2.15-2.17 show three transmit antennas (red dots) with unit distance to each other, which perform beamforming to the location of one receiver (green dot). The contour plot with color range purple to white shows the beamforming gain in the plane. To compute the beamforming gain, we compare the the multiple antennas with a single antenna placed in the center. We do not show the beamforming gain in the near field of the sending antennas with a distance smaller than 2λ (black bordered area around senders). Figure 2.15 shows the focus of the main beam towards the receiver in

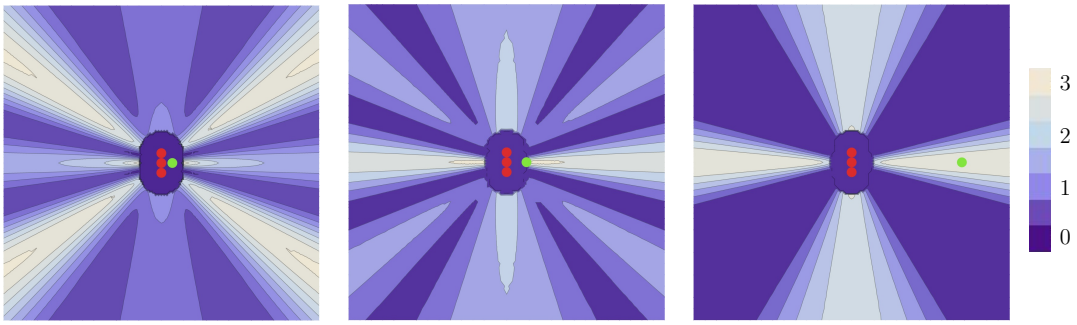

(a) $\lambda = 1$, $d = \lambda$ (b) $\lambda = 1$, $d = 1.8\lambda$ (c) $\lambda = 1$, $d = 10\lambda$

Figure 2.15: Beamforming gain of 3 senders and 1 receiver for different distances d

different distances and the length of the main beam increases with increasing receiver distance. The next graphics in Figure 2.16 show how the main beam can be rotated to

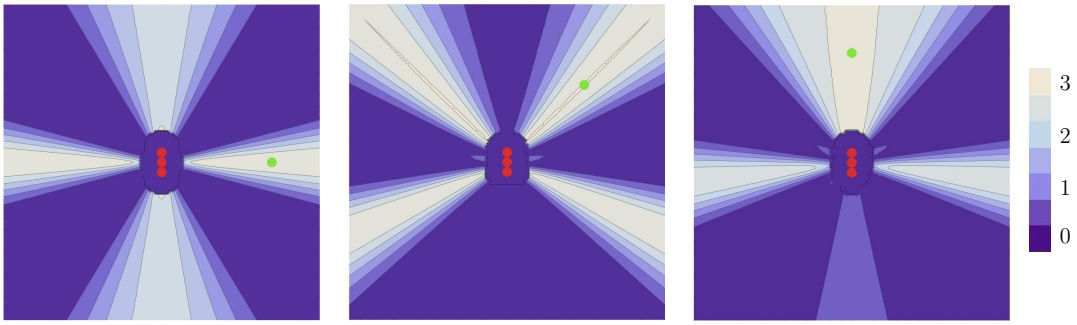

(a) $\lambda = 1$, $\alpha = 0$ (b) $\lambda = 1$, $\alpha = \pi/4$ (c) $\lambda = 1$, $\alpha = \pi/2$

Figure 2.16: Beamforming gain of 3 senders and 1 receiver for different main beam angle α

three different directions. Corresponding of the positioning of the antenna array, the main beam perpendicular to the line of sender antennas is sharper (Fig. 2.16(a)) than the beam alongside the line of senders (Figure 2.16(c)). The wavelength plays also an important role for beamforming (Figure 2.17). In scenario (a) the sending antennas are

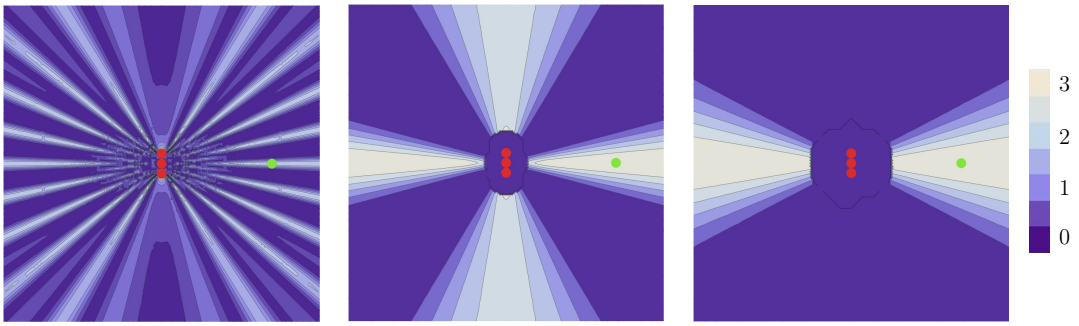

(a) $\lambda = 0.2$ (b) $\lambda = 1$ (c) $\lambda = 2$

Figure 2.17: Beamforming gain of 3 senders and 1 receiver for different wavelengths λ

approximately five wavelengths apart from each other, in (b) one wavelength, and in (c) only half a wavelength. We can see that the beams get more narrow with decreasing wavelength.

As the preceding example shows, beamforming produces more than one beam and the naming convention for the beams is as follows.

Definition 7 *A beam originates of an array of antennas and defines the space with increased beamforming gain. The boundaries of the beams are typically a* 3 *or* 6 *dB attenuation compared to the maximum beamforming gain in the center of a beam. The* ***main beam*** *specifies the beam from a sender towards an adjusted receiver point. As byproduct there are other* ***side beams*** *also called* ***side lobes*** *with a strong signal when adjusting the main beam.*

Side beams can cause strong interference or might be used for additional communication. In Figure 2.17(c) we can see the main beam white colored around the receiver (red dot) and a side beam in reverse direction.

The above definitions and analysis likewise hold for send beamforming with multiple sending antennas and a single receiver antenna (MISO) as well as for receive beamforming with a single sending antennas and multiple receiving antennas (SIMO). If we set the phase shifts of the receiving antennas $v_1, \ldots, v_m$ to $(\arg g_k) := 2\pi f \left|u - v_k\right| / c$ for a signal from sending antenna u, the channel attenuation is

$$\max |h| = \max \sum_{k=1}^{m} \frac{|g_k|}{|u - v_k|} \ .$$

However, for true MIMO beamforming with multiple sending and receiving antennas, we are not able in most cases to adjust the phasing that there is no phase shift in the super-positioned signal at all receiving antennas. Then the channel between sender

and receiver not only causes an attenuation due to path loss but also an attenuation due to phase errors of super-positioned signals.

There also exist beamforming techniques to optimize the beam-formed electromagnetic field for a receiver position and nulling other positions to filter interference. This is not considered in this work and we might refer to other work for instance [RXS11].

2.5 Summary of Communication Model

We consider an ad hoc network with n nodes that are placed stationary in the plane. The network area grows proportional to n, i.e. the mean node density is constant. The nodes communicate wirelessly without an external infrastructure (e.g. access points).

For communication, each device is equipped with a half-wave dipole antenna which is aligned perpendicular to the plane. The devices communicate solely on a single carrier frequency f with corresponding wavelength $\lambda = c/f$ for an electromagnetic wave propagating with speed of light c. The far-field radiation pattern, which holds for distance $d \geq 2\lambda$, is omnidirectional in the plane, i.e. the line-of-sight signal for distance d attenuates with amplitude d^{-1} and power d^{-2}. Dipole antennas are vertically polarized and for an elevation (angle) θ the power is additionally attenuated by factor $\sin^2 \theta$.

The nodes communicate in half-duplex mode, i.e. a node can either send or receive at the same time. Data is modulated with amplitude/phase shift keying (e.g. QAM) on the carrier. The transmission power of each node is constant $\mathcal{O}(1)$ if not stated otherwise. We assume the communication between a sender and receiver is successful if the signal-to-noise ratio SNR at the receiver is over a given threshold β. For SNR $\geq \beta$ we assume a constant data rate.

For send beamforming, we use the following input-output model with input signal X and output signal Y at receiver v with noise w_v modeled as AWGN.

$$Y = X \cdot h + w_v$$

The channel from all senders u_i to receiver point v effects $h \in \mathbb{C}$ with

$$h = \left(\sum_{i=1}^{n} h_i \right) = \left(\sum_{i=1}^{n} s_i \cdot \frac{\mathrm{e}^{-j2\pi f |u_i - v|/c}}{|u_i - v|} \right)$$

where the i-th sender can attenuate and phase shift the input signal X with value $s_i \in \mathbb{C}$.

We assume that we can phase-synchronize the nodes at least for the transmission of one message, such that we are able to perform send beamforming. For send beamforming, all nodes will emit the same signal X containing a message with a necessary delays in parameter s_i to correct the phase-synchronization for a receiver point. The superposition principle holds for the electric fields of all senders, and the overall signal power of n senders can increase by a factor of up to n^2 compared to a single sender.

3 Analysis of Beamforming with Multiple Antennas

We investigate in this chapter how to configure nodes of an ad hoc network for collaborative beamforming and what are the characteristics of wireless transmissions with beamforming. We start the analysis with extending the SINR model, which is designed for transmissions with single antennas, for multiple antennas performing beamforming[1]. Then we proceed in Section 3.3 with the analysis of an efficient distribution of transmission power among multiple antennas that perform send beamforming. We analyze in Section 3.4 the beamforming pattern of multiple antennas. We model an antenna array with uniformly at random positioned nodes in a disk. We derive the antenna configuration for beamforming from the antenna geometry in the free space model. Since beamforming has the feature of enhancing the signal strength in certain beams, we investigate in Section 3.5 the maximum signal strengths.

The signal-to-noise-plus-interference ratio (SINR) for node v receiving the signal of transmitter u_i is [GK00]

$$\mathrm{SINR}(v) \quad = \quad \frac{\frac{P(u_i)}{|u_i - v|^\alpha}}{w + \sum_{k \neq i} \frac{P(u_k)}{|u_k - v|^\alpha}} \; . \tag{3.1}$$

In this case, each node has a single antenna. The received signal contains the signal of sender u_i and the interfering signals of senders u_k with $k \neq i$. Furthermore, some noise w will be received which we will take care of soon. The SINR value determines the

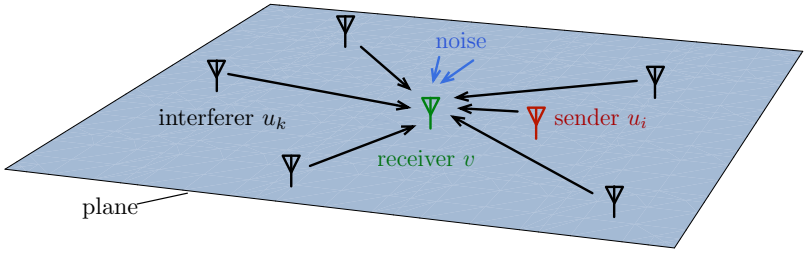

Figure 3.1: SISO case: receiver v receives from sender u_i and nodes u_k with $k \neq i$ interfere

data rate with $f \cdot \log(1 + \mathrm{SINR})$ where f is the carrier frequency (see Definition 2).

[1]The extension of the SINR model for coordinated antennas is published in our work [JS13].

A minimum SINR threshold is necessary to establish a connection. In this section, we extend the SINR model for nodes with multiple antennas performing beamforming respectively multiple nodes performing collaborative beamforming with their antennas.

In the following, we assume that nodes are placed in the plane with antennas aligned perpendicular to the plane (see Figure 3.1), where no polarization effect occurs. We first consider the SIMO case with ℓ uncoordinated senders $u_1, \ldots, u_\ell$ with independent inputs and m coordinated receivers $v_1, \ldots, v_m$ that perform receive beamforming. The

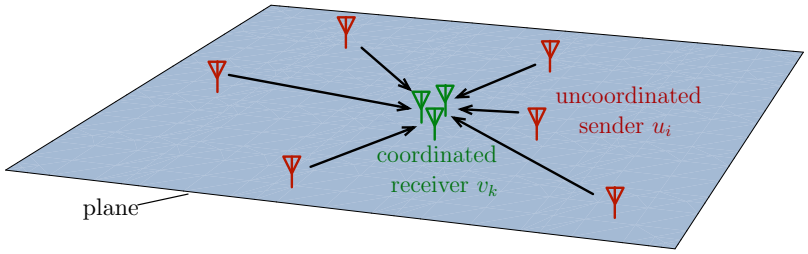

Figure 3.2: MU-SIMO case: coordinated nodes $v_1, \ldots, v_m$ receive from uncoordinated senders $u_1, \ldots, u_m$ which are multiple independent users (MU) with single input (SI)

coordinated receiver array intends to receive the signal of sender u_i and filter the interfering signals of the other senders u_k with $k \neq i$. The power of sender u_i can be described by $|h_i|^2$ as well as the power of the uncoordinated signals is $|\sum_{k \neq i} h_k|^2$. Since we assume independent choices of the phase shifts of the interferers u_k, we can simplify this term.

Lemma 1 *The expected power of uncoordinated senders $u_1, ..., u_\ell$ with characteristic scalars $s'_1, ..., s'_\ell$ at the coordinated receivers $v_1, ..., v_m$ is*

$$\mathbb{E}[P] = \mathbb{E}\left[|h|^2\right] = \sum_{k=1}^{m} \sum_{i=1}^{\ell} |g_k|^2 \frac{|s'_i|^2}{|u_i - v_k|^2}$$

where g_k denotes the signal gain of the k-th receiver.

The following proof of Lemma 1 approves the superposition of power of unsynchronized interferences in the SINR model.

Proof of Lemma 1: Given n senders with characteristic scalars $s'_i = a_i \, e^{j\phi_i}$ and distance $|u_i - v|$ to a receiver v. The sender antennas are not synchronized with phase angle ϕ_i and produce an interference at v. The electrical field strength E of sender u_i with far field approximation is $E = k_{\text{phy}} \cdot \Re(X \cdot h_i) + \sqrt{N_0}$ (see Def. 1) for AWGN N_0. We assume all senders are sending on the same carrier frequency with input $X = e^{j2\pi ft}$ as worst-case interference. The transfer function h_i for sender u_i of the line-of-sight channel is therefore

$$h_i = \frac{a_i \cdot e^{j\phi_i}}{|u_i - v|} \; .$$

The power equivalent (without physical factors) produced by sender u_i at v alone is

$$P_i = \left| \frac{a_i \cdot \mathrm{e}^{j\phi_i}}{|u_i - v|} \right|^2 = \frac{a_i^2}{|u_i - v|^2} \ .$$

The superposition principle can be applied to the electric field respectively h and not to the power or $|h|^2$.

$$E_v = (\textstyle\sum_{i=1}^{n} E_{u_i}) + \sqrt{N_0}$$

The power equivalent of the superposed field is then

$$P_v = (\textstyle\sum_{i=1}^{n} h_i)^2 \ . \tag{3.2}$$

The expected power of the interfering noise is then

$$\begin{aligned}
\mathbb{E}[P] &= \mathbb{E}\left[\left| \sum_{i=1}^{n} \frac{a_i \cdot \mathrm{e}^{j\phi_i}}{|u_i - v|} \right|^2 \right] \\
&= \mathbb{E}\left[\sum_{i=1}^{n} \frac{a_i \cdot \mathrm{e}^{j\phi_i}}{|u_i - v|} \cdot \sum_{i=1}^{n} \frac{a_i \cdot \mathrm{e}^{-j\phi_i}}{|u_i - v|} \right] \\
&= \mathbb{E}\left[\sum_{i \in \{1..n\}} \left(\frac{a_i}{|u_i - v|} \right)^2 \right] + \underbrace{\mathbb{E}\left[\sum_{i=1}^{n} \sum_{k=1, i \neq k}^{n} e^{j(\phi_i - \phi_k)} \right]}_{=0} \frac{a_i}{|u_i - v|} \cdot \frac{a_k}{|u_k - v|} \\
&= \mathbb{E}\left[\sum_{i=1}^{n} \frac{a_i^2}{|u_i - v|^2} \right] \ .
\end{aligned}$$

□

This corresponds to the well known SINR model. The noise power is amplified like all other signals at the m coordinated receivers by a factor of $|g_k|^2$ with signal gain g_k at the k-th receiver. Since electric fields superpose we get the following signal-to-noise ratio.

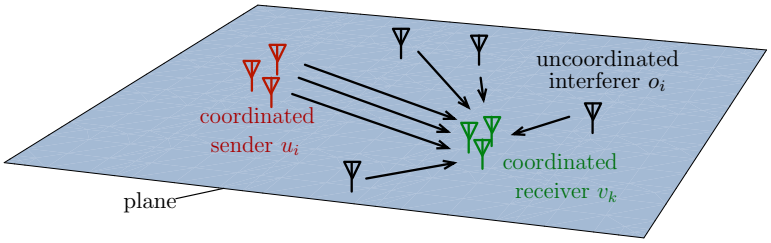

Figure 3.3: MIMO case: coordinated senders $u_1, \ldots, u_n$ transmit to coordinated receivers $v_1, \ldots, v_m$ and uncoordinated senders $o_1, \ldots, o_\ell$ interfere

Definition 8 *For n coordinated senders at positions $u_1, \ldots, u_n$ and m coordinated receivers at positions $v_1, \ldots, v_m$ the signal-to-interference+noise-ratio (SINR) can be determined as*

$$SINR = \frac{\left| \sum_{i=1}^{n} \sum_{k=1}^{m} s_i \cdot \frac{e^{-j\frac{2\pi}{\lambda}|u_i - v_k|}}{|u_i - v_k|} \cdot g_k \right|^2}{\sum_{k=1}^{m} |g_k|^2 \left(w + \sum_{i=1}^{\ell} \frac{P'_i}{|o_i - v_k|^2} \right)} = \frac{|s \cdot H \cdot g|^2}{w' + I} \tag{3.3}$$

where $u = (u_1, \ldots, u_n) \in \mathbb{R}^n$ is the set of the coordinated sending antenna positions, $v = (v_1, \ldots, v_m) \in \mathbb{R}^m$ is the set of the coordinated receiving antenna positions, and $o = (o_1, \ldots, o_\ell) \in \mathbb{R}^\ell$ is the set of uncoordinated sender antenna positions.

The positions of the coordinated senders and receivers describe the channel matrix H of the signal in free space

$$H_{i,k} = \frac{e^{-j\frac{2\pi}{\lambda}|u_i - v_k|}}{|u_i - v_k|} \quad i \in [n],\ k \in [m]\ .$$

In the denominator of (3.3), w is the power equivalent of the noise at each receiving antenna v_k and P'_i describes the power of the interfering antenna o_i.

$$I = \sum_{i \in [\ell], k \in [m]} |g_k|^2 \frac{P'_i}{|o_i - v_k|^2}$$

is the sum of the received signal power from uncoordinated senders. And the received noise is given by

$$w' = w \cdot \textstyle\sum_{k \in [m]} |g_k|^2\ .$$

The vectors $s = (s_1, \ldots, s_n) \in \mathbb{C}^n$ with $|s_i|^2 \leq P_{u_i}$ and $g = (g_1, \ldots, g_m) \in \mathbb{C}^m$ can be chosen arbitrarily.

Power Gain We can experience a power gain of a factor m for a single sender, if we use m coordinated antennas for receiving with beamforming (SIMO, Figure 3.4). Likewise we obtain a power gain of factor n when using n coordinated antennas for sending with beamforming (MISO).

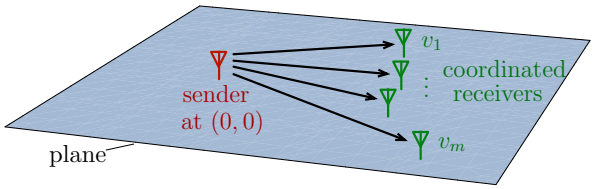

Figure 3.4: SIMO case: a single antenna at $(0,0)$ transmits to coordinated receiver $v_1, \ldots, v_m$

Theorem 1 *Consider multiple coordinated antennas performing send or receive beamforming to a single antenna.*

a) SIMO: Given a sender at the origin 0 and m coordinated receivers $0 < |v_1| < \ldots < |v_m|$ *performing receive beamforming. Let* $SINR_{1,m}$ *be the SINR of these receivers and let* $SINR_{1,1}$ *be the SINR of a single receiver at* v_m*.*
Then, $SINR_{1,m} \geq m \cdot SINR_{1,1}$*.*

b) MISO: Given a receiver at the origin 0 and n coordinated senders $0 < |u_1| < \ldots < |u_n|$ *performing send beamforming. Let* $SINR_{n,1}$ *be the SINR of these senders and let* $SINR_{1,1}$ *be the SINR of a single sender at* u_n *with transmission power P. Then,*

- $SINR_{n,1} \geq n \cdot SINR_{1,1}$ *for constant total transmit power* $P = \sum_{i=1}^{n} |s_i|^2$*.*
- $SINR_{n,1} \geq n^2 \cdot SINR_{1,1}$ *for constant power* $P = |s_i|^2$ *for each sender i.*

Proof: of (a) SIMO: Choose $s_1 = \sqrt{P}$ and $g_k = \mathrm{e}^{j\frac{2\pi}{\lambda}|v_k|}$. This results in

$$\begin{aligned}
\mathrm{SINR}_{1,m} &= \frac{\left|\sum_{k=1}^{m} \sqrt{P} \cdot \frac{\mathrm{e}^{-j\frac{2\pi}{\lambda}|v_k|}}{|v_k|} \cdot \mathrm{e}^{j\frac{2\pi}{\lambda}|v_k|}\right|^2}{\sum_{k=1}^{m} \left|\mathrm{e}^{j\frac{2\pi}{\lambda}|v_k|}\right|^2 (w+I)} \\
&= P \cdot \frac{\left|\sum_{k=1}^{m} \frac{1}{|v_k|}\right|^2}{m\,(w+I)} \text{ whereas } v_m = \max_k\{v_k\} \\
&\geq m \frac{P}{|v_m|^2 \cdot (w+I)} \\
&= m \cdot \mathrm{SINR}_{1,1}
\end{aligned}$$

of (b) MISO: Choose $s_i = \mathrm{e}^{j\frac{2\pi}{\lambda}|u_i|}\sqrt{P/n}$ and $g_k = 1$. This results in

$$\begin{aligned}
\mathrm{SINR}_{n,1} &= \frac{\left|\sum_{i=1}^{n} \mathrm{e}^{j\frac{2\pi}{\lambda}|u_i|}\sqrt{P/n} \cdot \frac{\mathrm{e}^{-j\frac{2\pi}{\lambda}|u_i|}}{|u_i|}\right|^2}{w+I} \\
&= P \cdot \frac{\left|\sum_{i=1}^{n} \frac{1}{|u_i|}\right|^2}{n\,(w+I)} \text{ whereas } u_n = \max_i\{u_i\} \\
&\geq n \frac{P}{|u_n|^2 \cdot (w+I)} \\
&= n \cdot \mathrm{SINR}_{1,1}
\end{aligned}$$

If we increase the overall power from P to $(n \cdot P)$, each node has constant power with $s_i = \mathrm{e}^{j\frac{2\pi}{\lambda}|u_i|}\sqrt{P}$ and we get $\mathrm{SINR}_{n,1} \geq n^2 \cdot \mathrm{SINR}_{1,1}$ instead. □

Again this results in an extension of the transmission range.

Corollary 1 *In comparison to a single antenna, beamforming of n coordinated antennas extends the transmission range for transmitting to (or receiving from) a single antenna by factor $\sqrt{n}$ (in the free-space model and the same transmission power). For transmit beamforming, the transmission range increases by factor n, if each transmitter has constant transmission power and the total power increases by factor n as well.*

Line Placement The following analysis is restricted to nodes placed on a one-dimensional line in the plane. With the same calculation of Theorem 1, one can

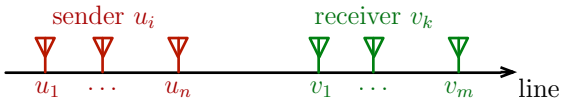

Figure 3.5: Placement of nodes on a one-dimensional line

see a power gain in MIMO.

Theorem 2 *Given n coordinated senders $u_1 < \ldots < u_n < 0$ and m coordinated receivers $0 < v_1 < \ldots < v_m$. Let $SINR_{n,m}$ be the SINR of these senders and receivers and let $SINR_{1,1}$ be the SINR of a single sender at u_1 and a single receiver at v_m. Then, $SINR_{n,m} \geq nm \cdot SINR_{1,1}$.*

Proof: Choose $s_i = \mathrm{e}^{j\frac{2\pi}{\lambda}u_i}\sqrt{P/n}$ and $g_k = \mathrm{e}^{-j\frac{2\pi}{\lambda}|v_k|}$. This results in

$$\begin{aligned}\mathrm{SINR}_{n,m} &= \frac{\left|\sum_{i=1}^{n}\sum_{k=1}^{m}\mathrm{e}^{j\frac{2\pi}{\lambda}u_i}\cdot\sqrt{P/n}\cdot\frac{\mathrm{e}^{-j\frac{2\pi}{\lambda}|u_i-v_k|}}{|u_i-v_k|}\mathrm{e}^{-j\frac{2\pi}{\lambda}v_k}\right|^2}{\sum_{k=1}^{m}\left|\mathrm{e}^{-j\frac{2\pi}{\lambda}v_k}\right|^2\cdot(w+I)} \\ &= \frac{\frac{P}{n}\cdot\left|\sum_{i=1}^{n}\sum_{k=1}^{m}\frac{1}{|u_i-v_k|}\right|^2}{m\cdot(w+I)}\,.\end{aligned}$$

With $u_1 = \min_i\{u_i\}$ it follows

$$\mathrm{SINR}_{n,m} \geq \frac{n\cdot P\cdot\left|\sum_{k=1}^{m}\frac{1}{|u_1-v_k|}\right|^2}{m\cdot(w+I)} \geq \frac{n\cdot P\cdot\left|\sum_{k=1}^{m}\frac{1}{|v_k|}\right|^2}{m\cdot(w+I)}\,.$$

With $v_m = \max_k\{v_k\}$ it follows

$$\mathrm{SINR}_{n,m} \geq \frac{n\cdot m\cdot P}{|u_1-v_m|^2\,(w+I)}$$

□

We get for the special case of MISO a ratio of $\mathrm{SINR}_{n,1} \geq n\cdot\mathrm{SINR}_{1,1}$ with beamforming gain n, and for the case of SIMO we get $\mathrm{SINR}_{1,m} \geq m\cdot\mathrm{SINR}_{1,1}$.

In all fairness, it should be noted that we bound the beamforming gain for the highest path loss between farthest nodes, which are sender u_1 and receiver v_m. And if senders are in the vicinity of receivers, the low path loss can have a higher impact than the beamforming gain of far distant nodes (we discuss this in Section 3.3 which is about the distribution of transmission power among beamforming senders).

The result implies that although the overall transmission power is the same, the signal range with n coordinated send and m coordinated receive antennas extends by a factor of $\sqrt{n \cdot m}$ in the free space model. This phenomenon is long known and is called power gain in MISO [WMGG67].

Corollary 2 *Assume a single sender with transmission power P can transmit to single receiver at distance d. Then any n coordinated senders with total transmission power P and m coordinated receivers (which are placed on a line) can have a transmission distance $d \cdot \sqrt{n \cdot m}$.*

This is not contradicting the principle of conservation of power, since we consider only the power on the line, whereas the power distribution in the rest of the space changes drastically.

3.1 Deliberate Attenuation

For nodes placed on a line, beamforming of n senders can attain a power gain of factor n^2 when each sender has constant transmission power (Theorem 2). The signal power is then $\frac{n^2}{d^2}$ in distance d to the senders. The collaborative senders also produce

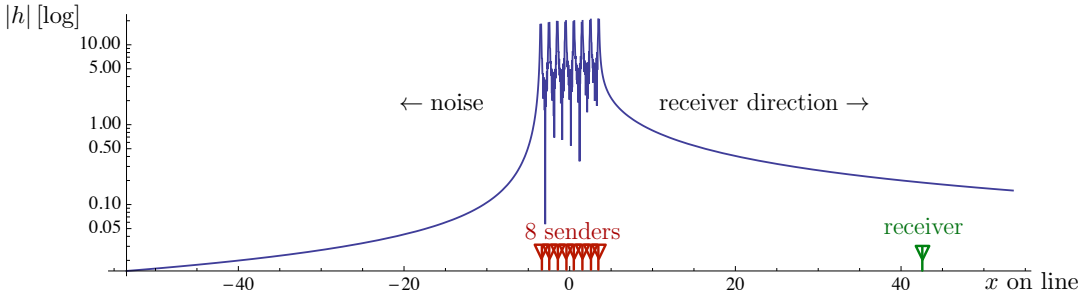

Figure 3.6: Signal strength $|h|$ of 8 beamforming senders (wavelength $\lambda \approx 0.027$)

noise at the nodes, which are in the opposite direction of the receiver on the line (see Figure 3.6). If we assume that the senders are uncoordinated for the opposite direction (i.e. the phases are uncorrelated if the carrier wavelength is not an integer multiple of the distance between senders), the produced noise has according to Lemma 1 an expected power less than $\frac{n}{d^2}$ in distance d to the senders. With a technique, we call *deliberate attenuation*, we can attenuate this noise by increasing the path loss exponent

α with an attenuation of the signal power of $d^{-\alpha}$. The attenuation of the noise in one direction will be at the expense of decreasing the power gain towards the receiver in the other direction. While power gain of beamforming is well known, the observation, that one can deliberately attenuate the signal in one direction, is new to our knowledge. For this, we first show in Lemma 2 how to increase the path loss exponent α for an attenuation of the signal power with $d^{-\alpha}$ and then use this in Theorem 3 to produce deliberate attenuation and power gain in the other direction at the same time.

Lemma 2 *Any n coordinated antennas in general positions on the line can produce a fast signal attenuation on the line which decreases with SINR $\Theta\left(1/d^{2n}\right)$ in distance d. We call this technique 'deliberate attenuation'.*

Proof: To increase the path-loss exponent to $\alpha = 2n$ or a signal amplitude decreasing with $1/d^n$, we want to ensure that

$$h\left(x\right) = \sum_{i=1}^{n} s_i \cdot \frac{\mathrm{e}^{-j\frac{2\pi}{\lambda}(x-u_i)}}{x-u_i} = \frac{\gamma}{\Theta\left(x^n\right)}$$

for the complex antenna characteristics s_i and some constant γ. Without loss of generality, we only consider x-values outside the sender group with $x > u_i$. We extend all summands to the same denominator and the goal is to simplify the nominator to a constant γ to decrease the signal strength to $\mathcal{O}\left(x^{-n}\right)$.

$$\begin{aligned} h\left(x\right) &= \sum_{i=1}^{n} \frac{s_i \cdot \mathrm{e}^{-j\frac{2\pi}{\lambda}(x-u_i)} \cdot \prod_{k=1,k\neq i}^{n}\left(x-u_k\right)}{\left(x-u_i\right)\cdot\prod_{k=1,k\neq i}^{n}\left(x-u_k\right)} \\ &= \frac{\sum\limits_{i=1}^{n} s_i \cdot \left(d_{0,i}\cdot x^{n-1} + d_{1,i}\cdot x^{n-2} + \cdots + d_{n-1,i}\right)}{\prod_{k=1}^{n}\left(x-u_k\right)} \qquad (3.4) \\ &= \frac{\gamma}{\prod_{k=1}^{n}\left(x-u_k\right)} \qquad (3.5) \end{aligned}$$

There is a choice for $(s_1, \ldots, s_n)$ resolving (3.4) to (3.5), since there is a solution to the following equation.

$$D\left(x^{n-1}\ldots x^0\right)\cdot\begin{pmatrix} d_{0,1} & \ldots & d_{0,n} \\ \cdots & & \cdots \\ d_{n-1,1} & \ldots & d_{n-1,n} \end{pmatrix}\cdot\begin{pmatrix} s_1 \\ \vdots \\ s_n \end{pmatrix} = \begin{pmatrix} 0 \\ \vdots \\ 0 \\ \gamma \end{pmatrix}$$

Because n vectors of length $(n-1)$ are linear dependent there is always a non-trivial solution $(s_1, \ldots, s_n) \neq (0, \ldots, 0)$ to this equation. To compute the coefficients d_{ki} of the polynomial consider the following submatrix M' and vector y.

$$\overbrace{\phantom{\begin{pmatrix} M' & \boxed{\begin{matrix} y_1 \\ \vdots \\ y_{n-1} \end{matrix}} \end{pmatrix}}}^{n}$$
$$(n-1)\left\{\begin{pmatrix} M' & \boxed{\begin{matrix} y_1 \\ \vdots \\ y_{n-1} \end{matrix}} \end{pmatrix}\right. \cdot \begin{pmatrix} s_1 \\ \vdots \\ s_{n-1} \\ s_n \end{pmatrix} = \begin{pmatrix} 0 \\ \vdots \\ 0 \\ \gamma \end{pmatrix}$$

We can write instead

$$M' \cdot \begin{pmatrix} s_1 \\ \vdots \\ s_{n-1} \end{pmatrix} = -\begin{pmatrix} y_1 \\ \vdots \\ y_{n-1} \end{pmatrix} \cdot s_n \ .$$

With the inverse of M', we can compute the sender parameters $s_1, \ldots, s_n$.

$$\begin{pmatrix} s_1 \\ \vdots \\ s_{n-1} \end{pmatrix} = (M')^{-1} \cdot \left(-\begin{pmatrix} y_1 \\ \vdots \\ y_{n-1} \end{pmatrix} \cdot s_n\right)$$

Accordingly, parameters $s_1, \ldots, s_{n-1}$ have to be relatively chosen to s_n, which can be set non-zero with some default value. □

One may object that the neglected near-field components have stronger asymptotics than this attenuated signal. However, this proof technique also applies to a more accurate model chosen, which reflects far-field and near-field, and yields the same result, i.e. a near-field component for the electromagnetic field of $\mathcal{O}\left(\frac{1}{d^2}\right)$ with distance d to the sender (see Equation 2.1).

We see in Figure 3.7 an example of deliberate attenuation where (b) shows the complex phases and signal strengths of six antennas for deliberate attenuation. We see in the first quadrant three complex values and multiplying these values with $e^{j\pi}$ gives the complex values in the third quadrant. Adding these 3 pairs of values would cancel them out. Since these values are additionally multiplied with path loss $\frac{1}{x-u_i}$, we only get deliberate attenuation and not a complete cancellation.

Instead of sending a second signal with phase shift π for cancellation, we can send the inverted signal as well since $e^{j\pi} = -1$. The inverted signal does not depend on the wavelength. Thus, this setting holds for a frequency band and not only a carrier frequency, and we can deliberately attenuate data transmission which needs a frequency band around the carrier frequency for transitioning from one symbol to another.

Since deliberate attenuation includes canceling out signals, it needs antenna parameters s_i closely as possible with precise phases and signal strengths. We estimate deliberate attenuation in the next Lemma if the s_i's are error-prone.

Lemma 3 *If n coordinated antennas perform deliberate attenuation (see Lemma 2) and the parameters of the transmit antennas s_i are error-prone with a (complex) error*

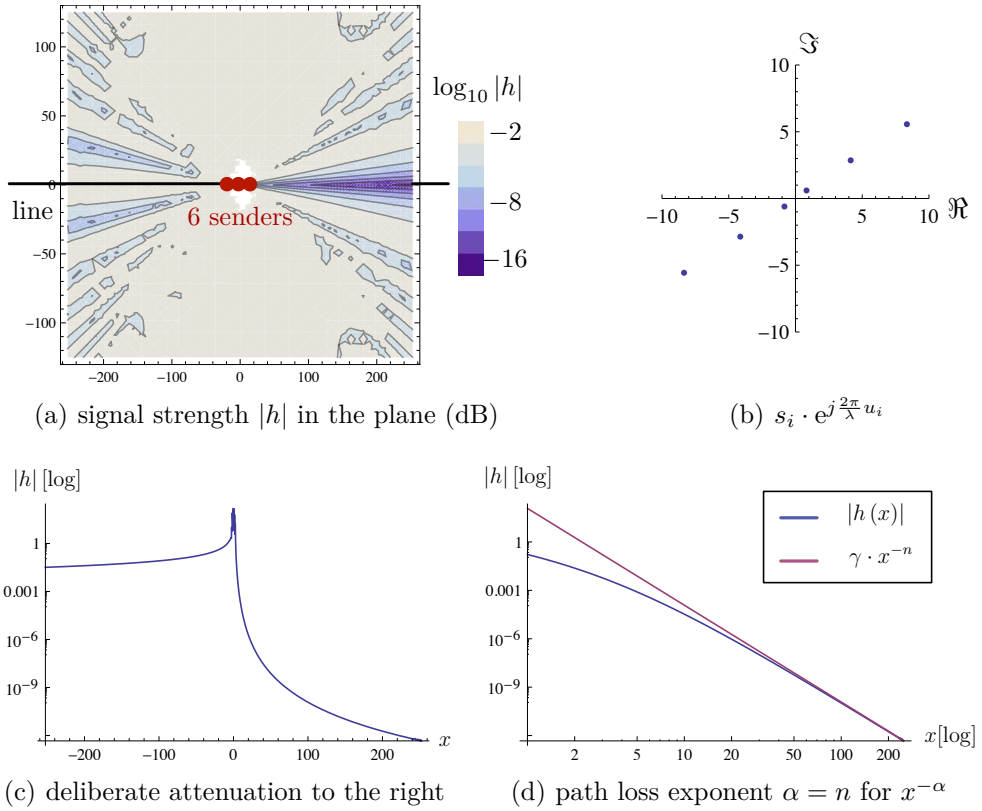

(a) signal strength $|h|$ in the plane (dB)

(b) $s_i \cdot \mathrm{e}^{j\frac{2\pi}{\lambda}u_i}$

(c) deliberate attenuation to the right

(d) path loss exponent $\alpha = n$ for $x^{-\alpha}$

Figure 3.7: Example of $n = 6$ senders positioned on a line around $x = 0$ which perform deliberate attenuation towards $x > 0$ whereby $s_n = 1$, $\lambda/n \approx 0.03$, and $|\gamma| = 120$

$(1+\epsilon) \cdot s_i$, *deliberate attenuation is only valid at distance* d *from the antenna array if the error is less than* $\epsilon = \mathcal{O}\left(\frac{1}{n \cdot d^{n-1}}\right)$.

Proof: Let us consider a group of m antennas whose complex parameters s_i with $i \in \{1, m\}$ and $m < n$ cancel each other out for deliberate attenuation, such that

$$\sum_{i=1}^{m} s_i \cdot \mathrm{e}^{j\frac{2\pi}{\lambda} \cdot u_i} = 0 \ .$$

An upper bound of a super-posed error is then

$$s_{\text{error}} \quad \leq \quad \sum_{i=1}^{n} \epsilon \cdot |s_i| < n \cdot \max_{i \in \{1,n\}} \left(|s_i|\right) \cdot \epsilon \ .$$

Without loss of generality, let us assume that $\max\{u_i\} = 0$. If we super-pose the complex vectors of exact deliberate attenuation and the upper bound of the error, we get

$$|h| \quad \leq \quad \frac{\gamma}{x^n} + \frac{s_{\text{error}}}{x} \ .$$

The second summand only attenuates with $\Theta\left(x^{-1}\right)$. Without loss of generality, let us assume that we can only uphold a fast attenuation of $\Theta\left(x^{-n}\right)$ as long as

$$s_{\text{error}} \leq \frac{\gamma}{x^{n-1}} .$$

For a valid deliberate attenuation the maximum error is then

$$\epsilon = \mathcal{O}\left(\frac{1}{n \cdot x^{n-1}}\right) .$$

□

We can see that the error has to be zero, that deliberate attenuation of x^{-n} is valid for every $x > 0$. The example in Figure 3.8 shows how deliberate attenuation can be realized up to a certain distance x depending on the error s_{error} (with comparison of free-space attenuation $\frac{1}{x}$).

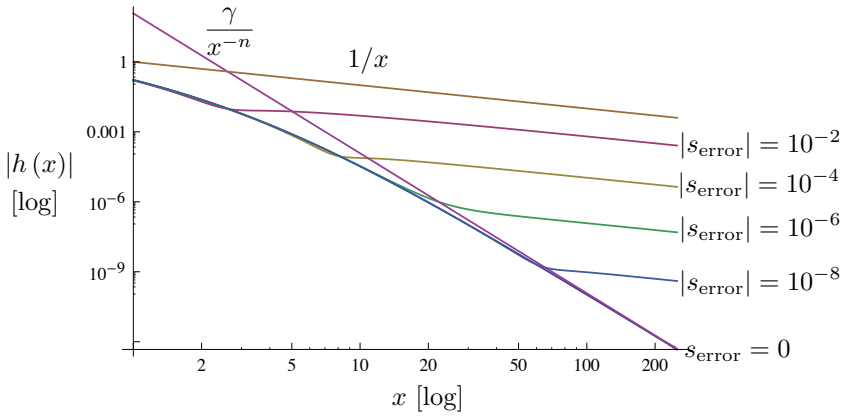

Figure 3.8: Signal amplitude $|h(x)|$ at distance x of deliberate attenuation with error-prone sender parameters s_i containing error s_{error}(Example with 6 senders from Figure 3.7)

However, it is important to remember that deliberate attenuation is particularly important in the vicinity of an array of senders. For remote positions with a large x, the signal will be low even for a moderate path loss less than x^{-n}. In the next Theorem, we show how to combine deliberate attenuation in one direction on the line with free-space attenuation in the opposite direction.

Theorem 3 *Given $n = \rho \cdot \beta$ (for $\rho \geq 2$) coordinated senders with power P each, we can obtain in opposite directions a power gain $\Theta\left(\beta P/d^2\right)$ and a deliberate power attenuation of $\Theta\left(\beta P/d^{2\rho-2}\right)$ in expectation. If we also use beamforming, the power increases by factor β and we get in opposite directions a power gain $\Theta\left(\beta^2 P/d^2\right)$ and a deliberate power attenuation of $\mathcal{O}\left(\beta^2 P/d^{2\rho-2}\right)$. If the distance between senders is approximate to a multiple of half a wavelength with $\frac{k\lambda}{2} + \epsilon \cdot \frac{\lambda}{2}$ for $k \in \mathbb{N}$ and $\epsilon > 0$, free-space path loss is only available at a minimum distance depending on ϵ.*

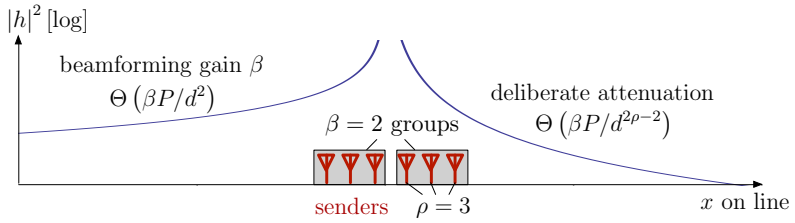

Figure 3.9: $n = 6$ senders have a beamforming gain $\beta = 2$ to the left and additionally deliberate attenuation with path loss exponent $(2\rho - 2) = 4$ to the right. The blue line illustrates the signal power in logarithmic scale

Proof Sketch. Let $u = (u_1, \ldots, u_n)$ be the sender antennas divided into β groups of ρ antennas. Each group of the ρ antennas will deliberately attenuate for a position $x > \max\{u_i\}$ and distance $d = (x - \max\{u_i\})$ with a power of $\Theta(\frac{P}{d^{2\rho-2}})$ and send a signal of power of at least $\Theta\left(P/d^2\right)$ to a position $x < \min\{u_i\}$ and the distance $d = (\min\{u_i\} - x)$ to the group of antennas.

In order to achieve this claim we have to prevent deliberate attenuation to the left. Without loss of generality, let us consider the first group of senders positioned at u_i with $i \in \{1, \rho\}$. Then the deliberately attenuated signal to the right is

$$h\left(x\right) \quad = \quad \mathrm{e}^{-j\frac{2\pi}{\lambda}x} \cdot \sum_{i=1}^{\rho} \frac{\overbrace{s_i \cdot \mathrm{e}^{j\frac{2\pi}{\lambda}u_i}}^{=s_{hi}}}{(x - u_i)} \ . \tag{3.6}$$

Now we analyze the signal $g\left(x\right)$ for $x < \min\{u_i\}$, which should not be attenuated.

$$g\left(x\right) \quad = \quad \mathrm{e}^{j\frac{2\pi}{\lambda}x} \cdot \sum_{i=1}^{n} \frac{\overbrace{s_i \cdot \mathrm{e}^{-j\frac{2\pi}{\lambda}u_i}}^{=s_{gi}}}{(u_i - x)} \tag{3.7}$$

The phase shift s_{hi} of sender i in $h\left(x\right)$ and and the phase shift s_{gi} in $g\left(x\right)$ differs by

$$s_{hi} \quad = \quad s_{gi} \cdot \mathrm{e}^{-j\frac{2\pi}{\lambda} \cdot 2 \cdot u_i} \ .$$

We get deliberate attenuation to the left and to the right if $s_{hi} = s_{gi}$. This is the case if the distance between neighboring nodes is $\frac{k\lambda}{2}$ with $k \in \mathbb{N}$, since

$$s_{gi} = s_{hi} \cdot \mathrm{e}^{j\frac{2\pi}{\lambda} \cdot 2 \cdot u_i} = s_{hi} \cdot \mathrm{e}^{j2\pi \cdot k} = s_{hi} \ .$$

In this special case, we have the same phases in both directions. Since each amplitude $|s_i|$ is adjusted for deliberate attenuation, we have deliberate attenuation in both directions in this case. So we require, that the distance between nodes is not an integer multiple of $\frac{\lambda}{2}$.

If the distance between senders has only a small deviation from a multiple of a half wavelength with $\frac{k\lambda}{2} + \epsilon \cdot \frac{\lambda}{2}$ with $\epsilon > 0$, this deviation will already lead to free-space path loss with exponent $\alpha = 2$ according to Lemma 3. The free-space path loss will be available at a minimum distance which depends on the magnitude of error.

Otherwise the probability that the phase shifts $\mathrm{e}^{j\frac{2\pi}{\lambda}\cdot 2\cdot u_i}$ from s_{hi} to s_{gi} map again to phase angles, which effect deliberate attenuation, might be non zero. For this situation, we can use a second degree of freedom s_{n-1} besides s_n to choose a configuration $(s_1, \ldots, s_n)$ where this is not the case. Therefore, we add to Equation (3.5) the additional term $(\gamma_2 \cdot x) / \Theta(x^n)$ resulting into (3.9), which decreases the path loss exponent by two with attenuation $\Theta\left(P/d^{2\rho-2}\right)$ at distance d.

$$
\begin{aligned}
h(x) &= \sum_{i=1}^{n} \frac{s_i \cdot \mathrm{e}^{-j\frac{2\pi}{\lambda}(x-u_i)} \cdot \prod_{k=1,k\neq i}^{n} (x-u_k)}{(x-u_i) \cdot \prod_{k=1,k\neq i}^{n} (x-u_k)} \\
&= \frac{\sum_{i=1}^{n} s_i \cdot \left(d_{0,i} \cdot x^{n-1} + d_{1,i} \cdot x^{n-2} + \cdots + d_{n-2,i} \cdot x + d_{n-1,i}\right)}{\prod_{k=1}^{n} (x-u_k)} \qquad (3.8) \\
&= \frac{\gamma + \gamma_2 \cdot x}{\prod_{k=1}^{n} (x-u_k)} \qquad (3.9)
\end{aligned}
$$

There is a choice for $(s_1, \ldots, s_n)$ resolving (3.8) to (3.9), since there is a solution to the following equation.

$$
D\begin{pmatrix} x^{n-1} \ldots x^1 & x^0 \end{pmatrix} \cdot \begin{pmatrix} d_{0,1} & \ldots & d_{0,n} \\ \cdots & & \cdots \\ & & \\ d_{n-2,1} & \ldots & d_{n-2,n} \\ d_{n-1,1} & \ldots & d_{n-1,n} \end{pmatrix} \cdot \begin{pmatrix} s_1 \\ \vdots \\ \\ s_{n-1} \\ s_n \end{pmatrix} = \begin{pmatrix} 0 \\ \vdots \\ 0 \\ \gamma_2 \cdot x \\ \gamma \end{pmatrix}
$$

Because n vectors of length $(n-2)$ are linear dependent there is always a non-trivial solution $(s_1, \ldots, s_n) \neq (0, \ldots, 0)$ to this equation. To compute the coefficients d_{ki} of the polynomial consider the following submatrix M'' and submatrix y.

$$
\begin{array}{l}
\overbrace{}^{n} \\
\left.\begin{array}{l} \\ \\ \end{array}\right\}(n-2)
\end{array}
\left(\begin{array}{cc|c}
 & y_{1,1} \; y_{1,2} & \\
M'' & \vdots & \\
 & y_{n-2,1} \; y_{n-2,2} & \\
\hline
 & \cdots &
\end{array}\right) \cdot \begin{pmatrix} s_1 \\ \vdots \\ s_{n-2} \\ \hline s_{n-1} \\ s_n \end{pmatrix} = \begin{pmatrix} 0 \\ \vdots \\ 0 \\ \hline \gamma_2 \\ \gamma \end{pmatrix}
$$

We can write instead

$$
M'' \cdot \begin{pmatrix} s_1 \\ \vdots \\ s_{n-2} \end{pmatrix} = -\begin{pmatrix} y_{1,1} & y_{1,2} \\ \vdots & \\ y_{n-2,1} & y_{n-2,2} \end{pmatrix} \cdot \begin{pmatrix} s_{n-1} \\ s_n \end{pmatrix} .
$$

With the inverse of M'' we can compute the sender parameters $s_1, \ldots, s_{n-2}$.

$$\begin{pmatrix} s_1 \\ \vdots \\ s_{n-2} \end{pmatrix} = (M'')^{-1} \cdot \left(- \begin{pmatrix} y_{1,1} & y_{1,2} \\ \vdots & \\ y_{n-2,1} & y_{n-2,2} \end{pmatrix} \cdot \begin{pmatrix} s_{n-1} \\ s_n \end{pmatrix} \right)$$

Accordingly, parameters $(s_1, \ldots, s_{n-2})$ have to be relatively chosen to s_{n-1} and s_n. The parameter s_{n-1} can be set non-zero with some default value and parameter s_n is the additional degree of freedom to be chosen that the signal to the left is not attenuated.

We see two interesting choices to adjust the phases between the β groups. Either we simply add a random phase shift or we can correlate the signals of the β groups to produce beamforming to left. In the first case of random phases, the expected power will be (by the argument of Lemma 1) the sum of all signal powers of the sub-groups. From this, we can induce the existence of a choice such that the signal is attenuated by $\Theta\left(\beta \cdot P/d^2\right)$ to the left and $\Theta\left(\beta P/d^{2\rho-2}\right)$ to the right.

For beamforming to the left with $x < \min\{u_i\}$, we multiply each of the β groups with a phase shift such that the signals of all groups are correlated to the left. We get an overall signal power to the left of

$$|h|^2 = \left(\sum_{i=1}^{\beta} h_i \right)^2 = \beta^2 \cdot |h_\rho|^2$$

where $|h_\rho|$ denotes an estimated power for each group of ρ senders. To the right, the wavelength might be some harmonics of the node distances such that the signals of some sub-groups are also correlated and we get a signal in $\mathcal{O}\left(\beta^2\right)$. Overall, when applying beamforming between the subgroups, the expected signal is $\Theta\left(\beta^2 \cdot P/d^2\right)$ to the left and $\mathcal{O}\left(\beta^2 P/d^{2\rho-2}\right)$ to the right. □

Corollary 3 *Among many others, the following combination of deliberate attenuation and power gain to opposite directions are possible for antennas with power P each.*

1. $\Theta\left(P/d^2\right)$ *to the left and* $\Theta\left(P/d^{2n-2}\right)$ *to the right ($\rho = n$, $\beta = 1$)*
2. $\Theta\left(\sqrt{n}P/d^2\right)$ *to the left and* $\Theta\left(\sqrt{n}P/d^{2\sqrt{n}-2}\right)$ *to the right ($\rho = \sqrt{n}$, $\beta = \sqrt{n}$)*
3. $\Theta\left(nP/d^2\right)$ *to the left and* $\Theta\left(nP/d^{2c}\right)$ *to the right for any integer $c \geq 1$ ($\rho = c+1$, $\beta = n/(c+1)$).*
4. $\Theta\left(n^2P/d^2\right)$ *to the left and* $\mathcal{O}\left(n^2P/d^{2c}\right)$ *to the right for any integer $c \geq 1$ ($\rho = c+1$, $\beta = n/(c+1)$), and applying beamforming.*

3.2 Diversity Gain

The power gain of beamforming helps to extend the communication distance. However, there is also a direct possibility to increase the data rate using the so-called diversity

gain.

It is often mentioned in literature (e.g. in [PAK03]) that angular spread is essential for MIMO transmission. Our first observation is that in principle such a diversity gain is possible on the line even in free space.

Lemma 4 *For coordinated senders $u_1 < \ldots < u_n$ and coordinated receivers $v_1 < \ldots < v_m$ on a line with $u_n < v_1$ or $v_m < u_1$ the channel matrix H has rank $\min\{n, m\}$.*

Proof: Without loss of generality, we consider only the case $u_n < v_1$. Let $n = m$, then the channel matrix is

$$\begin{aligned} H &= \left(\frac{\mathrm{e}^{-j\frac{2\pi}{\lambda}|u_i - v_k|}}{|u_i - v_k|} \right)_{k,i\in[n]} \\ &= \left(\frac{\mathrm{e}^{-j\frac{2\pi}{\lambda}(v_k - u_i)}}{v_k - u_i} \right)_{k,i\in[n]} \\ &= D\left(\left(\mathrm{e}^{-j\frac{2\pi}{\lambda}v_k} \right)_{i\in[n]} \right) \cdot \left(\frac{1}{v_k - u_i} \right)_{k,i\in[n]} \cdot D\left(\left(\mathrm{e}^{j\frac{2\pi}{\lambda}u_i} \right)_{k\in[n]} \right) \end{aligned}$$

where $D(a)$ denotes the diagonal matrix of vector a, which has full rank if a has no zero entry. The matrix $C = \left(\frac{1}{v_k - u_i}\right)_{k,i\in[n]}$ is a Cauchy matrix and thus is invertible for all u, v if for all i, k: $u_i \neq v_k$. Since the inverse of $(A \cdot B)^{-1} = B^{-1} \cdot A^{-1}$ for matrices A, B and the inverse of $D\left((d_i)_i\right)^{-1} = D\left(\left(d_i^{-1}\right)_i\right)$, the inverse of channel matrix H is

$$H^{-1} = D\left(\left(\mathrm{e}^{-j\frac{2\pi}{\lambda}u_i} \right)_{k\in[n]} \right) \cdot C^{-1} \cdot D\left(\left(\mathrm{e}^{j\frac{2\pi}{\lambda}v_k} \right)_{i\in[n]} \right)$$

where the inverse of the Cauchy matrix C^{-1} can be computed with [Sch59]. □

An example for computing the inverse of the channel matrix of two senders and two receivers is in Appendix A.

Theorem 4 *For coordinated senders $u_1 < \ldots < u_n$ and non coordinated receivers $v_1 < \ldots < v_m$ on a line with $m < n$ and $u_n < v_1$ or $v_m < u_1$, it is possible to send to any subset of receivers without producing a signal at the other receivers.*

Proof: Consider the vector $a_1, \ldots, a_m$ such that $a_i = 1$ if i is in the subset of aimed receivers and $a_i = 0$ otherwise. Now, we use only m senders. Then let H^{-1} be the inverse of H, which exists because of Lemma 4. Then each sender u_i uses the parameter $qH^{-1}a$, where $q = \sqrt{P}/\max\{|(H^{-1}a)_i|\}$, where P denotes the maximum possible transmission power. The resulting signal is therefore $qHH^{-1}a = qa$. □

Example

Consider the case $n = m = 2$ and $a = (0,1)^T$, i.e. receiver v_2 gets the signal while keeping silence at receiver v_1 (see Figure 3.10(a)). The parameters for sending are

$$s = \begin{pmatrix} s_1 \\ s_2 \end{pmatrix} = H^{-1} \cdot a = \frac{(v_2 - u_1)(v_2 - u_2)}{(u_2 - u_1)(v_2 - v_1)} \cdot \begin{pmatrix} -(v_1 - u_1) \cdot e^{j\frac{2\pi}{\lambda}(v_2 - u_1)} \\ (v_1 - u_2) \cdot e^{j\frac{2\pi}{\lambda}(v_2 - u_2)} \end{pmatrix}$$

and sender u_1 delays/attenuates the signal with s_1 and u_2 with s_2. Comparing s_1 and s_2, we see that the signals of u_1 and u_2 cancel out at position v_1, because both signals arrive in the same phase at v_1 and v_2, the signal amplitudes are matched at position v_1 with factors $(v_1 - u_1)$ and $(v_1 - u_2)$, and the signal of u_1 is negated for canceling out. For position v_2 the signal strengths won't match and there is a signal as Figure 3.10(b) shows. But the signal at v_2 is weaker compared to beamforming to both receivers with $a = (1,1)^T$.

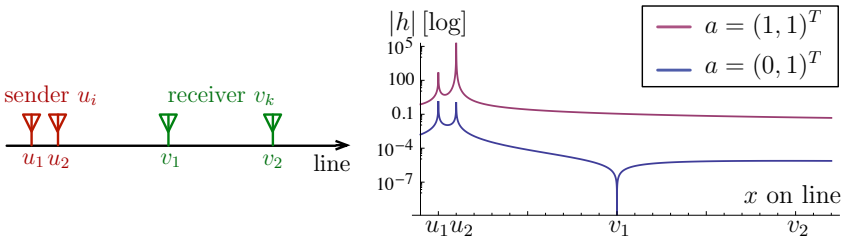

(a) antennas positioned on line (b) signal strength on line

Figure 3.10: Example for diversity gain of two senders and two receivers

Using this theorem, it is possible to send n messages in parallel from n coordinated senders to n uncoordinated receivers, which can be seen as parallel MISO. For this, we choose a receiver and modulate a signal, which can be received at this receiver only, while the other receivers get no signal (compare the preceding example). Now, we repeat this for all receivers and send the superposed signal from the n coordinated senders. As a result, each uncoordinated receiver gets only "his message". This seems to increase the bandwidth between senders and receivers on the line by a factor of n. However, the delimiting factor is the attenuation of the signals imposed by the maximum transmission power P and the entries of the inverse channel matrix H^{-1}.

Lemma 5 *Fix a set of n senders $u_1, \ldots, u_n$ and n receivers $v_1, \ldots, v_n$. Consider the channel matrix of u and $(v_1 + d, \ldots, v_n + d)$ for increasing distance d on the line. Then, the maximum absolute value of the inverse of the channel matrix is $\Theta(d^{2n-1})$.*

Proof: The absolute values of the channel matrix are described by the Cauchy matrix

$$M = \left(\frac{1}{(v_k + d) - u_i} \right)_{k,i \in [n]} .$$

The determinant of a Cauchy matrix is (see [Sch59])

$$\begin{aligned} \det M &= \frac{\prod_{k=2}^{n} \prod_{i=1}^{k-1} (v_k - v_i)(u_i - u_k)}{\prod_{k=1}^{n} \prod_{i=1}^{n} (d + v_k - u_i)} \\ &= \Theta\left(\frac{1}{d^{n^2}} \right) . \end{aligned}$$

The inverse $D = (d_{ki})_{k,i \in [n]}$ of a matrix can be computed as

$$d_{ki} = (-1)^{k+i} \frac{\det(M_{ki})}{\det(M)}$$

where M_{ki} is the submatrix of M without the k-th row and i-th column. Note that M_{ki} is also a Cauchy matrix. Therefore,

$$|d_{ki}| = \Theta\left(\frac{d^{n^2}}{d^{(n-1)^2}} \right) = \Theta\left(d^{2n-1} \right)$$

□

So, the usage of Theorem 4 leads to an attenuation by a factor of $\mathcal{O}\left(1/d^{2n-2}\right)$, which is close to the deliberate attenuation which we have discussed before. On the positive side, we show that it is possible to send n message in parallel from n coordinated senders to n uncoordinated receivers even in free space. However, the power of each antenna must be chosen extremely large with respect to the noise, interference power, and distance, i.e. $P \geq (w + I)d^{4n+2}$. For such powerful senders, the diversity gain of MIMO is larger than the data rate increase using the classic Shannon bounds even in the free space communication model.

3.3 Distribution of Transmission Power among Antennas

Wireless transmissions with low power are essential in mobile communications to prolong battery lifetime of mobile nodes and to reduce interferences of parallel transmissions, which in result can increase the data rate. Assume several sender nodes are available to send the same information to a specific receiver node. Obviously, the sender being closest to the receiver is the best choice for transmitting because it has the lowest path-loss $1/d^2$ for distance d and can send with less power. In the example in Figure 3.11(a), this would be the node with distance d_5. Now assume we have multiple coordinated nodes available for a cooperative transmission with beamforming and all nodes send with the same transmit power $P = P_i$. Recall that the signal strength

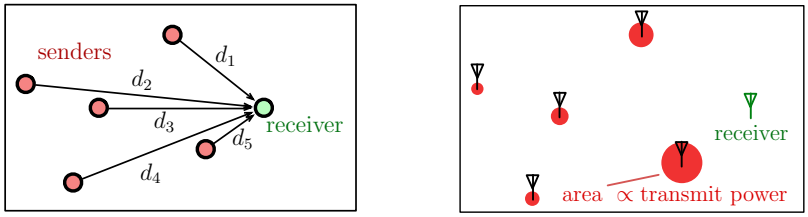

(a) sender-receiver distances d_i (b) optimal power distribution

Figure 3.11: Example of a power distribution among $n = 5$ senders for a single receiver

of n senders is at the receiver $h = \sum_{i=1}^{n} \sqrt{P_i}/d_i$ where sender i transmits with power P_i at distance d_i from the receiver. We get full beamforming (power) gain of factor n^2 if $\forall i \in [1, n] : d_i = d, P_i = P$ and therefore $h = n \cdot \sqrt{P}/d$. If distances $d_1, \ldots, d_n$ are non-uniform, the beamforming gain is reduced and the receiver gets a stronger signal of senders that are closer to the receiver and have lower path-loss with $1/d_i$.

In result, if we have a fixed power budget P_c available for all n senders with $P_c = \sum_{i=1}^{n} P_i$, we have an optimization problem with a tradeoff between a uniform and a non-uniform power distribution among the senders; a uniform power distribution enables more beamforming gain while a non uniform power distribution can allocate more power to senders, which are closer to the receiver and can transmit more power to the receiver with less path loss. In the example of Figure 3.11(b), it is beneficial to allocate more power to the sender with the shortest distance d_5.

In the following, we will first describe the optimal power distribution for arbitrary positioned nodes (Section 3.3.1). Then we turn our attention to two special cases of node placements: nodes positioned on a line (Section 3.3.2) and nodes positioned in a grid in the plane (Section 3.3.3). We will use both placements later on in the analysis of routing algorithms in Sections 4.2-4.4.

3.3.1 Arbitrary Placement of Senders

Lemma 6 *Assume one node receives from n senders in the plane at distance d_i with $1 \leq i \leq n$ (see Figure 3.11). The overall power budget of all n senders is $P_c \leq \sum_{i=1}^{n} P_i$ and sender i has transmission power P_i. All n senders are coordinated and perform beamforming. Then, a maximum signal strength is reached at the receiver, if the i-th sender has amplitude a_i with*

$$a_i = \frac{\sqrt{P_c}}{d_i \cdot \sqrt{\sum_{k=1}^{n} \frac{1}{d_k^2}}} \; . \tag{3.10}$$

The resulting signal power is therefore

$$|h|^2 = P_c \cdot \sum_{i=1}^{n} \frac{1}{d_i^2} \; . \tag{3.11}$$

Proof: Denote P_c the overall transmission power available for a transmission with multiple coordinated senders. In the first setting we have two nodes with amplification a_1 and a_2 with resulting power constraint

$$P_c \leq a_1^2 + a_2^2 \ .$$

The grey area in Figure 3.12 shows the possible configuration for amplifications (a_1, a_2). The signal strength at the receiver with distances d_1 and d_2 to the sender nodes is for

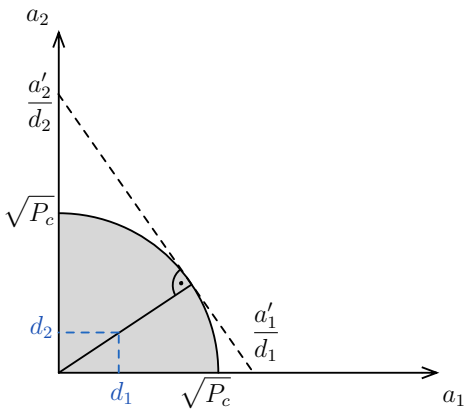

Figure 3.12: Graphical solution for power allocation to cooperative beamforming senders with distances d_1, d_2, amplitudes a_1, a_2 and overall power budget P_c.

a configuration with amplifications (a_1, a_2)

$$h = \frac{a_1}{d_1} + \frac{a_2}{d_2} \ .$$

The normal vector of the linear equation $f(a_1) = a_2$ is

$$\mathbf{n} = \begin{pmatrix} \frac{1}{d_1} & \frac{1}{d_2} \end{pmatrix}, \ |\mathbf{n}| = \sqrt{\frac{1}{d_1^2} + \frac{1}{d_2^2}}$$

and the normalized vector is $\mathbf{n}_0 = \mathbf{n}/|\mathbf{n}|$. To solve the problem graphically, we move the linear equation in such a way that it has distance $\sqrt{P_c}$ from the origin and maximum sending power is used. For that, we multiply the normal vector $\mathbf{n}_0$ with the length $\sqrt{P_c}$ with the solution

$$\begin{pmatrix} a_1 \\ a_2 \end{pmatrix} = \frac{\sqrt{P_c}}{\sqrt{\frac{1}{d_1^2} + \frac{1}{d_2^2}}} \cdot \begin{pmatrix} \frac{1}{d_1} \\ \frac{1}{d_2} \end{pmatrix} \ .$$

For three dimensions, the solution is a single intersection point of a sphere, which is the power constraint with radius $\sqrt{P_c}$, and a plane described by three amplification values (a_1, a_2, a_3).

The general case for n antennas and power limitation P_c is then

$$a_i \quad = \quad \frac{\sqrt{P_c}}{d_i \cdot \sqrt{\sum_{k=1}^{n} \frac{1}{d_k^2}}} \; .$$

Inserting the optimal amplification factors a_i gives the following signal power at the receiver:

$$|h_i|^2 \quad = \quad \left(\sum_{i=1}^{n} \frac{a_i}{d_i} \right)^2 = \left(\sum_{i=1}^{n} \frac{\sqrt{P_c}}{d_i^2 \cdot \sqrt{\sum_{k=1}^{n} \frac{1}{d_k^2}}} \right)^2 = P_c \frac{\left(\sum_{i=1}^{n} \frac{1}{d_i^2} \right)^2}{\sum_{k=1}^{n} \frac{1}{d_k^2}} = P_c \cdot \sum_{i=1}^{n} \frac{1}{d_i^2}$$

□

When several nodes are available to collaborate for send beamforming to a receiver node, each sender node i has an individual path-loss with d_i^{-2} for receiver distance d_i reducing the signal level. In result, if all senders have a common budget of transmission power P_c, it is beneficial to allocate more transmission power to the senders, which are nearer to the receiver and have lower path-loss. On the other hand, an uneven power distribution among the senders will reduce the beamforming gain. There is a tradeoff between reducing path-loss and enabling beamforming gain. The optimum solution is the signal amplitude $\frac{s}{d_i}$ for sender i and receiver distance d_i and factor $s = \sqrt{P_c / \sum_{k=1}^{n} d_k^{-2}}$ norming the sum of all sender's power to P_c (see Lemma 6).

In the next sections, we will discuss the power allocation to sender nodes placed on a line and a rectangular area in the plane. The routing algorithms in the next chapter use clusters of sender nodes with these geometries.

3.3.2 Senders Placed on a Line

Assume an infinite number of nodes placed with equidistance 1 on a line, which perform send beamforming to a receiver at distance d to this line of sender nodes. Each node

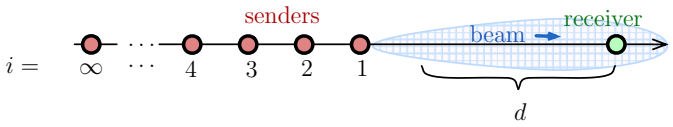

Figure 3.13: Infinite number of beamforming senders on a line and a receiver in distance d

has a single antenna, the line is in a plane, and all antennas are perpendicular to this

plane, i.e. there is no polarization effect. We choose the power of the i-th sender with distance $(d+i)$ according to Equation 3.10, which is

$$a_i = \frac{\sqrt{P_c}}{(d+i)\cdot s}$$

with constant s such that the overall power budget of all senders is $P_c = \sum_{i=1}^{\infty} P_i$ where $P_i = a_1^2$ denotes the power of the i-th sender.

Lemma 7 *For an infinite number of senders placed on a line with equidistance* 1*, the beamforming (power) gain at a receiver at distance d on the line is $\Theta(d)$ compared to a single node with the same transmission power, if the transmission power is distributed according to Equation (3.10) among the senders.*

When allocating the power evenly to an infinite number of senders, the signal strength at the receiver is zero.

Proof: When adjusting the amplitudes of the sender nodes with Equation (3.10), we can compute the signal power at the receiver with distance d to the infinite line of senders with Equation (3.11) and get

$$|h|^2 \;=\; P_c \cdot \sum_{i=1}^{\infty} \frac{1}{(d+i)^2} = P_c \cdot \Psi^{(1)}(d+1)$$

where $\Psi^{(k)}(\cdot)$ is the k-th polygamma function of order k. The polygamma function of first order can be replaced by the first derivative of the digamma function $\frac{\mathrm{d}}{\mathrm{d}x}\Psi(x)$ for some x. The digamma function in turn can be replaced by the $(x-1)$-st harmonic number H_{x-1} such that $\frac{\mathrm{d}}{\mathrm{d}x}\Psi(x) = \frac{\mathrm{d}}{\mathrm{d}x}H_{x-1} - \gamma$ where $\gamma \approx 0.58$ is the Euler-Mascheroni constant. It follows

$$\begin{aligned} |h|^2 &= P_c \cdot \frac{\mathrm{d}}{\mathrm{d}x}\Psi(x) \text{ with } x := d+1 \\ &= P_c \cdot \frac{\mathrm{d}}{\mathrm{d}x}\left(-\gamma + \sum_{k=1}^{x-1}\frac{1}{k}\right) . \end{aligned}$$

We can upper bound the d-th partial sum of the harmonic series with $\ln(x)$ resulting into

$$|h|^2 \;\geq\; P_c \cdot \frac{\mathrm{d}}{\mathrm{d}x}(-\gamma + \ln(x)) \geq \frac{P_c}{x} \geq \frac{P_c}{d+1} .$$

Comparing Equation (3.10) with (3.11), we can derive from the preceding equation the amplitude a_i of the i-th sender with distance $(d+i)$

$$a_i = \frac{\sqrt{P_c}}{(d+i)\cdot s} \tag{3.12}$$

whereby $s \geq \sqrt{d+1}$ such that the overall power budget of all senders is $P_c = \sum_{i=1}^{\infty} a_i^2$. When comparing the infinite number of senders to a single sender at distance d, the beamforming gain is $\frac{d^2}{d+1} = \Theta(d)$.

In contrast, if we distribute the overall power P_c equally among the infinite number of senders, we get

$$|h|^2 = \lim_{n\to\infty} \left(\sum_{i=1}^{n} \frac{\sqrt{P_c/n}}{d_i} \right)^2 = \lim_{n\to\infty} \frac{P_c}{n} \left(\sum_{i=1}^{n} \frac{1}{d_i} \right)^2 = \lim_{n\to\infty} \frac{P_c}{n} \left(\ln(n+1) + o(1) \right)^2 = 0 \ .$$

□

The comparison of optimal and equal power allocation shows two things: the equation of the optimal power allocation scheme forms a converging series with terms $1/d_i^2$ and consequently most of the power is allocated to the senders which are close to the receiver ("head of the line"). An equal power distribution in contrast forms a diverging harmonic series and the the power is allocated to the "long tail" and the overall signal strength is approaches zero when the number of senders goes to infinity.

In Equation (3.12), we can approximate the scaling factor with $s \geq \sqrt{d+1}$ and a receiver's amplitude a_i only depends on its own position with factor $(d+i)$ and not on the remaining nodes' positions. Thus, we can allocate the power only with a small constant deviation from the optimum without knowing the number of sender nodes n on the line.

However, the following lemma shows the asymptotic beamforming gain for n beamforming senders (see Figure 3.14).

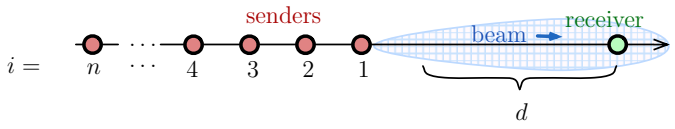

Figure 3.14: n beamforming senders on a line and a receiver in distance d

Lemma 8 *If we choose the optimal power distribution of Lemma 6 for n senders placed on a line with equidistance* 1*, the beamforming (power) gain at a receiver at distance d on the line is* $\Theta(\min\{d, n\})$ *compared to a single node with the same transmission power.*

The proof structure follows the proof of Lemma 6 and thus is kept short.

Proof: The signal power of multiple senders performing beamforming with the power allocation scheme of Lemma 6 is

$$\begin{aligned}
|h|^2 &= P_c \cdot \sum_{i=1}^{n} \frac{1}{(d+i)^2} \\
&= P_c \cdot \left(\Psi^{(1)}(d+1) - \Psi^{(1)}(n+d+1)\right) \\
&= P_c \cdot \left(\frac{\mathrm{d}}{\mathrm{d}x_1}\Psi(x_1) - \frac{\mathrm{d}}{\mathrm{d}x_2}\Psi(x_2)\right) \text{ with } x_1 := d+1 \text{ and } x_2 := n+d+1 \ .
\end{aligned}$$

We can replace the digamma function $\Psi(x)$ for some x by a harmonic series resulting into

$$\begin{aligned}
|h|^2 &= P_c \cdot \left(\frac{\mathrm{d}}{\mathrm{d}x_1}\left(\sum_{k=1}^{x_1-1}\frac{1}{k}\right)\right) - P_c \cdot \left(\frac{\mathrm{d}}{\mathrm{d}x_2}\left(\sum_{k=1}^{x_2-1}\frac{1}{k}\right)\right) \\
&\geq P_c \cdot \left(\frac{\mathrm{d}}{\mathrm{d}x_1}\ln(x_1)\right) - P_c \cdot \left(\frac{\mathrm{d}}{\mathrm{d}x_2}\ln(x_2)\right) \text{ (lower estimate of first term larger)} \\
&= P_c \cdot \left(\frac{1}{x_1} - \frac{1}{x_2}\right) \\
&= P_c \cdot \left(\frac{1}{d+1} - \frac{1}{n+d+1}\right) \\
\Rightarrow |h|^2 &\geq P_c \cdot \left(\frac{n}{(d+1)\cdot(d+1+n)}\right) \ .
\end{aligned}$$

In case of $\frac{n}{d} \to \infty$ beamforming gain is $\Theta(n)$ according to Lemma 7 since

$$\lim_{n\to\infty}\left(\frac{1}{d+1} - \frac{1}{n+d+1}\right) = \frac{1}{d+1} \ .$$

In case of $d \gg n$ the signal power converges to $\Theta\left(\frac{P_c \cdot n}{d^2}\right)$ since

$$\frac{1}{d+1} - \frac{1}{n+d+1} = \frac{n}{(d+1)^2 + n(d+1)}$$

where $(d+1)^2$ is the dominating term of the denominator for $d \gg n$.

If the receiver's distance d is proportional to the number of senders n with $n = k \cdot d$ for a constant $k > 0$, the signal power at the receiver is

$$|h|^2 \geq P_c \cdot \left(\frac{k\cdot d}{(d+1)\cdot(d+1+k\cdot d)}\right) \geq \frac{P_c \cdot \frac{k}{k+1}\cdot d}{(d+1)^2} = \Theta\left(\frac{P_c}{d}\right) = \Theta\left(\frac{P_c \cdot n}{d^2}\right) \ .$$

□

Lemma 9 *If n senders are placed on a line with equidistance 1 and perform beamforming with an even power distribution among senders, the beamforming gain g at a receiver at distance d on the line is $\frac{\ln n}{n} \leq g \leq n$ compared to a single node with the same transmission power.*

Proof: For an even power distribution, each of the n senders transmits with power $\frac{P_c}{n}$ and corresponding amplitude $\frac{\sqrt{P_c}}{\sqrt{n}}$. The n senders produce at distance d a super-posed signal with power

$$\begin{aligned} |h|^2 &= \frac{P_c}{n}\left(\sum_{i=1}^{n}\frac{1}{d+i}\right)^2 \\ &= \frac{P_c}{n}\left(\Psi\left(d+n+1\right)-\Psi\left(d+1\right)\right)^2 \\ &= \frac{P_c}{n}\left(\left(\sum_{k=1}^{d+n}\frac{1}{k}\right)-\left(\sum_{k=1}^{d}\frac{1}{k}\right)\right)^2 \\ &= \frac{P_c}{n}\left(\ln\left(d+n\right)+\varepsilon_{d+n}-\ln\left(d\right)-\varepsilon_d\right)^2 \ . \end{aligned}$$

Here, $\varepsilon_k \sim \frac{1}{2k}$ and thus $\varepsilon_{d+n} - \varepsilon_d < 0$.

$$|h|^2 \leq \frac{P_c}{n}\left(\ln\left(1+\frac{n}{d}\right)\right)^2 \tag{3.13}$$

We can estimate the function with the Taylor series

$$\ln\left(1+x\right) = \sum_{k=1}^{\infty}\left(-1\right)^{k+1}\cdot\frac{x^k}{k} = x - \frac{x^2}{2} + \frac{x^3}{3} - \frac{x^4}{4} + \dots \ .$$

This gives

$$|h|^2 \leq \frac{P_c}{n}\left(\frac{n}{d} - \frac{n^2}{2d^2} + \frac{n^3}{3d^3} - \frac{n^4}{4d^4} + \dots\right)^2 \ .$$

When only considering the first term of the series for a upper bound of the signal power, we get

$$|h|^2 \leq \frac{P_c\cdot n}{d^2}$$

which corresponds to a maximum beamforming (power) gain of n. For the lower bound we set $d = 1$ and get

$$|h|^2_{d=1} = \frac{P_c}{n}\left(\sum_{i=1}^{n}\frac{1}{i}\right)^2 \geq \frac{P_c\cdot\ln\left(n+1\right)}{n} \ .$$

Thus, the lower bound for the signal power at a receiver with distance $d \geq 0$ is

$$|h|^2 \geq \frac{P_c}{d^2} \cdot \frac{\ln(n+1)}{n}$$

which is a lower bound for the beamforming gain of $\frac{\ln(n+1)}{n}$. This lower bound is tight for small distances d and large sender arrays with n nodes. □

Figure 3.15 shows the path loss for $n = 1000$ senders placed equidistant on a line at a receiver at distance d. Notably, for even power distribution and small distances d the

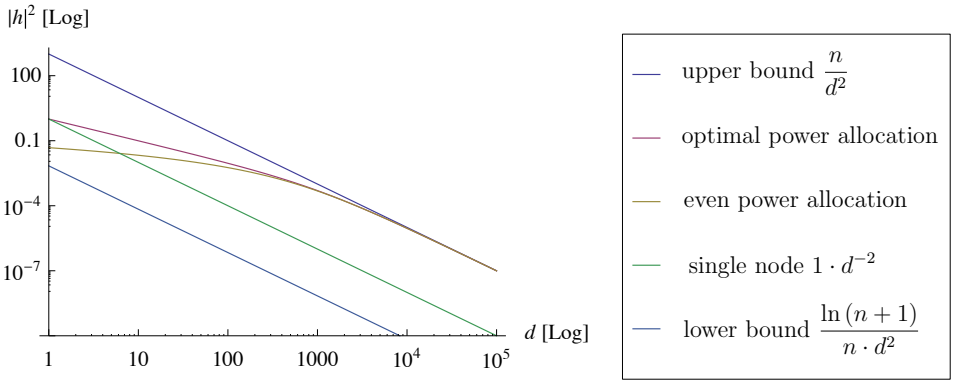

Figure 3.15: Log-Log Plot of the signal power $|h|^2$ of $n = 100$ senders placed on a line at a receiver distance d (see Figure 3.14) for optimum and even power distribution. Compare Lemma 9 for the upper and lower bound (blue).

beamforming gain is smaller than 1 and a single sender with all transmission power at distance d would produce a higher signal strength (green line). For long distances d, the beamforming gain approaches the upper bound with full beamforming gain, illustrated by the blue line with power $\frac{n}{d^2}$ of n senders at distance d.

Beamforming gain of nodes placed equidistantly on a line can be summarized as follows. An infinite number of senders has beamforming gain $\Theta(d)$ at a receiver at distance d when applying the optimal power allocation scheme of Lemma 6. As result, the (power) attenuation reduces to d^{-1} at distance d (a single sender has attenuation d^{-2}). However, the beamforming gain of n senders is $\Theta(\min\{d, n\})$ (Lemma 8) when using an optimal power distribution. In contrast, the beamforming gain g is only $\frac{\ln n}{n} \leq g \leq n$ when applying an even power distribution among the senders (Lemma 9). For long distances $d \gg n$, optimal and even power distribution approach to full beamforming gain n.

3.3.3 Senders Placed in a Rectangular Area

We analyze the beamforming gain of n senders placed in a rectangular area (see Figure 3.16) in the following. The n senders are placed in a grid with grid distance 1 and

dimensions $(w \times b)$ such that $n = w \cdot b$. We consider the signal strength at a single receiver at position $(x, y) = (0, 0)$ and the sender array is placed centered on the x-axis at distance d to the receiver.

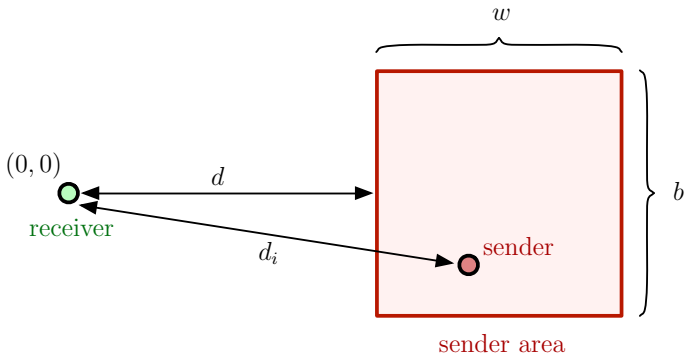

Figure 3.16: Scenario for $n = w \cdot b$ beamforming senders which are placed in a rectangle with dimensions (width $\times$ height) $= (w \times b)$. The distance of the receiver to the rectangle is d.

If all senders are coordinated to perform send beamforming to the receiver, the signal power at the receiver is

$$|h|^2 \quad = \quad \left(\sum_{x=d}^{d+w} \sum_{y=-b/2}^{b/2} \frac{\sqrt{P_i}}{|(x,y)|} \right)^2 .$$

We can upper bound the superposition of the signals of n senders at discrete positions in the grid by the integral over the area. Therefore, we assume a continuous transmission power distribution in the area $P_{(x,y)}$ which results into

$$|h|^2 \quad \leq \quad \int_0^w \int_{-b/2}^{b} \frac{P_{(x,y)}}{\sqrt{(d+x)^2 + y^2}} \, \mathrm{d}y \, \mathrm{d}x \; .$$

When using the optimum power allocation scheme of Lemma 6, we get

$$|h|^2 \quad \leq \quad P_c \cdot \int_0^w \int_{-b/2}^{b/2} \frac{1}{(d+x)^2 + y^2} \, \mathrm{d}y \, \mathrm{d}x \; .$$

The inner integral over y solves to

$$\int_{-b/2}^{b} \frac{1}{(d+x)^2 + y^2} \, \mathrm{d}y \quad = \quad \frac{2 \operatorname{arccot}\left(\frac{2(d+x)}{b}\right)}{d+x} \; .$$

Inserting gives

$$\begin{aligned}
|h|^2 &= \int_0^w \int_{-b/2}^{b} \frac{1}{(d+x)^2 + y^2} \, \mathrm{d}y \, \mathrm{d}x \\
&= \int_0^w \frac{2 \operatorname{arccot}\left(\frac{2(d+x)}{b}\right)}{d+x} \, \mathrm{d}x \\
&= j\mathrm{polylog}\left(2, j\frac{b}{2d}\right) - j\mathrm{polylog}\left(2, -j\frac{b}{2d}\right) \\
&\quad + j\mathrm{polylog}\left(2, -j\frac{b}{2\,(d+w)}\right) - j\mathrm{polylog}\left(2, j\frac{b}{2\,(d+w)}\right)
\end{aligned}$$

where the polylog-function (with first parameter equals 2) is defined as

$$\mathrm{polylog}\,(2, z) = \sum_{i=1}^{\infty} \frac{z^i}{i^2} \; .$$

Replacing gives

$$\begin{aligned}
|h|^2 &= j\sum_{i=1}^{\infty} \frac{\left(j\frac{b}{2d}\right)^i}{i^2} - j\sum_{i=1}^{\infty} \frac{\left(-j\frac{b}{2d}\right)^i}{i^2} + j\sum_{i=1}^{\infty} \frac{\left(j\frac{b}{2(d+w)}\right)^i}{i^2} - j\sum_{i=1}^{\infty} \frac{\left(-j\frac{b}{2(d+w)}\right)^i}{i^2} \\
&= j\sum_{i=1}^{\infty} \frac{\left(-j\frac{b}{2d}\right)^i}{i^2} - \frac{\left(j\frac{b}{2d}\right)^i}{i^2} + j\sum_{i=1}^{\infty} \frac{\left(j\frac{b}{2(d+w)}\right)^i}{i^2} - \frac{\left(-j\frac{b}{2(d+w)}\right)^i}{i^2} \; .
\end{aligned}$$

All terms with an even index i cancel out since

$$(-j)^i - j^i = j^i - (-j)^i = 0 \; .$$

We can use the following conversions to simplify the terms with uneven index value i:

$$\begin{aligned}
j \cdot \left((-j)^i - j^i\right) &= -2 \cdot (-1)^{(i+1)/2} \\
j \cdot \left(j^i - (-j)^i\right) &= 2 \cdot (-1)^{(i+1)/2}
\end{aligned}$$

Then,

$$\begin{aligned}
|h|^2 &= 2\sum_{i=0}^{\infty} \frac{(-1)^{(i+1)/2} \cdot \left(\left(\frac{b}{2(d+w)}\right)^{2i+1} - \left(\frac{b}{2d}\right)^{2i+1}\right)}{(2i+1)^2} \\
|h|^2 &= 2\sum_{i=0}^{\infty} \frac{\left(\frac{b}{2d}\right)^{4i+1} - \left(\frac{b}{2(d+w)}\right)^{4i+1}}{(4i+1)^2} + \frac{\left(\frac{b}{2(d+w)}\right)^{4i+3} - \left(\frac{b}{2d}\right)^{4i+3}}{(4i+3)^2} \; . \qquad (3.14)
\end{aligned}$$

To simplify the series we can use

$$\sum_{i=0}^{\infty} \frac{z^{4i+1}}{(4i+1)^2} - \frac{z^{4i+3}}{(4i+3)^2} = \frac{z}{16} \cdot \Phi\left[z^4, 2, \frac{1}{4}\right] - \frac{z^3}{16} \cdot \Phi\left[z^4, 2, \frac{3}{4}\right] \tag{3.15}$$

where the Lerch transcendent is given by

$$\Phi\left[z, s, \alpha\right] = \sum_{i=0}^{\infty} \frac{z^i}{(i+\alpha)^s} \ .$$

Applying Equation (3.15) to Equation (3.14) gives

$$\begin{aligned} |h|^2 = {} & \tfrac{b}{16d} \cdot \Phi\left[\left(\tfrac{b}{2d}\right)^4, 2, \tfrac{1}{4}\right] - \tfrac{b^3}{64d^3} \cdot \Phi\left[\left(\tfrac{b}{2d}\right)^4, 2, \tfrac{3}{4}\right] \\ & + \tfrac{b^3}{64(d+w)^3} \cdot \Phi\left[\left(\tfrac{b}{2(d+w)}\right)^4, 2, \tfrac{3}{4}\right] - \tfrac{b}{16(d+w)} \cdot \Phi\left[\left(\tfrac{b}{2(d+w)}\right)^4, 2, \tfrac{1}{4}\right] \end{aligned} \tag{3.16}$$

Indeed, the simplified closed-form solution still contains the Lerch-transcendent-function, which makes further analysis difficult. But we can compute the signal power for specific parameters and can plot the function as shown in Figure 3.17 (magenta curve). The optimum power distribution outperforms an even power distribution by a small

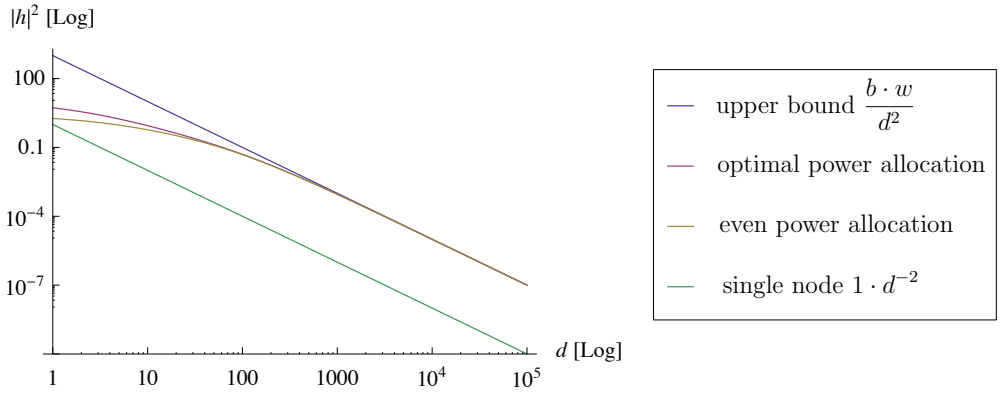

Figure 3.17: Log-Log plot of the optimum signal power of Equation 3.16 for senders placed in a $(w \times b) = (100 \times 10)$-rectangle and a receiver in distance d (see Figure 3.16).

constant factor. Notably, beamforming with an even power distribution outperforms a single node at all distances $d \geq 1$ (green curve) and has a beamforming gain $g > 1$, which was not the case for senders placed on a line (compare Figure 3.15). For both power distributions, full beamforming gain of $b \cdot w = 1000$ with signal power $\frac{b \cdot w}{d^2}$ (blue curve) is approximately reached at distance $d = 1000$. In another experiment with senders placed in a (10×10)-square, we could not spot any performance difference between optimum and even power distribution among the senders.

The plots in Figure 3.18 show the performance for different aspect ratios of the sender rectangle. The rectangles have dimensions $(w \times b) = (n^r, n^{1-r})$ with aspect ratio r, e.g. $r = 0$ is a vertical line with dimensions $(1 \times n)$, $r = 1/2$ is a square with dimensions $(\sqrt{n} \times \sqrt{n})$, and $r = 1$ is a horizontal line $(n \times 1)$. The first graphics in Figure 3.18(a) shows the signal power $|h|^2$ in logarithmic scale for a varying aspect ratio r and several curves are plotted for the receiver's distances $d \in [2, 22, 42, 62, 82]$. We can spot a maximum signal power for a certain aspect ratio r of the senders' rectangle, where the senders are "closest" to the receiver. A rough explanation gives the distance of the sender furthest away from the receiver which is at distance $\sqrt{(d+w)^2 + b^2/4}$. For a close receiver with $d = 1$, the distance to the furthest receiver is for a vertical or horizontal line of receivers $\Theta(n)$ while the distance is only $\sqrt{n}$ for a quadratic area of senders.

Given $n = 100$ sender nodes in a rectangular area, Figure 3.18(b) shows which aspect ratio of the rectangle maximizes the signal strength at a receiver at distance d, e.g. for $d = 50$ it is $r = 0.25$ with dimensions (width $\times$ height) $= (3 \times 33)$. Comparing Figure 3.18(b) with Figure 3.18(a), we can identify the maximum aspect ratio $r' \approx 0.403$ for $d = 2$. Rectangles with an aspect ratio greater than r' turn out to be no optimal choice for any distance d. To see the impact of the rectangle's aspect ratio on the signal power, we see in Figure 3.18(c) what is the gain when choosing the "best" instead of the "worst" aspect ratio at a receiver's distance d. For small d, the gain is up to 7 while for far distant receivers the influence of the aspect ratio drops to nothing with no gain 1.

Summarizing, the beamforming gain of senders placed in a rectangular area in the plane depends on the rectangle ratio (width to height) and the power allocation among senders. A quadratic rectangle might be used for an approximation of senders placed in a disk in the plane. We can solve the signal power of $(w \times b)$ senders and a receiver distance d in a closed-form solution in Equation (3.16) (containing the Lerch-transcendent-function). A visual analysis (Figure 3.17) reveals a dependence of the beamforming gain and the receiver's distance similar to senders placed on a line (Figure 3.15). Main difference is that nodes placed in a rectangular area instead of a line have more beamforming gain at near distant receivers, because the senders are placed with a higher density and a shorter mean distance to the receiver.

We present algorithms in the following Chapter 4, which utilize transmit beamforming to increase the transmission range and speed up routing algorithms. In this regard, we do not attempt to reduce the transmission power of short distant transmissions. Thus, the usage of the optimal distribution of transmission power among beamforming senders will only have a small effect on improving the transmission range. Nevertheless, the optimal power distribution can improve constant factors of the running time of these algorithms, but will not change the asymptotic. We focus in the following on the analysis of the asymptotic behavior of transmission algorithms and assume therefore even power distribution among transmitters.

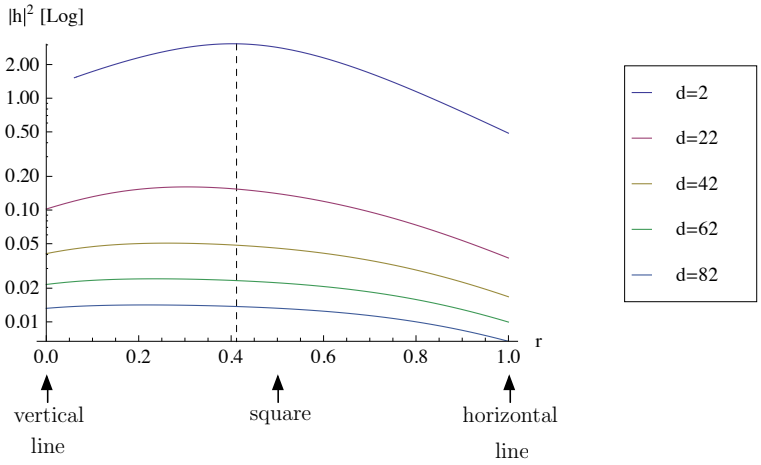

(a) Signal strength $|h|^2$ depending on the rectangle ratio r

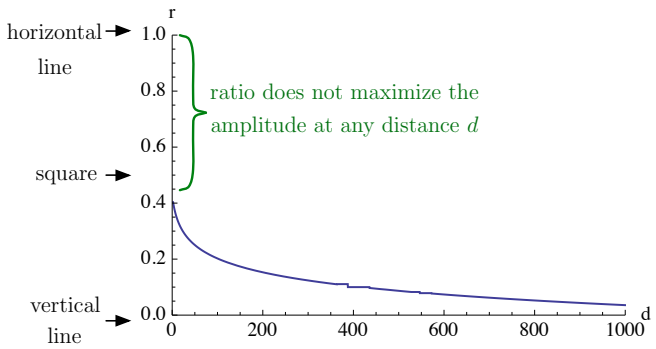

(b) Aspect ratio r maximizes signal power $|h|^2$ at distance d

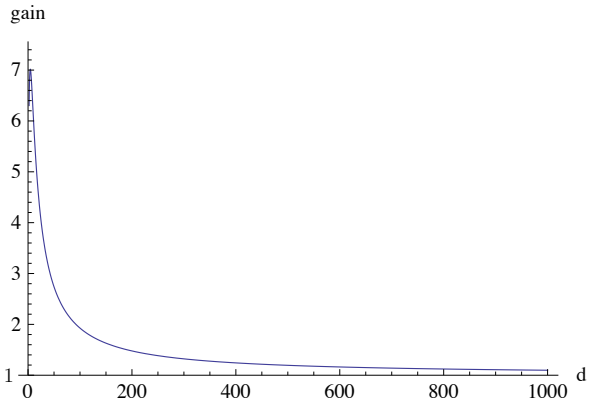

(c) Power gain when using rectangle's aspect ratio with the highest instead of lowest signal strength at a receiver at distance d

Figure 3.18: Send beamforming from $n = 100$ senders placed in a rectangular area with dimensions $\left(n^r \times n^{1-r}\right)$ and aspect ratio r to a receiver at distance d (see Figure 3.16)

3.4 Beamforming Pattern

In the preceding section 3.3, we have concentrated on the beamforming gain of multiple sender antennas at one specific receiver position and have therefore optimized the phase-synchronization and transmission power. In this section, we extend this analysis and characterize the signal strength $|h|$ of the complete radiation pattern. This includes the signal strength in all directions and at all distances. We limit the analysis to the

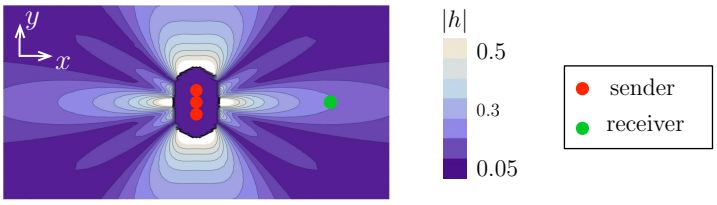

Figure 3.19: Beamforming pattern of three senders performing beamforming to one receiver

far field with distances $d > 2\lambda$ (for wavelength λ) from all sending antennas. In Figure 3.19, the black bordered area around the senders excludes the near field around the senders. While a single antenna has an omnidirectional radiation pattern, we will see that multiple sender antennas in superposition have not. An intuitive explanation therefore is that focusing more transmission power towards a specific receiver position with beamforming reduces in reverse the power towards other directions. The results of this section answer two questions. Firstly, how strong is the interference power of a beamforming sender in other directions than towards the receiver? This is important because the data rate of a communication channel depends on the signal-to-noise-and-interference ratio (SINR). Secondly, how large is the angle range in the radiation pattern with strong beamforming gain and can we reach an area of several receivers with beamforming gain? To come to the point: it is actually possible and we will exploit this feature to broadcast a message to a specific region with beamforming gain (see Chapter 4). We present in this section the results of our article [JS12].

In this section we consider line-of-sight propagation and discuss the geometric properties of beamforming by reference to the geometry of multiple antennas. We choose a random uniform placement of antennas in a disc of diameter d to overcome the shortcomings of a linear equidistant placement. This matches a practical scenario where antennas are non uniformly attached to a device or even are flexible installed. Furthermore, we do not consider the channel matrix $\mathbf{H}$ but directly compute the signal strengths in a given direction. This way, we derive bounds which generally describe the signal beam angle with respect to the antenna geometry parameter d, the wavelength λ, the number of sender/receiver antennas m_s, respectively m_r, and the distance between sender and receiver. We classify the angles into three classes, the main beam which is useful for transmission or reception, the side beams which may cause interferences with other nodes, and the random noise, which adds only little noise to the

system, see Figure 3.20.

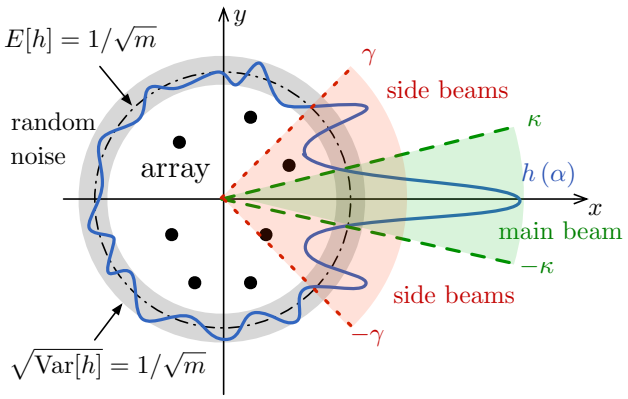

Figure 3.20: Example of seven randomly placed antennas (black dots) in a disc (white disc in the center) which perform send beamforming towards the x-axis. The blue line shows the signal strength $h(\alpha)$ for angle α. The main beam around the sending direction $\alpha = 0$ has angle range $[-\kappa, \kappa]$, side beams are within angle range $[-\gamma, \gamma]$, and we get average white Gaussian noise in other directions.

Problem Setting We consider a network node with m transmit antennas performing beamforming to a single receiver antenna. The corresponding input-output model with multiple inputs X_i with $i \in [1, m]$ of the sending antennas and output Y at the single receiver is

$$Y = \left(\sum_{i=1}^{m} h_i \cdot X_i \right) + w = h \cdot X + w$$

where we assume that all antennas emit the same input signal $X = X_i$ to perform beamforming. The parameter w defines additive white Gaussian noise (AWGN). Thus, the channel from sending antennas located at u_i with $i \in [1, m]$ to receiver position v is defined by

$$h \quad = \quad \sum_{i=1}^{m} h_i = \sum_{i=1}^{m} s_i \cdot \frac{\mathrm{e}^{-j\frac{2\pi}{\lambda}|u_i - v|}}{|u_i - v|}$$

where each sending antenna can have an extra phase shift and attenuation with parameter $s_i \in \mathbb{C}$.

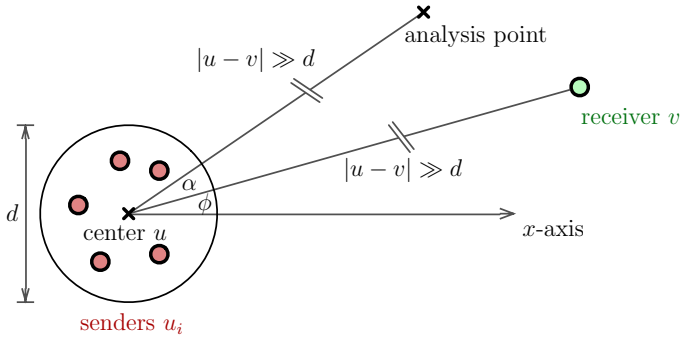

Figure 3.21: Sending antennas u_i with $1 \leq i \leq m$ are randomly placed on a disc with diameter d and center position u. The receiver v is at angle ϕ and distance $|u-v| \gg d$. We analyze the signal at a point at radiation angle $(\phi + \alpha)$

The sending antennas u_i are placed independently and uniformly at random on a disc in the plane with diameter d and position u denotes the centroid of the disc. Thus, the maximum distance between two antennas placed at positions u_i and u_ℓ is

$$d \quad \geq \quad \max_{i,\ell \in [1,m]} |u_i - u_\ell| \,.$$

We require that diameter d is at least $\Omega\left(\lambda \cdot \sqrt{m}\right)$ for carrier wavelength λ and the number of antennas m.

We assume that two communication nodes u and v are in far distance compared to d, i.e. $|u-v| \gg d$. So, we estimate the received signal strengths from all sender antennas u_i with $i \in [1,m]$ at position v as

$$h \quad = \quad \frac{1}{|u-v|} \cdot \sum_{i=1}^{m} s_i \cdot \mathrm{e}^{-j\frac{2\pi}{\lambda}|u_i - v|} \quad . \tag{3.17}$$

In this section, the path loss is not our matter of concern and we set the sender gain to

$$|s_i| := \frac{|u-v|}{m} \quad . \tag{3.18}$$

Let us define the sender's phase shift for beamforming as $\arg s_i := \theta$. Then the channel is specified by

$$h \quad = \quad \frac{1}{m} \sum_{i=1}^{m} \mathrm{e}^{j\left(\theta - \frac{2\pi}{\lambda}|u_i - v|\right)} \quad .$$

If the signals of all senders have the same phase, which is the case for beamforming to receiver position v, the signals add up and we get $h = \left(\frac{1}{m} \cdot m\right) = 1$ and thus we have adjusted the channel gain to 1 for receiver position v. Please note that the total transmission power of all sending antennas is proportional to $\frac{1}{m}$ in this case.

Due to different path lengths $|u_i - v|$ between transmit antenna u_i and a target position v, the signals of the different transmit antennas u_i are time-displaced at v. We only consider the phase shift for the carrier wavelength λ expressed by a complex value $e^{j\kappa}$ with phase angle κ. The phase angle κ effects a modulo computation of the time for propagation $|u_i - v|/c$ between a transmit antenna u_i and position v modulo the period $1/f = \lambda/c$. The superpositioned time-displaced signals of the antennas u_i produce a spatial attenuation of the signal. This effect is called *beamforming* where the signal is strong in certain spatial beams and attenuated otherwise.

In the next Section 3.4.1, we configure the antenna parameters s_i of m sending antennas for a maximum signal strength at a given receiver, i.e. Equation (3.17) is resolved to $Y = X + w$. Then, we identify the angular ranges of the main and side beams (also called side lobes) where such a strong signal can be received (Section 3.4.2). In the remaining angle range, we estimate the attenuated signal by average white Gaussian noise (Section 3.4.3).

The superpositioned output signal of the multiple antennas in Equation (3.17) is calculated from the addition of complex values which can be represented as two-dimensional vectors. When assuming unit power at all antennas, all vectors have unit length and only the angles differ caused by the phase shifts. Figure 3.22 shows

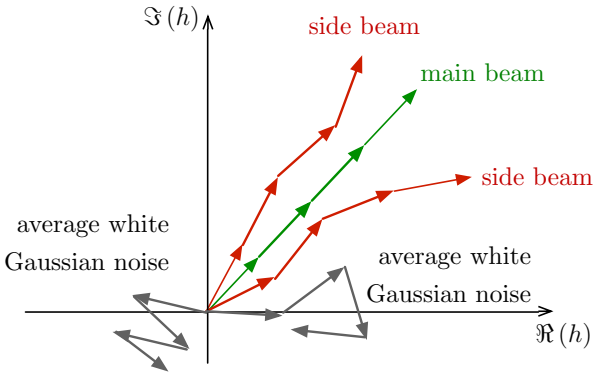

Figure 3.22: Example for calculating the signal strength $h(\alpha)$ with $h = \left(\frac{1}{m} \cdot \sum_i e^{j\beta_i}\right)$ for different angles α. The signal of all antennas has the same signal amplitude $\frac{1}{m}$ (same complex vector length) but different phase angles β_i.

an example for the different cases with maximum signal strength in the main beam where the signals of all antennas arrive with the same phase angle. In the side beams, which are spatially close to the main beam (compare Figure 3.20), the phase angles are again highly correlated. Otherwise for a radiation angle differing more from the target direction ($\alpha \geq \gamma$, see Sec. 3.4.3) we observe random phase angles resulting into a strong attenuated signal which we denote as average white Gaussian noise (dark grey).

3.4.1 Configure Beamforming for Arbitrary Placed Antennas

To achieve maximum signal strength of multiple transmitting antennas at a given target with output $Y = X + w$, one can adjust the phases of the multiple antennas in such a way that they are highly correlated at the target. For that, the signal is delayed at the input antennas in such a way that the delay time plus the transmission time from each antenna to the target is the same. For an explanation consider the antenna array in Figure 3.23 with two antennas positioned at u_1 and u_2 where u_1 has a longer path to the target in direction ϕ than u_2.

Reflections can be seen as additional signal sources but with an attenuated and time shifted signal. The running time from an antenna via a reflecting obstacle to the target and the line-of-sight time from the antenna to the target depend on each other. Thus, we cannot adjust both signals in any way that both arrive at the same time at the target. A reflected signal always arrives delayed at the target in comparison to the line-of-sight signal and produces additional noise. We will only consider the line-of-sight case in the latter.

Now we will define how to set up the phase shifts of an antenna array with arbitrary antenna positions to gain maximum signal strength in a certain target direction. This theoretic approach neglects reflections and similar effects, which is the reason why in existing MIMO systems the measured channel matrix is the target for optimization. Here, we consider the simplified scenario of line-of-sight communication in the plane.

We assume the node-to-target distance to be much larger than the maximum distance of each nodes' antennas. So, the antennas' rays reach the target nearly as parallel lines [2]. Assume a virtual antenna in the centroid of the antenna array $\mathbf{u}$ with phase 0. The target direction of this array is ϕ. The input signal X is shifted in time at all

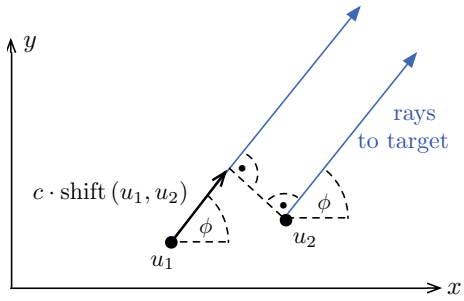

Figure 3.23: Phase shift of $\text{shift}(u_1, u_2, \phi)$ between reference antenna u_1 and antenna u_2 for beamforming towards target direction ϕ (the spatial shift between both antennas towards the target is $c \cdot \text{shift}(u_1, u_2, \phi)$)

[2] When we apply both assumptions of far distant communication nodes and no angular spread between multiple antennas to a MIMO channel, the channel matrix $\mathbf{H}$ has rank 1. Hence, beamforming, respectively the SNR, dominates then the channel capacity.

antennas such that it reaches the target in direction ϕ at the same time. The time shift of each antenna u_i can be derived from a geometrical argument, i.e. the difference of distances between u and u_i and the target divided by the speed of light c. For distant targets this time shift can be approximated by a function depending only on the sender antenna positions and the sending angle ϕ. In Figure 3.23, this time shift is shown for the positions u_1 and u_2 with label $c \cdot \text{shift}(u_1, u_2)$.

Let vector v and angle ϕ describe a ray towards the target. Vector v has an arbitrary non-zero length.

$$v \quad := \quad |v| \cdot \begin{pmatrix} \cos\phi \\ \sin\phi \end{pmatrix}$$

We can use the scalar projection of $(u_i - u)$ and v and angle ϕ to compute the spatial shift

$$c \cdot \text{shift}(u, u_i, \phi) \quad = \quad (u_i - u) \cdot \frac{v}{|v|}$$

where c denotes the speed of light. The time shift or delay is then

$$\text{shift}(u, u_i, \phi) \quad = \quad \frac{(u_x - u_{ix})}{c} \cdot \cos\phi + \frac{(u_y - u_{iy})}{c} \cdot \sin\phi \ . \tag{3.19}$$

Without loss of generality, the centroid is at $(u_x, u_y) = (0, 0)$. So, the phase shift θ of the signal for antenna u_i and a communication partner in direction ϕ is then

$$\text{shift}(u_i, \phi) = \frac{u_{ix}}{c} \cdot \cos\phi + \frac{u_{iy}}{c} \cdot \sin\phi. \tag{3.20}$$

We assume that we send the same signal long enough and therefore we can represent delays as phase shifts. Producing beamforming with these phase shifts gives the output signal $Y = X + w$ at the communication partner.

3.4.2 Characterization of the Main Beam and Side Beams

If we optimize the phases at multiple antennas for the transmission of input signal X in one particular direction, the phase angles around that sending angle are still correlated and not random. The signal strength of the superpositioned output is maximum at the sending angle with $Y = X + w$ and attenuates with increasing angle difference from the sending angle. We claim that the signal strength is proportional to the maximum signal strength in an angle range $\alpha \in [-\kappa, \kappa]$ (see Figure 3.20).

Theorem 5 *The angle range of the main beam tends to $\Theta(\lambda/d)$ when d/λ grows to infinity.*

We analyze the case where multiple antennas perform beamforming towards the target angle ϕ and input signal X has a phase shift on the multiple antennas according to Equation (3.20). To analyze the signal in the angle range $\alpha \in [-\kappa, \kappa]$ around the target direction ϕ (compare Figure 3.21), we insert an additional delay for angle $(\phi + \alpha)$ into the equation to calculate the signal in direction $(\phi + \alpha)$. When adjusting beamforming for target direction ϕ, the transfer function of the channel from the multiple senders towards angle α is

$$h(\phi, \alpha) \quad = \quad \frac{1}{m} \cdot \sum_{i=1}^{m} \mathrm{e}^{-j2\pi f \mathrm{shift}(u_i, \phi)} \cdot \mathrm{e}^{j2\pi f \mathrm{shift}(u_i, \phi+\alpha)} \ .$$

Notice that if the receiver is in target direction ϕ with $\alpha = 0$, both delays in the previous equation eliminate each other and we get the maximum signal strength $|h(\phi, \alpha = 0)| = 1$. Without loss of generality, we set the target direction $\phi = 0$ resulting into

$$\begin{aligned} h(\phi = 0, \alpha) \quad &= \quad \frac{1}{m} \cdot \sum_{i=1}^{m} e^{-j\frac{2\pi}{\lambda}(u_{ix} \cdot (\cos\alpha - 1) + u_{iy} \cdot \sin\alpha)} \\ &\approx \quad \frac{1}{m} \cdot \sum_{i=1}^{m} e^{-j\frac{2\pi}{\lambda} u_{iy} \cdot \alpha} \ . \end{aligned} \tag{3.21}$$

The last approximation in Equation (3.21) uses $\sin\alpha = \alpha$, $\cos\alpha = 1$ for small α. For $\alpha = 0$ all antennas have the same phase angle 0 and varying α rotates the phase angles with different speed depending on the vertical position u_{iy} of the i-th antenna. At

(a) target angle $\alpha = 0$ (b) in the main beam with $\alpha > 0$

Figure 3.24: Complex vectors h_i of senders u_i in the channel with $h(\phi = 0, \alpha) = \sum_i h_i$

direction α the phase angle is then limited by range $[-\tau, \tau]$ with

$$\tau \quad := \quad \frac{2\pi}{\lambda} \cdot d \cdot \alpha.$$

Based on our assumption of randomly distributed antennas we further assume equally distributed phase angles in range $[-\tau, \tau]$. Thus, we can estimate the sum by an integral

over the range $[-d, d]$ resulting into

$$\begin{aligned} h_2(\phi = 0, \alpha) &\approx \frac{m}{m} \cdot \frac{\int_{-d}^{d} e^{-j\frac{2\pi\alpha}{\lambda}y}\, \mathrm{d}y}{2\tau} \\ &= -\frac{m}{m} \cdot \left[\frac{e^{-j\frac{2\pi\alpha}{\lambda}y}}{j\frac{2\pi\alpha}{\lambda} \cdot 2d}\right]_{y=-d}^{d} \\ &= -\left[\frac{\cos\left(-\frac{2\pi\alpha}{\lambda}y\right) + j\sin\left(-\frac{2\pi\alpha}{\lambda}y\right)}{j\frac{2\pi\alpha}{\lambda} \cdot 2d}\right]_{y=-d}^{d} \\ &= \frac{\sin\left(\frac{2\pi\alpha}{\lambda} \cdot d\right)}{\frac{2\pi\alpha}{\lambda} \cdot d} \\ &= \operatorname{sinc}\left(\frac{2d}{\lambda} \cdot \alpha\right). \end{aligned}$$

According to the $\operatorname{sinc}(\cdot)$-function, the main beam is bounded by angle region

$$\alpha \in [-\kappa, \kappa] \text{ with } \kappa = \frac{\lambda}{2d}.$$

For instance, when the antennas are placed on a disc with radius 2λ and a typical wavelength $\lambda = 12.5$ cm the main beam has the range $[-\kappa', \kappa']$ with angle $\kappa' \approx 7$ degree.

Besides, the main beam at $\alpha = 0$ there are recurrent side beams (also called side lobes) at the maxima of the $\operatorname{sinc}(\cdot)$-function. The signal gain of these side beams is limited according to the $\operatorname{sinc}(\cdot)$-function by $\lambda/(2\pi \cdot d \cdot \alpha)$. In the next section, we will show that the side beams are within angle range $[-\gamma, \gamma]$ with $\gamma \approx \frac{\lambda}{d}\sqrt{m}$.

3.4.3 Average White Gaussian Noise Produced by Multiple Antennas

Now we analyze the random noise of a sender with an angle outside of the main and side beams. Recall that for u_i chosen uniformly at random from a disc of diameter d

$$h(0, \alpha) = \frac{1}{m} \cdot \sum_{i=1}^{m} e^{-j\frac{2\pi}{\lambda}(u_{ix} \cdot (\cos\alpha - 1) + u_{iy}\sin\alpha)}. \tag{3.22}$$

Let β_i denote the random variable of the phase angle with

$$\beta_i = \frac{2\pi}{\lambda}\left(u_{ix} \cdot (\cos\alpha - 1) + u_{iy}\sin\alpha\right) .$$

Figure 3.25 shows the distribution of this random variable for wavelength $\lambda = 2\pi$.

Note that for growing d/λ the range of the random variable increases linearly. Let $[-\ell, \ell]$ denote the range of β_i. The maximum value for ℓ is $\frac{4\pi}{\lambda}d$, for small α. We can approximate ℓ by $\ell \approx (\frac{2\pi}{\lambda}\alpha d)$, since $\sin\alpha \approx \alpha$ and $\cos\alpha \approx 1$ for small α.

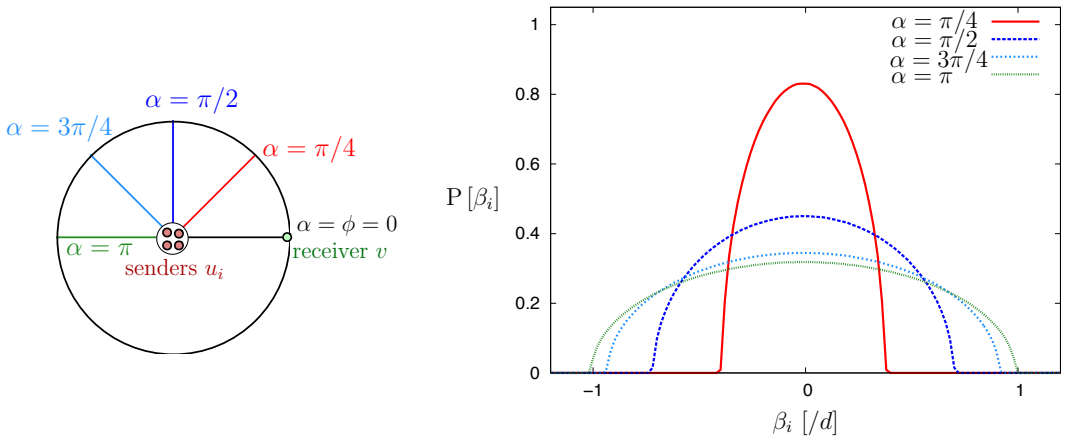

(a) radiation angles α (b) addition of complex values h_i

Figure 3.25: Probability distribution of phase angle β_i in $\sum_i e^{-j\beta_i}$ of Equation (3.21). For illustration purposes only, we set $\lambda = 2\pi$ and the angle range is $\beta_i/d \in [-1, 1]$.

We approximate this random variable by a uniform distribution over $[-\ell, \ell]$. The following Lemma shows that for $\ell \geq 2\pi\sqrt{m}$ the absolute value of the random variable H has an expectation of at most $\frac{a}{\sqrt{m}}$ and a standard deviation of $2\frac{a}{\sqrt{m}}$. For uniform β_i the signal strength can be reduced to the length of a 2-dimensional geometric random walk with unit steps in the plane. Here, the diameter d of the disk for antenna placement has to be in the order of $\Omega(\lambda \cdot \sqrt{m})$ that the phase angles β_i are uniformly distributed.

Lemma 10 *Let $H_{m,\ell} := \sum_{i=1}^{m} e^{j\beta_i}$ for uniformly distributed β_i from $[-\ell, \ell]$.*

1. $\mathbb{E}\left[|H_{m,\ell}|^2\right] = \frac{1}{m}$ *for $\ell \neq 0$ which are a multiples of 2π*
2. $\mathbb{E}\left[|H_{m,\ell}|\right] = \mathcal{O}\left(\frac{1}{\sqrt{m}}\right)$ *for all $\ell \geq 2\pi\sqrt{m}$*
3. $\mathbb{E}\left[|H_{m,\ell}|^2\right] = \mathcal{O}(m)$ *for all ℓ*

Proof: If $\ell > 0$ is a multiple of 2π all angles are uniformly distributed. A two-dimensional geometric walk starts at $s_0 = (0, 0)$ and continues for m steps at points $s_1, \ldots, s_m$ where each step $s_{i+1} - s_i$ has unit length and an independently randomly chosen direction. Such geometric walks have been studied for a long time, see [MW40] and the following theorem is well-known and its proof can be found in standard text-books.

Each vector s_i with length $\frac{1}{m}$ and direction β_i can be represented as complex value $s_i = \frac{1}{m}e^{j\beta_i} = \frac{1}{m} \cdot (j \sin\beta_i + \cos\beta_i)$ where $j = \sqrt{-1}$. The distance between start and end point of the random walk is then the vector length of the sum of all vectors.

$$h = \frac{1}{m}\sum_{i=1}^{m} e^{j\beta_i} \tag{3.23}$$

Let $\overline{h}$ denote the complex conjugate of h.

$$\begin{aligned} |h|^2 &= h \cdot \overline{h} \\ &= \underbrace{\frac{1}{m}\sum_{i=1}^{m} e^{j\beta_i}}_{h} \cdot \underbrace{\frac{1}{m}\sum_{k=1}^{m} e^{-j\beta_k}}_{\overline{h}} \\ &= \frac{1}{m^2}\sum_{i=1}^{n}\sum_{k=1}^{m} e^{j(\beta_i-\beta_k)} \\ &= \frac{1}{m} + \frac{1}{m^2}\sum_{i=1}^{m}\sum_{\substack{k=1,\\ i\neq k}}^{m} e^{j(\beta_i-\beta_k)} \end{aligned}$$

For each index tuple (i,k) with $i \neq k$ there exists a symmetric (k,i) with the negated imaginary value.

$$\forall i \neq k: \qquad \Im\left(e^{j(\beta_i-\beta_k)}\right) + \Im\left(e^{j(\beta_k-\beta_i)}\right) = 0$$

So, we get only a sum of real numbers.

$$\sum_{i=1}^{n}\sum_{\substack{k=1,\\ i\neq k}}^{n} e^{j(\beta_i-\beta_k)} = \sum_{i=1}^{n}\sum_{\substack{k=1,\\ i\neq k}}^{n} \cos\left(\beta_i - \beta_k\right)$$

We have assumed that angles $\beta_i \in [0, 2\pi)$ are independently, identically and uniformly distributed over $[0, 2\pi)$. So the expectation of $\cos(\beta_i)$ is

$$\frac{1}{2\pi}\int_{\beta=0}^{2\pi} \cos\beta \ \mathrm{d}\beta = 0 \ .$$

And, the expected value of the sum is

$$\begin{aligned} \mathbb{E}\left[|H_m|^2\right] &= \frac{1}{m} + \frac{1}{m^2}\sum_{i=1}^{n}\sum_{\substack{k=1,\\ i\neq k}}^{n} \underbrace{\mathbb{E}\left[\cos\beta_i - \beta_k\right]}_{0} \\ \Rightarrow \mathbb{E}\left[|H_m|^2\right] &= \frac{1}{m} \ . \end{aligned}$$

The root mean square of $|h|$ is therefore

$$|H_m|_{\mathrm{rms}} = \frac{1}{\sqrt{m}} \ .$$

For the expectation there is no closed form known. Notice that even for small number of hops the analysis is complex, i.e. for $m \leq 4$, see [BNSW09]. A good approximation

has been presented in 1905 by Lord Rayleigh [PL05] with the the probability distribution $\frac{2x}{m}e^{-x^2/m}$ for large m. The expectation of this approximation is $\frac{1}{2}\sqrt{\pi}\sqrt{m}$. Using the local central limit theorem leads to Proposition 2.1.2 (2.7) in [LL10]:

$$\text{Prob}\left[|H_m| \geq s/\sqrt{m}\right] \quad \leq \quad c \cdot \mathrm{e}^{-\beta s^2}$$

in accordance with Rayleigh's approximation for some positive constant c and β. So, $\mathbb{E}\left[(\right]|H_m|) = \mathcal{O}\left(1/\sqrt{m}\right)$ follows from this proposition.

If ℓ is not a multiple of 2π, note that $\mathbb{E}\left[|H_{m,\ell}|\right]$ is possibly non-zero. We observe for $\beta_i \in [-\underline{\ell}, \underline{\ell}]$ for $\underline{\ell} = 2\pi\left\lfloor \ell/(2\pi)\right\rfloor$ the expectation above. The other case happens with probability $(\ell - \underline{\ell})/\ell \leq 2\pi/\ell$. So, the expected value of $|\beta_i|$ is at most $2\pi/\ell$. So, the overall expected number of $|H_{\ell,m}|$ is bounded by $2\pi m/\ell$. For $\ell > 2\pi\sqrt{m}$ we have

$$\mathbb{E}\left[|H_{\ell,m}|\right] \quad \leq \quad \frac{1}{\sqrt{m}} \; .$$

Therefore the standard deviation for general ℓ remains $\mathcal{O}\left(\sqrt{m}\right)$ since the random variables β are independent. □

Clearly the distribution of phases differs from the uniform distribution. However, the simulations of the next section give some evidence that this behavior also holds for the correct distribution. For $\ell \geq 2\pi\sqrt{m}$ and $\ell \approx \frac{2\pi}{\lambda}\alpha d$ (for small enough α) we get $\alpha \geq \frac{\lambda}{d}\sqrt{m}$ as the minimum angle for the random noise area. This bounds the side beams in our model to be within an angle range $[-\gamma, \gamma]$ with $\gamma \approx \frac{\lambda}{d}\sqrt{m}$.

To this point we have only considered directed sending with beamforming. When we also consider, that the receiver has directed reception with multiple antennas in a random direction, the overall attenuation of interference is

$$h \quad = \quad \underbrace{\frac{1}{\sqrt{m}}}_{\text{sender}} \cdot \underbrace{\frac{1}{\sqrt{m}}}_{\text{receiver}} = \frac{1}{m} \; .$$

Conjecture 1 *In SIMO (Single Input Multiple Output) the expected noise produced by a sender with a single antenna is $\mathcal{O}\left(1/\sqrt{m}\right)$ when the receiver has m multiple antennas randomly placed in the plane on a disk with diameter d and the receiving angle is at random.*

Conjecture 2 *In MISO (Multiple Input Single Output) the expected noise produced by a sender with m multiple antennas randomly placed in the plane on a disk with diameter d is $\mathcal{O}\left(1/\sqrt{m}\right)$ at a receiver with a single antenna when the sending angle is at random.*

Conjecture 3 *In MIMO (Multiple Input Multiple Output) the expected noise produced by a sender with m_s multiple antennas randomly placed in the plane on a disk with*

diameter d is $\mathcal{O}\left(1/\left(\sqrt{m_s}\cdot\sqrt{m_r}\right)\right)$ at a receiver with m_r multiple antennas randomly placed in the plane on a disk with diameter d when sending respectively receiving angle are at random. If sender and receiver antennas are homogenous with $m = m_r = m_s$ the noise is $\mathcal{O}(1/m)$.

3.4.4 Simulation

In this section, we present numerical simulations to support the estimations presented in the analysis. In a first experiment (Figure 3.26), we illustrate the complex vector

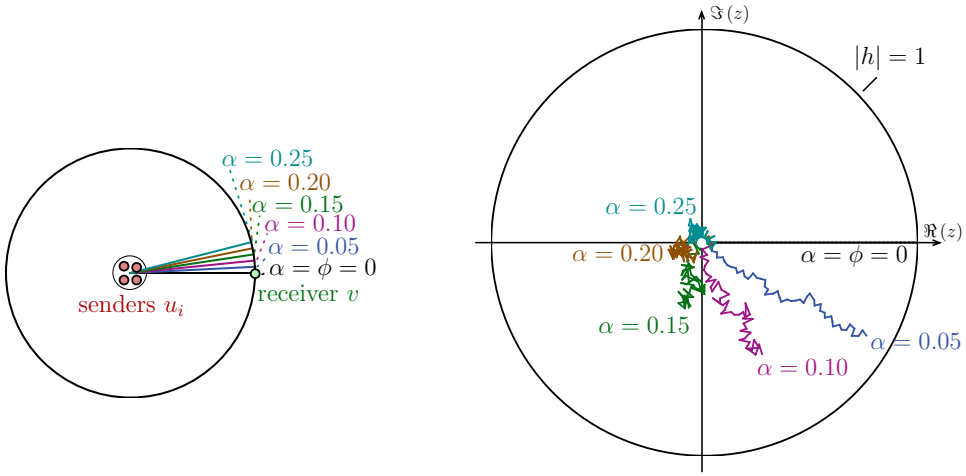

(a) radiation angles α (b) addition of complex values h_i

Figure 3.26: Beamforming of $m = 50$ senders u_i to a single receiver v at angle $\phi = 0$. Figure (b) shows the addition of signals in the channel $h = \sum_{i=1}^{m} h_i$ for radiation angle α

addition $h = \left(\frac{1}{m}\sum_{i=1}^{m} e^{j\beta_i}\right)$ of Equation (3.23). The beamforming is adjusted for a receiver at angle $\phi = 0$ and we see the addition for angle $\alpha = \{0, 0.05, 0.1, 0.15, 0.2, 0.25\}$. For a radiation angle equal to the receiver angle with $\alpha = \phi = 0$, all vectors h_i have the same argument and we see in Figure 3.26(b) a black straight line. For growing α

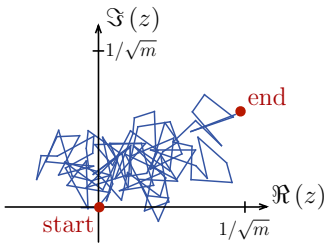

Figure 3.27: Random walk with $m = 100$ steps and step length $1/m$

the range of phase angles β_i also increases and the total path of added vectors gets shorter. For $\alpha \geq 0.2$ the path "wanders" around the origin. In enlarged view, we can see a pure random walk of 100 steps in Figure 3.27.

Figure 3.28 shows the angle-dependent signal strength of a multiple antenna array where angle $\alpha = 0$ is the sending direction for directed communication. The signal strengths are mean values of several random placement with maximum value 1 and computed for infinite distant targets to obtain our assumptions without an error. We compute the radiation pattern for different numbers of antennas $m \in$

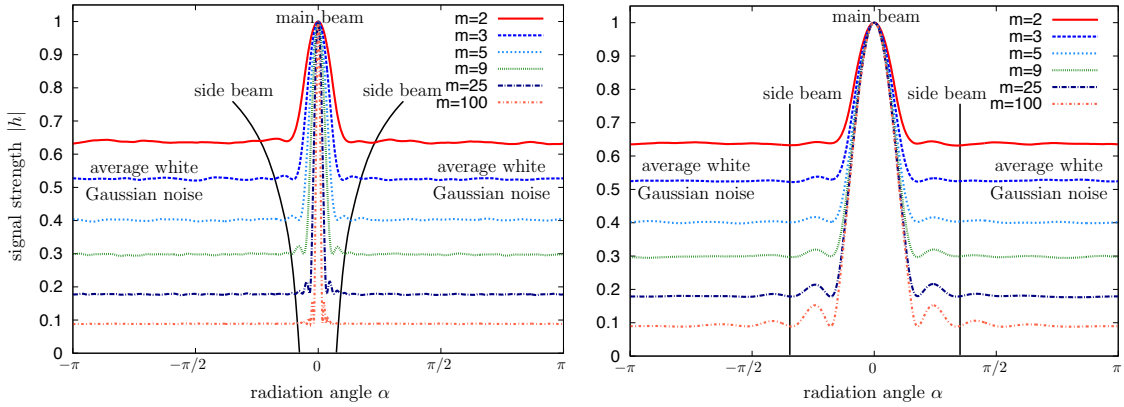

(a) $d = 2\lambda\sqrt{m}$ (b) $d = 2\lambda$

Figure 3.28: mean angular signal strength $|h|$ in the plane for varying number of antennas m and disc diameter d for antenna placement. Angle $\alpha = 0$ is the target direction.

$\{2, 4, 6, 8, 10, 100, 1000\}$. For each number of antennas we average over $10,000$ simulations with a random positioned antenna array and a random transmission direction. The random noise aside from the main and side beams is $1/\sqrt{m}$ as expected, i.e. $m \approx |h|^{-2}$ (for instance $100 = 0.1^{-2}$, $25 = 0.2^{-2}$, $9 = 0.3^{-2}$). The diameter of the antenna arrays in Figure 3.28(a) is $d = 2\lambda\sqrt{m}$. The angle range of the main beam around $\alpha = 0$ decreases with increasing number of antennas. Especially for a high number of antennas one can spot two major side beams around the main beam. The distances of the side beams to the transmission direction $\alpha = 0$ also decrease with increasing number of antennas because of an increasing disc diameter d. In the next experiment in Figure 3.28(b), we keep the disc area constant with a diameter of $d = 2\lambda$ instead of increasing the area with the number of antennas m. The result shows that the main and side beams have for all numbers of antennas m the same angle range. But the average white Gaussian noise decreases with $1/\sqrt{m}$ and strength of the side beam increases with increasing number of antennas m.

In the simulation presented in Figure 3.29, we keep the number of antennas constant to $m = 9$ and vary the disc area by increasing the disc diameter $d = k \cdot 2\lambda \cdot \sqrt{m}$ with a constant factor $k \in \{0.1, 0.3, 0.5, 0.7, 0.9\}$. The average white Gaussian noise keeps the

same for all chosen k but the angle range of the main beam and side beams decreases with increasing disc diameter d.

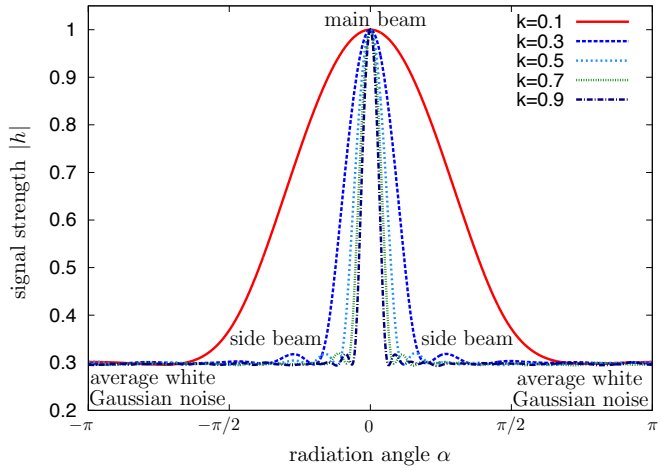

Figure 3.29: mean angular signal strength $|h|$ in the plane for $m = 9$ sending antennas. Angle $\alpha = 0$ is the target direction. The disc for antenna placement has diameter $d = 2k \cdot \sqrt{m} \cdot \lambda$.

The signal strength in target direction $\alpha = 0$ is set up to be maximum and thus has variance 0 for random antenna placements under the given assumptions. We analyze the variance of the signal strength in the range of average Gaussian noise with angle $\alpha = \pi$ in Figure 3.30. We test the signal strength $|h|$ for the number of antennas $m \in [2, 1000]$ and $10,000$ random antenna placements each. The blue colored function

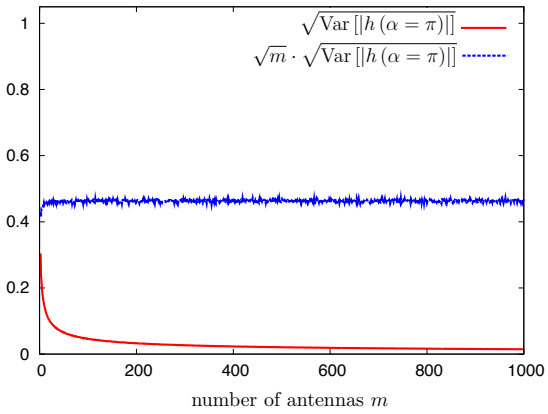

Figure 3.30: standard deviation $\sqrt{\text{Var}\,[|h|]}$ of signal strength $|h|$ at angle $\alpha = \pi$ when $\alpha = 0$ is the target direction. We estimate the average white Gaussian noise to be in $\mathcal{O}\,(1/\sqrt{m})$.

is the standard deviance of the normalized signal strength $|h|$ multiplied with $\sqrt{m}$ and turns out to be constant with the conclusion of an average white Gaussian noise in the order of $1/\sqrt{m}$ as expected.

Only considering angular transmission simplifies indeed the network model since we only need to know the direction of the target and not the actual location with additional distance information. But neglecting the distance leads to a small angle error resulting in not completely synchronized phases in the main beam. Figure 3.31 shows the simulation results for the signal strength in the main beam depending on the distance between the multiple antenna array and the target location. There is no attenuation due to path loss because the sender gain $|s_i|$ is adjusted accordingly (Eq. 3.18). This is the result likewise for MISO and SIMO with communication between m multiple antennas with a single antenna. The m multiple antennas are randomly placed on a disc with diameter $d = 2\lambda$ with the wavelength λ. The distance between the array and the single antenna is measured from the centroid of the disc. The

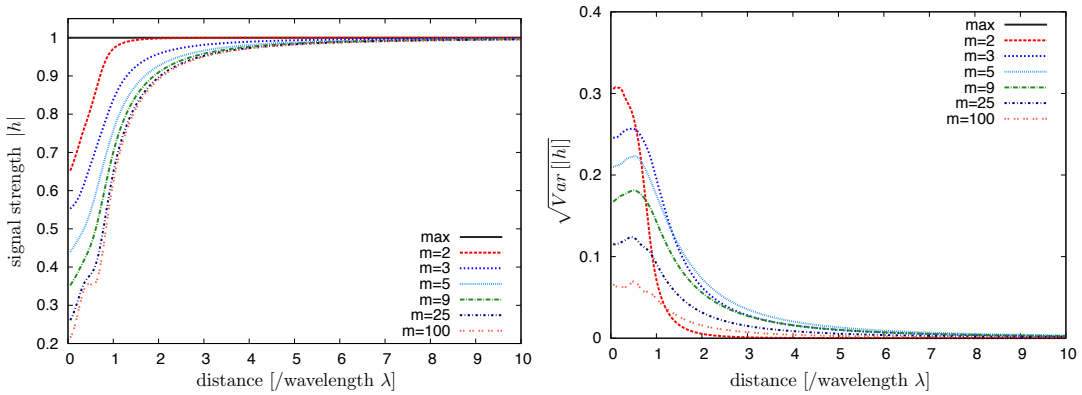

(a) Mean normalized signal strength $|h|$ (b) Standard deviation of signal strength $|h|$

Figure 3.31: The beamforming setup with Equation (3.20) for a target direction only causes a phase error depending on the distance to the target. This leads to an attenuation of the signal strength $|h|$, where m denotes the number of antennas.

estimation error is maximum when placing the target position in the centroid of the disc of the antenna array with distance 0. Here, the signal strength $|h|$ decreases with $1/\sqrt{m}$ comparable to the average white Gaussian noise in a random direction. With increasing distance the error fades away and the signal strength converges to the maximum value possible, that is 1.

In summary, we analyze in this section the beamforming gain of m multiple antennas placed independent at random in a disk with diameter $d \in \Omega\left(\lambda \cdot \sqrt{m}\right)$ for wavelength λ of the carrier. We classify the angles into three classes: the main beam is useful for transmission or reception and has an angle range $[-\kappa, \kappa]$ with $\kappa = \lambda/\left(2d\right)$ around the target angle ; besides the main beam there are side beams that may cause interferences with other nodes; Beyond an angular deviation of $\frac{\lambda}{d}\sqrt{m}$ from the target direction, the random noise range adds only little noise to the system. Another conclusion is that the beamforming capabilities can be improved by increasing the distance between the antennas or using frequencies with smaller wavelengths.

3.5 Maximum Electromagnetic Field Strength

We can use beamforming to enhance the transmission distance. For that, beamforming concentrates transmission power on a beam towards the target position and increases the signal-to-noise ratio which might have a high path loss over a long distance. A longer transmission distance can mean faster routing in a multi-hop routing if less hops are needed. But on the other hand, when enabling communication with beamforming, there should not be any spots where the electromagnetic field exceeds certain limits, e.g. governmental regulated limits of electromagnetic radiation. The path loss is $1/d^2$ for distance d in the free-space model and hence the highest power is right next to an antenna. To reduce the power of one strong antenna covering a huge area, one can

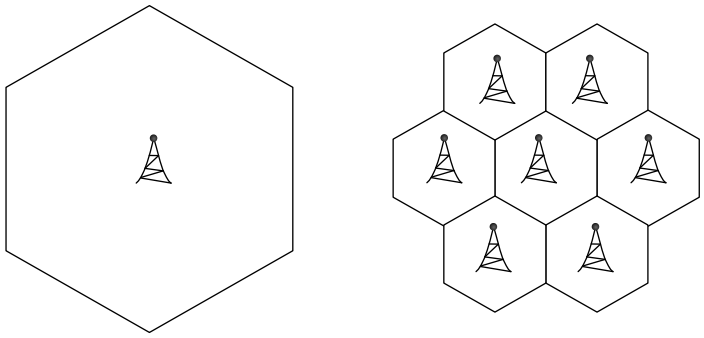

(a) large cell $k = 1$ (b) small cells $k = 7$

Figure 3.32: Example for covering an area with either one strong antenna (a) or several weak antennas (b).

fragment the area into k cells with equal size and an antenna with reduced power of factor $\Theta(1/k)$ (see Figure 3.32). With multiple antennas performing beamforming, we basically do the same and spread the transmission power on multiple antennas in some area. The difference is that we couple the multiple senders to increase the reception distance. In the following, we will give upper-bounds for the signal power of the coordinated multiple senders. The bounds are only rough estimates since we will assume perfect signal correlation with same phase at a spot with maximum signal power. We present in the next Chapter (4) transmissions schemes, which use send beamforming to transmit to far distant receivers. Therefore, we analyze in this section the maximum electromagnetic field strengths. The results of this section show which causes the strongest field strength: this can be either the strong signal in the vicinity of a sender or the strength of the entire super-positioned field of multiple senders.

3.5.1 Senders Placed on a Line

In the following, we determine the maximum signal power for beamforming with senders placed on a line and analyze in which case the array of beamforming senders has

a higher impact on the signal power than the peak values in the vicinity of antennas.

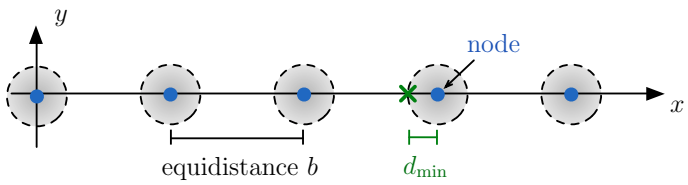

Figure 3.33: Beamforming senders (blue dots) are placed along the x-axis with equidistance b. The grey-shaded areas around the nodes with radius $d_{\min}$ are excluded in the analysis and denote the minimum distance from a sender (where the far-field assumption holds).

Lemma 11 *Consider ℓ nodes placed on a line with equidistance b, each node has the same transmit power P_0, and $d_{\min}$ defines the minimum distance we can approach an antenna where the far-field assumption is satisfied. The signal power in the vicinity of an antenna in distance $d_{\min}$ is $\mathcal{O}\left({d_{\min}}^{-2} + \ln \ell\right)$ and the signal of the antenna at distance $d_{\min}$ is stronger than the signal of the remaining field if $b \in o\left(d_{\min} \cdot \ln \ell\right)$.*

Proof: In the following we will upper bound the signal power. First consider two nodes placed at $(0,0)$ and $(b,0)$. The signal power is then

$$|h(x)| = \sqrt{P_0} \cdot \left(\frac{e^{-j2\pi \frac{|x|}{\lambda}}}{x} + \frac{e^{-j2\pi \frac{|x-b|}{\lambda}}}{|x-b|} \right) \leq \sqrt{P_0} \cdot \left(\frac{1}{|x|} + \frac{1}{|x-b|} \right)$$

We get three domains for x with $x < 0$, $0 < x < b$, and $x > b$. The strongest signal is clearly between both antennas. For this range, the derivation is

$$\frac{\partial |h(x)|^2}{\partial x} = -\sqrt{P_0} \left(\frac{1}{x^2} - \frac{1}{(b-x)^2} \right)$$

which is zero for $x = b/2$ which is a minimum. So we get the highest signal value when approaching one of the antennas. Let $d_{\min}$ denote the smallest distance to an antenna with $d_{\min} \geq 2\lambda$ to satisfy the far-field assumption. Then the maximum signal strength is

$$\max |h(x)| \leq \sqrt{P_0} \left(\frac{1}{d_{\min}} + \frac{1}{b - d_{\min}} \right) .$$

Now consider the node placement in Figure 3.33 where ℓ nodes are positioned equidistant on the line with distance b and position $u_i = (b \cdot i, 0)$ for $i \in \{1, \ell - 1\}$. The nodes perform beamforming towards the x-axis. To upper-bound the signal power at all places, let us assume for the moment that the signals of all nodes have the same

phase. In this case, we can additionally reduce the analysis of the upper bound to the case $y = 0$ because the path loss is larger for $y \neq 0$ and it holds

$$|h(x, y = 0)| \geq |h(x, y \neq 0)| \ .$$

The signal power is then along the x-axis

$$|h(x)| \ \leq \ \sqrt{P_0} \sum_{i=0}^{\min(\ell-1, \lfloor x/b \rfloor)} \frac{1}{x - b \cdot i} + \sqrt{P_0} \sum_{i=\min(\ell-1, \lceil x/b \rceil)}^{\ell-1} \frac{1}{b \cdot i - x} \ .$$

We have used the far field-assumption and thus $|x - b \cdot i| > 2\lambda$ for $i \in \{1, 2, \ldots, \ell\}$. Let us assume without loss of generality that ℓ is odd. Then, we get the maximum signal strength when approaching the node in the middle (from the right).

$$\begin{aligned}
|h(x)| \ &\leq \ \underbrace{2\sqrt{P_0} \left(\sum_{i=0}^{(\ell-1)/2-1} \frac{1}{x - b \cdot i} \right)}_{\text{remaining nodes}} + \underbrace{\frac{\sqrt{P_0}}{x - (\ell - 1)/2}}_{\text{node next to } x} \\
&\leq \ 2\frac{\sqrt{P_0}}{b} \left(\sum_{i=1}^{(\ell-1)/2} \frac{1}{i} \right) + \frac{\sqrt{P_0}}{x - (\ell - 1)/2} \\
&\leq \ \sqrt{P_0} \left(\frac{2}{b} \left(\ln \left(\frac{\ell - 1}{2} \right) + o(1) \right) + \frac{1}{d_{\min}} \right) \\
|h(x)| \ &\leq \ \sqrt{P_0} \left(\frac{2}{b} \left(\ln(\ell) + o(1) \right) + \frac{1}{d_{\min}} \right) \text{ with } \ell > 2 \qquad (3.24)
\end{aligned}$$

If we want to assure that the next antenna for a position x is dominant for the signal strength, the second term has to be greater

$$\frac{2}{b} \left(\ln \left(\frac{\ell - 1}{2} \right) + o(1) \right) \ \leq \ \frac{1}{d_{\min}} \ .$$

From this, it follows that

$$b \ \geq \ 2d_{\min} \left(\ln \left(\frac{\ell - 1}{2} \right) + o(1) \right)$$

with asymptotic approximation $b \in o(d_{\min} \cdot \ln \ell)$. □

Corollary 4 *Consider an invariant of Lemma 11, where ℓ nodes are placed with equidistance, and only each b-th node is an active sender with power $(b^2 \cdot P_0)$ to reach the b-th next neighbor. Assume we can approach an antenna up to distance $d_{\min}$ (where the far-field assumption is satisfied). Then the maximum signal power are local peak values in close distance $d_{\min}$ to senders if $b \in o(d_{\min} \cdot \ln \ell)$.*

A larger value for b causes a higher overall transmission power and increases the effect of local maxima in the vicinity of senders with a sending power that is stronger by factor b^2. So, we can control with b the density of senders and what dominates in the maximum field strength – the super-positioned field of beamforming or single nodes with a strong signal strength in the vicinity. In Section 4.2, we will see that the transmission distance for beamforming with $\frac{\ell}{b}$ nodes on the line and power $(b^2 \cdot P_0)$ each is invariant from b.

3.5.2 Senders Placed in a Grid

Consider ℓ senders which are placed in a grid in the plane with grid distance b.

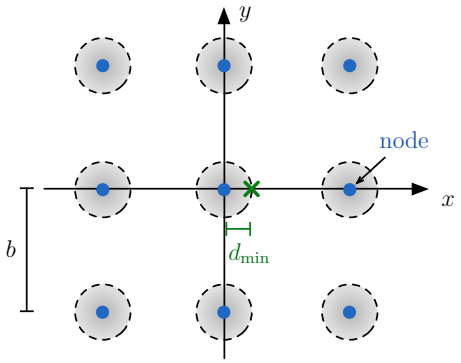

Figure 3.34: Beamforming senders (blue dots) are placed in a square grid with distance b. The grey-shaded areas around the nodes with radius $d_{\min}$ are excluded in the analysis and denote the minimum distance from a sender (where the far-field assumption holds).

Lemma 12 *Assume ℓ nodes are placed in a grid with size $\sqrt{\ell} \times \sqrt{\ell}$ and grid distance b and all nodes send a signal with power $\sqrt{P_0}$. If the signal is synchronized at the center of the grid with same phases, the signal strength at the center is $(k\sqrt{P_0 \cdot \ell}/b)$ respectively power $(k^2 P_0 \ell / b^2)$ for some constant $k > 1$. The maximum signal power is driven by local peak values in close distance $d_{\min}$ of senders if $b \in o\left(d_{\min} \cdot \sqrt{\ell}\right)$.*

Proof: Given ℓ nodes in a grid with size $\sqrt{\ell} \times \sqrt{\ell}$ and grid distance b, the signal strength in the center is

$$\begin{aligned} |h| &= \frac{4\sqrt{P_0}}{b} \cdot \sum_{x=1/2}^{(\sqrt{\ell}-1)/2} \sum_{y=1/2}^{(\sqrt{\ell}-1)/2} \frac{1}{\sqrt{x^2+y^2}} \\ &\leq \frac{8\sqrt{P_0}}{b} \cdot \int_{x=0}^{\sqrt{\ell}/2} \int_{y=0}^{\sqrt{\ell}/2} \frac{1}{\sqrt{x^2+y^2}} \, \mathrm{d}y \, \mathrm{d}x \\ &= \frac{k'\sqrt{P_0 \cdot \ell}}{b} \end{aligned}$$

with $k' = 4 \ln\left(2 + \sqrt{8}\right)$. Now consider the field strength of a spot at distance $d_{\min}$ to a node at the center producing a field strength $1/d_{\min}$. The influence of this node is the same as the field strength of the remaining multiple senders if

$$\frac{1}{d_{\min}} \geq \frac{c'\sqrt{P_0 \cdot \ell}}{b} \Rightarrow b \in o\left(d_{\min} \cdot \sqrt{\ell}\right) .$$

□

While factor $\ln(\ell)$ in Lemma 11 can be approximated as a constant in most practical scenarios, the $\sqrt{\ell}$ in Lemma 12 might not. Thus, when multiple senders are placed in the small area of a quadratic grid the concentration of senders in that area is high and produces local maxima of strong field strengths in the area of senders. In Section 4.3, we present a routing algorithm where nodes in a rectangular area collaborate for beamforming. Fortunately, the rectangular shaped areas are not square-shaped and thus the concentration of senders is less.

Lemma 13 *Assume ℓ sender nodes that are placed in a grid with grid distance b and an area $(b^2 \cdot \ell)$ with width $\left(b \cdot k^{-\frac{1}{3}} \cdot \ell^{\frac{2}{3}}\right)$ and height $\left(b \cdot k^{\frac{1}{3}} \cdot \ell^{\frac{1}{3}}\right)$. The signal power is $\mathcal{O}\left(\ell^{2/3} \cdot \ln \ell + {d_{\min}}^{-2}\right)$ at a position with distance $d_{\min}$ to the next antenna. The signal power driven by the next antenna at distance $d_{\min}$ (where the far-field assumption still holds) if $b \in o\left(d_{\min} \cdot \sqrt[3]{\ell} \cdot \ln \ell\right)$.*

Proof: Consider a rectangular area of senders with dimensions $(w \times h)$ with

$$\begin{aligned} w &= b \cdot k^{-\frac{1}{3}} \cdot \ell^{\frac{2}{3}} \\ h &= b \cdot k^{\frac{1}{3}} \cdot \ell^{\frac{1}{3}} \end{aligned}$$

where $k \geq \lambda/4$ for wavelength λ (see Equation (4.10)). The senders perform beamforming to a target alongside to the width of the rectangle. We can upper bound the signal strength of each line with Equation 3.24 to

$$\begin{aligned} |h_{\text{line}}| &\leq \sqrt{P_0}\left(\frac{2}{b}\left(\ln\left(w/b\right) + o\left(1\right)\right) + \frac{1}{d_{\min}}\right) \text{ with } w > 2 \\ &\leq \sqrt{P_0}\left(\frac{2}{3b}\left(2\ln\left(\ell\right) + \ln\left(k\right) + o\left(1\right)\right) + \frac{1}{d_{\min}}\right) . \end{aligned}$$

Having h lines in the rectangle we have an overall upper bound of

$$|h_{\text{rect}}| \leq \sqrt{P_0}\left(\frac{2k^{\frac{1}{3}} \cdot \ell^{\frac{1}{3}}}{3b}\left(2\ln\left(\ell\right) + \ln\left(k\right) + o\left(1\right)\right) + \frac{1}{d_{\min}}\right) .$$

When considering the wavelength in variable k as given constant, the asymptotic approximation in the number of nodes ℓ is $b \in o\left(d_{\min} \cdot \sqrt[3]{\ell} \cdot \ln\left(\ell\right)\right)$. □

From Corollary 1, we know that ℓ nodes can increase the transmission range by factor ℓ when applying collaborative beamforming. In a network with n nodes, where the nodes are placed in a grid with grid distance g and dimensions $(g\sqrt{n}) \times (g\sqrt{n})$, we only need $\Theta(\sqrt{n})$ nodes collaborating for send beamforming to transmit to any point in the network. Combining this with Lemma 13, we get the following corollary.

Corollary 5 *Assume that only nodes in a rectangular area with a maximum size of width* $\left(b \cdot k^{-\frac{1}{3}} \cdot n^{\frac{1}{3}}\right)$ *and height* $\left(b \cdot k^{\frac{1}{3}} \cdot n^{\frac{1}{6}}\right)$ *collaborate for send beamforming. This makes at most* $\sqrt{n}$ *nodes which can transmit to any node in a grid network with grid distance* b *and dimensions* $b\sqrt{n} \times b\sqrt{n}$*. Let* $d_{\min}$ *denote the minimum distance we can approach an antenna where the far-field assumption is satisfied. Then the signal power is* $\mathcal{O}\left(n^{1/6} \cdot \ln n + {d_{\min}}^{-2}\right)$ *in the vicinity of an antenna at distance* $d_{\min}$ *and the signal of the antenna at distance* $d_{\min}$ *is stronger than the signal of the remaining field if* $b \in o\left(d_{\min} \cdot \sqrt[6]{n} \cdot \ln(n)\right)$*.*

The main conclusion of this section is that send beamforming can reduce peaks of maximum electromagnetic field strengths of wireless transmissions. A single antenna needs power $\Theta(d^2)$ to send to distance d with corresponding field strengths in the same order. With beamforming we distribute the transmission power among multiple antennas and reduce the overall transmission power as well. In the next Chapter, we present transmission schemes which let nodes placed on a line or in a rectangular area collaborate for send beamforming. $\Theta(d)$ senders with constant transmission power each and placed on a line can send to distance d if they collaborate for beamforming and the peak values of the electromagnetic field have strength $\Theta(\log d)$. However, the field strength produced by $\Theta(d)$ nodes in a rectangular area (see Lemma 13) has a maximum signal power of $\Theta\left(d^{2/3} \cdot \ln d\right)$. The peak value is higher for a placement in a rectangular area in comparison to a placement on a line because the transmission power per area is higher.

4 Transmission Schemes with Collaborative Beamforming

In this chapter, we present routing algorithms for ad hoc networks using collaborative transmit beamforming. We start in Section 4.1 with a first example limited to a two-hop routing and show how collaborative beamforming can be applied. In Section 4.2, we present a multi-hop broadcast algorithm for nodes placed on a line. This algorithm is extended to a unicast algorithm in Section 4.3 for nodes placed in a two-dimensional grid. We further optimize the unicast algorithm for energy efficiency in Section 4.4 and, moreover, consider nodes placed in a three-dimensional grid.

4.1 Example: Two-Hop Relaying

A first example of applying collaborative beamforming is a two-hop transmission from a sender to a receiver via a relay (see Figure 4.1). In the following, we will first describe the case of a relay node with a single antenna and compare that later on with a relay consisting of multiple nodes performing collaborative transmit beamforming.

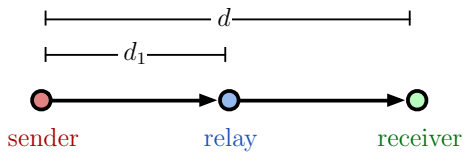

Figure 4.1: Transmission from a sender via a relay node to the final receiver node.

If the receiver is not in reach of the sender node due to limited sending power, it is necessary to amplify and relay a signal at a node "on the way" that the receiver can receive the signal. Another advantage of using relay nodes is to reduce energy consumption. A signal emitted by a sender node decays for distance d with $1/d^2$ in the free-space model. If we put a relay between sender and receiver, we have two hops with distance $d/2$ and power $d^2/4$. In sum, the transmission power is halved.

When relaying a signal at a relay node, we have to distinguish between two cases whether we perform noise filtering at the relay node or not. With noise filtering, the relay filters noise from the noisy signal and retrieves the data symbols, recreates the original signal for the symbols with an amplification according to the receiver's

distance, and sends this signal to the receiver. We assume that signal processing for noise filtering needs constant power P_{filter} at each relay node. Without noise filtering, the relay only records the noisy signal, amplifies it, and resends the received signal containing noise. We assume that the energy consumption for recording and errors due to quantizing the analog signal to a digital recording are negligible.

Single relay with noise filter This case describes the situation of Figure 4.1 with a single relay node between sender and receiver and the relay performs noise filtering which needs power P_{filter}, i.e. the relay forwards the signal without any further noise.

Lemma 14 *For a two-hop transmission from a sender to a single relay to a receiver (see Figure 4.1), the total transmission power is minimum if the relay is placed in the middle between sender and receiver. However, a direct transmission from sender to receiver with transmission power $P \cdot d^2$ for distance d needs less power than a two-hop transmission, if $P_{filter} > P_0 \cdot \frac{d^2}{2}$ where P_{filter} is the power for noise filtering at the relay.*

Proof: For a given noise power N, let us assume we need a SNR $\geq \frac{P_0/d^2}{N}$ for a successful transmission over distance d. The distance from sender to relay is d_1 and d_2 is the distance from relay to receiver. Then, the necessary overall power is

$$P \quad = \quad P_0 \left(d_1^2 + d_2^2\right) + P_{\text{filter}}$$

where P_{filter} denotes the power for signal processing at the relay node. The derivation of this function has a zero for $d_1 = d/2$ and we get minimum total power consumption when placing the relay node in the middle between sender and receiver, i.e. the distance from the relay to the receiver is $d_2 = d - d_1$. For the overall minimum, we have to compare the solution of a two-hop relayed transmission with direct transmission from sender to receiver.

$$\begin{aligned} P_0 \cdot d^2 &\geq P_0 \left(d_1^2 + (d - d_1)^2\right) + P_{\text{filter}} \\ \Rightarrow P_{\text{filter}} &\leq P_0 \cdot 2d_1 \left(d - d_1\right) \end{aligned}$$

Obviously, when choosing $d_1 = d$ and placing the relay node directly next to the receiver, it is always a better choice to use direct communication since the relay node would need additional power P_{filter}. And when placing the relay node in the middle between sender and receiver with $d_1 = d/2$, we get

$$P_{\text{filter}} \quad \leq \quad P_0 \cdot \frac{d^2}{2} \ .$$

The overall minimum for two-hop relaying or direct transmission is then

$$P \quad = \quad P_0 \cdot \min\left(d^2, d_1^2 + (d - d_1)^2 + \frac{P_{\text{filter}}}{P}\right) \ .$$

And when choosing $d_1 = d/2$ we get

$$P \quad = \quad P_0 \cdot \min\left(d^2, \frac{d^2}{2} + \frac{P_{\text{filter}}}{P}\right) \ .$$

□

Single relay without noise filter in this second case, the relay node records and resends the received signal without noise filtering. Then the energy consumption at the relay node is only the power for sending and we assume fixed costs for operating the node are negligible. The noise at the relay node is N_1 and the noise at the receiver is N_2 which is AWGN and with the same absolute power level $|N| = |N_1| = |N_2|$. For simplicity let us assume that the power of the signal P_0 has the same level with $N = P_0$ and the sender can boost it with (power) amplification a_1. Then the signal to noise ratio at the relay node at distance d_1 is

$$\beta_1 = \frac{\frac{a_1}{d_1^2} P_0}{N_1} = \frac{a_1}{d_1^2} \ . \tag{4.1}$$

When the relay node relays the signal without signal processing and just amplification with factor a_2, the noise at the receiver consists of the noise N_2 at the receiver plus the amplified and relayed noise at the relay node with power $(N_1 a_2/d_2^2)$. See Figure 4.2 for illustration of the signal and noise levels at the sender, relay, and receiver. Please note that without signal processing at the relay node, noise N_1, which the relay receives as well, is also amplified and forwarded by the relay node (orange curve).

The signal to noise ratio at the receiver is thus

$$\beta_2 = \frac{\frac{a_2}{d_2^2} \cdot \frac{a_1}{d_1^2} P_0}{\frac{a_2}{d_2^2} \cdot N_1 + N_2} = \frac{\frac{a_1}{d_1^2}}{1 + \frac{d_2^2}{a_2}} = \frac{\beta_1}{1 + \frac{d_2^2}{a_2}} \ .$$

Solving the equation to a_2 gives then

$$a_2 \quad = \quad \frac{d_2^2}{\frac{\beta_1}{\beta_2} - 1} \ .$$

In the next step, we limit the position of the relay node to the line-of-sight between sender and receiver with $d = d_1 + d_2$.

$$a_2 \quad = \quad \frac{(d - d_1)^2}{\frac{\beta_1}{\beta_2} - 1}$$

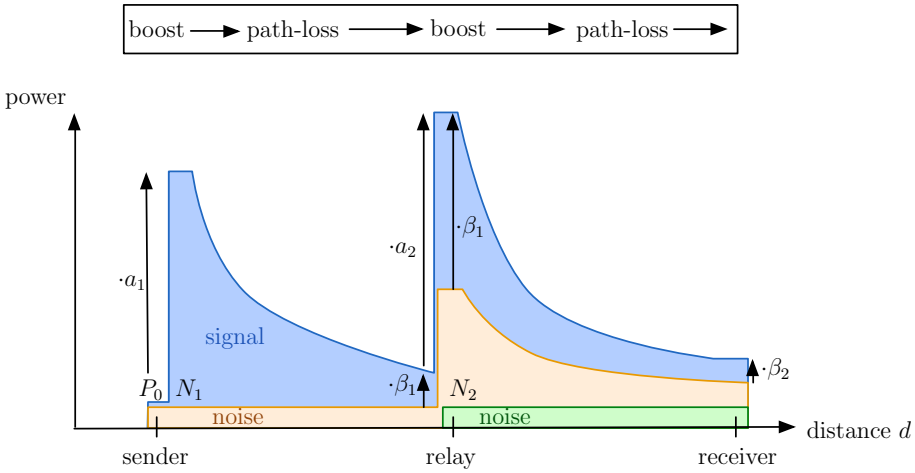

Figure 4.2: Sender boosts signal power P_0 with a_1, relay boosts received signal with a_2. N_1, N_2 denote noise levels at the relay and receiver; d_1, d_2 are distances to relay and receiver; $\beta_0, \beta_1, \beta_2$ are SNR at sender, relay, and receiver.

The overall power for the two hop transmission is therefore

$$\begin{aligned} P &= \underbrace{a_1 \cdot P_0}_{\text{sender}} + \underbrace{a_2 \cdot (\beta_1 \cdot P_0 + N_1)}_{\text{relay node}} \\ \Rightarrow P &= P_0 \cdot (a_1 + a_2 \cdot (\beta_1 + 1)) \\ \Rightarrow P &= P_0 \cdot \left(a_1 + \frac{\beta_1 + 1}{\frac{\beta_1}{\beta_2} - 1} \cdot (d - d_1)^2 \right) \text{ where } a_1 = \beta_1 \cdot d_1^2 \\ \Rightarrow P &= P_0 \cdot \left(\beta_1 \cdot d_1^2 + \frac{\beta_1 \cdot \beta_2 + \beta_2}{\beta_1 - \beta_2} \cdot (d - d_1)^2 \right) . \end{aligned} \tag{4.2}$$

Without loss of generality, let us assume that a SNR of $\beta_2 = 1$ at the receiver is sufficient and we set distance d between sender and receiver to $d = 1$. Then

$$P/P_0 = \beta_1 \cdot d_1^2 + \frac{\beta_1 + 1}{\beta_1 - 1} \cdot (1 - d_1)^2 .$$

We see in Figure 4.3 a comparison of the power for transmission with a relay node and direct transmission where it holds $P/P_0 = \frac{a_1}{d^2} = 1$. We see that direct transmission outperforms transmission with a relay if no signal processing is performed at the relay and the received noise is forwarded as well.

Lemma 15 *Transmission with a single relay node between sender and receiver needs always more power than direct communication if no signal processing is performed at the relay which filters noise from the received signal.*

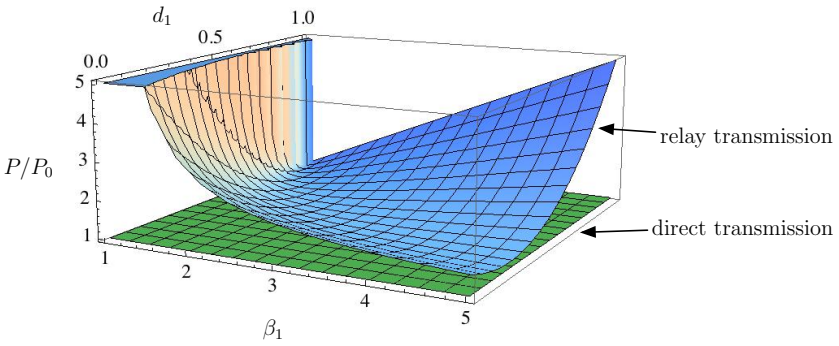

Figure 4.3: Comparison of the transmission power for direct transmission from sender to receiver and transmission with a relay at position d_1 between sender and receiver whereby β_1 denotes the SNR at the relay and the relay performs no signal processing

Proof: To proof that a transmission with a relay always needs more power we show that both functions of the transmission power do not intersect and insert one value in both functions to decide which function values are larger. When both functions intersect it holds

$$1 \quad = \quad \beta_1 \cdot d_1^2 + \frac{\beta_1 + 1}{\beta_1 - 1} \cdot (1 - d_1)^2 \ .$$

Solving to d_1 gives

$$d_1 \quad = \quad \frac{1 + \beta_1 \pm \sqrt{2\beta_1 - \beta_1^2 - 1}}{\beta_1^2 + 1} \ .$$

We demand that the SNR at the receiver is $\beta_2 = 1$. Thus, the SNR at the relay has to be $\beta_1 \geq \beta_2$ since the SNR only gets worse if the relay resends the noisy signal which it has received. For $\beta_1 \geq 1$, the term $\sqrt{2\beta_1 - \beta_1^2 - 1}$ is only real-valued for $\beta_1 = 1$. In this case, the noise $N_2 > 0$ at the receiver has to be 0 which is not true. This proofs that both functions do not intersect. Finally, we test one point $\left(\beta_1 = 2, d_1 = \frac{1}{2}\right)$ resulting into $1 < 2 \cdot \frac{1}{4} + \frac{3}{1} \cdot \frac{1}{4} = \frac{5}{4}$ and conclude that transmission with a relay always needs more power than direct communication if no signal processing is performed at the relay. □

Multiple relays with noise filter Now we consider $n \geq 1$ multiple relay nodes which perform collaborative beamforming. The sender broadcasts the message to all relay nodes at once in one hop and the relay nodes resend the message with collaborative beamforming to the receiver node. For collaborative beamforming we have to coordinate the relay nodes, i.e. synchronize the relay nodes and set up phase shifts for transmit beamforming to the receiver node. We assume a non-fading channel in the free-space model where the relay nodes have to be coordinated only once, and we do not take these fixed energy costs into account.

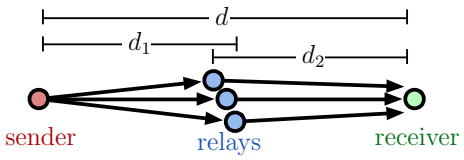

Figure 4.4: Communication from a sender of a relay node to the final destination node.

Lemma 16 *Assume we have n relay nodes for a two-hop transmission from a sender node to the relay nodes to the receiver. The n relay nodes are synchronized and perform cooperative transmit beamforming. Each relay node performs noise filtering which needs power P_{filter}. In comparison, a direct transmission from sender to receiver needs more power if $N \geq (n+1) \cdot P_{filter}$ whereby N is AWGN.*

Please note that we consider in Lemma 16 the theoretical case where all relays can be placed on the same optimum position. This describes the lower bound for energy consumption. In a realistic physical model, the relays have a minimum distance and thus a spatial expansion (compare Figure 4.4), which will increase path loss and reduce energy savings.

Proof: Denote d_1 the maximum distance of the first hop from sender to multiple relay nodes and d_2 the maximum distance of any relay node to the receiver. The first hop from the sender to the multiple relay nodes is a broadcast. To reach a SNR of $\beta = 1$, the sender has to send with power $N \cdot d_1^2$ where N is the power of AWGN and $d_1 = \max_{k=1..n} \{d_{1k}\}$ of all distance d_{1k} from the sender to the k-th relay node. We assume that the relay nodes are phase-synchronous, know the position of the receiver node and can send with cooperative transmit beamforming. Additionally, we assume that all relays send with the same power level, i.e. given overall power P_0 for relaying each relay node sends with power $P_k = \frac{P_0}{n}$. The k-th relay node has distance p_{k2} to the receiver with $d_2 = \max_{k=1..n} \{d_{2k}\}$. Therefore the SNR at the receiver is

$$\beta_2 \geq \frac{\left(\sum_{k=1}^{n} \frac{\sqrt{P_0/n}}{d_{2k}}\right)^2}{N} \geq \frac{n}{d_2^2} \cdot \frac{P_0}{N} \ .$$

To reach SNR $\beta_2 = 1$, each relay has to send with power $\frac{N}{n^2} \cdot d_2^2$. The overall power for broadcasting from the sender to the relays and transmit beamforming from the relays to the receiver is

$$\begin{aligned} P &\leq N \cdot d_1^2 + n \cdot \left(\frac{N}{n^2} \cdot d_2^2 + P_{\text{filter}}\right) \\ \Rightarrow P &\leq N \cdot \left(d_1^2 + \frac{d_2^2}{n}\right) + n \cdot P_{\text{filter}} \end{aligned}$$

We assume the ideal case where all nodes can be placed at the same position somewhere on the line between sender and receiver to minimize the path-loss. The distance

between sender and receiver is $d = 1$. Then,

$$P \leq N \cdot \left(d_1^2 + \frac{(1-d_1)^2}{n} \right) + n \cdot P_{\text{filter}}$$

We derive P to d_1 to find the optimum position

$$\frac{\mathrm{d}P}{\mathrm{d}d_1} = 2 \cdot N \cdot \left(\left(1 + \frac{1}{n} \right) d_1 - \frac{1}{n} \right)$$

and equating to zero gives

$$\begin{aligned} 0 &= \left(1 + \frac{1}{n} \right) d_1 - \frac{1}{n} \\ \Rightarrow d_1 &= \frac{1}{n+1} \end{aligned}$$

The second derivation

$$\frac{\mathrm{d}P}{\mathrm{d}d_1^2} = 2 \cdot N \left(1 + \frac{1}{n} \right) > 0$$

shows that it is a minimum. So when more relay nodes are available, it is more energy-efficient to perform a small first hop and then relaying with more beamforming gain. Inserting the minimum into the equation gives

$$P \leq \frac{1}{n+1} \cdot N + n \cdot P_{\text{filter}} \ .$$

We can see in Figure 4.5 the transmission power depending on the number of relays n and the power P_{filter} for filtering noise at each relay. The values are normed by P_0 which is power equivalent for transmission without path loss, i.e. transmission power $P_0 \cdot d^2$ to reach SNR $\beta_2 = 1$ at noise floor N.

In the following we analyze in which case direct sending from sender to receiver with power $N \cdot d^2 = N$ needs more power than a two-hop transmission with n relays.

$$\begin{aligned} N &\geq \frac{1}{n+1} \cdot N + n \cdot P_{\text{filter}} \\ \Rightarrow N &\geq (n+1) \cdot P_{\text{filter}} \end{aligned}$$

□

Since each relay node has fixed costs for noise filtering P_{filter} in this setting, more relays, which perform collaborative beamforming, does not necessarily mean less total energy consumption.

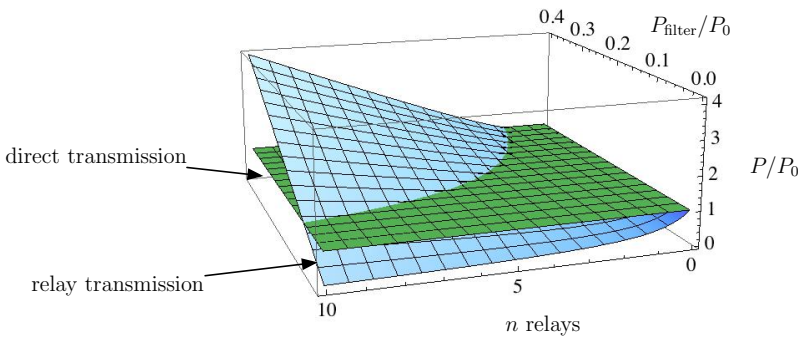

Figure 4.5: Comparison of the transmission power P of direct transmission from sender to receiver and a two-hop transmission with n relays performing transmit beamforming. Noise filtering at each relay needs power P_{filter}.

Multiple relays without noise filter In this case n relay nodes resend a received signal without performing any noise filtering and received noise is also resend. The n relay nodes will phase shift the signal to perform cooperative transmit beamforming. A more detailed analysis of this problem can be found in the related work [HNSGL08].

Lemma 17 *Assume a two-hop transmission scheme where n relay nodes between sender and receiver perform cooperative beamforming and forward the sender's signal with appropriate delays for beamforming (see Figure 4.4). The relays only record and resend the received signal without noise filtering needing negligible power. In comparison to a direct transmission from sender to receiver, the two-hop scheme can need less overall power if* $n > \frac{2}{\beta_1} + 1$ *with SNR* β_1 *at the relays.*

Proof: We sketch the upper bound for power-reduction with multiple relay nodes and assume that all n relay nodes are in the middle between sender and receiver and the noise $N_{1,1}, \ldots, N_{1,n}$ at the relays is nonetheless uncorrelated. The SNR at the receiver is then

$$\beta_2 = \frac{\frac{a_2}{d_2^2} \cdot \frac{a_1}{d_1^2} \cdot n^2 \cdot P_0}{\sum_{i=1}^{n} \frac{a_2}{d_2^2} \cdot N_{1,i} + N_2} = \frac{n \cdot \beta_1}{1 + \frac{d_2^2}{n \cdot a_2}} \ .$$

Solving the equation to (power) amplification a_2 at the relays gives

$$a_2 \quad = \quad \frac{d_2^2}{n^2 \cdot \frac{\beta_1}{\beta_2} - n} \ .$$

We place all n relays at the same position, which is on the line between sender and receiver. Without loss of generality, we set the distance between sender and receiver to 1, such that $d_2 = 1 - d_1$ and the SNR at the receiver to $\beta_2 = 1$.

$$a_2 \quad = \quad \frac{(1 - d_1)^2}{n^2 \cdot \beta_1 - n}$$

The overall power for a two-hop transmission is therefore

$$\begin{aligned} P &= \underbrace{a_1 \cdot P_0}_{\text{sender}} + \underbrace{n \cdot a_2 \cdot (\beta_1 \cdot P_0 + N_1)}_{n \text{ relay nodes}} \\ \Rightarrow P/P_0 &= a_1 + n \cdot a_2 \cdot (\beta_1 + 1) \text{ where } a_1 = \beta_1 \cdot d_1^2 \\ \Rightarrow P/P_0 &= \beta_1 \cdot d_1^2 + n \cdot \frac{(1-d_1)^2}{n^2 \cdot \beta_1 - n} \cdot (\beta_1 + 1) \\ \Rightarrow P/P_0 &= \beta_1 \cdot d_1^2 + \frac{\beta_1 + 1}{n \cdot \beta_1 - 1} \cdot (1-d_1)^2 \end{aligned} \tag{4.3}$$

To check, when a direct transmission from sender to receiver over distance d needs more power than the two-hop transmission scheme, we set $P_0 \cdot d^2 \geq P$ and get

$$n \geq \frac{2 + \beta_1 - 2 \cdot (1 + \beta_1)\, d_1 + d_1^2}{\beta_1 - \beta_1^2 \cdot d_1^2} .$$

Setting $d_1 = 0$ minimizes the right term, where all relay nodes are placed at the position of the sender without any path loss. Therefore,

$$n = \frac{2}{\beta_1} + 1$$

and for $n > \frac{2}{\beta_1} + 1$ it is theoretically possible to save transmission power when using n relay nodes performing beamforming. The power equivalent is for this case

$$P/P_0 = \frac{\beta_1 + 1}{n \cdot \beta_1 - 1} .$$

□

Please note that a realistic positioning with a minimum distance between sender and relay nodes, which increases the distances to sender and receiver, will reduce and possibly void the power savings shown in the preceding proof.

Since the beamforming gain of the collaborating relay nodes increases the SNR level, we can conclude from Lemma 17 the following.

Corollary 6 *Multiple relay nodes, which collaborate for beamforming, can be used as noise filter, i.e. the spatial filter enhances the SNR and filters noise from other directions. As a consequence, each relay node individually might not be able to decode the forwarded information due to a low SNR, which can be a security feature.*

We can conclude two things from the example of two-hop relaying. First, a simple amplify and resend strategy without noise filtering accumulates noise from each hop and thus is not feasible for multi-hop routing. Second, relaying with collaborative sender beamforming can save energy. If energy reduction is not the goal, we can extend the transmission distance without increasing energy consumption, which leads to less routing hops and shorter routing time. The broadcast algorithm of the following section accomplishes exactly this goal.

4.2 Broadcast on a Line

In this section, we consider a routing algorithm for ad hoc network nodes which are placed equidistantly on a line. Basically, the algorithm informs all intermediate nodes between a given source node and destination node. We use a multi-hop routing scheme and nodes collaborate in each hop for transmit beamforming to increase the transmission distance and decrease the total number of hops.

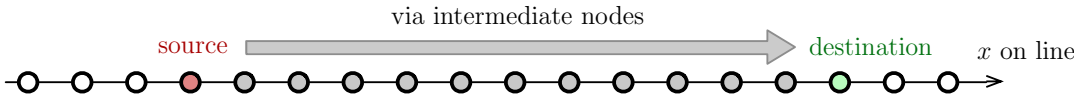

Figure 4.6: Routing for nodes on a line from source to destination via intermediate nodes

With this operation we can implement a unicast operation from one source to one destination as well. When we perform the operation twice starting from the originating source node to the left and to the right to both ends of the line, we get a broadcast operation. Respectively for a geocast, which transmits an information to a contiguous geographical area, we have to perform the operation from the source through the geographical area which is in this case a range of the line.

The goal of the algorithm is to reach fast routing and small energy consumption at the same time. In Table 4.1, the here presented algorithm (beamforming multi-hop*) is compared to a direct transmission from a source to a destination in distance d and 'nearest-neighbor multi-hop' denotes the routing strategy where a message is forwarded sequentially from the source to the nearest neighbor on the line towards the destination until the destination has been reached. Interference-free distance denotes

	running time	**transmission energy**	**interference-free distance**
direct transmission	$\Theta(1)$	$\Theta(d^2)$	$\Theta(d)$
nearest-neighbor multi-hop	$\Theta(d)$	$\Theta(d)$	$\Theta(1)$
beamforming multi-hop*	$\Theta(\log d)$	$\Theta(d)$	$\Theta(d)$

Table 4.1: Comparison of runtime, energy consumption, and interference in dependency on the transmission distance d

the minimum distance between parallel operations in which operations can be executed without such strong interference in expectation that an operation fails[1]. We can see that our algorithm combines fast routing with small energy consumption. The nearest-neighbor routing strategy provides minimum energy consumption for the operation and our algorithm is as well asymptotically optimal.

[1] see Lemma 35 in the appendix for the interference-free distance of direct transmissions.

We also show that our algorithm is self-synchronizing, i.e. relay nodes are phase-synchronized when receiving a message and can instantly collaborate for beamforming. Please note that phase-synchronization between nodes is the necessary property for collaborative beamforming.

Setting We consider n wireless ad hoc network nodes equidistantly placed on a line (with unit distance). Each node is equipped with one antenna and the antenna is placed perpendicular to the line at the node's position, i.e. there is no polarization effect. The transmission power of each node is just large enough to reach its nearest neighbors.

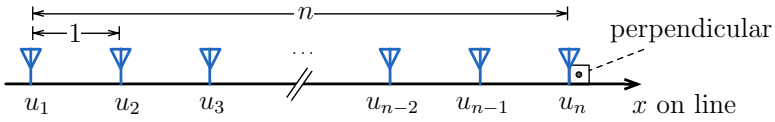

Figure 4.7: Setting with n nodes placed on a line at positions $u_1, \ldots, u_n$

4.2.1 Broadcasting Algorithm

Without loss of generality, assume the first node of the line u_1 is the originator of the broadcast message. The broadcast scheme works in rounds. In the first round, the only informed node u_1 transmits the message to neighbor u_2. The informed node synchronizes with the first node and thus becomes coordinated. In the subsequent rounds, all coordinated senders use beamforming gain to reach the next neighbors and synchronize them. This process continues until all nodes are informed. Using our previous observations of the beamforming gain we can prove that this way the number of coordinated nodes increases exponentially inducing a logarithmic time for the broadcast.

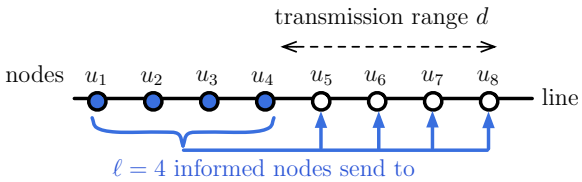

Figure 4.8: Four coordinated nodes $u_1, \ldots, u_4$ broadcast with transmit beamforming on the line and double the the number of informed nodes to $u_1, \ldots, u_8$

Theorem 6 *The broadcast problem of n equidistant nodes on a line, where each node has only constant transmission power to establish a point-to-point connection to each*

neighbor, can be solved in time $\Theta(\log n)$ *and energy* $\Theta(n)$ *using transmit beamforming and wireless self-coordination.*

Proof: Without loss of generality, the nodes have unit distance and the carrier wavelength is $\lambda < \frac{1}{2}$ that the far-field approximation holds. For a given noise N and a required threshold SNR_0, the minimum power P_0 to reach a neighbor in unit distance is $P_0 \geq N \cdot \mathrm{SNR}_0$.

First let us analyze the transmission range d of ℓ adjacent, coordinated, and informed nodes. Each informed node u_i uses the characteristic $s_i = \sqrt{P_0} \cdot e^{j\frac{2\pi}{\lambda} \cdot i}$ (see Definition 4) and sends with unit power P_0. The ℓ nodes produce at distance d the signal power

$$\begin{aligned} |h(\ell, d)|^2 &= \left| \left(\sum_{i=1}^{\ell} \underbrace{\sqrt{P_0} \cdot e^{j\frac{2\pi}{\lambda} \cdot i}}_{s_i} \cdot \frac{\mathrm{e}^{-j\frac{2\pi}{\lambda}(d+i)}}{d+i} \right)^2 \right| \\ &= P_0 \cdot \left(\sum_{i=1}^{\ell} \frac{1}{d+i} \right)^2 \\ &= P_0 \cdot \left(\Psi(d+\ell+1) - \Psi(d+1) \right)^2 \\ &> P_0 \cdot \ln\left((d+\ell)/d \right)^2 \end{aligned}$$

where $\Psi(\cdot)$ is the digamma function.

Now, the receiver in distance d gets the message and can be coordinated with the other informed nodes if $\frac{|h(\ell,d)|^2}{N} \geq \mathrm{SNR}_0$.

$$\frac{P_0 \cdot \ln\left((d+\ell)/d \right)^2}{N} \geq \mathrm{SNR}_0 .$$

So, for $\ln\left((d+\ell)/d \right)^2 \geq 1$ the node in distance d can be reached. This is the case for $d \leq \frac{1}{\mathrm{e}-1}\ell$. If the number of informed and coordinated nodes in round i is ℓ_i then in the next round

$$\ell_{i+1} \geq \ell_i + \max\left\{ 1, \left\lfloor \frac{1}{\mathrm{e}-1} \ell_i \right\rfloor \right\}$$

nodes are informed. Clearly $\ell_i = \Omega(\kappa^i)$ for any $\kappa < \frac{\mathrm{e}}{\mathrm{e}-1}$. Hence, all n nodes are informed after $T = \mathcal{O}(\log n)$ rounds.

The energy is bounded by

$$\mathcal{O}\left(\sum_{i=1}^{T} P_0 \ell_i \right) = \mathcal{O}\left(P_0 \sum_{i=1}^{T} \kappa^i \right) = \mathcal{O}\left(P_0 \sum_{i=0}^{T-1} \frac{n}{\kappa^i} \right) = \mathcal{O}(nP_0) .$$

□

Figure 4.9 illustrates the execution of one round in the routing algorithm where 6 senders inform the next 6 nodes on the line. We see the transmission power $|h|^2$ in the plane which is produced by the 6 senders collaborating for beamforming. The antennas of the nodes are aligned orthogonally to the plane.

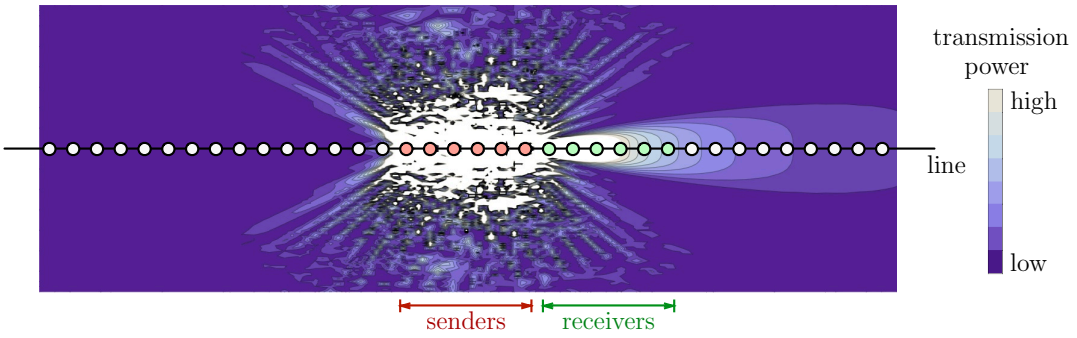

Figure 4.9: Transmission power $|h|^2$ of 6 beamforming senders (red) informing 6 receivers (green) with unit distance between nodes and wavelength $\lambda \approx \frac{1}{8}$

4.2.2 Parallel Execution

An interesting feature of this broadcasting process is that it can be performed in parallel, since we can bound the interfering energy by the following theorem.

Theorem 7 *For an infinite number of equidistant nodes on the line, the broadcasting algorithm of Theorem 6 can be performed in continous groups of ℓ nodes if the minimum distance between these groups is $\Omega(\ell)$.*

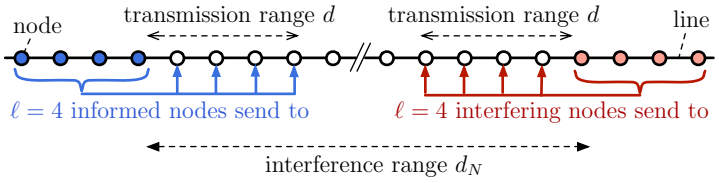

Figure 4.10: parallel transmissions: $\ell = 4$ nodes (blue) send to range d with interference in distance d_N (red).

The following proof shows for Theorem 7 that the noise produced by unsynchronized simultaneous sending groups of antennas is independent from the number of nodes in the network n.

Proof of Theorem 7: Let $\ell \leq n$ be the number of active senders in a group of nodes collaborating for beamforming and let d_N denote the minimum distance between groups of active senders. Assume each sender i has a characteristics with $|s| = s_i$. When ℓ senders collaborate for beamforming and are phase synchronized, they have an upper bounded signal strength of $(|s| \cdot \ell/d)$ in distance d. Then the signal strength of an infinite number of sender groups with distance d_N to each other and unsynchronized

phase angle β_i is

$$|h_N| \leq \sum_{i=1}^{\infty} \frac{|s| \cdot \ell}{i \cdot d_N} \cdot \mathrm{e}^{j\beta_i} = \frac{|s| \cdot \ell}{d_N} \cdot \sum_{i=1}^{\infty} \frac{\mathrm{e}^{j\beta_i}}{i} = \frac{|s| \cdot \ell}{d_N} \cdot c_N \ .$$

Let $\overline{c_N}$ denote the complex conjugate of c_N.

$$\begin{aligned} |c_N|^2 &= c_N \cdot \overline{c_N} \\ &= \sum_{i=1}^{\infty} \frac{\mathrm{e}^{j\beta_i}}{i} \cdot \sum_{k=1}^{\infty} \frac{\mathrm{e}^{-j\beta_k}}{k} \\ &= \left(\sum_{i=1}^{\infty} \frac{1}{i^2} \right) + \left(\sum_{i=1}^{\infty} \sum_{k=1, i \neq k}^{\infty} \frac{\mathrm{e}^{j(\beta_i - \beta_k)}}{i \cdot k} \right) \\ &= \frac{\pi^2}{6} + \sum_{i=1}^{\infty} \sum_{k=1, i \neq k}^{\infty} \frac{\mathrm{e}^{j(\beta_i - \beta_k)}}{i \cdot k} \end{aligned}$$

For each index tuple (i, k) with $i \neq k$ there exists a symmetric (k, i) with the negated imaginary value.

$$\forall i \neq k: \qquad \Im\left(\mathrm{e}^{j(\beta_i - \beta_k)}\right) + \Im\left(\mathrm{e}^{j(\beta_k - \beta_i)}\right) = 0$$

So, we get only a sum of real numbers.

$$\sum_{i=1}^{\infty} \sum_{k=1, i \neq k}^{\infty} \frac{\mathrm{e}^{j(\beta_i - \beta_k)}}{i \cdot k} = \sum_{i=1}^{\infty} \sum_{k=1, i \neq k}^{n} \frac{\cos\left(\beta_i - \beta_k\right)}{i \cdot k}$$

We have assumed that angles $\beta_i \in [0, 2\pi)$ are independently, identically, and uniformly distributed over $[0, 2\pi)$. So the expectation of $\cos(\beta_i)$ is $\left(\frac{1}{2\pi} \int_{\beta=0}^{2\pi} \cos\beta \ \mathrm{d}\beta\right) = 0$. And the expected value of the sum is

$$\mathbb{E}\left[|c_N|^2\right] = \frac{\pi^2}{6} + \sum_{i=1}^{\infty} \sum_{k=1, i \neq k}^{\infty} \frac{\overbrace{\mathbb{E}\left[\cos\beta_i - \beta_k\right]}^{0}}{i \cdot k} = \frac{\pi^2}{6} \ .$$

The root mean square of h_N is therefore

$$|h_N|_{\mathrm{rms}} = \frac{|s| \cdot \ell}{d_N} \cdot \frac{\pi}{\sqrt{6}} = \mathcal{O}\left(\frac{\ell}{d_N}\right) \ . \tag{4.4}$$

□

Figure 4.11 illustrates the result of Theorem 7 for the noise strength $|h_N|_{\mathrm{rms}} = \frac{|s|\ell}{d_N} \frac{\pi}{\sqrt{6}}$. In the experiment, we $\frac{|s| \cdot \ell}{d_N} := 1$ and the phase angels of the interfering groups of senders are chosen uniform at random with $\beta_i \in [0, 2\pi)$. Each number of interfering sender groups was tested 100 times and averaged. The total average measured strength of noise was ≈ 1.17 whereas the factor in the proof is $\frac{\pi}{\sqrt{6}} \approx 1.28$.

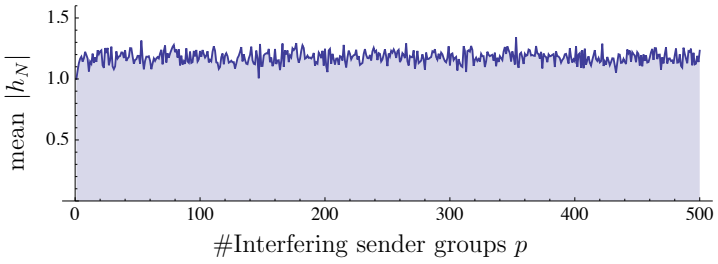

Figure 4.11: Measurement of the signal strength $|h_N|$ for different number of sender groups p. The size of each group and distance between groups is constant with $|s| \cdot \ell / d_N = 1$

The ingredients for a high network throughput are a combination of fast routing with few hops and high parallelism of simultaneous transmissions in the network at the same time. We have shown in Theorem 6 a fast routing algorithm for nodes placed on a line with runtime $\mathcal{O}(\log n)$ and and energy $\mathcal{O}(n)$ and we also have shown in Theorem 7 how it can be processed in parallel in the network. The following lemma shows how we can use the algorithm to achieve a high network throughput.

Lemma 18 *In a network with n nodes equidistantly placed on a line, every node can broadcast a message to every other node in time $\Theta(n)$, if it is possible to uphold synchronization over time $\Theta(n)$, and in time $\Theta(n \cdot \log n)$ otherwise. This needs energy $\Theta(n^2)$ and $\Theta(\log n)$ routing hops for each message.*

Proof: Consider the broadcasting scheme of Theorem 6 for n nodes placed equidistantly on a line. An easy approach to broadcast a message from every node to every other node is to perform the broadcasting scheme of Theorem 6 sequentially n times starting from node i in the i-th run. Since broadcasting takes time $\Theta(\log n)$ and energy consumption $\Theta(n)$, this needs for n executions time $\Theta(n \cdot \log n)$ and energy $\Theta(n^2)$. In this case, each message is routed in $\Theta(\log n)$ subsequent hops.

The preceding approach is only sequential. We can add parallelism to the transmission scheme and increase the throughput by applying a divide and conquer approach (see Figure 4.12). The basic idea is to exchange in $\log n$ rounds all messages between neighboring groups of nodes. In the first round $i = 1$, single neighboring nodes exchange their message (with $\Theta(n)$ parallel transmissions). In the last round $i = \log n$, half the network exchanges messages with the other half of the network (with a transmission distance $\Theta(n)$).

The groups of nodes of each routing step (illustrated in Figure 4.12 by colored rectangles) are coordinated, i.e. are synchronized for beamforming and each node has all messages of all other nodes in this group and thus can transfer all messages with collaborative beamforming to the adjacent group of nodes (connected by an line in the graphics) in time $\Theta(m)$ where m denotes the number of messages.

In each routing step of the divide an conquer scheme, we require that we can double the number of informed and coordinated nodes with collaborative beamforming. In

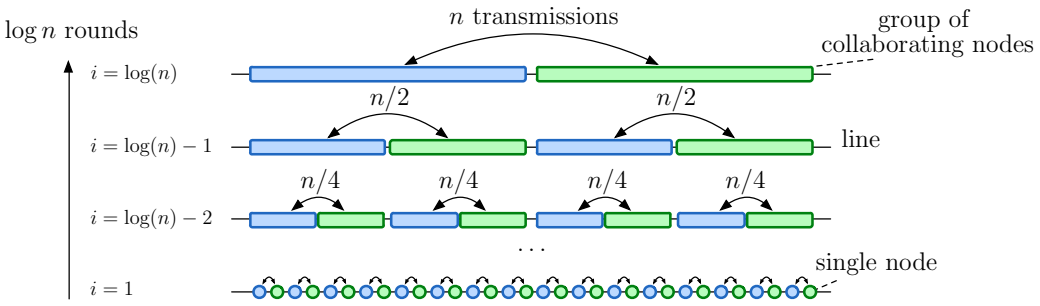

Figure 4.12: Broadcast from every node to any other node in a network placed on a line by applying a divide & conquer approach to increase parallelism

case, the exponential growth of our line broadcasting algorithm of Theorem 6 is only b^x for x rounds and base $b < 2$, the number of routing hops will be more than one. To double the number of informed nodes we need x rounds with $b^x \geq 2$ which holds for $x = \left\lceil \frac{\log 2}{\log b} \right\rceil$.

From Theorem 7, we know that the noise of parallel and unsynchronized transmissions is constant for an infinite number of parallel transmissions. This requires that the ratio $\frac{\ell}{d_N}$ of the group size of coordinated senders ℓ and the distance between groups of parallel senders d_N is constant. To reduce interference to a level that the receivers can receive the information and become synchronized, we can apply a TDMA (Time Division Multiple Access) scheme and transmit in K rounds only at each K-th group of senders. In return, the running time increases by constant factor K.

In the first round $i = 1$, we only coordinate single neighboring nodes and pairs of neighbors exchange their message, which takes two rounds. Combining with TDMA, we have $2K$ sequential sub-rounds where in round $\kappa = 1..2K$, all nodes u_s with $s = 1, \ldots, n$ send to its right neighbor for which holds $((s-1)/2 + \kappa \mod K) = 0$ and to its left neighbor if it holds $((s-2)/2 + \kappa \mod K) = 0$. Please note that the pairs of neighboring nodes have exchanged a message in both ways and thus are coordinated for beamforming to the left and to the right along the line. In general for round i of the divide and conquer approach, a group of 2^{i-1} nodes informs the adjacent 2^{i-1} nodes to the left if it holds $\left((s-1)/2^i + \kappa \mod K\right) = 0$ and to the left if it holds $\left((s-2)/2^i + \kappa \mod K\right) = 0$. Here the time of each sub-round in the TDMA scheme increases by factor 2^{i-1} because the group of 2^{i-1} has 2^{i-1} messages. So the overall time of round i is $\left(\log(b) \cdot 2K \cdot 2^{i-1}\right)$.

In round $i = \log(n)$, we get a group of $2^{\log n} = n$ nodes and all nodes have received all messages and the broadcast is finished. We get the overall running time

$$T = \sum_{i=1}^{\log n} \lceil \log 2 / \log b \rceil \cdot 2K \cdot 2^{i-1} = \lceil \log 2 / \log b \rceil \cdot 2K \cdot (n-1) = \Theta(n) \ .$$

Since the synchronization of one group of nodes for collaborative beamforming is established in a preceding routing step, we have to assume that we can uphold the synchronization for the complete execution of the broadcasting scheme in time $T = \Theta(n)$. This includes for one divide and conquer step pausing the routing for interleaved execution in the TDMA scheme and upholding synchronization for sequential transmission of 2^{i-1} messages in round i.

In round i, a group of 2^{i-1} nodes needs for transmitting 2^{i-1} messages (and energy consumption k_2 per message and node) an overall energy of $(k_2 \cdot \log(b) \cdot 2^{2i-2})$. We have $\frac{n}{2^{i-1}}$ groups in round i. The overall energy consumption is then

$$\begin{aligned}
\sum_{i=1}^{\log n} \left(\lceil \log 2 / \log b \rceil \cdot k_2 \cdot 2^{2i-2} \right) \cdot \frac{n}{2^{i-1}} &= \lceil \log 2 / \log b \rceil \cdot k_2 \cdot n \cdot \sum_{i=1}^{\log n} 2^{i-1} \\
&= \lceil \log 2 / \log b \rceil \cdot k_2 \cdot \left(n^2 - n \right) \\
&= \Theta\left(n^2 \right) .
\end{aligned}$$

□

For the case we can uphold synchronization for time $\Theta(n)$, this broadcasting scheme reaches the same throughput as using a broadcasting scheme with nearest-neighbor communication. Although nearest-neighbor transmissions are short distant and need $\Theta(n)$ hops to reach from a source all other nodes, the operation can provide high parallelism with spatial mutliplexing in $\Theta(n)$ because only small areas have to be blocked for short-range communication between neighbors. So we get in both cases time $\Theta(n)$ and energy $\Theta(n^2)$. The advantage of our scheme might be that each message has only $\Theta(\log n)$ hops on its way to reach all nodes in the network. This may reduce the possibility of error. Also extra times on each hop, e.g. for processing may be less which we see in the last rounds of the divide and conquer approach where many messages are sequentially send over the same channel (in the last round these are $n/2$ messages).

Summarizing this section, we present a broadcast scheme using transmit beamforming for n nodes placed on a line in time $\Theta(\log n)$. The scheme only needs a constant times more energy with $\Theta(n)$ than sequential direct-neighbor communication. We show that the algorithm can be executed in parallel on the line if the groups of senders have size $\mathcal{O}(n)$ and the distance between groups is $\Omega(n)$. When combining the broadcast scheme with a divide and conquer approach, we can even show that a broadcast from each node to every other node is possible in time $\Theta(n)$ which is asymptotical the same for a scheme with direct-neighbor communication. This requires to uphold phase-synchronization for $\Theta(n)$ rounds but has the advantage, that each message is only routed over $\Theta(\log n)$ rounds which might have less sources of error.

4.3 Unicast in the Plane

For nodes placed on a line (Section 4.2), we could enhance the routing time from time $\Theta(d)$ to $\Theta(\log d)$ for transmission distance d when using collaborative transmit beamforming. Therefore, we still have the same asymptotic energy consumption $\Theta(d)$. We show in this section, that if we can choose the collaborating nodes from plane instead of a line, we can further improve the runtime from $\Theta(\log d)$ to $\Theta(\log \log d)$.

	node placing	**running time**	**transmission energy**
direct transmission	*	$\Theta(1)$	$\Theta(d^2)$
nearest-neighbor multi-hop	*	$\Theta(d)$	$\Theta(d)$
beamforming broadcast	line	$\Theta(\log d)$	$\Theta(d)$
beamforming unicast	plane	$\Theta(\log \log d - \log \lambda)$	$\Theta(d)$

Table 4.2: Comparison of runtime and energy consumption for transmission distance d, wavelength λ, and equidistant node placement (* denotes placing in 1D, 2D, or 3D)

We present a unicast operation which transfers a message from a source node to a target node. This result is published in [JS14c] respectively in the technical article [JS14a]. First, we consider n nodes in a grid where the transmission power per node is restricted to reach the neighboring node. The basic idea of the algorithm is a multi-

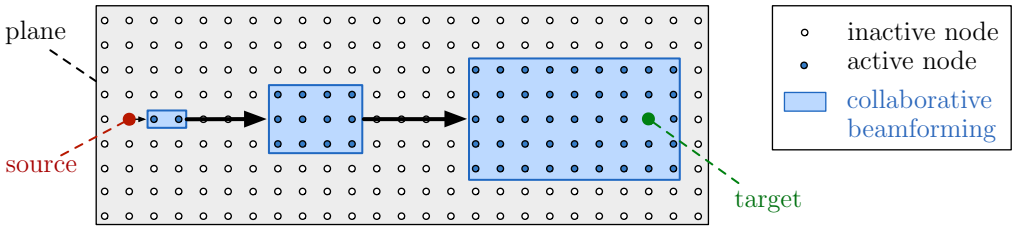

Figure 4.13: Unicast in the plane with multi-hop scheme combined with collaborative send beamforming between blue areas

hop scheme where in each hop, nodes in rectangular areas (blue areas in Figure 4.13) collaborate for transmit beamforming to increase the transmission distance of the hop. The number of nodes in the rectangular areas of successive hops grows in each round which increases the beamforming gain. The higher beamforming gain increases the transmission range and results in a speed-up with only $\Theta(\log \log n)$ hops. In contrast to broadcasting on the line, we do not use completely all nodes between source and target as intermediate nodes. In the example of Figure 4.13, the disjoint blue colored areas contain intermediate nodes. Thus, this operation is not suitable for broadcasting to an area between source and destination.

This algorithm is self-synchronizing as well as the the broadcast on the line (Theo-

rem 6). Multiple receivers in a rectangular area can deduce their phase synchronization from the reception time alone. The key argument is that the propagation direction of receiving a message in the previous round and resending in the current round is nearly the same. If all intermediate nodes resend the received information in the next hop with the same delay, then the synchronization allows the desired beamforming gain. The wavelength λ of the carrier plays here an important role for phase-synchronization and influences the runtime, which is $\Theta(\log\log d - \log\lambda)$ for distance d. So a long wavelength λ enhances the runtime.

After analysing the algorithm in a grid of n nodes, we consider n randomly distributed nodes in a square of area n. We show for a transmission range of $\Theta(\sqrt{\log n})$ and a wavelength of $\lambda = \Omega(\log^{-1/2} n)$ that the unicast problem can be solved in $\mathcal{O}(\log\log n)$ rounds as well. The corresponding transmission energy increases to $\mathcal{O}(\sqrt{n}\log n)$.

Our main method is to assign rectangular areas for suitable relay nodes. These nodes cooperate for the beamforming of the unicast message. For this, nodes store the received message and resend it at time points depending on the reception times. We restrict the corresponding transmission power such that each node can only reach its neighborhood without beamforming. The overall goal is to minimize the transmission time of a single unicast message with asymptotic linear transmission energy at the same time.

Model and Setting We use the input-output model of Definition 4. Interfering radio signals and errors occurring during the modulation and demodulation are modeled as being uncorrelated to a line-of-sight signal (of a transmission) as additive white Gaussian noise w, which is Gaussian distributed $w \sim \mathcal{N}(0, \sigma^2)$ with variance σ^2. A signal can be received if the signal-to-noise ratio is larger than a threshold τ, i.e. $\text{SNR} = \frac{P}{w} \geq \tau$. To normalize the physical values, we choose $\tau = 1$, $|w| = 1$. We assume a fixed data rate for the SNR τ and do not intend to increase the data rate by enhancing the SNR and using a modulation scheme with higher data rate.

We consider n wireless ad hoc network nodes placed in a quadratic area of size n in the plane. Each node is equipped with one antenna and the antenna is placed perpendicular to the plane, i.e. there is no polarization effect. We successively consider two scenarios:

(a) the nodes are placed in a grid with grid distance 1, wavelength $\lambda < \frac{1}{2}$ to meet the far-field assumption, and the transmission power is just large enough that a node reaches vertical and horizontal neighbors in the grid with amplitude $|s_i| \leq 1$ of sender i.

(b) the nodes are randomly distributed in the area and have a minimum distance of 2λ to satisfy the far-field assumption, the transmission power is $\Theta(\log n)$, and the wavelength is $\lambda = \Omega(\log^{-1/2} n)$.

Regarding the second scenario, it is shown in [GK98] that the minimum transmission distance for achieving connectivity in this model is $\Omega(\sqrt{\log n})$. Therefore, we increase

the maximum amplification of sender i to $|s_i| \leq k(\log n)^{1/2}$ for some constant k. For 'nearest-neighbor multi-hop' in Table 4.2 the power increases in the same order as well.

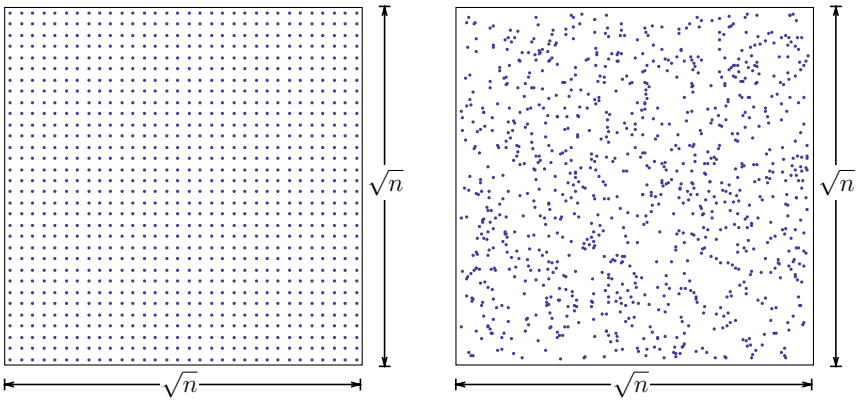

(a) grid (b) random placement

Figure 4.14: n nodes in a square of area n for the two scenarios in our setting

4.3.1 Unicast I: Unicast in the Grid

The basic idea of our unicast algorithm is a multi-hop algorithm with relays between sender and receiver shown in Figure 4.15(a) and each relay consists of multiple nodes which perform collaborative transmit beamforming, see Figure 4.15(b). With beam-

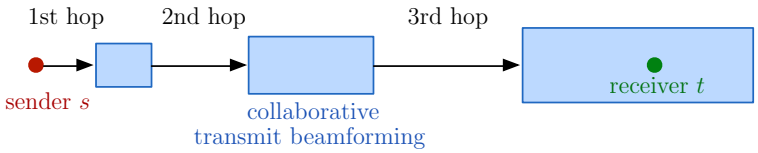

(a) Multi-hop between rectangles of beamforming senders.

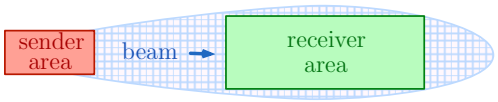

(b) Beamforming from sender to receiver rectangle

Figure 4.15: Scheme of the $\mathcal{O}(\log \log n)$-Unicast algorithm.

forming gain, the hop distance increases double exponentially such that this unicast algorithm needs $\mathcal{O}(\log \log n)$ hops from the source to the target.

We use transmit beamforming[2] (MISO) which requires, when performed with several senders in parallel, the distribution of the message to all senders and phase synchronization between all senders. As Figure 4.15(b) indicates, we will show that we can broadcast a message from a sender to a receiver area with rectangular shape such that all nodes in the receiver area have the same message for collaborative transmit beamforming in the next round. For synchronizing the sender phases, we present two algorithms. Algorithm 1 corrects the phase at the relay nodes using the position of the nodes, whereas Algorithm 2 is self-synchronizing. Algorithm 1 outperforms Algorithm 2 regarding the transmission time by a constant factor.

We first describe the $\mathcal{O}(\log \log n)$-unicast algorithm in a network with $\sqrt{n} \times \sqrt{n}$ nodes placed in a grid. For unit grid distance we assume $\lambda \leq \frac{1}{2}$ to meet the far-field assumption. We start to describe the algorithm for a message transmission along the x-axis in the middle of the grid and generalize it for other coordinates, later on. The source node is at coordinates $(0, 0)$ and the target node at $(\sqrt{n}, 0)$. The algorithm consists of two phases, an initial phase (Fig. 4.15(a) 1st hop) where we broadcast the message from the source to the first rectangle of relay nodes, and a second phase where we perform multi-hop with collaborative beamforming between rectangular areas (Fig. 4.15(a), 2nd, 3rd hop). The transition from first to second phase has special requirements arising from properties of the second phase which is thus presented first.

We first describe how to set up phases for distributed beamforming when the senders are placed on a line along the x-axis (see Fig. 4.16) and extend that for rectangles in the plane, later on. Assume we have senders placed at $(i, 0)$ with $1 \leq i \leq n$ performing

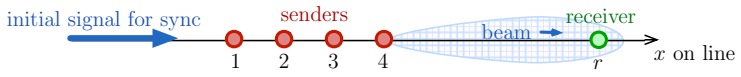

Figure 4.16: Synchronization in the one-dimensional case

beamforming to a receiver r at $(r_x, 0)$ with $r_x > n$. To attain full beamforming gain, the senders start the transmission with a delay of $(n - i)/c$ for propagation speed c such that all transmissions arrive exactly at the same time and consequently in the same phase. We synchronize all senders with the initial signal containing the message. A node placed at $(i, 0)$ receives the message at time $t = i/c$ and if each node resends the message immediately, it sends the message with delay $-i/c$, which is the desired beamforming setup to receiver r. Hence, broadcasting along a line achieves self-synchronization for distributed beamforming.

We use the same synchronization method for senders in a rectangular area, and each node u at coordinates (u_x, u_y) sends at time $t = u_x/c - t_0$ which only depends on the x-coordinate and offset time t_0 has to be chosen such that the sender with smallest

[2] We make no use of receive beamforming (SIMO). It requires that cooperative nodes exchange the received signals as quantized data for signal processing. For large sets of receivers, multi-hop transmissions of the signals are necessary, and more over, the message size grows exponentially if receiver beamforming is applied recursively since quantizing the signal has to be applied recursively.

u_x sends at time $t = 0$ without delay. If it holds $|u - v| = v_x - u_x$, which is the case for nodes along the x-axis, the synchronization is perfect. But for a rectangular area of nodes with width w_i and height h_i, the reception delay depends also on the y-coordinate. The delay function $\psi(i, v)$ computes for a receiver at coordinates $v = (v_x, v_y)$ the delay to attain synchronization, which is phase angle $\arg[e^{-j2\pi v_x/\lambda}]$.

$$\psi(i, v) = \frac{1}{f} + \frac{1}{2\pi f} \arg\left[\sum_{u \in (w_{i-1} \times h_{i-1})} \frac{e^{-j2\pi(|u-v|-v_x)/\lambda}}{|u - v|}\right] \tag{4.5}$$

When applying delay $\psi(i, v)$ at each receiver v, all nodes are synchronized for beamforming such that each node v sends with a delay of $-v_x/c$. By a proper choice of the dimensions of the rectangles (w_i, h_i), we can assure that the phase shift is less than $\pi/2$ and thus $\psi(i, v) > 0$ (compare Lemma 19).

This leads to Algorithm 1 where the delay $\psi(i, v)$ is used in line 3 in order to synchronize the receivers in the i-th round for the $w_i \times h_i$-receiver area. The if-condition in Line 2 assures that only receivers in the correct receiver area process the message.

Algorithm 1 Unicast I

```
1: procedure RECEIVE(receiver v, message m, time t)
2:     if ISINRECTANGLE(round (t), v) then      ▷ only process in active rectangle
3:         WAIT(ψ (round (t) , v))                              ▷ phase correction
4:         SEND(m)                          ▷ coordinated transmit beamforming
5: function ISINRECTANGLE(round i, position p)                ▷ true for active receivers
6:     return w_0 + w_i + 2 Σ_{k=1}^{i-1} w_k ≤ p_x ≤ w_0 + 2 Σ_{k=1}^{i} w_k & 0 ≤ p_y ≤ h_i
```

The following Lemmas 19-21 specify the dimensions and distances between rectangles of relay nodes where the multi-hop procedure of Algorithm 1 with distributed transmit beamforming is possible. Figure 4.17 illustrates the limitations of the dimensions. The

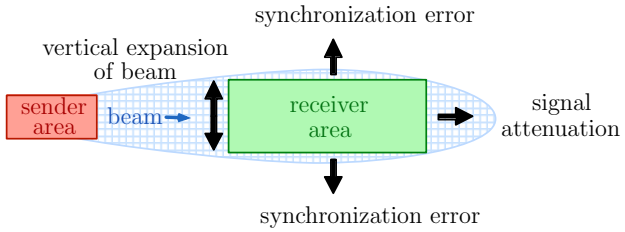

Figure 4.17: Limitations on the rectangle of receivers

send beam has an opening angle and becomes broader with the distance to the senders which makes a minimum distance necessary for a larger height of the rectangle of receivers. The height is again limited by the synchronization error. The width of the rectangle is limited by the signal attenuation due to path loss.

Lemma 19 *When a single sender node sends a signal to a $w \times h$ rectangular area in a distance of at least w (see Figure 4.18), the phase shift with respect to the phase $2\pi v_x/\lambda$ is at any receiver node v inside the area at most α if $h^2 \leq \frac{\alpha}{\pi}\lambda w$.*

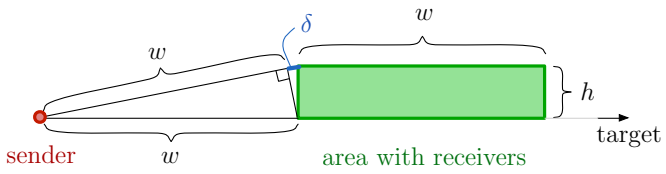

Figure 4.18: Broadcast of an single sender (red) to receivers in the green area.

Proof: Let X denote the signal of the sender u and Y the signal at v. Then,

$$Y = \frac{X}{|u-v|} \cdot \mathrm{e}^{-\frac{j2\pi}{\lambda}} \cdot |u-v| \quad .$$

Thus, the phase shift is described by $-\arg(\frac{Y}{X}) = \frac{2\pi}{\lambda}|u-v|$. The difference of phase shifts is therefore

$$\delta \quad = \quad \frac{2\pi}{\lambda}|u-v| - \frac{2\pi v_x}{\lambda} \quad = \frac{2\pi}{\lambda}\left(\sqrt{v_x^2+v_y^2} - v_x\right) = \frac{2\pi}{\lambda}v_x\left(\sqrt{1+\left(\frac{v_y}{v_x}\right)^2} - 1\right) \quad .$$

We can apply Lemma 36 (see Appendix A) and get

$$\delta \leq \frac{\pi}{\lambda}\frac{r_y^2}{r_x} \quad .$$

This phase difference is maximized for $v_y = h$ and $v_x = w$. Then,

$$\delta \leq \frac{\pi}{\lambda}\frac{h^2}{w} \quad .$$

From $h^2 \leq \frac{\alpha}{\pi}\lambda w$ it follows that $\delta \leq \alpha$. □

Note that the difference between the signal and the offset is so small, e.g. for $\alpha \leq \pi/4$, that it is less than one wavelength. So, if we repeat the message transmission after a fixed time offset in the next round, then the message modulated upon the carrier wave is in sync with all the other sender nodes provided by using the same time offset.

Lemma 20 *A $w_i \times h_i$-rectangular area of beamforming senders S can reach any node in a $w_{i+1} \times h_{i+1}$ rectangle at distance w_{i+1} if*

$$\begin{aligned} h_{i+1} &\geq h_i \ , && (4.6)\\ w_{i+1} &\geq w_i \ , && (4.7)\\ w_{i+1} &\leq \frac{1}{3\sqrt{2}} w_i h_i \ , && (4.8)\\ h_{i+1} &\leq w_{i+1} \ , \ \textit{and} && (4.9)\\ h_{i+1}^2 &\leq \frac{1}{4}\lambda w_{i+1} \ . && (4.10) \end{aligned}$$

Proof: Remember that all sending nodes u of a vertical column in the grid have the same phase which is created by characteristic $s_u = \mathrm{e}^{j\frac{2\pi u_x}{\lambda}}$. The channel from the set of senders S to the receiver v is

$$\begin{aligned} h &= \sum_{u\in S} s_u \cdot \frac{1}{|u-v|} \cdot \mathrm{e}^{-\frac{j2\pi}{\lambda}\cdot|u-v|} \\ &= \sum_{u\in S} \mathrm{e}^{j\frac{2\pi u_x}{\lambda}} \cdot \frac{1}{|u-v|} \cdot \mathrm{e}^{-\frac{j2\pi}{\lambda}\cdot|u-v|} \\ &= \sum_{u\in S} \frac{1}{|u-v|} \cdot \mathrm{e}^{-\frac{j2\pi}{\lambda}\cdot|u-v|+j\frac{2\pi u_x}{\lambda}} \ . \end{aligned}$$

And from Lemma 19 we get ($\alpha = \pi/4$) for

$$\beta_{s,r} := \frac{2\pi u_x}{\lambda} - \frac{2\pi}{\lambda}\cdot|u-v|$$

from $w_i \leq w_{i+1}$ and inequality (4.10)

$$0 \leq \beta_{s,r} \leq \frac{\pi}{4} \ . \tag{4.11}$$

We want to prove that $|h|^2 = \mathrm{SNR} \geq \tau = 1$. For this it suffices to prove that for the real part of h, i.e. that $\Re(h) \geq 1$, since $|h|^2 = \Im(h)^2 + \Re(h)^2$. Using

$$|u-v| \leq w_i + 2w_{i+1} \leq 3w_{i+1} \overset{\text{by}(4.8)}{\leq} \frac{1}{\sqrt{2}} w_i h_i = \frac{1}{\sqrt{2}}|S|$$

we get

$$\Re(h) = \sum_{u\in S} \frac{\Re\left(\mathrm{e}^{-j\beta_{u,v}}\right)}{|u-v|} = \sum_{u\in S} \frac{\cos\beta_{u,v}}{|u-v|} \geq \sum_{u\in S} \frac{\cos\frac{\pi}{4}}{w_i + 2w_{i+1}} \geq \frac{w_i h_i}{3w_{i+1}} \frac{1}{\sqrt{2}} \geq 1.$$

□

Figure 4.19 illustrates the relation between the sender and the receiver area. The delay δ illustrates the largest possible value $\beta_{u,v}$ in the range of Equation (4.11). If the

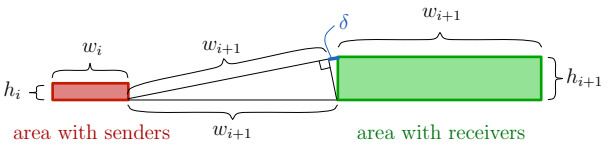

Figure 4.19: Area growth during broadcast step.

sender and the receiver are at the margin of the grid, we cannot expand the height of the relay node areas symmetrically along the line of sight between sender and receiver. To apply the algorithm also at the margin of the network, we only expand the height of the rectangle in one direction, i.e. towards the center of the network. This has been already addressed in Equation (4.10).

This leads to the double exponential growth of the rectangles given in closed form in the following lemma.

Lemma 21 *The equations*

$$w_i = \left(\frac{72}{\lambda}\right)\left(\frac{\lambda}{72}w_0\right)^{(3/2)^i}, \tag{4.12}$$

$$h_i = \sqrt{18}\left(18^{-\frac{1}{2}}h_0\right)^{(3/2)^i}, \tag{4.13}$$

for $i \in \{1, 2, \ldots\}$ *satisfy inequalities (4.6-4.10) for* $h_0 \geq 18^{\frac{1}{2}}$, $w_0 \geq \frac{72}{\lambda}$ *and* $h_0^2 = \frac{1}{4}\lambda w_0$.

Proof:

(4.6) : Merging Inequality (4.8) with (4.10) gives $h_{i+1} \leq \frac{\lambda}{4} \cdot \frac{1}{\sqrt{18}} \cdot w_i h_i \leq \frac{1}{\sqrt{18}} h_i^{3/2}$. Then, $h_i \leq h_{i+1}$ follows from $h_0 \geq \sqrt{18}$.

(4.7) : $w_i \leq w_{i+1}$ is true if $w_0 \geq \frac{72}{w_0}$.

(4.8) : $w_{i+1} \leq \frac{1}{3\sqrt{2}} w_i h_i$

Now $h_0 = 2\sqrt{\lambda w_0}$, which implies $w_0 h_0 = 2\sqrt{\lambda} w_0^{3/2}$. Therefore,

$$\begin{aligned} \frac{1}{\sqrt{18}} w_i h_i &= \frac{72}{\lambda}\left(\frac{\lambda}{72}\sqrt{\frac{\lambda}{72}} w_0^{3/2}\right)^{(3/2)^i} \\ &= \frac{72}{\lambda}\left(\frac{\lambda}{72} w_0\right)^{(3/2)^{i+1}} \\ &= w_{i+1} \,. \end{aligned}$$

(4.8) $h_i^2 \leq \frac{1}{4}\lambda w_i$: The following equations finalize the proof.

$$\begin{aligned} h_0^2 &= \frac{1}{4}\lambda w_0 \\ \frac{1}{18}h_0^2 &= \frac{\lambda w_0}{72} \\ 18\left(\frac{1}{18}h_0^2\right)^{(3/2)^i} &= \frac{1}{4}\lambda\left(\frac{72}{\lambda}\right)\left(\frac{\lambda}{72}w_0\right)^{(3/2)^i} \\ {h_i}^2 &= \frac{1}{4}\lambda w_i \end{aligned}$$

□

4.3.2 Unicast II: Unicast with Self-Synchronization

So far, we assume that a relay node calculates after the receipt of a message the received phase from the senders' positions and readjusts the phase such that all nodes of a vertical line are in phase. This step is not necessary if the dimensions of the rectangles are chosen according to Lemma 22. Then, the received signal can be sent without phase correction from each relay node. The algorithm then reduces to two steps: If a message has been received, relay nodes check from the message header whether they are in the correct rectangles. Then, each relay node repeats the messages after the same time offset.

Algorithm 2 Unicast II

```
1: procedure RECEIVE(receiver v, message m, time t)
2:     if ISINRECTANGLE(round (t), v) then      ▷ only process in active rectangle
3:         SEND(m)                              ▷ coordinated transmit beamforming
```

Lemma 22 *The routing of Unicast II can transmit a signal correctly without correcting the phase errors, if the following inequalities for the dimensions h_i and w_i of the relay rectangles are satisfied.*

$$h_{i+1} \geq h_i \ , \tag{4.14}$$

$$w_{i+1} \geq w_i \ , \tag{4.15}$$

$$w_{i+1} \leq \frac{1}{3\sqrt{2}} w_i h_i \ , \tag{4.16}$$

$$h_i \leq w_i \ , \ \textit{and} \tag{4.17}$$

$$h_i^2 \leq \frac{3}{2\pi^2}\frac{1}{(i+1)^2}\lambda w_i \ . \tag{4.18}$$

For Unicast I, we have shown a phase shift of at most α for the ratio of height and width of the rectangle with $h^2 \leq \frac{\alpha}{\pi}\lambda w$. Comparing this with Equation (4.18) of Unicast II,

we have an additional factor $\frac{3}{2\pi}(i+1)^{-2}$. The main idea to proof self-synchronization is that the phase shifts in each round form a convergent series $\alpha_i = \frac{3\pi}{2} \cdot \frac{1}{\pi^2 i^2}$, such that the sum of all phases $\sum_{i=1}^{\infty} \alpha_i \leq \frac{\pi}{4}$ can be bound. The proof is otherwise analogous to Lemma 20 and is combined with the proof of Lemma 23.

The dimensions of these rectangles can be chosen as follows.

Lemma 23 *The following recursions satisfy equations (4.14-4.18) for* $h_0^2 = \frac{3}{2\pi^2}\lambda w_0$ *for* $w_0 \geq \frac{96\pi^2 e \cdot c_4}{\lambda}$*, and* $h_0 \geq 4\sqrt{18}$*.*

$$w_{i+1} = \frac{1}{\sqrt{12}\pi} \cdot \frac{\sqrt{\lambda}}{i+1} \cdot w_i^{3/2} \tag{4.19}$$

$$h_{i+1} = 18^{-\frac{1}{4}} \frac{1+i}{2+i} \cdot h_i^{3/2} \ . \tag{4.20}$$

The recursions are satisfied by the following equations.

$$w_i \leq \left(\frac{\sqrt{\lambda}}{\sqrt{12}\pi}\right)^{2(3/2)^i-2} \cdot c_2^{-(3/2)^i} \cdot w_0^{(3/2)^i} \ \textit{with } c_2 \geq 12.011 \tag{4.21}$$

$$w_i \geq \left(\frac{\sqrt{\lambda}}{\sqrt{12}\pi}\right)^{2(3/2)^i-2} \cdot c_3^{-(3/2)^i} \cdot w_0^{(3/2)^i} \ \textit{with } c_3 \leq 1.58 \tag{4.22}$$

$$h_i = 18^{\frac{-(3/2)^i+1}{2}} \cdot \left(\frac{i+1}{i+2}\right)^{\frac{1}{2}(i-1)\cdot i} \cdot h_0^{(3/2)^i} \tag{4.23}$$

We see in the next section 4.3.3 that the initial phase of the algorithm needs a logarithmic number of rounds to reach the constant length w_0 and therefore $\log_{3/2}(w_0 \cdot \lambda) = 25$ for a moderate expansion with basis 3/2.

Proof: The recursions follow from combining Inequality (4.16) with (4.18).

$$w_{i+1} \overset{(4.16)}{=} \frac{1}{3\sqrt{2}} w_i h_i \overset{(4.18)}{=} \frac{1}{3\sqrt{2}} \left(\frac{3}{2\pi^2}\right)^{1/2} \frac{\sqrt{\lambda}}{i+1} w_i^{3/2} = \frac{1}{\sqrt{12}\pi} \cdot \frac{\sqrt{\lambda}}{i+1} \cdot w_i^{3/2}$$

$$h_{i+1} \overset{(4.18)}{=} \sqrt{\frac{3\lambda}{2\pi^2}} \frac{1}{i+1} w_{i+1}^{1/2} \overset{(4.16)}{=} \sqrt{\frac{3\lambda}{2\pi^2}} \frac{1}{i+1} \left(\frac{w_i h_i}{18^{1/2}}\right)^{1/2} \overset{(4.18)}{=} 18^{-\frac{1}{4}} \cdot \frac{i+1}{i+2} \cdot h_i^{3/2}$$

The equations (4.14-4.18) can be proven as follows:

(4.14) : To prove $h_i \leq h_{i+1}$, we insert h_0 into Equation (4.20).

$$h_1 = 18^{-\frac{1}{4}} \frac{1}{2} \cdot \left(4\sqrt{18}\right)^{3/2} = 4\sqrt{18} = h_0$$

Both factors $h_i^{3/2}$ and $\frac{1+i}{2+1}$ are monotonous increasing. In particular, the derivation of the latter is $(i+2)^{-2}$ which is positive for $i \geq 0$. Thus, if $h_1 = h_0$ then it holds that $h_{i+1} \geq h_i$.

(4.15) : To proof $w_{i+1} \geq w_i$, let us substitute $c_1 := \frac{\sqrt{\lambda}}{\sqrt{12\pi}}$ in Equation (4.19).

$$w_i = \frac{c_1}{i+1} \cdot w_{i-1}^{3/2}$$

Here are the first values of w_i:

$$\begin{aligned}
w_0 & \\
w_1 &= \frac{c_1}{2} \cdot w_0^{3/2} \\
w_2 &= \frac{c_1}{3} \cdot \frac{c_1^{3/2}}{2^{3/2}} \cdot w_0^{(3/2)^2} \\
w_3 &= \frac{c_1}{4} \cdot \frac{c_1^{3/2}}{3^{3/2}} \cdot \frac{c_1^{(3/2)^2}}{2^{(3/2)^2}} \cdot w_0^{(3/2)^3} \\
w_4 &= \frac{c_1}{5} \cdot \frac{c_1^{3/2}}{4^{3/2}} \cdot \frac{c_1^{(3/2)^2}}{3^{(3/2)^2}} \cdot \frac{c_1^{(3/2)^3}}{2^{(3/2)^3}} \cdot w_0^{(3/2)^4}
\end{aligned}$$

A closed-form solution for Equation (4.19) is

$$\begin{aligned}
w_i &= c_1^{\sum_{k=1}^{i} (3/2)^{k-1}} \cdot \prod_{k=1}^{i} (2+i-k)^{-(3/2)^{k-1}} \cdot w_0^{(3/2)^i} \\
w_i &\leq c_1^{2(3/2)^i - 2} \cdot c_2^{-(3/2)^i} \cdot w_0^{(3/2)^i} \qquad (4.24)
\end{aligned}$$

for a constant c_2 fulfilling the inequation

$$\begin{aligned}
c_2^{-(3/2)^i} &\geq \prod_{k=1}^{i} (2+i-k)^{-(3/2)^{k-1}} \\
&= 2^{\sum_{k=1}^{i} -(3/2)^{k-1} \cdot \log(2+i-k)} \\
&= 2^{\sum_{k=1}^{i} -(3/2)^{k-i-1} \cdot \log(2+i-k) \cdot (3/2)^i} .
\end{aligned}$$

When substituting $u := i - k$ we get

$$\begin{aligned}
c_2^{-(3/2)^i} &\geq 2^{\sum_{u=0}^{i-1} -(3/2)^{-u-1} \cdot \log(2+u) \cdot (3/2)^i} \\
&\geq (2^{c_4})^{-(3/2)^i}
\end{aligned}$$

where $c_2 = 2^{c_4}$ can be upper-bounded with

$$c_4 = \sum_{u=0}^{\infty} \frac{\log(2+u)}{(3/2)^{u+1}}$$

which converges to $c_4 \approx 3.586$ and we get for the constant

$$c_2 = 2^{c_4} = 12.011\ldots \qquad (4.25)$$

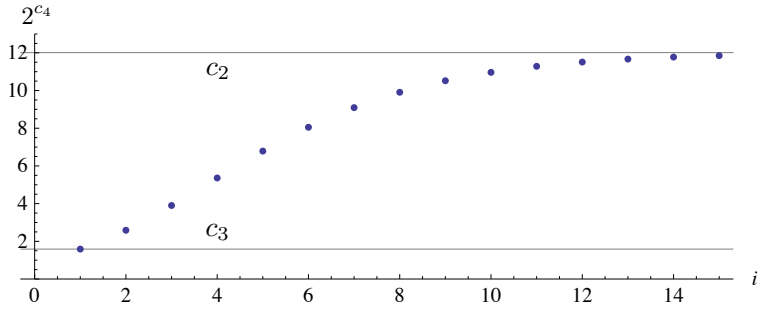

Figure 4.20: Constant c_4 in approximated closed solution of in Eq. (4.21) for width w_i.

Figure 4.20 shows a plot of 2^{c_4} for recursion step i with convergence to c_4 and a lower bound is also marked for $i = 1$ with

$$c_3 \leq 1.58 \,. \tag{4.26}$$

To satisfy $w_{i+1} \geq w_i$ we have to assure in Equation (4.21) that the initial value w_0 compensates from the beginning the limiting factors with c_1 and c_2. Thus,

$$w_0 \geq \frac{c_2}{c_1^2} = \frac{12\pi^2 \cdot c_2}{\lambda} \text{ for a constant } c_2 = 12.011 \,. \tag{4.27}$$

(4.23) : Here are the first values from the recursion of the height in Equation (4.20) with the constant $c_6 = 18^{-1/4}$.

$$\begin{aligned}
h_0 & \\
h_1 &= \frac{2}{3} c_6 \cdot h_0^{3/2} \\
h_2 &= \frac{3}{4} c_6 \cdot \left(\frac{2}{3}\right)^{3/2} c_6^{3/2} \cdot h_0^{(3/2)^2} \\
h_3 &= \frac{4}{5} c_6 \cdot \left(\frac{3}{4}\right)^{2/3} c_6^{2/3} \cdot \left(\frac{2}{3}\right)^{(3/2)^2} c_6^{(3/2)^2} \cdot h_0^{(3/2)^3}
\end{aligned}$$

The closed-form solution for h_i is therefore

$$\begin{aligned}
h_i &= c_6^{\sum_{k=0}^{i-1}(2/3)^k} \cdot \prod_{k=1}^{i} \left(\frac{i+1}{i+2}\right)^{i-k} \cdot h_0^{(3/2)^i} \\
&= c_6^{2(3/2)^i - 2} \cdot \left(\frac{i+1}{i+2}\right)^{\frac{1}{2}(i-1)i} \cdot h_0^{(3/2)^i} \,.
\end{aligned}$$

(4.16) : $w_{i+1} \leq \frac{1}{3\sqrt{2}} w_i h_i$

Now $h_0 = \sqrt{\frac{3\lambda}{2\pi^2} w_0}$, which implies $w_0 h_0 = \sqrt{\frac{3\lambda}{2\pi^2}} w_0^{3/2}$. Inserting w_{i+1} of Equation (4.19) gives

$$\begin{aligned} \frac{1}{\sqrt{12}\pi} \cdot \frac{\sqrt{\lambda}}{i+1} \cdot w_i^{3/2} &\leq \frac{1}{3\sqrt{2}} w_i h_i \\ \Rightarrow \frac{1}{\pi^2} \frac{\lambda}{(i+1)^2} \cdot w_i &\leq h_i^2 \text{ and replacing } h_i^2 \text{ with Equation (4.18)} \\ \Rightarrow w_i &\leq \frac{3}{2} w_i \Rightarrow \text{ true.} \end{aligned}$$

(4.17) We can show the inequation $h_i \leq w_i$ by comparing the closed solutions of w_i and h_i. Insertion of the lower bound for w_0 in Equation (4.21) gives

$$\begin{aligned} w_i &\geq \left(\frac{\lambda}{12\pi^2}\right)^{(3/2)^i - 1} \cdot c_2^{-(3/2)^i} \cdot \left(\frac{8e \cdot 12\pi^2 \cdot c_2}{\lambda}\right)^{(3/2)^i} \\ &= \frac{12\pi^2}{\lambda} (2e)^{(3/2)^i} \cdot 4^{(3/2)^i} . \end{aligned} \tag{4.28}$$

Insertion of h_0 into Eq. (4.23) gives

$$h_i = \sqrt{18}^{-(3/2)^i + 1} \cdot \left(\frac{i+1}{i+2}\right)^{\frac{1}{2}(i-1)\cdot i} \cdot \left(4 \cdot \sqrt{18}\right)^{(3/2)^i} = \sqrt{18} \cdot 4^{(3/2)^i} \tag{4.29}$$

For $w_i \geq h_i$ it follows $\lambda \leq 8 \cdot \pi^2 \cdot c_5^{3/2} \approx 353$ which is true.

(4.18) For proving $h_i^2 \leq \frac{3}{2\pi^2} \frac{1}{(i+1)^2} \lambda w_i$, we insert the the closed solutions of w_i (Equation (4.28)) and h_i (Equation (4.29)).

$$\begin{aligned} 18 \cdot 4^{2(3/2)^i} &\leq \frac{3}{2\pi^2} \cdot \frac{1}{(i+1)^2} \lambda \cdot \frac{12\pi^2}{\lambda} \cdot (8c_5)^{(3/2)^i} \\ \Rightarrow (i+1)^2 &\leq c_5^{(3/2)^i} \\ \Rightarrow 2 \cdot \log(i+1) &\leq \left(\frac{3}{2}\right)^i \cdot \log c_5 \\ \Rightarrow \frac{(3/2)^{i+1}}{\log(i+1)} &\geq \frac{4 \log c_5}{3} \\ \Rightarrow (i+1)\log(3/2) - \log\log(i+1) &\geq \log(4/3) + \log\log(c_5) \\ \Rightarrow i \cdot \log(3/2) - \log\log(i+1) &\geq \log(8/9) + \log\log(c_5) \end{aligned}$$

This inequality cannot be solved for i in closed form and therefore we compute a lower bound for the constant c_5 by analyzing the following function:

$$\frac{c_5^{(3/2)^i}}{(i+1)^2} \geq 1 \tag{4.30}$$

and setting the derivation for variable i equals zero gives

$$\begin{aligned} 0 &= \frac{(3/2)^i \cdot c_5^{(3/2)^i} \cdot \log(3/2) \log(c_5)}{(i+1)^2} - \frac{2c_5^{(3/2)^i}}{(i+1)^3} \\ \frac{2}{(i+1)} &= (3/2)^i \cdot \log(3/2) \log(c_5) \\ i_0 &= \frac{\text{ProductLog}\left(\frac{3}{\log(c_5)}\right) - \log(3/2)}{\log(3/2)} \end{aligned}$$

Here, the function $\text{ProductLog}(x) = w$ is the inverse function of $x \mapsto we^w$. The value i_0 is the location of the minimum. To find the minimum, i_0 needs to be substituted into Inequality (4.30). So, this implies

$$c_5 \geq \mathrm{e} \tag{4.31}$$

since $\frac{c_5^{(3/2)^{i_0}}}{(i_0+1)^2} = 1.00208 > 1$ for $c_5 = \mathrm{e}$.

□

4.3.3 Initial Phase of the Algorithm

It remains to show how to inform the first rectangle of the second phase. For this, we use the broadcast algorithm of Section 4.2 [JS13] in an initial phase.

Lemma 24 *A start phase of $\mathcal{O}(-\log \lambda)$ rounds allows to inform an initial area of nodes with $w_0 > \frac{72}{\lambda}$, $h_0 \geq \sqrt{18}$, $h_0^2 \leq \frac{1}{4}\lambda w_0$, and $h_0 \leq w_0$.*

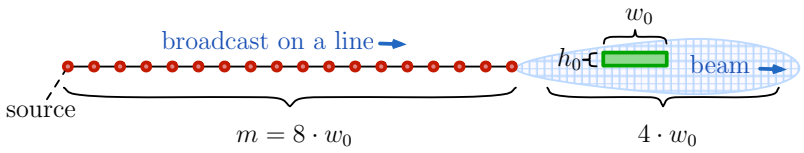

Figure 4.21: In an initial phase, a broadcast on a line with $m = 8w_0$ nodes is performed followed by a last hop of cooperative beamforming from the line of senders to the first rectangle with dimensions $w_0 \times h_0$.

Proof: To inform the first rectangle with dimensions $w_0 \times h_0$, we first inform $8w_0$ subsequent nodes placed on a line which together can inform and synchronize all nodes in the first rectangle with collaborative beamforming (see Figure 4.21). To initially inform a line of $m = 8w_0$ senders, we use the exponential broadcast algorithm of Section 4.2 [JS13], which informs m nodes placed on a line in $\mathcal{O}(\log m)$ rounds. Note

that the exponential broadcast algorithm has informed at least $(3/2)^i$ nodes after round i. We choose m large enough that this line can inform a rectangle of dimensions $w_0 \times h_0$ in distance w_0. We choose $m = 8w_0$ which results in a runtime $k \cdot \log\left(\frac{8 \cdot 72}{\lambda}\right) = \mathcal{O}(-\log\lambda)$ rounds for some constant k. Then, $8w_0$ nodes are in phase to inform not only the next $4w_0$ nodes on the line but also all other nodes in the beam including a rectangle with dimensions $w_0 \times h_0$. However, there will be a phase shift for the nodes of the rectangle, which are not on the line. By Lemma 19, this offset attenuates the signal by a factor of at most $\frac{1}{\sqrt{2}}$. Therefore, all nodes of this initial rectangle receive the message. Analogous to Equation (4.5), we can compute the delay error for each node in the first rectangle placed at $v = (v_x, v_y)$ with

$$\psi(i,v) \quad = \quad \frac{1}{f} + \frac{1}{2\pi f} \arg[\sum_{x=0}^{8w_0-1} \frac{\mathrm{e}^{-j2\pi\left(\sqrt{(x-v_x)^2+v_y^2}-v_x\right)/\lambda}}{\sqrt{(x-v_x)^2+v_y^2}}] \,. \tag{4.32}$$

□

The above lemmas lead to our main result of the $\mathcal{O}(\log\log n)$ unicast.

Theorem 8 *Assume n nodes are placed in a grid with unit distance. Each node has a transceiver with one antenna, only the transmission power to reach each neighbor, and uses the carrier wavelength $\lambda \leq \frac{1}{2}$. Then, any node can send a message to any other node in $\mathcal{O}(\log\log n - \log\lambda)$ rounds.*

Proof: The basic idea is, first to route on the x-axis until the correct y-coordinate has been reached and then to relaunch the algorithm orthogonally on the y-axis (compare Figure 4.22). Then, the claim follows by the above lemmas. □

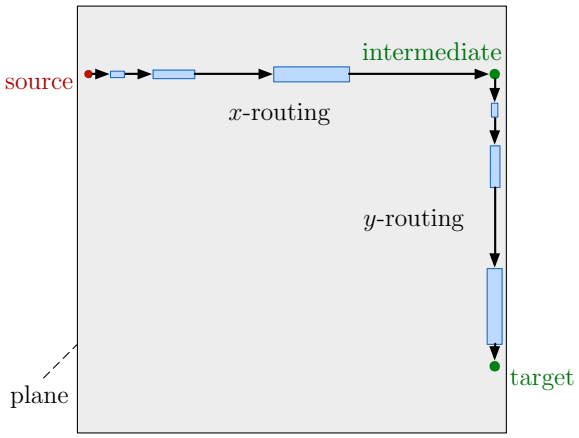

Figure 4.22: x-y routing for a routing between any nodes in the plane (Theorem 8)

The asymptotic energy is given by the sum of sending nodes, i.e. $\sum_{i=1}^{r} w_i h_i$ for r rounds, since each node sends with constant energy. Now, $w_i h_i = \Theta(w_{i+1})$, where $w_{i+1} = \Theta(d)$ and w_i grows double exponentially. So, for the sum of transmission energy, the last term asymptotically bounds the sum.

Corollary 7 *The overall transmission energy consumed by the $\mathcal{O}(\log\log n)$ unicast algorithm for sending a message over distance d is $\Theta(d)$.*

4.3.4 Unicast of Randomly Placed Nodes

Now, we apply this observation to randomly placed nodes in a square with area n. First, we establish a bound on the minimum number of nodes in some area.

Lemma 25 *Given n nodes randomly distributed in a square of area n with transmission range $k\sqrt{\log n}$ for some constant k. In every geometric object inside a square of an area of at least $k^2 \log n$ lie at least $\log n$ nodes with high probability, i.e. $1 - n^{-\ell}$ for some constant ℓ.*

Proof: This follows from a straight-forward application of the Chernoff bound. Let X denote the number of nodes in the square. Then, the probability for a node lying in it is $p = \frac{k^2 \log n}{n}$. The expected number of nodes is $\mu = pn = k^2 \log n$. Now, we use for $0 < \delta < 1$.

$$\mathbf{P}(X \leq (1-\delta)\mu) \;\leq\; e^{-\frac{\delta^2}{2}\mu} \tag{4.33}$$

For $\delta = \frac{\sqrt{\ell \ln 4}}{k}$, we have

$$\mathbf{P}(X \leq \left(1 - \frac{\sqrt{\ell \ln 4}}{k}\right) k^2 \log n) \;\leq\; n^{-\ell}\,. \tag{4.34}$$

For $k \geq \sqrt{4 + \ell \ln 4}$, we have $\left(1 - \frac{\sqrt{\ell \ln 4}}{k}\right) k^2 \geq 1$ and

$$\mathbf{P}(X \leq \log n) \;\leq\; n^{-\ell}\,. \tag{4.35}$$

□

If the transmission distance is asymptotically smaller, the network is disconnected with probability 1 in the limit [GK98].

Theorem 9 *Given n nodes randomly distributed in a square of area n with transmission range $k\sqrt{\log n}$ for some constant $k > 0$. Then, for wavelength $\lambda \geq \frac{3k}{\sqrt{\log n}}$ a node can send a message to any other node in time $\mathcal{O}(\log\log n)$ with high probability, i.e. $1 - n^{-\mathcal{O}(1)}$.*

Proof: We use the above observation which lower-bounds the number of nodes in the transmission range of the start node as $\log n$.

Now we consider a $k\sqrt{\log n} \times k\sqrt{\log n}$ square around the start node. We need to do a preparation step where we inform a rectangle satisfying the rectangle properties (4.6)-(4.10). Consider a rectangle $w_1 \times h_1$ in distance w_1 from the start square.

We choose

$$w_1 = \frac{1}{3}k \log^{3/2} n \tag{4.36}$$

$$h_1 = k\sqrt{\log n} \tag{4.37}$$

and prove that within one hop this rectangle can be informed from the start square which fulfills the rectangle properties (4.6)-(4.10) and can serve as a start rectangle for the double exponential growth of Theorem 8. We assume that all these nodes have position information which they can use to adapt the phase in order for the second phase of the algorithm.

This rectangle is in reach of the start square since we have at least $\log n$ nodes (with high probability). These nodes have transmission range $k\sqrt{\log n}$ each, since $w_1 \leq \frac{1}{3}k \log^{3/2} n$.

Inequality (4.10) states that $h_1^2 \leq \frac{1}{4}\lambda w_1$. Since $\lambda \geq \frac{3k}{\sqrt{\log n}}$, we have

$$h_1 = k^2 \log^2 n \leq \lambda w_1 \ .$$

The number of nodes in the $w_1 \times h_1$ rectangle has increased to $\Omega(\log^2 n)$ with high probability. From now on, the rest follows by the double exponential growth argument analogously to Theorem 8, where each step is successful with high probability. This can be proven by Chernoff bounds, since the transmission distance is a factor $\mathcal{O}(\sqrt{\log n})$ larger than in the grid model. □

Now each node sends with energy $\Theta(\log n)$, which is proportional to the square of the transmission range. Like in the first Corollary the number of sender nodes is again $\Theta(d)$. Therefore we have the following energy consumption.

Corollary 8 *The overall transmission energy in the randomly positioned case for sending a message over distance d is $\Theta(d \cdot \log n)$.*

4.3.5 Converging Towards the Speed of Light

For broadcast on the line, we have presented a method in Section 4.2 which needs $\mathcal{O}(\log n)$ rounds [JS13]. The processing time at each relay node consists of receiving the message, analyzing it, and re-sending it, which we denote by t_0. Note that t_0 is a constant. Let us denote the node distance from the start node by d and c denotes the speed of light as the signal speed.

Lemma 26 *For broadcast on the line, the maximum transmission speed is at most* $\frac{1}{\sqrt{2}}c$ *which is a constant slower than speed of light* c*.*

Proof: In each round i the transmission distance increases exponentially by $d_i = b^i$ for some basis $b \in (1,2)$. Then in round $r = \lceil \log_b d \rceil$ the target is reached.

So, the overall time $T(d)$ is

$$T(d) \quad \leq \quad r \cdot t_0 + \sum_{i=1}^{r} \frac{d_i}{c} = r \cdot t_0 + \frac{1}{c} \cdot \frac{b^{r+1}-1}{b-1} \ .$$

Since $d \cdot b \leq b^{r+1} \leq d \cdot b^2$, we have

$$T(d) \geq t_0 \lceil \log_b d \rceil + d \cdot \frac{1}{c} \cdot \frac{b - \frac{1}{d}}{b-1} \ .$$

Therefore, the transmission velocity $v(d) = d/T(d)$ is at most

$$v(d) \quad \leq \quad c\left(1 - \frac{1}{b} \pm o(1)\right) \ .$$

So, the maximum speed of transmission on the line is a constant fraction of the speed of light. □

In two dimensions the situation is different. However, the unicast algorithm presented in Theorem 8 sends a message along the x-axis and then along the y-axis and this detour reduces the transmission speed to at most $\frac{1}{\sqrt{2}}c$.

Theorem 10 *For carrier wavelength* $\lambda \in \Omega(1)$ *and a quadratic grid with* n *nodes with unit node distance and unit transmission distance, it is possible to send a message from any node to any other node with a speed of* $c(1 - o(1/n))$ *where* c *is the speed of light.*

Proof: We use the same construction as in Theorem 8, but now we tilt the rectangles such that the beamforming is straight from source to target node. The number of nodes in the rectangles does not change except to some boundary effects, the influence of which is negligible. The starting rectangle needs a width of $w_0 = \Omega(1/\lambda)$. Since $\lambda \in \mathcal{O}(1)$, we can inform all nodes of this rectangle in constant time sequentially by single hop messages and add delay instructions to set up beamforming in the starting rectangle.

Then, the distances w_i grow double exponentially, i.e. $w_i = (w_{i-1})^b = (w_0)^{b^i}$ for some $b > 1$ and $w_0 > 1$. The number of rounds is $r = \mathcal{O}(1) + \log_d \log_{w_0} d$ for distance d. Note that

$$\begin{aligned} w_i - \sum_{j=0}^{i-1} w_j \quad &= \quad (w_0)^{b^i} - \sum_{j=0}^{i-1} (w_0)^{b^j} \geq (w_0)^{b^i} \cdot \left(1 - i(w_0)^{-b^i(1-1/b)}\right) \\ &= \quad (w_0)^{b^i} \cdot (1 - o(1)) \ . \end{aligned}$$

Besides the signal propagation delay $\frac{d}{c}$, we get two additional kinds of delays: one for the message handling in each round at the nodes, i.e. $\Theta(\log\log d)$, and the other one for propagation delays inside the rectangles; we initiate the next round in a rectangle when all nodes of the rectangle have received the message in the last round which takes time $\frac{w_i}{c}$. So, in each round i we have a message delay of $\frac{w_i}{c}$ for all $i < r$. The last hop w_r dominates all other rounds, if we adapt the second last step by using a shorter beamforming step if necessary. This guarantees that the target is reached within the rectangle and that the last inequality above holds for w_r.

Note that $d = w_r + \sum_{i=1}^{r-1} 2w_i + w_0$ and therefore $\sum_{i=0}^{r-1} w_i = o(d)$. So, the overall time for the message transmission is

$$T(d) = \frac{d + o(d) + \Theta(\log\log d)}{c} = \frac{1}{c} \cdot d \cdot (1 + o(1)) \ .$$

So, the message velocity is

$$v(d) = \frac{d}{T(d)} = c(1 - o(1)) \ .$$

□

4.3.6 Upper Bound for Electromagnetic Field Strength

The unprecedented long transmission range of a rectangular field begs the question whether the received signal energy might become too strong to be tolerated. The following lemma shows that the signal strength, which is proportional to the square root of the received power, grows rather moderately.

Lemma 27 *In a grid network with $\sqrt{n} \times \sqrt{n}$ nodes, Unicast I and II produce signal amplitudes $\mathcal{O}\left(\max\left\{\ln n, \lambda^{1/3} \cdot n^{1/6} \cdot \ln\frac{n}{\lambda}\right\}\right)$.*

This lemma only considers the signal strength at receiver positions while Lemma 13 on page 89 shows the maximum field strengths.

Proof: In our setting, n nodes are placed in a grid in the plane with grid distance 1 and corresponding dimensions of the network $\sqrt{n} \times \sqrt{n}$. Then, the rectangle of the last step can have maximum width $w_{\ell+1} = \sqrt{n}/2$ with distance $\sqrt{n}/2$ to the sender rectangle with dimensions $w_\ell \times h_\ell$. We can compute the dimensions with the equations of Lemma 21.

$$w_{\ell+1} \quad = \quad \frac{72}{\lambda} \cdot \left(\left(\frac{\lambda}{72} w_0\right)^{(3/2)^\ell}\right)^{(3/2)} \quad \Rightarrow \quad w_\ell = w_{\ell+1}^{2/3} \cdot \left(\frac{72}{\lambda}\right)^{1/3}$$

Substituting $w_{\ell+1}$ with $\sqrt{n}/2$ gives

$$w_\ell \quad = \quad n^{1/3} \cdot \frac{18^{1/3}}{\lambda^{1/3}} \ .$$

Using Equation (4.10) we get the height of the rectangle

$$h_\ell = \frac{1}{2}\lambda^{1/2} \cdot w_\ell^{1/2} = \frac{1}{2}\lambda^{1/2} \cdot n^{1/6} \cdot \frac{18^{1/6}}{\lambda^{1/6}} = \frac{18^{1/6}}{2}\lambda^{1/3} \cdot n^{1/6} \ .$$

We can upperbound the signal amplitude at the end of one horizontal line in the rectangle with w_ℓ senders with

$$|h_{\text{line}}| \leq 2 \cdot \sum_{i=1}^{w_\ell} \frac{1}{i} \leq 2 + 2 \cdot \ln(w_\ell) = 2 + \frac{2}{3}\ln\left(\frac{18}{\lambda}\right) + \frac{2}{3}\ln(n) \ .$$

Now we consider the nearest node to the sender rectangle in the middle of the sender beam. We can upperbound the signal amplitude by adding the signal strength of all h_ℓ lines with length w_ℓ. With the beamforming setup and $w_\ell \gg h_\ell$ the phase error will be rather small and the bound will be tight. Then we have

$$\begin{aligned} |h_{\text{rect}}| &\leq h_\ell \cdot |h_{\text{line}}| = \frac{18^{1/6}}{2}\lambda^{1/3} \cdot n^{1/6} \cdot \left(2 + \frac{2}{3}\ln\left(\frac{18}{\lambda}\right) + \frac{2}{3}\ln(n)\right) \\ |h_{\text{rect}}| &= \mathcal{O}\left(\lambda^{1/3} \cdot n^{1/6} \cdot \ln\frac{n}{\lambda}\right) \ . \end{aligned}$$

Thus, the maximum signal strength of the unicast algorithm is polynomial.

For the final result, we have also to consider the case of the initial phase, when the line broadcast has been finished. For $\sqrt{n} \leq 12w_0 = \frac{12 \cdot 72}{\lambda}$ we are in the initial phase and therefore the amplitude is

$$2 + 2\ln\left(\frac{2}{3}\sqrt{n}\right) = 2 + 2\ln\frac{2}{3} + \ln n = \mathcal{O}(\ln n) \ .$$

Summarizing, we get an asymptotic upper bound of

$$h_{\text{Unicast I}} \in \mathcal{O}\left(\max\left\{\ln n, \lambda^{1/3} \cdot n^{1/6} \cdot \ln\frac{n}{\lambda}\right\}\right) \ .$$

In Unicast II, we have chosen the initial rectangle with dimensions $w_0 \times h_0$ in such a way, that in Equation (4.19), which states the recursion of the rectangle width, factor $w_i^{3/2}$ compensates factor $(i+1)^{-1}$ right from the start with width w_0. The same holds for the recursion for the height of the rectangle. Thus, although the rectangles of Unicast II compared with the rectangles of Unicast I have a larger width to satisfy the maximum phase error, for the asymptotic signal strength we observe

$$h_{\text{Unicast I}} \in \mathcal{O}(h_{\text{Unicast II}}) \ .$$

□

4.3.7 Lower Bound for Time

We will now investigate the principal bounds for time delay of disseminating a message in a two-dimensional grid. For this, we concentrate on the question, how many rounds it takes at minimum to reach a node in the Euclidean distance d, when in the first round only one node was informed.

The key question for the lower bound for time is, up to when we can safely assure that a node v has not received the message, yet. This is the case when all super-positioned signals cannot be distinguished from the background (or internal) noise.

We assume that each sender u has transmission power $|s_u|^2 = P$ and the channel from senders $u \in S$ to receiver v has the function

$$h \quad = \quad \sum_{u \in S} \frac{s_u}{|u - v|} \ .$$

The attenuation of the signal power is then

$$|h|^2 = \left| \sum_{u \in S} \frac{s_u}{|u - v|} \right|^2 \ .$$

If this term is smaller than a constant c_n we assume no signal can be received.

The following theorem shows the time optimality of our $\mathcal{O}(\log \log n)$ unicast algorithm.

Theorem 11 *In a grid with n nodes with constant transmission power, every unicast message takes at least $\Omega(\log \log n)$ rounds to reach its destination.*

Proof: Let u be the start node and let $C_d := \{v \in V : |u, v| \leq d\}$ denote all nodes within Euclidean distance at most d from u.

Now in round i, let d_i be the distance of the farthest node in this round carrying the (or some parts of the) message. Now consider a node v in distance $d' \gg d_i$.

The attenuation of the signal power at distance d' is

$$|h|^2 \leq \left| \sum_{u \in C_{d_i}} \frac{s_u}{|u - v|} \right|^2 \leq \left(\sum_{u \in C_{d_i}} \frac{\sqrt{P}}{d' - d_i} \right)^2 \leq P \frac{|C_{d_i}|^2}{(d' - d_i)^2} \ ,$$

where P is the maximum transmission power of each node (a constant). In order to receive the signal, this power must be larger than a constant $\tau > 0$. We want to investigate the case when we cannot receive a signal, i.e.

$$P \frac{|C_{d_i}|^2}{(d' - d_i)^2} \leq \tau \ .$$

Then, $d' \geq d_i + |C_{d_i}| \sqrt{\frac{\tau}{P}}$ which implies with $|C_d| \leq 2\pi d^2$ that

$$d' \geq d_i + 2\pi d_i^2 \sqrt{\frac{\tau}{P}} \ .$$

From this it follows that $d_{i+1} \leq k \cdot d_i^2$ for a constant $k > 0$ and thus

$$d_{i+1} \leq k^{2^i-1}(d_1)^{2^i} \ .$$

Therefore, it takes at least some $k' \log\log d$ rounds (for a constant $k' > 0$) to inform a node in distance d. □

4.3.8 Simulation

We have simulated collaborative transmit beamforming for nodes placed in a rectangle in the plane. The dimensions of the rectangles correspond to Unicast I (compare Fig. 4.15(b)). Figure 4.23 shows the signal strength respectively phase shift of a 1705×186 grid network with grid distance 1 (one pixel=1 node) and the wavelength is $\lambda = 0.1$. We see sender beamforming from a rectangle with 341×6=2046 nodes to a receiver area with 482×7=3374 nodes (the areas are white bordered).

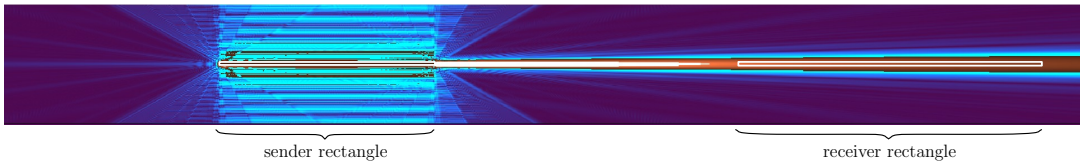

(a) SNR with color range [orange,white) over threshold τ and [purple, cyan) under τ

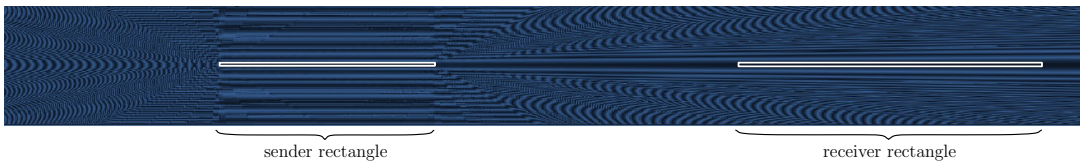

(b) Phase error with angle range $[0, \pi)$ and colors [black, blue)

Figure 4.23: Simulation of beamforming senders which are placed in a rectangle and produce a beam to the right. An animation with varying wavelength λ is available at `www.youtube.com/watch?v=3TJ2Gz8uhbc`.

The first picture 4.23(a) shows the signal strength where the blue color range depicts amplitudes under the SNR threshold $\tau = 1$ and the orange-white color range represents signal strengths over τ. We can spot a sharp beam around the receiver rectangle with a signal over the SNR threshold. The light blue lines over and under the sender rectangle indicate strong non receivable interferences for nodes not involved in the Unicast operation. We can also see two side lobes with 45 degree alongside the main beam. The second figure 4.23(b) shows the phase shift for synchronized beamforming. The black corridor from sender to receiver rectangle makes clear, that all nodes receiving the message within this corridor will be synchronized for beamforming to the right. The blue lines around the corridor mark a phase shift of π and the subsequent next black rays around have a phase error of 2π, i.e. one period $1/f_c$ of carrier frequency f_c.

Notably, the spatial variation of the phases of the super-posed signal is much smaller than the wavelength (=0.1 pixels) and scales with the size of the sender rectangle.

Figure 4.24(a) shows the beamforming gain for the wavelengths $\lambda \in \left\{\frac{1}{8}, \frac{1}{4}, \frac{1}{2}, 1, 2\right\}$. The $n = 2048$ cooperating senders are selected according to Unicast I and highlighted with an orange rectangle on the left and the signal is over the SNR threshold in the blue colored area. We did not intend to show the special case where the wavelength is an integer multiple of the grid distance and thus added a small ϵ to the wavelength. The reception distance of the beam is nearly equal to n showing full beamforming gain

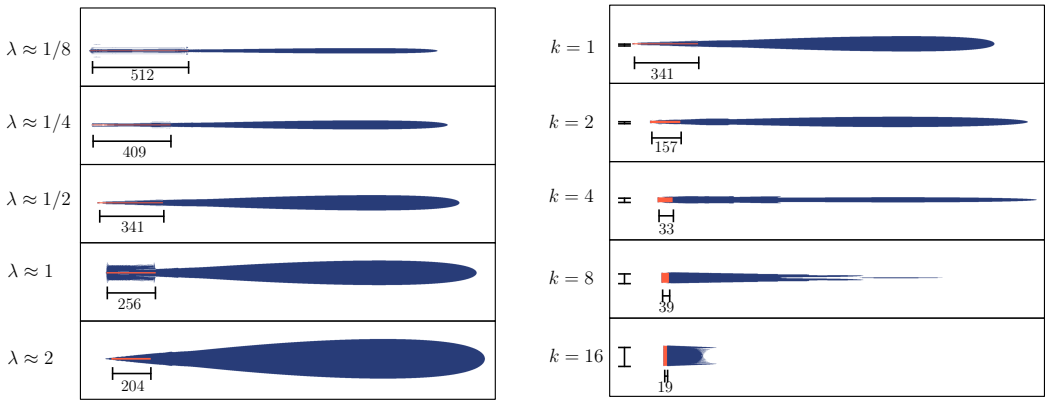

(a) $n = 1000$, height $h^2 = \lambda w$.

(b) $n = 2048$, $\lambda = \frac{1}{2}$ and varying rectangle sizes.

Figure 4.24: Simulation of n beamforming senders placed in a rectangle (orange colored at the left) which produce a beam to the right.

in the middle of the beam. The height of the beam increases with the wavelength λ.

In a second experiment, we manipulate for a constant wavelength $\lambda = 0.5$ the ratio of the rectangle with factor k, i.e. $w := A/k$ and $h := A \cdot k$. When we increase the height, we can spot two effects. First, the beam is sharper and we cannot reach a rectangle with larger height in the multicast. In the examples $k \geq 4$ the height even shrinks. Second, the perception range decreases and we can only multicast to a short distance.

We simulated the phase error which occurs in the initial phase (see Equation (4.32)) when informing the first rectangle with $w_0 \cdot h_0$ receivers from a line of $8w_0$ senders in distance w_0. We set the parameters to $\lambda = 0.1$, $w_0 = 2 \cdot \frac{72}{\lambda} = 1440$, and $h_0 = \sqrt{\lambda \cdot w_0/4} = 6$. Figure 4.25 shows the phase error compared to the synchronized phase for the coordinates (x, y) where $y = h_0$ is the top border of the first rectangle. We see that the phase shift around the line of senders for $0 \leq x \leq 8w_0$ is arbitrary in the range $[0, 2\pi)$ and for $x \geq 9w_0$ the phase shift is smaller than $1/\sqrt{2}$ as assumed.

Figure 4.26 shows an example for the propagation velocity during the execution of algorithm Unicast I. The vertical line separates the initial phase using the line-broadcast

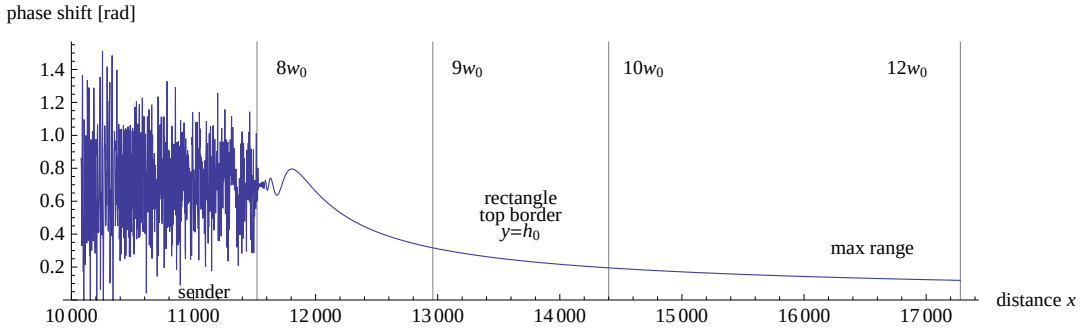

Figure 4.25: Phase shift error for broadcasting from a line of $8w_0$ senders to a rectangle of $w_0 \cdot h_0$ receivers in distance w_0 with parameters $\lambda = 0.1$ and $w_0 = 1440$.

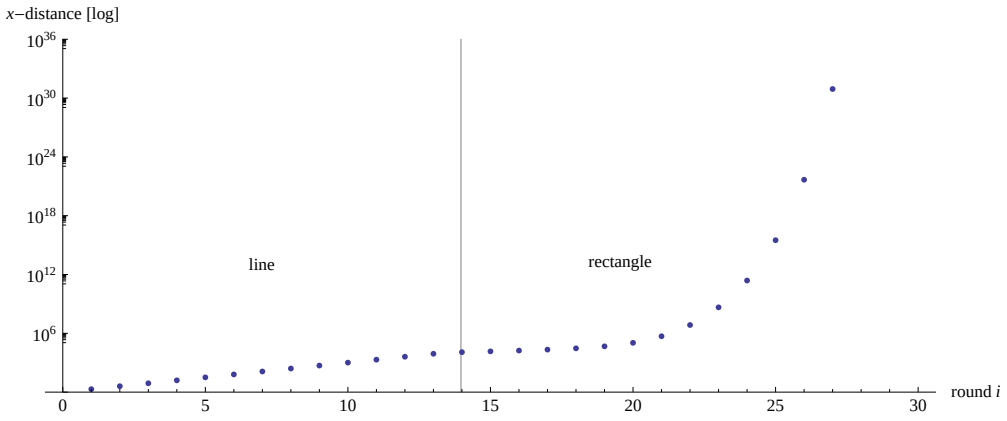

Figure 4.26: Progress of the algorithm Unicast I for $\lambda = 0.1$, $w_0 = 1000$, and the source at $x = 0$. The graph shows for round i the x-coordinate of the farthest informed node.

with exponential growth from the second phase applying Unicast I with double exponential growth. The constant slope in linear-log scale suggests an exponential growth in the first phase. When transitioning into the second phase, the slope of the progress first decreases and it takes around 5 rounds that Unicast algorithm can pick up speed and disseminates faster than the exponential growth in the initial phase. But from round $i = 26$ on, the information dissemination literally explodes. But of course, the time for each round increases with hop distance and though speed of light c is the limiting factor as the graph in Figure 4.27 shows, where the propagation distance x is plotted for time t. In this experiment, we assume a distance between nodes of 1 meter and a processing time of 10^{-2} seconds at each relay node. The brown line shows the propagation with speed of light, i.e. one hop broadcast.

In this section, we have presented a unicast algorithm for ad hoc networks on a grid with n nodes, which needs only $\mathcal{O}(\log \log n)$ rounds for wavelength $\lambda \in \Omega(1)$. This

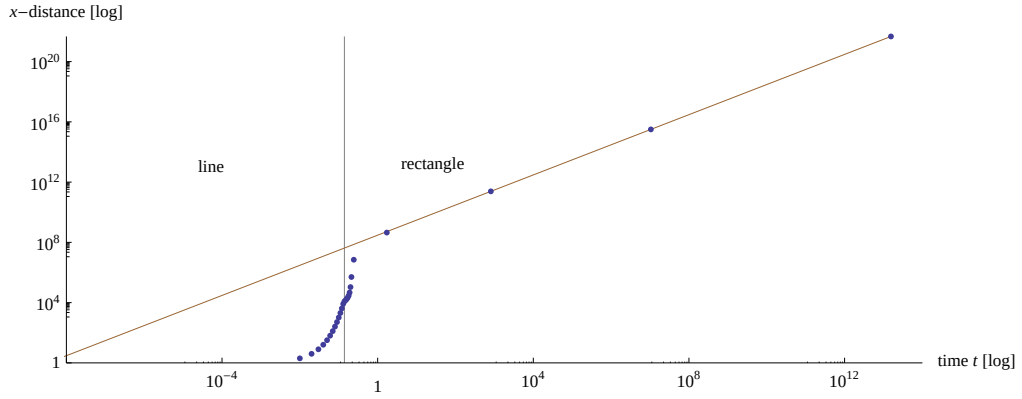

Figure 4.27: Progress of the algorithm Unicast I for $\lambda = 0.1$, $w_0 = 1000$, and the source at $x = 0$. The graph shows for round i the x-coordinate of the farthest informed node.

algorithm combines beamforming with multi-hop routing. Beamforming increases the hop distances to a double exponentially growth, i.e. $\Theta\left({w_0}^{(b^i)}\right)$ for round i. This growing beamforming gain is realized by a set of increasing rectangular areas containing relay nodes. Similar results can be shown for randomly placed nodes in a square, if the transmission range is increased by a factor of $\Omega(\sqrt{\log n})$. The overall transmission velocity of such unicast algorithms converges towards the speed of light and for the grid we show the optimality of the routing time $\mathcal{O}(\log \log n)$. Such a unicast algorithm does not asymptotically use more energy than the basic multi-hop algorithm.

Unlike in the one-dimensional case, the wavelength plays a large role in the construction and performance of the algorithm. Short wavelengths compared to the node distance increase the run-time, since it takes longer until the double exponential growth phase begins. For random placement it is not clear how beamforming can be utilized for wavelengths shorter than $\mathcal{O}(1/\log n)$, while for larger wavelengths our algorithm provides a solution. In the grid, the unicast algorithm has only logarithmic run-time if the wavelength is $\mathcal{O}(1/n^c)$. Note that the wavelength is taken relative to the node density. So, for fixed wavelength the node density plays the same role, where small node distances allow faster unicast.

Since we only use beam-formed sending with Multiple Input Single Output (MISO), the main component of the algorithm is to obey a fixed time delay between receiving the full message and residing it. Besides this, only a check is needed, whether the relay node is in one of the rectangles necessary for transport. This can be computed from the message header and the position information of the relay node. An exact position information is therefore not necessary. This is an extreme simplification compared to the way beamforming is usually achieved.

4.4 Energy-Efficient Unicast in the Plane and in Space

The efficiency of routing algorithms in ad hoc networks can be measured by delay, throughput, and power consumption. In mobile networks, most of the power at the nodes is consumed by radio transmission. Compared to centralized network structures, ad hoc networks allow a reduction of this factor, since shorter distances can reduce the transmission energy. While in practice this factor is limited, since there is some base power consumption at the electronic devices, in theory this effect favors long paths with very small hops over shorter paths with long hops [HSVG04]. Furthermore, trade-offs between power, delay, and network throughput can be observed. Here, we focus on power consumption while providing small routing delay, and optimize the unicast scheme of the preceding section 4.3 for energy efficiency. We present 3 different algorithms namely Unicast III, IV, and V with different trade-offs between runtime and power consumption.

	node placing	**running time**	**transmission energy**
direct transmission	*	$\Theta(1)$	$\Theta(d^2)$
nearest-neighbor multi-hop	*	$\Theta(d)$	$\Theta(d)$
beamforming broadcast	line	$\Theta(\log d)$	$\Theta(d)$
Unicast I + II	plane	$\Theta(\log\log d)$	$\Theta(d)$
Unicast III	plane	$\Theta(\log d)$	$\Theta\left(\sqrt{d}\right)$
Unicast IV	plane	$\Theta\left(\frac{1}{\varepsilon}\log\log d\right)$	$\Theta\left(\sqrt{d}^{1+\varepsilon}\right)$
Unicast V	space	$\Theta(\log d)$	$\Theta(\log d)$

Table 4.3: Comparison of runtime and transmission energy for transmission distance d, wavelength λ, and equidistant node placement (* denotes placing in 1D, 2D, or 3D)

In Unicast III, we can reduce the power consumption for transmission distance d from linear $\Theta(d)$ to sublinear $\Theta\left(\sqrt{d}\right)$, which is at the expense of an increased point-to-point delay $\Theta(\log d)$. In Unicast IV, we incorporate in an ϵ-approximation sublinear power consumption $\Theta((\sqrt{d})^{1+\varepsilon})$ with fast routing in $\Theta\left(\frac{1}{\varepsilon}\log\log d\right)$. In Unicast V, we generalize the operation to nodes placed in a three-dimensional grid and can show a transmission delay of $\Theta(\log d)$ where we can reduce the transmission power to $\Theta(\log d)$.

Model and Setting First, we assume the same setting as in the preceding section (4.3) to enhance the Unicast scheme for n nodes in a grid in the plane and extend this afterwards for a model of a three-dimensional space. The scenarios are:

(a) the nodes are placed in a two-dimensional unit distance grid with antennas perpendicular to the plane

(b) the nodes are placed in a three-dimensional unit distance grid with antennas perpendicular to the xy-plane

The wavelength is $\lambda < \frac{1}{2}$ to meet the far-field assumption. We do not restrict the

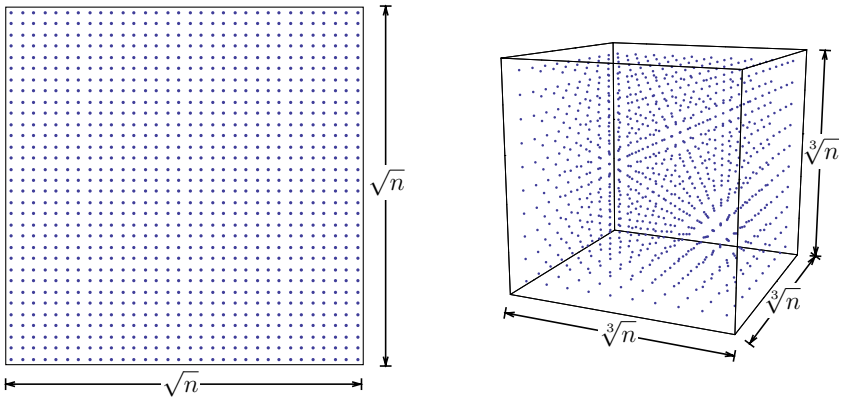

(a) plane (b) space

Figure 4.28: n nodes in a grid with two or three dimensions

individual transmission power of each node $p_i = |s_i|^2$, but try to minimize the sum of all nodes' transmission power during the unicast of a message. Please note that the model for three-dimensions also includes the polarization effect with an elevation angle θ. The angle occurs twice, at the sender and receiver antenna, and $\theta = \pi/2$ denotes by definition a transmission in the plane (compare Figure 2.5 on page 19). We extend input-output model of Definition 4 with polarization and get

$$h = \left(\sum_{i=1}^{n} s_i \cdot \frac{\mathrm{e}^{-j2\pi f |u_i - v|/c} \cdot \sin^2 \theta}{|u_i - v|} \right) .$$

4.4.1 Unicast III: Delay $\Theta(\log d)$ and Energy $\Theta(\sqrt{d})$

The routing algorithm Unicast III consists of $\log_b n$ subsequent multi-hop steps for some $b > 1$. The i-th multi-hop step is performed with transmit beamforming from an area of coordinated senders to an area of receivers, which get coordinated when receiving (see Figure 4.29). The geometry of each array performing transmit beamforming is a

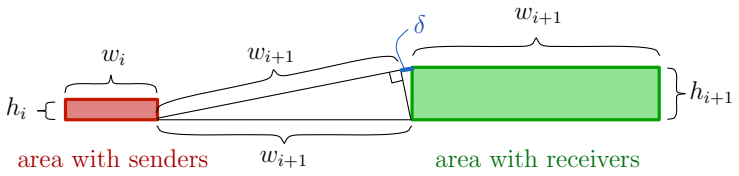

Figure 4.29: Unicast step with transmit beamforming from a $(w_i \times h_i)$ sender array to a $(w_{i+1} \times h_{i+1})$ receiver array in distance w_{i+1}

rectangle. We choose in the i-th hop the dimensions $(w_i \times h_i)$ of each array with width w_i, height h_i, and transmission power p_i of each node as stated in Lemma 28.

Lemma 28 *Sender nodes in a rectangular area $(w_i \times h_i)$ can reach with collaborative transmit beamforming and transmission power p_i per node all nodes in a rectangle in distance w_{i+1} and dimensions $(w_{i+1} \times h_{i+1})$ if the following inequalities are satisfied.*

$$\begin{aligned} h_{i+1}^2 &\leq \frac{1}{4}\lambda \cdot w_{i+1} \ , & (4.38)\\ w_{i+1} &\leq \frac{1}{3\sqrt{2}} h_i \cdot w_i \cdot \sqrt{p_i} \ , & (4.39)\\ w_{i+1} &\geq q \cdot w_i \ , & (4.40)\\ h_i &\leq w_i \ , & (4.41)\\ p_i &\leq 1 \ . & (4.42) \end{aligned}$$

Besides a successful transmission to all nodes in the $(w_{i+1} \times h_{i+1})$ rectangular area, we also like to synchronize the phases of these nodes for the successive next hop of transmit beamforming. Just as in Unicast I in Section 4.3.1, we set the ratio of width w_{i+1} and height h_{i+1} according to Equation (4.38) to make sure that all nodes have a phase-synchronization error less than $\frac{\pi}{4}$ for beam-formed sending to the target, i.e. if all nodes repeat the received message after a fixed delay then the phase shift in the super-positioned signal is less than $\frac{\pi}{4}$ at the target position. Equation (4.39) ensures that the reception range $3w_{i+1}$ of the beamforming senders is large enough to reach all nodes in the receiver array. The proof of Equations (4.38-4.39) can be found in Lemma 22 and 23.

In Equation (4.40), factor q is the base of the exponential speed-up, i.e. progress $\Theta\left(q^i\right)$ in round i. The power is limited by a constant in Equation (4.42), i.e. a node can reach all nearest neighbors.

Theorem 12 *The rectangular area $(w_i \times h_i)$ in round i with power p_i per node is*

$$\begin{aligned} w_i &= q^i \cdot w_0 \ , \\ h_i &= h_0 \cdot (\sqrt{q})^i \ \text{ with } h_0 = \sqrt{\frac{w_0 \cdot \lambda}{4}} \ , \\ p_i &\geq \frac{72 \cdot q^2}{w_0 \cdot \lambda} \cdot q^{-i} \ . \end{aligned}$$

The transmission with Unicast III over distance d needs $\Theta\left(\log_q d\right)$ hops and an overall transmission power of $\Theta\left(\sqrt{d/\lambda}\right)$.

Proof: The width w_i can be derived from (4.40) with the width w_0 of the start rectangle . The height of the rectangles is derived from rearranging (4.38).

$$h_i = \sqrt{\frac{1}{4}\lambda w_i} = h_0 \cdot (\sqrt{q})^i \text{ with } h_0 = \sqrt{\frac{w_0 \cdot \lambda}{4}}$$

The reception range in round i is

$$\begin{aligned} w_{i+1} &\leq \frac{1}{3\sqrt{2}} \cdot \underbrace{\left(h_0 \cdot q^{\frac{i}{2}}\right)}_{h_i} \cdot \underbrace{\left(w_0 \cdot q^i\right)}_{w_i} \cdot \sqrt{p_i} \\ &= \frac{w_0^{\frac{3}{2}}\sqrt{\lambda}}{3\sqrt{8}} \cdot q^{\frac{3}{2}i} \cdot \sqrt{p_i} \ . \end{aligned}$$

Inserting inequality (4.40) gives for the power p_i of a sender node in round i

$$\begin{aligned} q \cdot \underbrace{q^i \cdot w_0}_{w_i} &\leq \frac{w_0^{\frac{3}{2}}\sqrt{\lambda}}{3\sqrt{8}} \cdot q^{\frac{3}{2}i} \cdot \sqrt{p_i} \\ \sqrt{p_i} &\geq \frac{q \cdot 3\sqrt{8}}{\sqrt{w_0 \cdot \lambda}} \cdot q^{-i/2} \\ p_i &\geq \frac{72 \cdot q^2}{w_0 \cdot \lambda} \cdot q^{-i} \ . \end{aligned}$$

The power of all nodes involved in a unicast operation is then

$$\begin{aligned} P_{\text{tx,III}} &= \sum_{i=0}^{\lceil \log_q d \rceil - 1} h_i \cdot w_i \cdot p_i \\ &= \frac{36 \cdot q^2 \cdot \sqrt{w_0}}{\sqrt{\lambda}} \cdot \sum_{i=0}^{\lceil \log_q d \rceil - 1} (\sqrt{q})^i \\ &= \frac{36 \cdot q^2 \cdot \sqrt{w_0}}{\sqrt{\lambda}} \cdot \frac{\sqrt{d} - 1}{\sqrt{q} - 1} \\ &= \frac{36 \cdot q^2 \cdot \sqrt{w_0}}{\sqrt{\lambda} \cdot (\sqrt{q} - 1)} \cdot \left(\sqrt{d} - q^{-1/2}\right) \\ &= \Theta\left(\sqrt{d/\lambda}\right) \ . \end{aligned}$$

□

So, the energy consumption to transmit a message over distance d is $\Theta\left(\sqrt{d/\lambda}\right)$ and the transmission delay is $\Theta\left(\log_b d\right)$.

Corollary 9 *In an ad hoc network with n nodes placed in a $(\sqrt{n} \times \sqrt{n})$ grid, the energy consumption of Unicast III is $\Theta\left(\sqrt[4]{n}/\sqrt{\lambda}\right)$ with transmission delay $\Theta\left(\log_b n\right)$.*

The number of nodes n_3, which are involved in the execution of Unicast III with transmission distance d, is bounded by the following.

$$\begin{aligned} n_3 &= \sum_{i=0}^{\lceil \log_q d \rceil - 1} h_i \cdot w_i \\ &= \frac{\sqrt{\lambda} \cdot w_0^{3/2}}{2} \sum_{i=0}^{\lceil \log_q d \rceil - 1} \left(q^{3/2}\right)^i \\ &= \frac{\sqrt{\lambda} \cdot w_0^{3/2}}{2} \cdot \frac{\left(q^{3/2}\right)^{\log_q d} - 1}{q^{3/2} - 1} \\ &= \frac{\sqrt{\lambda} \cdot w_0^{3/2}}{2} \cdot \frac{d^{3/2} - 1}{q^{3/2} - 1} \\ &= \Theta\left(\sqrt{\lambda} \cdot d^{3/2}\right) \end{aligned}$$

We neglect the energy consumption for standby, but possibly have to consider the energy consumption by p_{rx} for signal-processing at each receiver node. This energy consumption of all nodes involved in the operation is then

$$P_{\text{rx,III}} = n_3 \cdot p_{\text{rx}} = \Theta\left(\sqrt{\lambda} \cdot d^{3/2}\right) .$$

There are different constant factors involved for the transmission power and the receiving power, and only if the reception power can be neglected compared to the transmission power, this unicast algorithm makes energy-wise sense.

4.4.2 Unicast IV: Delay $\Theta(\log \log d)$ and Energy $\Theta(\sqrt{d})$

In Unicast III, we slowed down the transmission delay of Unicast I in Section 4.3.1 from $\Theta(\log \log d)$ to $\Theta(\log d)$ in order to reduce the total energy consumption of the unicast. In the following algorithm Unicast IV, we combine small transmission delay $\Theta\left(\log_{1+\varepsilon} \log_{w_0} d\right)$ and small transmission power $\Theta\left(d^{\frac{1}{2}+2\varepsilon}\right)$. Yet, note that for a small ε it holds

$$\log_{1+\varepsilon} x = \frac{\log x}{\log(1+\varepsilon)} \geq \frac{\log x}{\varepsilon} .$$

So, for small $\varepsilon \to 0$, $\frac{1}{\varepsilon}$ will be the dominating factor which slows the delay down.

Lemma 29 *A $(w_i \times h_i)$ rectangle of beamforming senders can reach all nodes in an exponentially larger rectangle $(w_{i+1} \times h_{i+1})$, i.e. the areas have sizes $A_{i+1} \geq A_{i+1}^{\alpha}$ for $\alpha > 1$, if it holds for the rectangles*

$$\begin{aligned} h_{i+1}^2 &\leq \frac{1}{4}\lambda \cdot w_{i+1} \ , & (4.43)\\ w_{i+1} &\leq \frac{1}{3\sqrt{2}} h_i \cdot w_i \cdot \sqrt{p_i} \ , & (4.44)\\ w_{i+1} &\geq w_i^{\alpha} \ , & (4.45)\\ h_i &\leq w_i \ , & (4.46)\\ p_i &\geq 1 \ . & (4.47) \end{aligned}$$

The rectangular area of nodes in round i has dimensions

$$\begin{aligned} w_i &= (w_0)^{\alpha^i} \ \textit{and} \\ h_i &\leq \frac{\sqrt{\lambda}}{2} \cdot (\sqrt{w_0})^{\alpha^i} \ . \end{aligned}$$

Proof: The recursion of the i-th height of the rectangular area can be solved as follows.

$$\begin{aligned} h_{i+1}^2 &\leq \frac{1}{4}\lambda \cdot w_{i+1} = \frac{\lambda}{4} \cdot (w_0)^{\alpha^{i+1}} \\ h_i &\leq \frac{\sqrt{\lambda}}{2} \cdot (\sqrt{w_0})^{\alpha^i} \end{aligned}$$

□

This Lemma helps us to prove the following claim.

Theorem 13 *The delay of a point-to-point communication of distance d with Unicast IV is $\Theta\left(\log_{1+\varepsilon} \log_{w_0} d\right)$ for $\varepsilon > 0$. The corresponding transmission power is $\Theta\left(d^{\frac{1}{2}+2\varepsilon}\right)$. The energy consumption for signal processing of all nodes in a communication is $\Theta\left(\sqrt{\lambda} \cdot d^{3/2}\right)$.*

Proof: To reach a rectangle of size at least d we need k rounds. In round k, we have size $w_k \cdot h_k = \frac{\sqrt{\lambda}}{2} (w_0)^{3/2 \cdot \alpha^i}$.

$$\begin{aligned} d &= \left\lfloor (w_0)^{\alpha^k} \right\rfloor \\ k &= \lfloor \log_{\alpha} \log_{w_0} d \rfloor \end{aligned}$$

The power p_i of each sender in the i-th rectangle is the following.

$$\begin{aligned}
\sqrt{p_i} &\geq 3\sqrt{2} \cdot \frac{w_{i+1}}{h_i \cdot w_i} \\
&= 3\sqrt{2} \cdot \frac{(w_0)^{\alpha^{i+1}}}{\frac{\sqrt{\lambda}}{2} \cdot \left(\sqrt{w_0}\right)^{\alpha^i} \cdot (w_0)^{\alpha^i}} \\
&= \frac{6\sqrt{2}}{\sqrt{\lambda}} \cdot (w_0)^{\alpha^{i+1} - \frac{\alpha^i}{2} - \alpha^i} \\
&= \frac{6\sqrt{2}}{\sqrt{\lambda}} \cdot \left(w_0^{\alpha - \frac{3}{2}}\right)^{\alpha^i} , \\
p_i &\geq \frac{72}{\lambda} \cdot \left(w_0^{2\alpha-3}\right)^{\alpha^i} .
\end{aligned}$$

The energy consumption for transmitting to distance d is:

$$\begin{aligned}
P_{\text{tx,IV}} &= \sum_{i=0}^{\lfloor \log_\alpha \log_{w_0} d \rfloor} w_i \cdot h_i \cdot p_i \\
&\leq \sum_{i=0}^{\lfloor \log_\alpha \log_{w_0} d \rfloor} \underbrace{(w_0)^{\alpha^i}}_{w_i} \cdot \underbrace{\frac{\sqrt{\lambda}}{2} \cdot \left(\sqrt{w_0}\right)^{\alpha^i}}_{h_i} \cdot \underbrace{\frac{72}{\lambda} \cdot \left(w_0^{2\alpha-3}\right)^{\alpha^i}}_{p_i} \\
&= 36\sqrt{\lambda} \sum_{i=0}^{\lfloor \log_\alpha \log_{w_0} d \rfloor} (w_0)^{\left(\frac{3}{2}+2\alpha-3\right)\cdot\alpha^i} \\
&= 36\sqrt{\lambda} \sum_{i=0}^{\lfloor \log_\alpha \log_{w_0} d \rfloor} \left(w_0^{\left(2\alpha-\frac{3}{2}\right)}\right)^{\alpha^i}
\end{aligned}$$

To achieve a double-exponential growth, we need $\alpha > 1$ and choose $\alpha = 1 + \varepsilon$ and $\varepsilon > 0$. The energy consumption is then

$$P_{\text{tx,IV}} \leq 36\sqrt{\lambda} \sum_{i=0}^{\lfloor \log_{1+\varepsilon} \log_{w_0} d \rfloor} \left(w_0^{\left(\frac{1}{2}+2\varepsilon\right)}\right)^{(1+\varepsilon)^i} .$$

Note that

$$\begin{aligned}
\sum_{i=0}^{k} w^{q^i} &= w^{q^k} \cdot \sum_{i=0}^{k} w^{q^i - q^k} \\
&= w^{q^k} \cdot \left(1 + \sum_{i=0}^{k-1} w^{q^i - q^k}\right) \\
&\leq w^{q^k} \cdot \left(1 + \sum_{i=0}^{k-1} w^{q^{k-1} - q^k}\right) \text{ for } q > 1 \\
&= w^{q^k} \cdot \left(1 + \frac{k}{w^{q^k(1-1/q)}}\right) \\
&= w^{q^k} \left(1 + o\left(1\right)\right) \ .
\end{aligned}$$

Thus, the energy consumption for sending is

$$P_{\text{tx,IV}} \leq 36\sqrt{\lambda} \cdot \left(1 + o\left(1\right)\right) \cdot d^{\frac{1}{2}+2\varepsilon} \ .$$

The number of active nodes in Unicast IV is in the order of Unicast III

$$\begin{aligned}
n_4 &= \sum_{i=0}^{\left\lfloor \log_{1+\varepsilon} \log_{w_0} d \right\rfloor} w_i \cdot h_i \\
&\leq \sum_{i=0}^{\left\lfloor \log_{1+\varepsilon} \log_{w_0} d \right\rfloor} \underbrace{\left(w_0\right)^{(1+\varepsilon)^i}}_{w_i} \cdot \underbrace{\frac{\sqrt{\lambda}}{2} \cdot \left(\sqrt{w_0}\right)^{(1+\varepsilon)^i}}_{h_i} \\
&= \frac{\sqrt{\lambda}}{2} \sum_{i=0}^{\left\lfloor \log_{1+\varepsilon} \log_{w_0} d \right\rfloor} \left(w_0^{3/2}\right)^{(1+\varepsilon)^i} \\
&= \frac{\sqrt{\lambda}}{2} \cdot \left(1 + o\left(1\right)\right) \cdot d^{3/2} \ ,
\end{aligned}$$

and so is the constant power for signal processing at the receiving nodes with

$$P_{\text{rx,IV}} = n_4 \cdot p_{\text{rx}} = \Theta\left(\sqrt{\lambda} \cdot d^{3/2}\right) \ .$$

□

4.4.3 Unicast V: Delay $\Theta\left(\log d\right)$ and Energy $\Theta\left(\log d\right)$

There is a trade-off between the amount of nodes for transmit beamforming and energy consumption. Beamforming can focus the sender energy onto beams and increase reception range which can reduce transmission power. However, when the spatial expansion of beamforming senders is much larger than the distance to the receiver,

it gets unattractive to use the sender nodes being furthest away, because they have a high path loss to the receiver. For nodes placed on a one-dimensional line (Section 4.2) [JS13], we could show linear energy consumption $\Theta(d)$ for transmission distance d. The expansion of m beamforming sender is $\Theta(m)$ in this case. In the plane, we can decrease the expansion of m beamforming senders to a rectangle with a diameter $\Theta\left(m^{2/3}\right)$. This can decrease the transmission power to $\Theta\left(\sqrt{d}\right)$.

The spatial expansion of coordinated beamforming senders can be further increased compared to the one-dimensional line and two-dimensional rectangle when choosing beamforming senders in a three-dimensional cuboid (see Figure 4.31).

Lemma 30 *If a single sender u sends a signal to a $w \times h \times b$ cuboidal cell in a distance of at least w (see Figure 4.30), then all nodes in this cell are phase-synchronized for sender beamforming towards the target with a phase error less than α if $h^2 \leq \frac{\alpha}{2\pi}\lambda w$.*

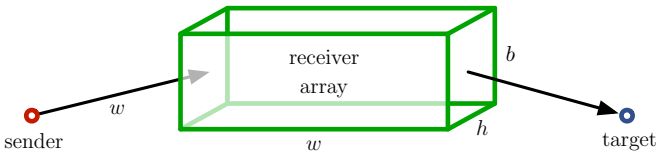

Figure 4.30: Nodes in the $w \times h \times b$ cuboid receive the message from sender u in distance w and are phase-synchronized for transmit beamforming to the target

Proof: Let X denote the signal of sender u and Y the signal at receiver v. Then,

$$Y = \frac{X}{|u-v|} \cdot \mathrm{e}^{-\frac{j2\pi}{\lambda}} \cdot |u-v| \quad .$$

Thus, the phase shift is described by $-\arg(\frac{Y}{X}) = \frac{2\pi}{\lambda}|u-v|$. The difference of phase shifts is therefore

$$\begin{aligned} \delta &= \frac{2\pi}{\lambda}|u-v| - \frac{2\pi v_x}{\lambda} \\ &= \frac{2\pi}{\lambda}\left(\sqrt{v_x^2+v_y^2+v_z^2} - v_x\right) \\ &\leq \frac{2\pi}{\lambda} v_x \left(\sqrt{1+\left(\frac{\sqrt{2}v_y}{v_x}\right)^2} - 1\right) \quad . \end{aligned}$$

This phase difference is maximized for $r_y = h$, $r_z = b$ and $r_x = w$ and by applying the relation $\sqrt{1+x^2} - 1 \leq \frac{x^2}{2}$ for all $x \geq 0$ (see Lemma 36), we get

$$\delta \leq \frac{\pi}{\lambda}\frac{2v_y^2}{v_x} = \frac{\pi}{\lambda}\frac{2h^2}{w} \quad .$$

From $h^2 \leq \frac{\alpha}{2\pi}\lambda w$ it follows that $\delta \leq \alpha$. □

We choose the dimensions of the cuboidal cells such that the error phase-synchronization is $\alpha \leq \pi/4$, i.e. less than a wavelength. For transmit beamforming, the nodes simply resend the message after a fixed time offset after receiving the message. The synchronization error α can be fixed with techniques presented for Unicast I (Section 4.3.1), which do not affect the energy consumption asymptotically.

In our model, the antennas of all nodes are aligned along the z-axis, i.e. a transmission between nodes with the same z-coordinate won't be affected by polarization. The polarization effect occurs when sending from a cuboid of beamforming senders to a cuboid of receivers. Assuming the distance between both cuboids in w_{i+1} and the height of the receiver cuboid is b_{i+1}, the elevation (angle) is at most

$$\theta = \frac{\pi}{2} - \arctan\left(\frac{b_{i+1}}{w_{i+1}}\right) .$$

Thus, the attenuation factor a_{pol} of polarization at sender and receiver is at most

$$a_{\text{pol}} \quad = \quad \sin\theta = \cos\left(\arctan\left(\frac{b_{i+1}}{w_{i+1}}\right)\right) = \frac{1}{\sqrt{1+\frac{b_{i+1}^2}{w_{i+1}^2}}} .$$

Furthermore, one has to consider the directional antenna behavior at the receiver. If we assume a dipole antenna along the z-axis this results in an extra factor of $\sin(\theta)$, which results in the same calculation and an extra factor of a_{pol}. The attenuation due to polarization at sender and receiver is then

$$a_{\text{pol}}^2 \quad = \quad \frac{1}{1+\frac{b_{i+1}^2}{w_{i+1}^2}} \geq \frac{1}{1+\frac{\lambda}{4w_{i+1}}} \geq \frac{4}{5} .$$

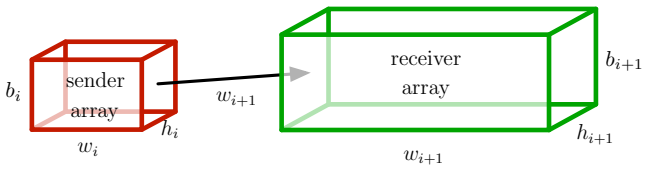

Figure 4.31: Transmission from a $w_i \times h_i \times b_i$ cuboid of coordinated beamforming senders to receivers in a $w_{i+1} \times h_{i+1} \times b_{i+1}$ cuboid

Lemma 31 *A $w_i \times h_i \times b_i$-cuboidal cell of beamforming senders with transmission power p_i can reach any node in a $w_{i+1} \times h_{i+1} \times b_{i+1}$-cuboidal cell at distance w_{i+1} if*

$$\begin{aligned} h_{i+1} &\geq h_i \ , && (4.48)\\ b_{i+1} &\geq b_i \ , && (4.49)\\ w_{i+1} &\geq w_i \ , && (4.50)\\ w_{i+1} &\leq \frac{1}{10\sqrt{5}}\sqrt{p_i}w_i h_i b_i \ , && (4.51)\\ h_{i+1} &\leq w_{i+1} \ , && (4.52)\\ b_{i+1} &\leq w_{i+1} \ , && (4.53)\\ h_{i+1}^2 &\leq \frac{1}{4}\lambda w_{i+1} \ , && (4.54)\\ b_{i+1}^2 &\leq \frac{1}{4}\lambda w_{i+1} \ . && (4.55) \end{aligned}$$

Proof: For a sender antenna and a receiving antenna with relative offset (w, h, b) we have $w \in [w_{i+1}, w_i + w_{i+1}], b \in [0, b_{i+1}], h \in [0, h_{i+1}]$. The signal phase shift with respect to w is therefore described by

$$\sqrt{w^2+h^2+b^2} - w = w\left(\sqrt{1+\frac{h^2+b^2}{w^2}} - 1\right) \leq \frac{1}{2}\frac{h^2+b^2}{w}$$

using $\sqrt{1+\frac{h^2+b^2}{w^2}} \leq \frac{1}{2}\frac{h^2+b^2}{w^2}$. The last term ist bounded by

$$\begin{aligned} \frac{1}{2}\frac{(h_{i+1})^2+(b_{i+1})^2}{w_{i+1}} &\leq \frac{1}{2}\frac{(h_{i+1})^2+(b_{i+1})^2}{w_{i+1}} \\ &\leq \frac{1}{4}\frac{\lambda w_{i+1}}{w_{i+1}} \leq \frac{1}{4}\lambda \ . \end{aligned}$$

For the amplitude note that

$$\sqrt{w^2+h^2+b^2} \leq \sqrt{(3w_{i+1})^2+(h_{i+1})^2+(b_{i+1})^2} \leq \sqrt{5}w_{i+1} \ .$$

The number of senders is given by $w_i h_i b_i$ and the attenuation is given by at most

$$\frac{a_{\text{pol}}^2}{4\cdot\sqrt{w^2+h^2+b^2}} \geq \frac{1}{\sqrt{5}w_{i+1}}\cdot\frac{1}{4}\cdot\frac{4}{5} = \frac{1}{5\sqrt{5}w_{i+1}} \ .$$

Since $\frac{w_i h_i b_i \sqrt{p_i}}{5\sqrt{5}} \geq 2w_{i+1} \geq w_i + w_{i+1}$ all receivers can be reached, if the original amplitude of each sender is $\sqrt{p_i}$. □

Again we increase the size of the cuboids in each round according to these equations. The power will be decreased as well. The following recursion gives a valid choice for appropriate constants c_1 depending on λ.

$$w_{i+1} := 2 \cdot w_i \tag{4.56}$$
$$h_i = \sqrt{w_i \lambda / 4} \tag{4.57}$$
$$b_i = \sqrt{w_i \lambda / 4} \tag{4.58}$$
$$p_i = \frac{c_1^2}{w_i^2} \tag{4.59}$$

Theorem 14 *For $\lambda \leq 1$, the delay for the three-dimensional beamforming algorithm is $\Theta(\log d)$ for distance d between source and target. The energy consumption for transmission is $\Theta(\frac{1}{\lambda} \log d)$ and for signal processing at the receivers is $\Theta\left(d^2\right)$.*

Proof: Note that

$$w_i = w_0 \cdot 2^i \ .$$

and $w_{i+1} \geq w_i$, $h_{i+1} \geq h_i$, and $b_{i+1} \geq b_i$.

Now

$$w_{i+1} = 2w_i = \frac{8}{c_1 \lambda} w_i h_i b_i \sqrt{p_i} \leq \frac{1}{10\sqrt{5}} \sqrt{p_i} w_i h_i b_i \ ,$$

if $\frac{8}{c_1 \lambda} \leq \frac{1}{10\sqrt{5}}$. So, we choose $c_1 = \frac{80\sqrt{5}}{\lambda}$.

We have $h_i \leq w_i$ and $b_i \leq w_i$, if $w_i \geq \frac{16}{\lambda^2}$. We have $h_i = \sqrt{w_i \lambda / 4} \leq w_i$ if $w_i \geq \lambda/4$. The delay is $\Theta(\log d)$ for distance d and the total energy for one round is given by

$$h_i b_i w_i p_i = \frac{c_1^2 \lambda w_i^2}{4 w_i^2} = \frac{8000}{\lambda} \ .$$

Summing over all $\log d$ rounds gives the total transmission energy of $\Theta(\frac{1}{\lambda} \log d)$.

To estimate the costs for signal processing at the receivers, we again count the number of nodes, which is for round i

$$m_i = h_i \cdot w_i \cdot b_i = w_i^2 \cdot \frac{\lambda}{4} \ .$$

These nodes have a reception range of

$$\sqrt{p_i} \cdot m_i = \frac{c_1}{w_i} \cdot \frac{w_i^2 \lambda}{4} = 80\sqrt{5} \cdot w_i \ .$$

The distance d from source to target is covered in round r, whereby for each round i we have to take into account the length of the rectangle w_i twice, for the rectangle and the transmission distance to the rectangle.

$$d \leq w_0 + \sum_{i=1}^{r} 2 w_0 \cdot 2^i = w_0 \left(4 \cdot 2^r - 3\right)$$
$$r \geq \log\left(\frac{d}{4w_0} + \frac{3}{4}\right) = \Theta\left(\log d\right)$$

Summing over all r rounds gives a total number of nodes of

$$\sum_{i=0}^{r} w_i^2 \cdot \frac{\lambda}{8} = \frac{4}{3w_0^2}d^2 + \frac{2}{w_0}d + 5w_0^2 = \Theta\left(d^2\right) \ .$$

□

For a network with diameter $\sqrt[3]{n}$, the number of nodes involved in a unicast operation is $\mathcal{O}\left(n^{2/3}\right)$, which is asymptotically smaller than for a unicast in the plane because of the smaller expected distance between source and target.

Corollary 10 *For wavelength $\lambda \leq 1$ and a three-dimensional network with diameter $\Theta\left(\sqrt[3]{n}\right)$, the delay for the three-dimensional beamforming algorithm is $\mathcal{O}(\log n)$. The energy consumption for transmission is $\mathcal{O}(\frac{1}{\lambda}\log n)$ and for signal processing at the receivers is $\mathcal{O}\left(n^{2/3}\right)$.*

With antennas aligned along the z-axis, the preceding algorithm is intended for routing in the x-y plane. If the the z-coordinates of source and target also differ, we can route in an inclined plane, which reduces the reception range of each node by a constant factor due to polarization. If the elevation (angle) is too large to reach the target in an inclined plane directly, we can gain height in a staircase like procedure. This only increases the routing delay and energy consumption by a constant factor and does not change the asymptotic results.

In this section, we demonstrated unicast algorithms for the two-dimensional plane and three-dimensional space, for which a total sublinear transmission power $\Theta(\sqrt{d})$ respectively $\Theta(\log d)$ for distance d from source to target is possible in principle. In particular, if we choose devices in the plane, we reach a transmission power of $\Theta((\sqrt{d})^{1+\varepsilon})$ and delay $\Theta\left(\frac{1}{\varepsilon}\log\log d\right)$. On the other hand, if we can choose devices for transmit beamforming in a cuboidal cell in the three-dimensional space, we can show a transmission energy of $\Theta(\log d)$ along with a transmission delay of only $\Theta\left(\log d\right)$. We achieve this by combining a multi-hop routing scheme with collaborative beamforming. In each hop, selected senders cooperate for beamforming in order to increase the transmission distance, while in each round each sender reduces its transmission power. We also analyze the incidental power consumption for e.g. signal processing at the receivers which is in $\mathcal{O}\left(d^2\right)$. However, if nodes are in reception mode anyway and energy consumption for that has not to be considered, these algorithms can be a real energy reduction.

5 A Distributed MAC Protocol Turning Interferences Into Noise

Beamforming is a spatial filter where super-posed signals are correlated in certain spatial regions called beams and uncorrelated otherwise in expectation. We can apply the same principle in the time domain instead of the spatial domain with the following idea: instead of m senders emitting the same signal (containing a symbol) with beamforming, one sender transfers a signal m times sequentially. To reproduce beam-

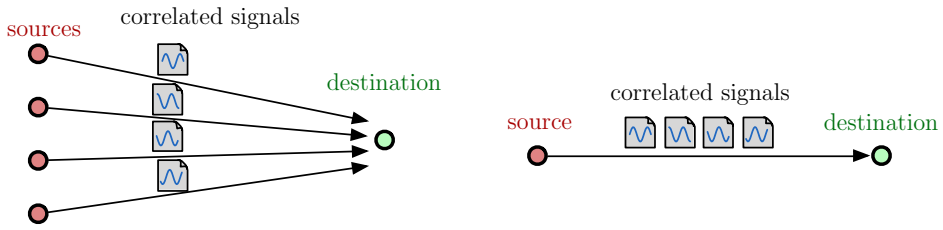

(a) spatial domain (b) time domain

Figure 5.1: phase-correlated signals of beamforming and in the time domain

forming, the transmitter emits the signal in each iteration with another phase shift. To attain power gain, the receiver reverses the phase shifts of each signal and adds all m signals (for superposition).

As Figure 5.1 indicates, the data rate decreases by factor $\frac{1}{m}$ when sending a message m times in a sequence. At first glance, this appears to be a step backwards. But a sender can now choose freely the phase shifts which do not depend on the nodes' positions anymore, because we are now in the time domain instead of the spatial domain (compare Figure 5.1). Each sender uses a unique sequence of phase shifts. Comparable to tuning in a channel by changing the frequency in frequency multiplexing, each receiver can tune in the signal of a specific sender by using the sender's signature of phase shifts with corresponding power gain. In contrast, if the used phase shifts of sender and receiver are uncorrelated, the receiver receives noise with no power gain. The application for this technique is a distributed medium access control (MAC) protocol where multiple parallel communications on the same carrier frequency can take place in a network without the need of spatial reuse or TDMA schemes. A second application is to use the power gain of this method to establish connectivity to remote communication partners.

Currently, the dominant method in off-the-shelf wireless network devices is to resolve problems in the medium access layer and the physical layer by using a central control infrastructure. Current standardized hardware for wireless communication solves medium access with division techniques in code, time, frequency, and space. Telecommunication standard UMTS for instance uses time division and code division multiple access (TDMA and CDMA) at the same time for parallel access and orthogonal frequency division multiplexing (OFDM) [EJRS14b] for higher bandwidth. Additionally, spatial reuse is established by communication with radio stations in individual cells. Allocation of frequency channel and time frame are scheduled by the infrastructure or are given by the location of the device, e.g. communication with radio tower with strongest signal. In contrast, ad hoc networks do not have an infrastructure for negotiation of the time frame/frequency allocation and distributed methods have to be applied here. Medium access usually needs coordination, distributed in ad hoc networks or centralized in a router of an infrastructure. We propose a coding scheme reducing this coordination constraint and making routing links more independent from each other.

Ad hoc networks can achieve connectivity, bandwidth gain, and energy reduction by cooperated routing, e.g. multi-hop routing or cooperated multiple input multiple output (MIMO). In a mobile environment with limited energy per device, users might not be willing to share energy if they have the choice specially when they are in idle mode and do not get anything in exchange. This problem of selfish-behavior is well known for example in peer-to-peer filesharing [LMSW06, AJS11], where so called free-riders do not want to share their upload bandwidth to others and only want to download. This reduces the capacity of the service provided by the p2p-system and only a fraction of free-riders can be compensated.

While wired networks can have a complete graph and arbitrary links, in wireless networks with limited power per node, we can only establish certain links because of the path loss between nodes. Specially, ad hoc networks have no reliable backbone with an area-covering infrastructure with wireless routers to interconnect wireless devices. This makes the problem even more challenging and can limit connectivity, i.e. if there are only free-riding nodes in a local area around a node, the node might be disconnect from the network. Irregular distributions of devices also limit connectivity of devices in sparse areas. Jamming devices might compromise connectivity as well. In all these cases of limited connectivity, the presented scheme can help to a certain extend by increasing the SNR with a power gain and the drawback of a reduced data rate. And establishing connectivity without coordination (e.g. TDMA) or cooperation (e.g. multi hop) means less network dependencies.

The basic idea of the approach is to use a modulation scheme where multiple nodes can access the medium at the same time and on the same frequency without interference, which reduces needed cooperation. The scheme increases the signal-to-noise ratio (SNR) to enhance the transmission distance while reducing the data rate. Connections to remote devices become possible where regular transmission power is insufficient. The scheme keeps interference in the network to a constant expected value which would

not be the case when increasing transmission power to gain transmission range. Our key method is to repeat symbols using additional pseudo-random PSK. So, we increase the SNR of the wireless channel above the reception threshold and remove the constraint of correlated interferences of parallel communication. We show a constant factor overhead for negotiating the initial data rate and establishing the connections.

5.1 Model and Modulation Scheme

We assume a channel with carrier frequency f respectively carrier wavelength $\lambda = c/f$ and a codeword modulated on the carrier. The input signal $X'(t)$ has duration T/R and can be decomposed into T samples with sample points $t \in \{0, 1, \ldots, T-1\}$ and sample rate R (with unit s^{-1}). We assume a fixed channel capacity W, which is the upper-bound of the data rate R, from a certain SNR threshold β on. We only intend in our communication scheme to increase the SNR of a communication channel over this threshold β to establish communication. Nevertheless, according to Shannon's law [Sha98] the data rate directly depends on the signal-to-interference-plus-noise ratio (SINR) with $\mathcal{O}(\log(1 + \mathrm{SINR}))$ and in a more refined model containing number of symbols (e.g. quadrature phase-shift keying (QPSK), 8PSK, ...) and the bit-error-rate (BER), the data rate can be variable depending on the SINR value of the wireless channel. However, if we increase the SINR expectedly in our scheme by factor K, the data rate will be reduced by $\frac{1}{K}$ in expectation and overall the bandwidth is throttled by $\mathcal{O}\left(\frac{1}{K}\log(1 + K \cdot \mathrm{SINR})\right)$. So the K-repetition scheme is only beneficial in the low-SINR regime where we use a static modulation scheme, e.g. QPSK.

In our modulation scheme, we repeat the signal of each symbol frame K times with random phase shifts ϕ_k for $k \in \{0, 1, \ldots, K-1\}$. This results in the input signal $X(t)$ at sample point $t \in [0, K \cdot T)$

$$X(t) = X'(t \mod T) \cdot \mathrm{e}^{j\phi_k}$$

with input signal $X'(t)$ of a symbol with T samples, which is repeated K times and multiplied with the pseudo-random phase angle ϕ_k with $k = \lfloor t/T \rfloor$. We assume that channel fading, which is caused by changes of the environment and node movement, is so slow that the channel is static for the transmission of one symbol, i.e. the phase and amplitude are stable in one symbol of the modulation scheme. The transmission manipulates the input with factor $h/d^{\alpha/2}$, where d^{α} is the path loss of the signal power for distance d between sender and receiver respectively $d^{\alpha/2}$ the path loss of the signal amplitude and h is a complex value expressing the phase shift. Then the input-output model is

$$Y(t) = \frac{h}{d^{\alpha/2}} \cdot X(t) \ .$$

Lemma 32 *When detecting a symbol in a signal with a frame length of T samples, which is repeated K times with random phases, the computation complexity only in-*

creases from T to $K \cdot T$ accumulations whereas the complexity for correlation remains the same with T multiplications.

Proof: For detection of the input codeword, we correlate the output signal $Y(t)$ with the complex carrier signal $\mathrm{e}^{-j2\pi f \cdot t}$ which is additionally modified with the random phase shifts $\mathrm{e}^{-j\phi_k}$. The correlation coefficient at sample point τ with sampling rate R, T samples per frame, and K repeated frames with phase shift ϕ_k is then

$$\rho(\tau) = \frac{h}{d^{\frac{\alpha}{2}}} \cdot \sum_{k=0}^{K-1} \sum_{t=0}^{T-1} Y(k \cdot T + t - \tau) \cdot \mathrm{e}^{-j(2\pi f \cdot t/R + \phi_k)} \ . \tag{5.1}$$

Instead of calculating the correlation of the received signal with the reference, we can also subtract the estimated phase angles of the received signal from the reference phase angles. For known synchronization and phase shifts ϕ_k, we can rearrange the correlation sum to

$$\rho(\tau) = \frac{h}{d^{\frac{\alpha}{2}}} \cdot \sum_{t=0}^{T-1} \mathrm{e}^{-j2\pi f \cdot t/R} \cdot \sum_{k=0}^{K-1} Y(k \cdot T + t_k(t) + t - \tau)$$

with

$$t_k(t) = \begin{cases} \frac{\phi_k \cdot R}{2\pi f} & \text{if } t \leq T - \frac{\phi_k \cdot R}{2\pi f} \\ -T + \frac{\phi_k \cdot R}{2\pi f} & \text{otherwise} \end{cases} \ .$$

Consequently, we can add the signals of all K frames and perform the correlation with the sine on the accumulated signal of one frame, whereas addition is a lightweight operation compared to a K times larger multiplication than the correlation. Accordingly, if synchronization is given, computation performance is not an issue since the data rate is lower by factor K. □

Lemma 33 *When repeating a symbol K times with pseudo random phases, the SINR increases by factor K in expectation.*

Proof: When superposing the signals of K repetitions, where the k-th repetition has power equivalent X_k^2, the overall output power is

$$Y^2 = \left(\sum_{k=0}^{K-1} \frac{h}{d^{\alpha/2}} \cdot X_k \right)^2 = K^2 \cdot \frac{h^2}{d^\alpha} \cdot X_0^2 \ .$$

Now assume that we apply the phase shifts ϕ_k to an interfering signal, which was modulated with uncorrelated phases ϕ'_k, for simplicity we can use a simple carrier with $\phi'_k = 0$. Neglecting transition effects between time frames, the superposition of the K time sequential signals Y'_k is then

$$Y' = \sum_{k=0}^{K-1} Y'_k \cdot \mathrm{e}^{j\phi_k} \ .$$

We know from Lemma 1 that the expected power of these K signals with equal power and uncorrelated phases is

$$(Y')^2 = K \cdot \frac{h'^2}{d'^\alpha} (X')^2 \ .$$

The overall SINR with AWGN w is then

$$\mathrm{SINR}_K = \frac{K^2 \cdot \frac{P}{d^\alpha}}{K \cdot \left(w + \sum_{i \in I} \frac{P_i}{d_i^\alpha}\right)} = \frac{K \cdot \frac{P}{d^\alpha}}{w + \sum_{i \in I} \frac{P_i}{d_i^\alpha}} \ . \tag{5.2}$$

□

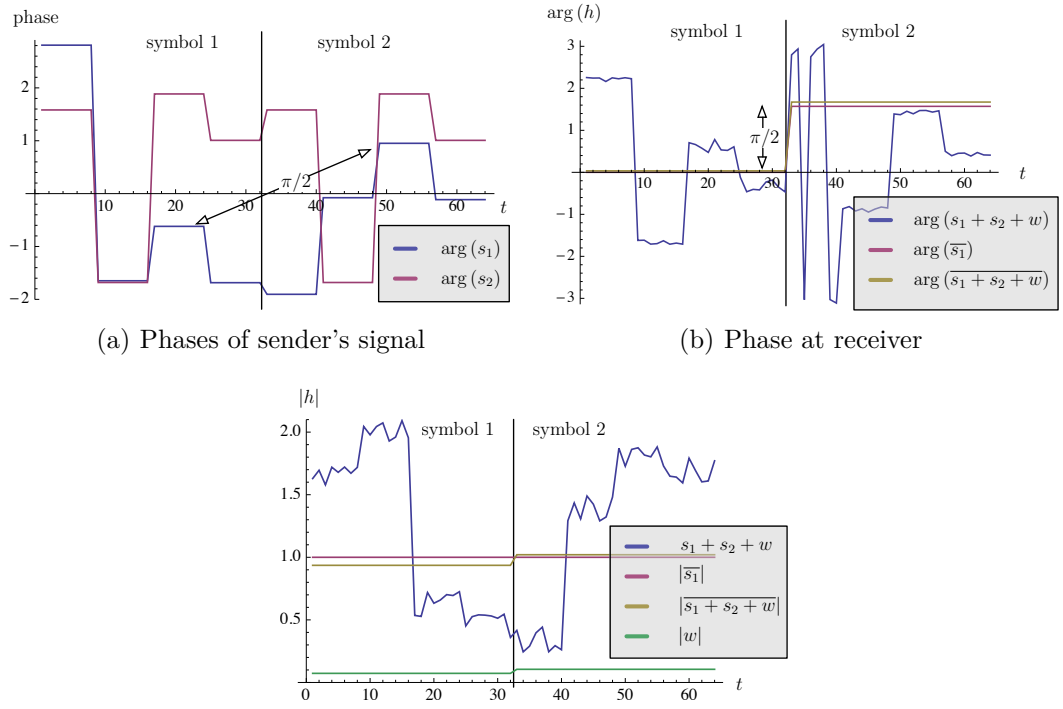

(a) Phases of sender's signal

(b) Phase at receiver

(c) Signal strength at receiver

Figure 5.2: Example: two senders s_1, s_2 transmit to the same receiver and s_1 transmits with PSK the symbols $(0, \pi/2)$, sender s_2 sequence $(0, 0)$. Each symbol is repeated $K = 4$ times with pseudo-random phases (see (a)). The signal amplitudes at the receiver are $|s_1| = |s_2| = 1$ plus AWGN $|w| = 0.1$. In the values marked with an overline, the receiver reveres the pseudo-random phases of sender s_1 and gets the sequence $\left(1 \cdot e^{j0}, 1 \cdot e^{j\pi/2}\right)$ with small error.

We can directly derive the data rate from Lemma 33.

Corollary 11 *If we can transmit with a given modulation at data rate W (unit bits/second) and signal-to-noise ratio β, we can also transmit with data rate W/K for a SNR of β/K in expectation when using the K-repetition scheme with the same modulation.*

We assume that interference and noise do not correlate with the K pseudo random phases.

A receiver resynchronizes to the sender's signal in each symbol frame. Since the data rate is decreased in our model by factor $\frac{1}{K}$, the error margin for fading in the wireless channel is reduced by the same factor.

5.2 Transmission Protocol

Our transmission protocol has two bottom-up states:

1. channel initialization to find an initial K
2. data transmission and update K for an appropriate SNR

If the data transmission fails the channel initialization has to be repeated to find a new K for successful transmission.

Each node has a unique ID. We use the ID as parameter in a pseudo-random number generator to produce the pseudo-random phases. We assume idealistically that the pseudo-random numbers are chosen independent at random (i.e. the assumptions in the proof of Lemma 1 apply for the pseudo-random phases).

A receiver can only receive a message if it listens to the correct modulation, i.e. sequence of K pseudo-random phases generated for a specific random seed. In our scheme each node v has a specific identifier ID_v for the random seed, comparable to the network address. Each node in receiving state listens to the modulation of its own seed and if another node can transmit a message by using the ID as random seed. For that, the receiver's ID has to be known in advance[1].

A sender node intending to establish a wireless connection to a specific receiver node does not know the noise level at the receiver and the path loss when transmitting to that node. Thus, parameter K has to be tested in a channel initialization phase, where K is incremented until an initialization message gets through to the receiver and is successfully acknowledged (see following Section 5.3).

Once a channel has been successfully initialized, we change the random seed for modulation from the receiver's to the sender's ID. If other nodes use the receiver's ID to establish a new channel, they won't 'interfere' with the transmission in the initialized channel. It is possible to receive data modulated with different IDs at the same time. The same holds for transmitting.

If only half duplex communication is possible, scheduling transmission and reception of data at a node is challenging for parallel channels with variable data rates. The time scheduling can be controlled by single nodes if only either parallel incoming or parallel outgoing links are allowed in the network. Then a node with parallel channels

[1] Standard techniques for local broadcast of hello-messages and multi-hop algorithms might be used to publish the attendance of a new node. The messages might be addressed to a dedicated ID receivable by all nodes.

has to set the length of time slots to the minimum length necessary for each individual channel. If a node can receive new messages for channel initialization, time slots for receiving should have an appropriate length that new communication partners with a low data rate are able to transmit in the time slot. With non-uniform data rates in our scheme, packet lengths have to be either adjusted non-uniformly to the time slots or the data rate is reduced to the slowest rate of all channels of a node. Figure 5.3(a) shows

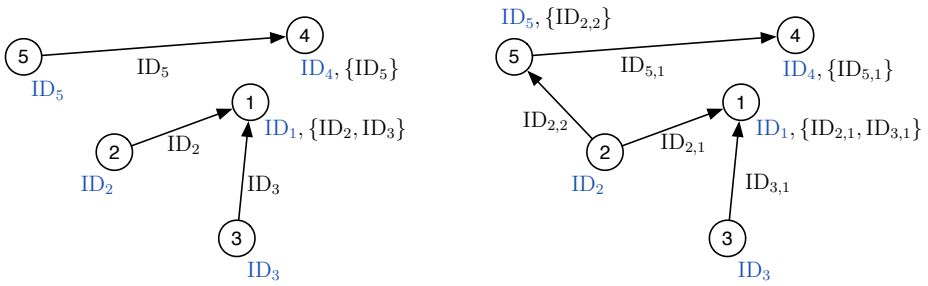

(a) half duplex (b) full duplex

Figure 5.3: Example for directed connections in a wireless network where edge labels denote the ID for modulation and node labels for demodulation

an example of a wireless network with 5 nodes and only half duplex communication. The node labeled '1' demodulates the received signal for its own random seed ID_1 and for two parallel incoming links with ID_2 and ID_3.

Full duplex communication on the same carrier frequency is also possible with wireless hardware [CHJ+12]. When transmitting and receiving at one antenna at the same time, the outgoing and incoming signals are super-posed. A circulator, which is a passive cancellation circuit [HMK12], can be used in the wireless hardware to filter the outgoing signal and the remaining part of the signal can be received. Besides, full duplex can also be emulated over a half duplex link and time or frequency division duplexing (TDD or FDD). Figure 5.3(b) shows the difference (compare with Fig. 5.3) where the node labeled with 5 receives from node 2 and transmits to node 4 at the same time. To make this possible, a node has to use another ID for an outgoing connection than its own, which is used to establish new incoming connections. Compare the identifiers in Figure 5.3(b) used at node 2, which uses ID_2 in a modulation to accept new incoming connections and at the same time it created two additional identifiers $ID_{2,1}$ and $ID_{2,2}$ for two outgoing connections. Since $ID_{2,1}$ and $ID_{2,2}$ are both pseudo-random, node 2 can super-pose the signals of both connections internally and send at the same time. So summarizing, if full duplex is given, we can simultaneously establish arbitrary connections (insofar the signal attenuation due to path loss does not nearly turns the data rate to zero).

The sequence diagram in Figure 5.4 shows an example for the communication protocol between a sender and a receiver node. The sender has the identifier ID_s which

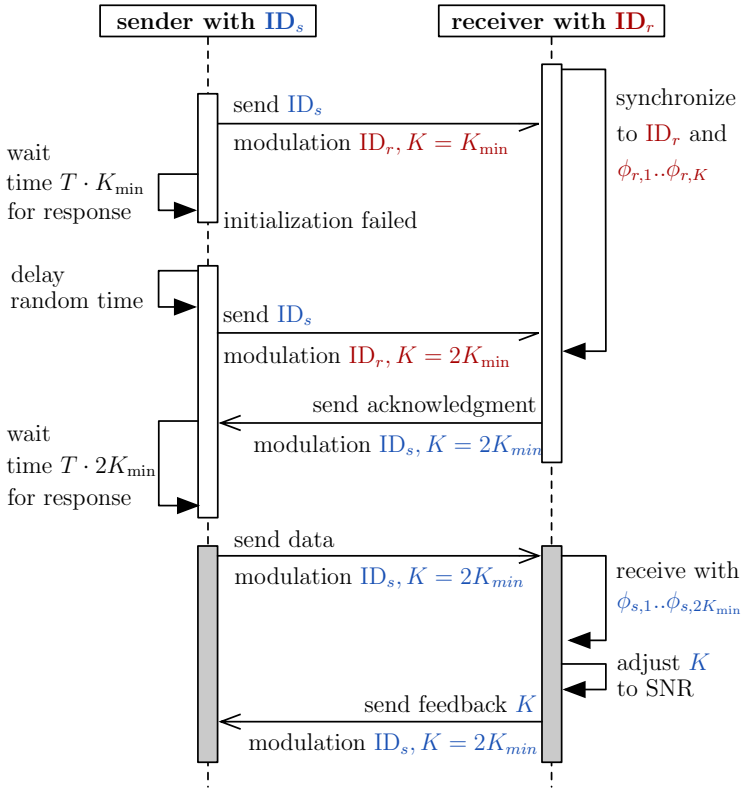

Figure 5.4: Sequence diagram for a point-to-point communication with a two round channel initialization followed by data transmission with feedback for optimizing K

it intends to use as seed in the data modulation with the K-repetition scheme. The receiver accepts new initialization messages which are modulated with the seed ID_r and is trying to synchronize to a pilot signal after demodulation with the K-repetition scheme with ID_r. The sender tries the first contact with a modulation with $K = K_{\min}$ and and does not get through. After a timeout for an acknowledgment from the receiver, it increases K to $2K_{\min}$ and resends the initialization message, which is successful this time and acknowledged by the the receiver. Both nodes know now that $K = 2K_{\min}$ is a proper choice in the modulation and can be used for data transmission. The initialization message contains ID_s from the sender and the receiver also starts demodulating the received signal for ID_s. The sender transmits data modulated with its identifier ID_s. After reception, the receiver computes the SNR after demodulation with the K-repetition scheme. The SNR value is used to optimize factor K and the receiver responds with a feedback containing a new value for K. Both nodes continue (de-)modulating the transmitted data with the new set K.

5.3 Channel Initialization

A transmission from a sender to a receiver is only successful if sender and receiver use the same ID and factor K for modulation respectively demodulation in the K-repetition scheme and other senders do not interfere with the same modulation.

In our protocol, all senders use the same carrier frequency without controlled medium access, and the frequency band of the carrier probably has a strong signal most of the time. Detecting a new started transmission in the superposition of many signals purely by the strength of the signal on the carrier is impossible. To achieve carrier sensing we have to perform demodulation with the K-repetition scheme first, which separates the super-posed channels on the same carrier frequency. For that, each node has a unique ID and all nodes intending to establish a connection have to use that ID for modulation in the first contact message. Each node ready to accept new connections demodulates the received signal with its ID and gets this way only initialization messages meant for itself and all other initialization messages intended for other nodes are filtered.

Data transmission is only successful if the SINR is greater than threshold β and a codeword can be identified in the presence of noise. When a node intends to establish a communication channel, it does not know the noise level at the receiver in advance and the signal attenuation due to path loss is also unknown. Hence, the initialization fails if the repetition factor K is chosen too small and, on the other side, initialization will take too long if K is chosen much larger as necessary. Therefore, we use the exponential binary search algorithm [BY76] to set up K.

Theorem 15 *A communication channel can be established with competitive factor eight for an unknown SINR-value compared to a known SINR-value. For that, an initialization message is transmitted with smallest possible repetition factor K and in the case of failure, repeated with a doubled factor K until an acknowledgment has been received. With established communication in both directions, the measured SINR value can be exchanged and K can be fine-tuned.*

Proof: Assume the optimal time for initialization is

$$T_{opt} = T \cdot (K'_s + K'_{ack}) \leq T \cdot 2K'$$

where T is the time for a single frame, K'_s denotes the minimum repetition factor for successful transmission of the initialization message and respectively K'_{ack} for a successful acknowledgement. We assume that a minimum repetition factor of K_{min} is necessary for successful transmission and a node can estimate this value by measuring the own noise level and the signal attenuation to nearby nodes is also known (e.g. $K_{min} \in \Theta(\log n)$ for n nodes in the plane, see Lemma 38 in the appendix). The optimal values for the communication are hence $K'_s, K'_{ack} \geq K_{min}$. Let us assume that the communication channel could be established in round i. The runtime of the

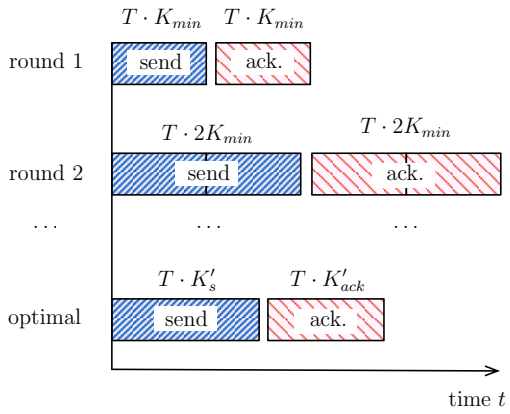

Figure 5.5: Illustration of initialization sequence with doubled transmission length for b=2 until transmission succeeds.

algorithm is then

$$T_{alg} \quad = \quad T \cdot 2K_{min} \cdot \sum_{\ell=0}^{i} b^{\ell} = T \cdot 2K_{min} \cdot \frac{b^{i+1}-1}{b-1}$$

including factor two for sending and acknowledging. For repetition factor K in round i, it holds $2K' \leq b^i \cdot 2K_{min} < b \cdot 2K'$. In round $(i-1)$, the algorithm failed and the optimum algorithm needs at least time

$$T_{opt} \geq \frac{T \cdot b^{i-1} \cdot 2K_{min}}{2}$$

where factor $\frac{1}{2}$ takes the estimation $K'_s + K'_{ack} \leq 2K'$ into account. The competitive ratio is hence

$$r \quad \leq \quad \frac{T_{alg}}{T_{opt}} = 2 \cdot \frac{b^{i+1}-1}{b^{i-1} \cdot (b-1)} = 2 \cdot \frac{b^2 - b^{-i+1}}{b-1} \leq \frac{2b^2}{b-1}$$

The ratio has for $b = 2$ a minimum and the optimal choice is to double K in each round. Then the competitive ratio is $r \leq 8$. □

Corollary 12 *Assume the minimum repetition factor is K_{min} and the maximum repetition factor is $r_K \cdot K_{min}$ with $r_K \geq 1$. If a new communication channel is established for an unknown repetition factor K, then the computation for synchronization increases to $\mathcal{O}(r_K)$ accumulations and $\mathcal{O}(\log r_K)$ correlations.*

For instance, if we consider a network with n nodes and area $\Theta(n)$ in the free-space model, possible values are $K_{min} = \Theta(\log n)$ and $r_K = \sqrt{n}$ (see Lemma 38).

Proof: If a receiver analyses the signal for all possible K values independently with $K \in (K_{min}, 2K_{min}, \ldots, r_K \cdot K_{min})$, the computation time for receiving the first frame for synchronization would increase to $2r_K \cdot K_{min}$. However, it is also possible here to accumulate the frames of length T iteratively and calculate the correlation when the number of summands $(K_{min}, 2K_{min}, 4K_{min}, \ldots, r_K K_{min})$ is reached. The processing can be stopped when the SINR threshold β is reached. This can already be the case before the complete sender sequence is analyzed when K is chosen too high at the sender. The overall computation then consists of $\mathcal{O}(r_K)$ accumulations and $\mathcal{O}(\log r_K)$ correlations. □

When several sender nodes try to contact the same receiver r with the same modulation ID_r for channel initialization, we might face interference because both signals can be correlated. But two senders only interfere if both signals are frame synchronous at the receiver, i.e. the frame with same pseudo-random phase overlaps. Otherwise we can assume that the pseudo-random phases have small auto-correlation property and the receiver can receive both signals at the same time. This is comparable to Chirp Spread spectrum (CSS) which spreads a signal over a frequency band to attain low auto-correlation, and overlapping chirp pulses can be received. We reach the same but in the phase domain instead of the frequency domain.

To solve interferences of simultaneous channel initializations at one receiver with synchronous pseudo-random phases, we include a random delay in the protocol if an initialization round has failed. This achieves that the frames with same pseudo-random phase do not overlap anymore and the channel initialization can succeed. In the case of several interfering nodes, it might be the case that a subset chooses the same random delay and they interfere in the round again. However, all senders without interference can establish the connection and are out of the game because after successful initialization they change the modulation to the sender ID. So the set of interfering senders shrinks in each round until all connections are established. The delay times have to be integer multiples of the frame time and can be chosen for instance with binary exponential backoff method [MB76].

5.4 Data Transmission

When a channel is initialized, data can be transmitted. The K-repetition scheme now uses the pseudo-random phases generated with the identifier of the sender ID_s (instead of the receiver's identifier ID_r in the channel initialization phase). This has the advantage that the receiver is able to receive new channel initialization messages because the established connection does not use the modulation with ID_r anymore. The receiver can establish multiple connections at the same time and handle parallel incoming data streams by analyzing the signal for all sender identifiers ID_s individually.

On the other hand, a sender can establish several outgoing connections by using multiple IDs, i.e. for the i-th outgoing connection the sender transmits during channel

initialization the identifier $\mathrm{ID}_{s,i}$. The signals of the multiple outgoing connections then have to be mixed at the sender before emitting the super-posed signal.

The interference values in the SINR-model are expected values with corresponding variance in the same magnitude. To cope with errors one can repeat the messages, codewords or increase the repetition value K for a sufficient high success rate. We include in the protocol to measure the SNR after demodulation with the K-repetition scheme and update factor K to keep the bit error rate small and do not loose synchronization. For that, the receiver gives feedback during transmission that factor K can be updated for modulation at the sender and demodulation at the receiver accordingly.

Another option to cope with the variance is that every node in the reception area will receive the messages with different interferences in the variance range and each of these nodes can receive and encode the message. So with relaying from a node which is closer to the actual receiver can increase the SINR and increase the robustness of the network if such a multi-hop procedure is possible.

The K-repetition scheme has constant transmission power but a variable data rate, and thus we analyze the energy consumption per bit of the K-repetition scheme.

Lemma 34 *When using the K repetition scheme, the expected energy per bit is proportional to the noise energy received in the same time.*

Consequently, the data rate is anti-proportional to the noise level.

Proof: For energy consumption, we have to consider transmission power and idle times. Since we prevent transmission interference with redundant transmissions, we have no idle times (e.g. for a TDMA schedule) and can transmit permanently. Assume we know the minimum noise $w_{\min}$ from the environment and adjust the transmission power accordingly that the receiver has a SNR

$$\mathrm{SNR}_{\min} \geq \frac{P_r}{w_{\min}} \tag{5.3}$$

with signal power P_r at the receiver. From (5.2) we already now that the the K-repetition scheme increases the SINR by factor K in expectation for any interferences which do not use the same pseudo random sequence of phases at the same time with

$$\mathrm{SINR}_K = \frac{K \cdot P_r}{w} \tag{5.4}$$

where w is the actual noise power at a receiver. Comparing (5.3) and (5.4) and setting $\mathrm{SNR}_{\min} = \mathrm{SINR}_K$ we have to choose

$$K = \left\lceil \frac{w}{w_{\min}} \right\rceil \geq 1 \ .$$

We assume here that noise w is correlated. In this case, changing the modulation or adjusting the transmission power has no effect since all devices in the ad hoc network would behave alike. □

5.5 Jammers

A so called jammer is a devices which actively interferes with a wireless transmission in order to prevent it. In other words, the goal of the jammer is to lower the signal-to-noise ratio at the receiver under a receivable level and the transmission fails. The interference power, a jammer can produce, depends on the jammer's sending power and the distance to the receiver with resulting signal attenuation. If the jammer is able to prevent a communication, the communication partners have two options: They can lower the distance to each other or the transmitter can increase transmission power to increase the signal level. But if the jammer is near the receiver and the transmitter has no realistic chance to increase the signal level above the interference level, the situation is hopeless.

Besides the sheer signal level of sender and jammer at a receiver, it is also important if both signals correlate. For instance if the jammer sends in another frequency band or only disturbs certain periods in the time domain, the interference is strongly lowered or even not present to the transmission. The sender and receiver might perform carrier sensing and adjust their communication according to the behavior of the jammer.

Far worse is the situation if the jammer knows the modulation and used frequency band respectively time frame of the sender in advance, e.g. the sender announces during transmission to the receiver the communication parameters that the receiver can adjust to it. In this case, only the transmitted data is unknown to the jammer. So the jammer cannot perfectly cancel out the signal with noise canceling techniques and the receiver will receive something. This is where a modulation scheme with redundant information like the K-repetition scheme can be applied, to retrieve the correct transmitted symbols from redundant error-prone symbols.

Theorem 16 *A jammer can only lower the data rate but not prevent a transmission if the K-repetition scheme is applied and the ID used in the K-repetition scheme is unknown to the jammer.*

For a given noise level w and signal power P_I of the jammer at the receiver, we choose

$$K = \lceil g \cdot (1 + P_I/w) \rceil$$

for a convenient constant g to cope with variance in the K repetition scheme.

Proof: Assume the signal-to-noise ratio at the receiver is without a jammer

$$\mathrm{SNR}_0 = \frac{P_s}{w}$$

with noise level w and signal power P_s of the sender at the receiver. Let us assume that a suitable modulation is chosen an the receiver can receive the transmission of the sender at a modest bit-error rate. When a jammer with signal power P_I at the

receiver becomes active, the SNR drops to

$$\mathrm{SINR}_1 = \frac{P_s}{w + P_I} \tag{5.5}$$

and the bit error rate increases or even the receiver might not be able to synchronize to the sender's signal anymore. We now apply the K-repetition scheme and can increase the ratio to

$$\mathrm{SINR}_K = \frac{K \cdot P_s}{w + P_I} \ . \tag{5.6}$$

Demanding $\mathrm{SNR}_0 = \mathrm{SINR}_K$ we get in expectation

$$K = \left\lceil 1 + \frac{P_I}{w} \right\rceil \ .$$

To cope with variance, we additionally increase K by factor $g = \Theta\left(\log\left(1 + P_I/w\right)\right)$ to receive with high probability. We can proof this by applying a Chernoff bound. The expected SNR for factor g is $g \cdot \mathrm{SNR}_0 = c_0 \cdot \log\left(1 + P_I/w\right) \cdot \mathrm{SNR}_0$. Then it holds for $0 < \delta \leq 1$:

$$\begin{aligned} \mathrm{Prob}\left[X \leq (1-\delta) \cdot \mathbb{E}\left[X\right]\right] &< \mathrm{e}^{-\frac{\delta^2 \cdot \mathbb{E}[X]}{2}} \\ \mathrm{Prob}\left[X \leq (1-\delta) \cdot c_0 \cdot \log\left(1 + P_I/w\right)\right] &< \mathrm{e}^{-\frac{\delta^2 \cdot c_0 \cdot \log\left(1+P_I/w\right)}{2}} \end{aligned}$$

The necessary ratio is $1 \cdot \mathrm{SNR}_0$ such that $(1-\delta) \leq \frac{1}{c_0 \log(1+P_I/w)}$. Solving to δ gives $\delta \geq 1 - \frac{1}{c_0 \log(1+P_I/w)}$. We choose $c_0 := 3$ so that $\delta \geq \frac{1}{2}$ for $\frac{P_I}{w} \geq 1$. Then the probability for the necessary SNR is

$$\mathrm{Prob}\left[X \leq 1\right] < \left(1 + P_I/w\right)^{-\frac{\left(\frac{1}{2}\right)^2 \cdot 3}{2}} = \left(1 + P_I/w\right)^{-c_2}$$

with $c_2 = \frac{3}{8}$. □

Corresponding to Corollary 11, we get the following data rate when a jammer is present.

Corollary 13 *If a jammer interferes a transmission with power P_I at the receiver, the data rate reduces by factor $\frac{1}{\lceil g \cdot (1+P_I/w) \rceil}$ when using the K-repetition scheme.*

In this chapter, we have presented a distributed MAC protocol which allows multiple devices in a wireless network to communicate simultaneously and independent from each other on the same carrier frequency. Interference of parallel communications is circumvented by repeating each symbol K times but with pseudo-random phase shifts. This increases the SNR of each transmission channel to a receivable level while reducing the data rate by factor $1/K$. The protocol can also be used to increase the transmission distance and establish connections to remote nodes if regular transmission power is insufficient, e.g. in wireless networks with inhomogeneous node densities. Also a device can handle multiple incoming connections at the same time with this protocol.

6 Conclusions and Outlook

We demonstrate in this thesis multi-hop transmission schemes for ad hoc networks, which use transmit beamforming to reduce the transmission delay and the overall transmission power at the same time. We consider in our model mobile devices with one dipole antenna each and a power constraint for transmitting. A transmission channel only consists of the line-of-sight path from sender to receiver in the free-space model.

At first, we analyze the characteristics of coordinated multiple antennas. The signal processing technique beamforming (or spatial filtering) enhances the signal-to-noise ratio of a transmission channel and extends the transmission range, i.e. the transmission range of n transmitters with total transmission power $\Theta(n)$ increases by factor $\Theta(n)$. For transmit beamforming, a non-uniform allocation of transmission power can increase the power transfer from multiple transmitters to a single receiver and, in result, increases the SNR for the same total transmission power. The optimal solution is a trade-off between many transmitters with large beamforming gain and a few transmitters near the receiver having a low signal attenuation. We use in our transmission schemes only uniform power allocations and the analysis of transmitters placed on a line and in rectangular areas suggests that a non-uniform power allocation does not improve the asymptotic results of our algorithms. Beamforming can achieve long distant transmissions, while the electromagnetic field strength does not increase proportional to the transmission distance. The reason is that the transmission power is distributed on many transmitting antennas. For a transmission distance d, the maximum signal power is $\mathcal{O}(\log d)$ for the line broadcast and $\mathcal{O}\left(d^{2/3} \cdot \ln d\right)$ for the unicast in the plane. Direct transmission produces field strengths of $\Theta\left(d^2\right)$ and nearest-neighbor routing $o(1)$.

On the other hand, diversity gain allows spatial multiplexing even for nodes placed on a line. The parallelism of multiplexing can increase the throughput but relies on a rich environment causing a channel matrix H with many large eigenvalues (which represent independent channels). Only one large eigenvalue is expected in a setting in the free-space model and a low angular spread between transmit and receive antennas being far distant from each other. The signal strength of this single channel can be enhanced by applying beamforming.

We develop a new technique called deliberate attenuation for nodes placed on a line, which can increase the path loss of n coordinated antennas in one direction to $\Theta\left(d^{2n-2}\right)$ while retaining free-space path loss d^{-2} in the opposite direction. This enhances the quality of the spatial filter of beamforming. We characterize the beam pattern of the

spatial filter of beamforming in the plane [JS12]. For m nodes randomly placed on a disk with diameter d, we classify three (angle) ranges: the main beam, side lobes, and white Gaussian noise. The main beam has an angle range of λ/d being proportional to the wavelength λ and side lobes around the main beam can produce interferences in the same order of magnitude of the main beam. Compared to the main beam with power $\Theta(m^2)$, the range of white noise has only expected power $\Theta(m)$.

We present multi-hop transmission schemes for the one-dimensional line, the two-dimensional plane, and three dimensional space. The first example of a one-hop relaying scheme shows that a simple amplify and resend strategy accumulates noise of each hop and thus is not feasible for multi-hop strategies without noise filtering. But the example shows that (collaborative) beamforming can reduce transmission power or increase transmission distance leading to less hops and improved delay in a multi-hop scheme.

	node placing	**running time**	**transmission energy**
direct transmission	*	$\Theta(1)$	$\Theta(d^2)$
nearest-neighbor multi-hop	*	$\Theta(d)$	$\Theta(d)$
beamforming broadcast	line	$\Theta(\log d)$	$\Theta(d)$
Unicast I + II	plane	$\Theta(\log\log d)$	$\Theta(d)$
Unicast III	plane	$\Theta(\log d)$	$\Theta\left(\sqrt{d}\right)$
Unicast IV	plane	$\Theta\left(\frac{1}{\varepsilon}\log\log d\right)$	$\Theta\left(\sqrt{d}^{1+\varepsilon}\right)$
Unicast V	space	$\Theta(\log d)$	$\Theta(\log d)$

Table 6.1: Comparison of runtime and transmission power for transmission distance d, wavelength λ, and equidistant node placement (* denotes placing in 1D, 2D, or 3D)

For n nodes placed on a line, our broadcasting scheme with beamforming can transmit a message from all nodes to every other node with $n(n-1)$ transmissions in total in time $\Theta(n)$. The same operation with nearest-neighbor multi-hop has also delay $\Theta(n)$. While nearest-neighbor routing requires $\Theta(n)$ hops to broadcast each message, our broadcast scheme with beamforming only needs $\Theta(\log n)$ hops, which might have less sources of error. However, if the network is in idle state, a single broadcast from one source to every other node has reduced delay $\Theta(\log n)$ in our scheme, whereas nearest-neighbor routing does not provide a speedup with delay $\Theta(n)$ for the same asymptotic power consumption $\Theta(n)$.

The unicast algorithm works in the two-dimensional plane or three-dimensional space. It is designed for ad hoc networks with small traffic, sparse energy supply, and small transmission delay, e.g. for wireless sensor networks. High traffic is discussed in the open problems section 6.1. We present different schemes (Unicast I-V) providing different trade-offs between transmission delay and power consumption. Unicast I has the shortest delay $\Theta(\log\log d)$ but needs phase-shifts at the relay nodes for synchro-

nization, whereas Unicast II is self-synchronizing but has larger constant factors in the transmission delay. We show a delay of $\Theta(\log\log d)$ is asymptotically optimal, if nodes have constant transmission power. Unicast I and II have the same asymptotic power consumption $\Theta(d)$ for transmission distance d if nodes are placed in a grid. Nearest-neighbor routing also needs linear power. Our unicast operation also works for nodes randomly placed in the plane. In this case, the transmission power of a node has to be increased by $\Theta(\log n)$ to reach neighboring nodes with high probability and the initial broadcast phase of a constant number of nodes needs extra synchronization, e.g. by position information. Unicast III reduces the power consumption for radio transmission to sublinear with $\Theta\left(\sqrt{d}\right)$ and the transmission delay is larger with $\Theta(\log d)$. Unicast IV provides an ε-approximation of sublinear power consumption $\Theta\left(d^{(1+\varepsilon)/2}\right)$ and double-logarithmic delay $\Theta(1/\varepsilon \cdot \log\log d)$. If we can choose the relay nodes from three-dimensional space, we can reach more nodes with the same transmission power to perform beamforming. Then, the total transmission power in Unicast V drops to $\Theta(\log d)$ for transmission delay $\Theta(d)$.

The broadcast operation on the line and the unicast operation in the plane and space can provide self-synchronization, i.e. phase synchronization is established on-the-fly in each routing hop. Phase-synchronization is necessary for beamforming to adjust the spatial filter. Other works assume here full-CSI. We show self-synchronization in the free-space model by geometrical arguments only. Our strongest assumption is that nodes know their position. A node decides by its position (accuracy can be low) if it should relay a received message.

Finally, we present a distributed medium access control (MAC) protocol that uses the basic concepts of beamforming and allows several devices in a wireless network to communicate on the same carrier frequency, at the same time, and without interfering each other. In the low-SINR regime, the scheme increases the signal-to-noise ratio of a transmission channel by $\Theta(K)$ while decreasing the data rate factor $1/K$. This is achieved by sending each symbol K times with pseudo-random phase shifts. Another possible application is establishing connectivity to remote nodes where regular transmission power is insufficient, e.g. in wireless networks with inhomogeneous node densities.

6.1 Open Problems

For data transmission, we want a short delay, high data rate, and small power consumption. We could show a short delay of $\Theta(\log\log d)$ for (sub-)linear transmission power consumption for our unicast scheme. The data rate of our scheme is the same as the data rate of a transmission between neighboring nodes in the network. But the channel will be blocked for time $\Theta(\log\log d)$ until the target at distance d receives the message and the next message transmission can be initialized by the source. This throttles the data rate by factor $\Theta\left(\frac{1}{\log\log d}\right)$. So pipelining is desirable, i.e. the source can initiate

sending the next message while the preceding message is still on the way to the target and handled by relay nodes. Figure 6.1 depicts a scenario where each rectangular clus-

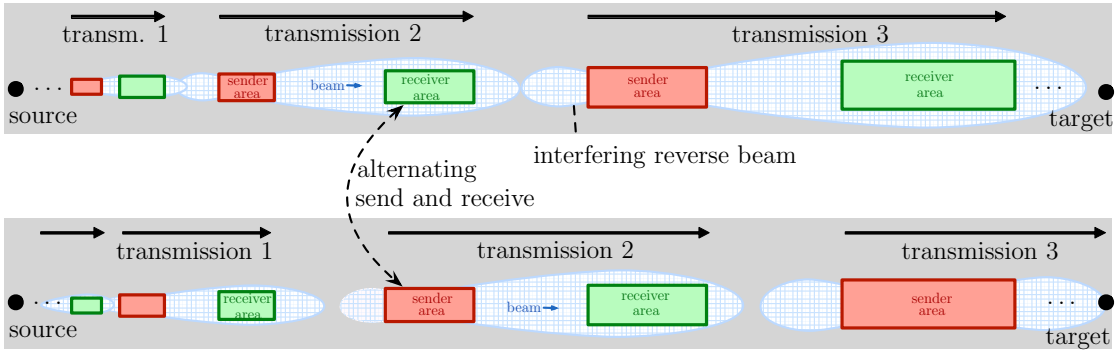

Figure 6.1: Unicast scheme combined with pipelining

ter between source and target is alternating transmitting or receiving. A proof idea is to show, that the maximum interference power between parallel operations is only a small constant for an arbitrary transmission distance d. When considering one receiving rectangle, we get interferences from rectangles in direction of the source and in direction of the target. With a little effort, it can be shown that interferences from the source's direction are a small constant, since the distances between rectangular grow double-exponentially. This is different for interferences from the target's direction, because the number of beamforming senders also grows double-exponentially. If we can assume that beamforming senders in a rectangular cluster have random positions, the signals of the senders are uncorrelated in expectation in direction to the target and it is also possible to show constant interference here where pipelining is possible. In case signals are correlated and produce a reverse beam towards the source (e.g. the grid distance is a multiple integer of the wavelength), interferences will grow in distance d and pipelining is not possible without any further steps. Here we might use deliberate attenuation to reduce interferences to the rear and have beamforming towards the target at the same time. For that it remains to show that deliberate attenuation is also usable in the plane.

Another open problem is how to maximize the overall network throughput when applying our unicast scheme in parallel in the network. Lemma 37 in Appendix A, gives a rough lower bound how unicast operations can be performed at the same time. The idea is to operate simultaneous x-routings in multiple rows (respectively y-routing in multiple columns) in the area of the network at the same time. The necessary distance between parallel lanes results here from the maximum signal strength, which we determined in Lemma 27.

We could decrease the transmission power for distance d to $\Theta\left(\sqrt{d}\right)$ in a grid network in the plane, and to $\Theta\left(\log d\right)$ in a grid network in three-dimensional space. If the

overhead of power consumption for signal processing at each receiving node cannot be neglected, we see a trade-off between power consumption for transmitting and receiving and it will be part of future work to find the optimal solution for this trade-off.

Another challenging topic is to use collaborative beamforming for efficient broadcasting in the plane. We simulated therefore a round based broadcasting scheme. A source node initiates the broadcast and each node, which detects a signal on the carrier frequency, simply repeats the signal in the following rounds. Tests suggest that the

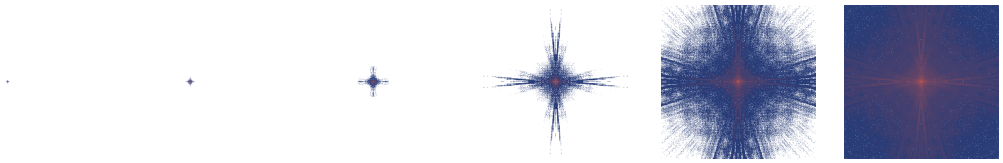

(a) round 3 (b) round 4 (c) round 5 (d) round 6 (e) round 7 (f) round 8

Figure 6.2: Simulation of broadcasting a carrier signal in a 500×500 grid with $\lambda \approx 0.21$

runtime is similar to the runtime of our unicast scheme. For the analysis of broadcasting in the plane, the model has to redefined to multipath-propagation although we are still in the free-space model. When we consider an arbitrary node in the network, a broadcasted message might arrive over multiple routing paths with different length and time. Several periods of the carrier, several symbols, or even several messages might superpose and each node has to ”decide” which is the dominant signal, and if it can be received and distinguished from the remaining signals.

Bibliography

[AEK+12] Chen Avin, Yuval Emek, Erez Kantor, Zvi Lotker, David Peleg, and Liam Roditty. SINR Diagrams: Convexity and Its Applications in Wireless Networks. *J. ACM*, 59(4):18, 2012.

[AJS11] Amir Alsbih, Thomas Janson, and Christian Schindelhauer. Analysis of peer-to-peer traffic and user behaviour. In *Fourth International Conference on Internet Technologies & Applications (ITA 2011)*, Wales, 2011.

[Ana14] Analog Devices, Inc, One Technology Way, P.O. Box 9106, Norwood, MA 02062-9106, U.S.A. *AD8341 1.5 GHz to 2.4 GHz RF Vector Modulator*, revision A edition, November 2014.

[Atm09] Atmel. *AVR121: Enhancing ADC resolution by oversampling*, 8003a-avr-09/05 edition, 05 2009.

[BNSW09] Jonathan M. Borwein, Dirk Nuyens, Armin Straub, and James Wan. Random walk integrals. Technical report, CARMA, University of Newcastle, Australia, October 2009.

[BWK05] I. Berenguer, Xiaodong Wang, and V. Krishnamurthy. Adaptive MIMO antenna selection via discrete stochastic optimization. *IEEE Transactions on Signal Processing*, 53(11):4315–4329, Nov 2005.

[BY76] Jon Louis Bentley and Andrew Chi-Chih Yao. An almost optimal algorithm for unbounded searching. *Information Processing Letters*, 5(3):82 – 87, 1976.

[CCJ90] Brent N. Clark, Charles J. Colbourn, and David S. Johnson. Unit disk graphs. *Discrete Mathematics*, 86(1–3):165–177, 1990.

[CH11] J.T. Chiang and Yih-Chun Hu. Cross-layer jamming detection and mitigation in wireless broadcast networks. *Networking, IEEE/ACM Transactions on*, 19(1):286–298, Feb 2011.

[CHJ+12] Jung Il Choi, S. Hong, M. Jain, S. Katti, P. Levis, and J. Mehlman. Beyond full duplex wireless. In *Signals, Systems and Computers (ASILOMAR), 2012 Conference Record of the Forty Sixth Asilomar Conference on*, pages 40–44, Nov 2012.

[CK85] Imrich Chlamtac and Shay Kutten. On Broadcasting in Radio Networks–Problem Analysis and Protocol Design. *IEEE Transactions on Communications*, 33(12):1240 – 1246, dec 1985.

[DF99] P. Driessen and J. Foschini. On the capacity formula for multiple input–

multiple output wireless channels: A geometric interpretation. *IEEE Transactions on Communications*, 47(2):173–176, 1999.

[dFdCdAM12] Edison Pignaton de Freitas, João Paulo C Lustosa da Costa, André Lima F de Almeida, and Marco Marinho. Applying mimo techniques to minimize energy consumption for long distances communications in wireless sensor networks. In *Internet of Things, Smart Spaces, and Next Generation Networking*, pages 379–390. Springer, 2012.

[DPP08] Lun Dong, AP. Petropulu, and H.V. Poor. A Cross-Layer Approach to Collaborative Beamforming for Wireless Ad Hoc Networks. *IEEE Transactions on Signal Processing*, 56(7):2981–2993, July 2008.

[EJRS14a] Alexander Ens, Thomas Janson, Leonhard M. Reindl, and Christian Schindelhauer. Robust Multi-Carrier Frame Synchronization for Localization Systems with Ultrasound. In *Proceedings of the 18th International OFDM Workshop 2014 (InOWo'14)*, Germany, 2014.

[EJRS14b] Alexander Ens, Thomas Janson, Leonhard M. Reindl, and Christian Schindelhauer. Robust multi-carrier frame synchronization for localization systems with ultrasound. In *Proceedings of the 18th International OFDM Workshop 2014 (InOWo'14)*, Essen, Germany, 2014.

[EKKG05] A. El-Keyi, T. Kirubarajan, and A.B. Gershman. Robust adaptive beamforming based on the Kalman filter. *IEEE Transactions on Signal Processing*, 53(8):3032–3041, Aug 2005.

[FLS06] Richard P. Feynman, Robert B. Leighton, and Matthew Sands. *The Feynman Lectures on Physics*, volume 1. Pearson Addison-Wesley, 2006.

[FTU10] Umberto Ravaioli Fawwaz T. Ulaby, Eric Michielssen. *Fundamentals of Applied Electromagnetics, 6/E.* Prentice Hall, 2010.

[GA02] David Gesbert and Jabran Akhtar. Breaking the barriers of shannon's capacity: An overview of MIMO wireless systems. *Telenor's Journal: Telektronikk*, 98(1):53–64, 2002.

[GK98] Piyush Gupta and Panganamala R Kumar. Critical power for asymptotic connectivity in wireless networks. In *Stochastic analysis, control, optimization and applications*, pages 547–566. Springer, 1998.

[GK00] Piyush Gupta and P. R. Kumar. The Capacity of Wireless Networks. *IEEE Transactions on Information Theory*, 46:388–404, 2000.

[Gol67] R. Gold. Optimal binary sequences for spread spectrum multiplexing. *IEEE Transactions on Information Theory*, 13(4):619–621, 1967.

[HCP11] F. Hutu, D. Cordeau, and J.-M. Paillot. 2.4 GHz antenna array using vector modulatorbased active phase shifters for beamforming. *Microwaves, Antennas Propagation, IET*, 5(2):245–254, Jan 2011.

[HMK12] Steven S. Hong, Jeffrey Mehlman, and Sachin Katti. Picasso: Flexible

rf and spectrum slicing. In *Proceedings of the ACM SIGCOMM 2012 Conference on Applications, Technologies, Architectures, and Protocols for Computer Communication*, SIGCOMM '12, pages 37–48, New York, NY, USA, 2012. ACM.

[HNSGL08] V. Havary-Nassab, S. Shahbazpanahi, A Grami, and Zhi-Quan Luo. Distributed beamforming for relay networks based on second-order statistics of the channel state information. *Signal Processing, IEEE Transactions on*, 56(9):4306–4316, September 2008.

[HSVG04] Friedhelm Meyer Heide, Christian Schindelhauer, Klaus Volbert, and Matthias Grünewald. Congestion, Dilation, and Energy in Radio Networks. *Theory of Computing Systems*, 37:343–370, 2004.

[Jay04] Sudharman K Jayaweera. Energy analysis of mimo techniques in wireless sensor networks. In *38th conference on information sciences and systems*, 2004.

[JES15] Thomas Janson, Alexander Ens, and Christian Schindelhauer. Turning Interferences into Noise in Ad Hoc Networks. *Telecommunication Systems*, accepted in June 2015.

[JS12] Thomas Janson and Christian Schindelhauer. Analyzing Randomly Placed Multiple Antennas for MIMO Wireless Communication. In *Fifth International Workshop on Selected Topics in Mobile and Wireless Computing (IEEE STWiMob'2012)*, pages 745–752, Barcelona, Spain, 2012.

[JS13] Thomas Janson and Christian Schindelhauer. Broadcasting in Logarithmic Time for Ad Hoc Network Nodes on a Line using MIMO. In *Proceedings of the 25th ACM Symposium on Parallelism in Algorithms and Architectures, SPAA'13*, pages 63–72, Montreal, Canada, July 2013. ACM.

[JS14a] Thomas Janson and Christian Schindelhauer. Ad-Hoc Network Unicast in O(log log n) using Beamforming. http://arxiv.org/abs/1405.0417, May 2014.

[JS14b] Thomas Janson and Christian Schindelhauer. Cooperative beamforming in ad-hoc networks with sublinear transmission power. In *2nd International Workshop on GReen Optimized Wireless Networks (GROWN'14)*, Larnaca, Cyprus, October 2014.

[JS14c] Thomas Janson and Christian Schindelhauer. Self-synchronized Cooperative Beamforming in Ad-Hoc Networks. In *16th International Symposium on Stabilization, Safety, and Security of Distributed Systems (SSS'14)*, number 8756 in Lecture Notes in Computer Science, pages 135–149, Paderborn, Germany, September 2014.

[Kar10] Klaus W. Kark. *Antennen und Strahlungsfelder*. Vieweg+Teubner, 3. edition, 2010.

[KMW04] Fabian Kuhn, Thomas Moscibroda, and Roger Wattenhofer. Unit Disk Graph Approximation. In *Proceedings of the 2004 joint workshop on Foundations of mobile computing*, DIALM-POMC '04, pages 17–23, New York, NY, USA, 2004. ACM.

[KV96] Hamid Krim and Mats Viberg. Two decades of array signal processing research: the parametric approach. *IEEE Signal Processing Magazine*, 13(4):67–94, July 1996.

[LBB+13] Ruizhi Liao, Boris Bellalta, Jaume Barcelo, Victor Valls, and Miquel Oliver. Performance analysis of IEEE 802.11ac wireless backhaul networks in saturated conditions. *EURASIP Journal on Wireless Communications and Networking*, 2013(1), 2013.

[LL09] E. Lebhar and Z. Lotker. Unit disk graph and physical interference model: Putting pieces together. In *IEEE International Symposium on Parallel Distributed Processing (IPDPS 2009)*, pages 1–8, may 2009.

[LL10] Gregory F. Lawler and Vlada Limic. *Random Walk: A Modern Introduction*. Cambridge University Press, July 2010.

[LMSW06] Thomas Locher, Patrick Moor, Stefan Schmid, and Roger Wattenhofer. Free riding in bittorrent is cheap. In *In HotNets*, 2006.

[MB76] Robert M Metcalfe and David R Boggs. Ethernet: distributed packet switching for local computer networks. *Communications of the ACM*, 19(7):395–404, 1976.

[MBC+01] Rex Min, Manish Bhardwaj, Seong-Hwan Cho, Eugene shih, Amit Sinha, Alice Wang, Anantha Chandrakasan, and Eugene Shih Amit Sinha. Low-power wireless sensor networks. In *In VLSI Design*, pages 205–210, 2001.

[MLÖ12] Alla Merzakreeva, Olivier Lévêque, and Ayfer Özgür. Hierarchical Beamforming for Large One-Dimensional Wireless Networks. In *IEEE International Symposium on Information Theory (ISIT)*, pages 1533 –1537, July 2012.

[MÖL13] Alla Merzakreeva, Ayfer Özgür, and Olivier Lévêque. Telescopic beamforming for large wireless networks. In *IEEE Int. Symposium on Information Theory*, Istanbul, 2013.

[MW40] W. H. McCrea and F. J. Whipple. Random paths in two and three dimensions. In *Proc. Roy. Soc. Edinburgh*, pages 281–298, 1940.

[MW04] A.F. Molisch and M.Z. Win. MIMO systems with antenna selection. *IEEE Microwave Magazine*, 5(1):46–56, March 2004.

[Net13] Meru Networks. Four reasons to deploy 802.11ac using a single-channel architecture (white paper), 2013.

[NGS09] Urs Niesen, Piyush Gupta, and Devavrat Shah. On Capacity Scaling in Arbitrary Wireless Networks. *IEEE Transactions on Information*

Theory, 55(9):3959–3982, 2009.

[NKH05] A. Natarajan, A. Komijani, and A. Hajimiri. A fully integrated 24-GHz phased-array transmitter in CMOS. *IEEE Journal of Solid-State Circuits*, 40(12):2502–2514, December 2005.

[ÖJTL10] Ayfer Özgür, Ramesh Johari, David Tse, and Olivier Lévêque. Information Theoretic Operating Regimes of Large Wireless Networks. *IEEE Transactions on Information Theory*, 56(1):427–437, 2010.

[ÖLT07] Ayfer Özgür, Olivier Lévêque, and David Tse. Hierarchical Cooperation Achieves Optimal Capacity Scaling in Ad Hoc Networks. *IEEE Transactions on Information Theory*, 53(10):3549–3572, October 2007.

[OMPT05] H. Ochiai, P. Mitran, H.V. Poor, and Vahid Tarokh. Collaborative beamforming for distributed wireless ad hoc sensor networks. *IEEE Transactions on Signal Processing*, 53(11):4110–4124, November 2005.

[OTA+07] U. Olgun, C.A. Tunc, D. Aktas, V.B. Erturk, and A. Altintas. Optimization of Linear Wire Antenna Arrays to Increase MIMO Capacity using Swarm Intelligence. In *Proceedings of the 2nd European Conference on Antennas and Propagation (EuCAP 2007)*, pages 1–6, November 2007.

[PAK03] Tony S. Pollock, Thushara D. Abhayapala, and Rodney A. Kennedy. Introducing Space into MIMO Capacity Calculations. *Journal on Telecommunications Systems*, 24:415–436, 2003.

[PC14] Carla Passiatore and Pietro Camarda. A fair mac protocol for resource sharing in ad-hoc cognitive networks. *Telecommunication Systems*, 56(2):269–283, 2014.

[PCLM12] Yu Pei, Ying Chen, D.M.W. Leenaerts, and R. Mahmoudi. A phase-shifting up-converter for 30GHz phased array applications. In *IEEE Radio Frequency Integrated Circuits Symposium (RFIC)*, pages 499–502, June 2012.

[Pha99] A.G. Phadke. *Handbook of Electrical Engineering Calculations*. Electrical and Computer Engineering. Taylor & Francis, 1999.

[PL05] Karl Pearson and Lord Rayleigh. The problem of the random walk. *Nature*, 72(1867):342, August 1905.

[RXS11] Mariel Rivas, Shuguo Xie, and Donglin Su. A wideband beamformer with interference and noise suppression capabilities employing only spatial signal processing. In *International ITG Workshop on Smart Antennas (WSA 2011)*, pages 1–5, Aachen, Germany, February 2011.

[Sch59] Samuel Schechter. On the inversion of certain matrices. *Mathematical Tables and Other Aids to Computation*, 66(13):73–77, 1959.

[Sha49] C.E. Shannon. Communication in the Presence of Noise. *Proceedings of the IRE*, 37(1):10–21, 1949.

[Sha98] Claude E. Shannon. Communication in the Presence of Noise. *Proceedings of the IEEE*, 86(2):447 –457, February 1998.

[SL07] M. Sandell and Beng-Sin Lee. Pseudo-Random Scrambling for Quasi-Static MIMO Channels. In *IEEE 18th International Symposium on Personal, Indoor and Mobile Radio Communications (PIMRC)*, pages 1–5, 2007.

[TV05] David Tse and Pramod Viswanath. *Fundamentals of wireless communication*. Cambridge University Press, New York, NY, USA, 2005.

[WFGV98] P.W. Wolniansky, G.J. Foschini, G.D. Golden, and R. Valenzuela. V-BLAST: an architecture for realizing very high data rates over the rich-scattering wireless channel. In *International Symposium on Signals, Systems, and Electronics (ISSSE 98)*, pages 295–300, September 1998.

[WM04] Konrad Wrona and Petri Mähönen. Analytical model of cooperation in ad hoc networks. *Telecommunication Systems*, 27(2-4), 2004.

[WMGG67] B. Widrow, P.E. Mantey, L.J. Griffiths, and B. B. Goode. Adaptive antenna systems. *Proceedings of the IEEE*, 55(12):2143–2159, 1967.

A Appendix

A.1 Related Work

The following approximate computations shall confirm the analysis of [MÖL13] in related work section (1.4). In the following, we analyze the two-cluster scheme. As noted in [MÖL13], the optimal choice of parameters $a = 1/(n^{2/3}P)$ and $M \geq n^{1/3}$ and we use for computation the case $M = n^{1/3}$. According to Equation (6) in [MÖL13], the amplification at the nodes collaborating for beamforming is then

$$|C_k|, |D_j| = \sqrt{\frac{anP}{M}} = 1 \ .$$

The SNR at the relay nodes around the receiver at distance $\sqrt{n}$ is then

$$\mathrm{SNR}_{\mathrm{relay}} = \frac{\left(\sum_{k=1}^{n^{1/3}} \frac{|C_k|\sqrt{P}}{\sqrt{n}}\right)^2}{w} = \frac{n^{2\cdot(1/3-1/2)} \cdot P}{w} = \frac{P}{n^{1/3} \cdot w} \ .$$

So, the relay nodes receive the signal at a very low SNR and might not be able to notice it. When these relay nodes beam-form the signal to the receiver with assumed longest distance $\sqrt{n}$, the SNR will improve at the receiver as follows.

$$\mathrm{SNR}_{\mathrm{destination}} = \frac{\left(\sum_{i=1}^{n^{1/3}} \frac{\sqrt{P}}{\sqrt{n^{1/3}}\cdot\sqrt{n}}\right)^2}{\sum_{i=1}^{n^{1/3}} \left(\frac{1}{\sqrt{n}}\right)^2 \cdot w + w} = \frac{P \cdot n^{-2/3}}{(n^{-2/3}+1)\cdot w} \approx 1$$

The signal magnitude at the relay nodes (before forwarding to the destination) might be far below quantization resolution of sampling at the relay nodes. Since we also have additive noise at the receivers, this quantization resolution might again increase when the signals are forwarded and super-posed at the destination. This effect is similar to a method of enhancing the resolution of an analog-digital converter (ADC) with adding noise to the signal and oversampling (e.g. see [Atm09]). It might be interesting if the transmission power has to be further increased for that at the second routing step.

The energy consumption of all three steps of the scheme is $\Theta(\sqrt[3]{n})$: The broadcast from the source node to the area $M = n^{1/3}$ needs power $\Theta(\sqrt[3]{n})$; the relay nodes performing beamforming need constant power $|C_k|^2$ and $|D_j|^2$ each and with M senders the total power is $\Theta(\sqrt[3]{n})$.

A.2 Communication Model

Signal to Interference plus Noise Ratio (SINR) The signal-to-noise ratio is independent from the absolute scale of the network, e.g. constant node density or constant network area (see [GK00]), if the antenna pattern is omnidirectional, i.e. signal power $\frac{P}{d^\alpha}$ for distance d from the sender, path loss exponent α, and sender power P. Assume we need a signal power P_{rx} at a receiver in distance d for successful transmission. Then, the sender needs transmission power $P_{\text{tx}} = P_{\text{rx}} \cdot d^\alpha$ to compensate attenuation due to path loss. Replacing the sender power P_{tx} in Equation (2.10) gives

$$\text{SINR}(v) \quad = \quad \frac{P_{\text{rx}}(u_i) \cdot \frac{d_i^\alpha}{|u_i - v|^\alpha}}{w + \sum_{k \neq i} P_{\text{rx}}(u_k) \cdot \frac{d_k^\alpha}{|u_k - v|^\alpha}} = \frac{P_{\text{rx}}(u_i)}{w + \sum_{k \neq i} P_{\text{rx}}(u_k) \cdot \frac{d_k^\alpha}{|u_k - v|^\alpha}} \ .$$

When we rescale the distances in the network by factor $\kappa > 0$, we still have

$$\frac{P_{\text{rx}}(u_i)}{w + \sum_{k \neq i} P_{\text{rx}}(u_k) \cdot \frac{(\kappa \cdot d_k)^\alpha}{|\kappa \cdot u_k - \kappa \cdot v|^\alpha}} = \text{SINR}(v) \ .$$

because the transmission powers P_{tx} of all nodes and the signal attenuations due to path loss change by the same factor κ^α.

For beamforming in contrast, the signal-to-noise ratio is only independent from the absolute scale of the network, if the wavelength is set proportional to the diameter of the network. The beamforming pattern of a sender (or receiver) array depends on the distances between the antennas and the carrier wavelength. Keeping the ratio of distances between nodes and the wavelength constant results in the same beamforming pattern. For that, we can consider the signal superposition of Equation (2.15) for n sender and m coordinated receiver antennas

$$h \quad = \quad \sum_{i=1}^{n} \sum_{k=1}^{m} s_i \cdot \frac{\mathrm{e}^{j \frac{2\pi}{\lambda} |u_i - v_k|}}{|u_i - v_k|} \cdot g_k$$

If we likewise increase the wavelength λ, the scale of the network u_i, v_k, and the signal strength s_i by factor $\kappa > 0$ to compensate the path loss, we again get the same channel.

$$\sum_{i=1}^{n} \sum_{k=1}^{m} \kappa \cdot s_i \cdot \frac{\mathrm{e}^{j \frac{2\pi}{\kappa \cdot \lambda} |\kappa \cdot u_i - \kappa \cdot v_k|}}{|\kappa \cdot u_i - \kappa \cdot v_k|} \cdot g_k \quad = \quad h$$

A.3 Analysis of Beamforming with Multiple Antennas

Diversity Gain (Lemma 4) In the following example, we compute the inverse of the channel matrix H. The scenario contains two senders at positions u_1 and u_2 and two receivers positioned at v_1 and v_2 on the line.

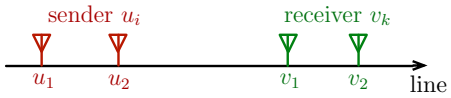

Figure A.1: Example for 2 senders and two receivers placed on the line

$$
\begin{aligned}
H &= \begin{pmatrix} \mathrm{e}^{-j\frac{2\pi}{\lambda}v_1} & 0 \\ 0 & \mathrm{e}^{-j\frac{2\pi}{\lambda}v_2} \end{pmatrix} \cdot \underbrace{\begin{pmatrix} \frac{1}{v_1-u_1} & \frac{1}{v_1-u_2} \\ \frac{1}{v_2-u_1} & \frac{1}{v_2-u_2} \end{pmatrix}}_{=C} \cdot \begin{pmatrix} \mathrm{e}^{j\frac{2\pi}{\lambda}u_1} & 0 \\ 0 & \mathrm{e}^{j\frac{2\pi}{\lambda}u_2} \end{pmatrix} \\
&= \begin{pmatrix} \frac{\mathrm{e}^{-j\frac{2\pi}{\lambda}v_1}}{v_1-u_1} & \frac{\mathrm{e}^{-j\frac{2\pi}{\lambda}v_1}}{v_1-u_2} \\ \frac{\mathrm{e}^{-j\frac{2\pi}{\lambda}v_2}}{v_2-u_1} & \frac{\mathrm{e}^{-j\frac{2\pi}{\lambda}v_2}}{v_2-u_2} \end{pmatrix} \cdot \begin{pmatrix} \mathrm{e}^{j\frac{2\pi}{\lambda}u_1} & 0 \\ 0 & \mathrm{e}^{j\frac{2\pi}{\lambda}u_2} \end{pmatrix} \\
&= \begin{pmatrix} \frac{\mathrm{e}^{-j\frac{2\pi}{\lambda}(v_1-u_1)}}{v_1-u_1} & \frac{\mathrm{e}^{-j\frac{2\pi}{\lambda}(v_1-u_2)}}{v_1-u_2} \\ \frac{\mathrm{e}^{-j\frac{2\pi}{\lambda}(v_2-u_1)}}{v_2-u_1} & \frac{\mathrm{e}^{-j\frac{2\pi}{\lambda}(v_2-u_2)}}{v_2-u_2} \end{pmatrix}
\end{aligned}
$$

We get the output $(y_1, y_2)^T$ when multiplying the input $(x_1, x_2)^T$ with the channel matrix, i.e. $y \cdot g = H \cdot x \cdot s$. The equation contains additional delays/attenuation at senders s and receivers g.

$$
\begin{pmatrix} y_1 \\ y_2 \end{pmatrix} = \begin{pmatrix} g_1 \left(x_1 \cdot s_1 \frac{\mathrm{e}^{-j\frac{2\pi}{\lambda}(v_1-u_1)}}{v_1-u_1} + x_2 \cdot s_2 \frac{\mathrm{e}^{-j\frac{2\pi}{\lambda}(v_1-u_2)}}{v_1-u_2} \right) \\ g_2 \left(x_1 \cdot s_1 \frac{\mathrm{e}^{-j\frac{2\pi}{\lambda}(v_2-u_1)}}{v_2-u_1} + x_2 \cdot s_2 \frac{\mathrm{e}^{-j\frac{2\pi}{\lambda}(v_2-u_2)}}{v_2-u_2} \right) \end{pmatrix}
$$

The Cauchy-matrix contained in the channel matrix H is

$$
C = \left\{ \frac{1}{v_k - u_i} \right\}_{k,i} .
$$

According to [Sch59], the inverse is

$$
C^{-1} = \left\{ (v_i - u_k) \cdot A_i(u_k) \cdot B_k(v_i) \right\}_{ki}
$$

where

$$
\begin{aligned}
A(x) &= \prod_k (x - v_k) = x^2 - (v_1 + v_2)\, x + v_1 v_2 \ , \\
B(x) &= \prod_i (x - u_i) = x^2 - (u_1 + u_2)\, x + u_1 u_2 \ , \\
A'(x) &= 2x - v_1 - v_2 \ , \\
B'(x) &= 2x - u_1 - u_2 \ , \\
A_i(x) &= \frac{A(x)}{A'(v_i) \cdot (x - v_i)} = \frac{x^2 - (v_1 + v_2)\, x + v_1 v_2}{(2v_i - v_1 - v_2)\,(x - v_i)} \ , \\
B_i(x) &= \frac{B(x)}{B'(u_i) \cdot (x - u_i)} = \frac{x^2 - (u_1 + u_2)\, x + u_1 u_2}{(2u_i - u_1 - u_2) \cdot (x - u_i)} \ .
\end{aligned}
$$

The entries of the inverse are

$$\begin{aligned} c_{ki}^{-1} &= (v_i - u_k) \cdot A_i(u_k) \cdot B_k(v_i) \\ &= (v_i - u_k) \cdot \frac{u_k^2 - (v_1+v_2)u_k + v_1 v_2}{(2v_i - v_1 - v_2)(u_k - v_i)} \cdot \frac{v_i^2 - (u_1+u_2)v_i + u_1 u_2}{(2u_k - u_1 - u_2)\cdot(v_i - u_k)} \,. \end{aligned}$$

The inverse is then

$$\begin{aligned} C^{-1} &= \frac{1}{(v_1 - v_2)(u_1 - u_2)} \cdot \\ &\quad \begin{pmatrix} (u_1 - v_1)(u_2 - v_1)(v_2 - u_1) & (v_1 - u_1)(u_1 - v_2)(u_2 - v_2) \\ (u_1 - v_1)(u_2 - v_1)(v_2 - u_2) & (u_2 - v_1)(u_1 - v_2)(u_2 - v_2) \end{pmatrix} \,. \end{aligned}$$

For matrix M and scalar x it holds for the inverse $(x \cdot M)^{-1} = x^{-1} \cdot M^{-1}$. Thus, the inverse of $(-C)^{-1} = -C^{-1}$ and the inverse of the channel matrix H is

$$H^{-1} = \begin{pmatrix} \mathrm{e}^{-j\frac{2\pi}{\lambda}u_1} & 0 \\ 0 & \mathrm{e}^{-j\frac{2\pi}{\lambda}u_2} \end{pmatrix} \cdot C^{-1} \cdot \begin{pmatrix} \mathrm{e}^{j\frac{2\pi}{\lambda}v_1} & 0 \\ 0 & \mathrm{e}^{j\frac{2\pi}{\lambda}v_2} \end{pmatrix} \,.$$

The example is continued in Chapter 3 below the definition of Theorem 4. The inverse H^{-1} is used to send a message to v_2 while keeping silence at v_1.

A.4 Transmission Schemes with Collaborative Beamforming

Lemma 35 *Assume an infinite number of nodes are placed on a line with equidistance 1. Senders transmit to targets in a distance less than d with maximum transmission power $d^2 \cdot P$ with power equivalent P. The minimum distance between parallel and unsynchronized senders is $d_{\min} = d \cdot k$ for constant $k = \pi \cdot \sqrt{2/3}$. Then the expected SINR at each receiver is SINR $\geq \frac{P}{P+w}$ where w is AWGN.*

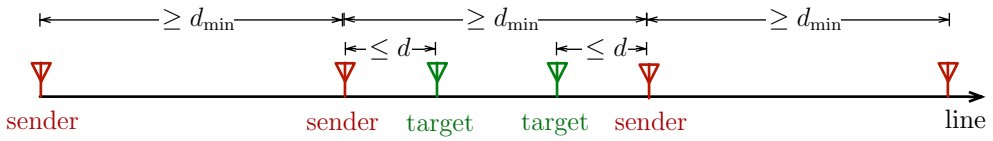

Figure A.2: Simultaneous transmissions between nodes placed on a line with minimum distance of senders $d_{\min}$ and transmission distance at most d

Proof: Let us assume we have an infinite number of nodes which are placed equidistance 1 on a line. A sender can reach its nearest neighbors on the line with power P. Let us assume active senders only communicate with a destination node in distance

d with corresponding transmission power $(d^2 \cdot P)$. If the minimum distance of active senders is $d_{\min}$ and the senders are uncoordinated, i.e. unsynchronized, the expected interference at a receiver is (by applying Lemma 1)

$$\mathbb{E}\left[P_{\text{interference}}\right] \leq \frac{d^2 \cdot P}{(d_{\min} - d)^2} + 2 \cdot \sum_{i=1}^{\infty} \frac{d^2 \cdot P}{(i \cdot d_{\min})^2} .$$

We set $d_{\min} := d \cdot \sqrt{2/3} \cdot \pi$ and get

$$\mathbb{E}\left[P_{\text{interference}}\right] \leq \frac{1}{\left(\pi \cdot \sqrt{2/3} - 1\right)^2} \cdot P + \frac{3}{\pi^2} \cdot \sum_{i=1}^{\infty} \frac{P}{i^2} .$$

Since $\sum_{i=1}^{\infty} i^{-2} = \pi^2/6$ and $\left(\pi \cdot \sqrt{2/3} - 1\right)^{-2} < \frac{1}{2}$, we get

$$\mathbb{E}\left[P_{\text{interference}}\right] \leq P .$$

With a maximum transmission power $d^2 \cdot P$, the signal power at a receiver is at least P in the free space model and with AWGN with power w we get a SINR level of

$$\mathbb{E}\left[\text{SINR}\right] \geq \frac{P}{P + w} .$$

□

Lemma 36 *For all* $x \geq 0$

$$\frac{x^2}{2} \geq \sqrt{1 + x^2} - 1 .$$

Proof: The claim is equivalent to $\frac{x^2}{2} + 1 \geq \sqrt{1 + x^2}$. Squaring both sides yields

$$\frac{x^4}{4} + x^2 + 1 \geq 1 + x^2$$

which always holds. □

Lemma 37 *Consider a network with n nodes in the plane with dimensions* $\sqrt{n} \times \sqrt{n}$. *To perform x-routing of the unicast scheme in parallel, we divide the network into horizontal rows of height* $\Theta\left(\max\left\{\ln n, \lambda^{1/3} \cdot n^{1/6} \cdot \ln \frac{n}{\lambda}\right\}\right)$. *If we only operate one x-routing in each row at a time, the expected interference is constant. With a TDMA schedule, where neighboring rows alternately transmit, we can lower the expected constant interference. The same holds for y-routing.*

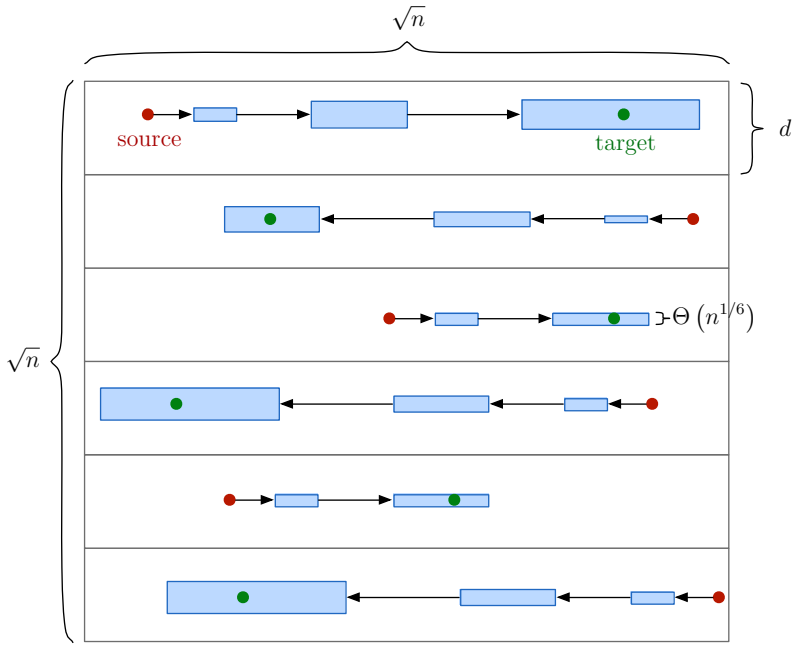

Figure A.3: Parallel execution of x-routing with the unicast scheme in horizontal rows

Proof: We choose the distance of parallel operations in such a way, that interfering beamforming senders have such a high attenuation (due to path loss) to each other that the sum of interferences forms a converging series for an infinite number of parallel transmissions. From Lemma 27, we know that the maximum signal strength is $\mathcal{O}\left(\max\left\{\ln n, \lambda^{1/3} \cdot n^{1/6} \cdot \ln \frac{n}{\lambda}\right\}\right)$. So we set the row height to $d := k \max\left\{\ln n, \lambda^{1/3} \cdot n^{1/6} \cdot \ln \frac{n}{\lambda}\right\}$ for some constant k. If we assume at least a 2-TDMA scheme, i.e. neighboring rows do not send at the same time, the distance to the i-th parallel operation is

$$d_i \quad \geq \quad i \cdot d \text{ with } 1 \leq i \leq \frac{\sqrt{n}}{d}$$

The expected interference is therefore

$$\mathbb{E}\left[|h|^2\right] \quad \leq \quad \sum_{i=1}^{\sqrt{n}/d} \left(\frac{d}{d_i}\right)^2 \leq \sum_{i=1}^{\infty} \frac{1}{i^2} = \frac{\pi^2}{6} \ .$$

□

Lemma 38 *Consider n nodes randomly placed in a quadratic area of size $\Theta(n)$ and sending at the same time with constant power P. When receiving from one of these nodes, the expected interference of the remaining $(n-1)$ uncoordinated nodes is $\Theta(\log n)$ in the free-space model.*

Proof: Assume interfering nodes have power P/d^2 for distance d and a power equivalent P in Watts/m^2. If n nodes are placed uniformly at random in an area $\sqrt{n} \times \sqrt{n}$, the expected number of interfering nodes within distance d on a disk with perimeter $2\pi d$ is $\Theta(d^2)$ and the probability density function (pdf) is $\Theta(d)$. Then the interference of $(n-1)$ interfering nodes with uncorrelated signals is

$$\sum_{i \in I} \frac{P_i}{d_i^2} \leq \int_{d=1}^{\sqrt{n}} 2\pi \cdot d \cdot \frac{P}{d^2} \leq c_1 \cdot P \cdot \log(n)$$

for some constant c_1. □

Glossary

ad hoc network an ad hoc network is a dynamic and wireless network establishing communication between mobile devices without an infrastructure, e.g. access points. 17, 39

AWGN (Additive White Gaussian Noise) is modeled with a normal distribution $\mathcal{N}(0, \sigma^2)$ with variance σ^2. A device receives the signal of a transmitter and additionally AWGN. 26, 39

beam-pattern or radiation pattern specifies the signal power for specific radiation angle, which are the azimuth angle and the elevation angle. An isotropic radiator has the same signal power in all directions. An omnidirectional antenna (dipole antenna) has the same signal strength for the same elevation angle and is vertically polarized, i.e. the signal power changes with factor $\sin^2\theta$ for elevation angle θ. 9

beamforming is a spatial filter for multiple omnidirectional antennas and creates a directed radiation pattern with an amplified signal in certain angular directions, so called beams. The direction can be electronically adjusted. 19, 36, 39

broadcast a source node transmits a message to all other $(n-1)$ nodes in a network with n nodes. iv, vi, 100

CDMA Code division multiple access allows multiple transmitters to simultaneously access a channel with same carrier frequency without interfering each other. Each sender sends its information in a sufficient redundant code such that simultaneous transmissions are orthogonal, i.e. each message can be retrieved from the superposed signal. The method is suitable for distributed medium access. 16, 147

deliberate attenuation denotes a technique for intentionally lowering the signal towards a direction in order to prevent interference. This also includes that the signal is still strong towards another direction where we intend to transfer a message. 163

elevation angle We assume dipole antennas in our model which are vertically polarized, i.e. the signal power changes with factor $\sin^2\theta$ for elevation angle θ. If sender and receiver are in the plane and the antennas are orthogonal to the plane, then $\sin^2(\pi/2) = 1$ and there is no polarization effect. 134

full-CSI Full-Channel State Information means that sender and receiver know the channel transition h from input X to output signal Y with $Y = h \cdot X$. iv, vi, 4

isotropic antenna sends a signal with same power in every direction and receives with same sensibility form every direction. 9

MAC A medium access control controls how multiple transmitters can access a radio channel without interfering each other. v, vi, 4, 146, 162

MIMO (Multiple Input Single Output) a signal is emitted by multiple sending antennas and received at a single output antenna. 30

MISO (Multiple Input Single Output) a signal is emitted by multiple sending antennas and received at a single output antenna. 30

MU-MIMO (Multiple User-Multiple Input Single Output) a wireless device e.g. access point establishes to multiple users a connection at the same time, and each connection has multiple spatial streams. (SU-)MIMO in contrast has only multiple spatial streams to a single user (SU). 10

MU-SIMO (Multiple User-Single Input Single Output) multiple users with single input (one antenna) transmit to a base station with multiple antennas (multiple output). 41

multi-hop In an ad hoc network, a message might be forwarded on several hops via several relay nodes from source to target. vi

multicast in a multicast operation, a message is transmitted from a source node to m multiple destination nodes in a network network with n nodes and $1 \leq m \leq n$. 130

nearest-neighbor routing denotes a multi-hop routing scheme. Starting at the source node, a message is forwarded in each hop to the neighboring node which is closest to the target. This is repeated until the target has been reached. For nodes placed on a line, the neighbors of a node are the two closest nodes to the left and to the right on the line. 4, 100, 108, 110, 133, 161, 162

omnidirectional antenna or dipole antenna has a radio pattern, where the signal strength is the same in all directions (with same elevation angle θ). With vertical polarization, the signal power changes with factor $\sin^2\theta$ for elevation angle θ. If sender and receiver are in the plane and the antennas are orthogonal to the plane, then $\sin^2(\pi/2) = 1$. In the free-space model, the signal amplitude attenuates with $\frac{1}{d}$ for the distance d (in the far-field with $d \geq 2\lambda$ for carrier wavelength λ). 3, 18, 20, 35, 39

QAM (Quadrature Amplitude Modulation) is a modulation scheme combining amplitude modulation and phase modulation. The notation of the number of different symbols $x \in (4, 16, 64, 256, 1024, 2048)$ is x-QAM which corresponds to $\log_2 x$ bits. 10, 25, 39

RF front end (Radio Frequency front end) is the transceiver hardware between the digital baseband system and the antenna. 32

self-synchronizing we denote an algorithm applying collaborative beamforming as *self-synchronizing*, if the algorithm is able to establish phase-synchronization between nodes collaborating for beamforming on-the-fly while transferring data (and without additional costs). This excludes algorithms that rely on full channel state information (full-CSI). 101, 108, 111, 117

sensor node A wireless sensor network (WSN) consists of sensor nodes. Sensor nodes have different sensors to measure physical conditions like temperature and the measured data is sent to a gateway of the network, where a user can access the data. Sensor nodes are battery-driven and are supposed to operate over years without recharging the battery. Thus, energy constraints for wireless transmission are very critical in these networks. 9

signal processing denotes processing of time-varying analog or digital signals. This can be for example delaying a signal at an antenna for beamforming. 9

SIMO (Single Input Multiple Output) a signal is emitted by a single sending antenna and received by multiple receiving antennas. 30

SINR (Signal to Interference and Noise Ratio) describes the quality of a received signal and how strong the signal is disrupted by interferences and noise. iv, vi

speed of light in vacuum is the physical constant $c = 299\,792\,458 \frac{\mathrm{m}}{\mathrm{s}} \approx 3 \cdot 10^8 \frac{\mathrm{m}}{\mathrm{s}}$. 20, 39

TDMA (Time Division Multiple Access) Several simultaneous transmitters can prevent interfering each other on the same carrier frequency by sending in disjunct time slots. 146, 147, 157

throughput the maximum data rate possible, i.e. if a complete transmission is successful, the throughput is equal the data rate. 13

unicast In a unicast operation, a message is transmitted from a source node to one destination node in the network. 108–112, 116, 122, 123, 131–133

wavelength λ specifies the distance which an electromagnetic wave with frequency $f = \frac{c}{\lambda}$ propagates with speed of light c in the time of one period $T = 1/f$. 20, 24

Variables and Constants

b_i	depth of a cuboid (in number of nodes)
c	speed of light
d	a distance
E_v	electric field at receiving node v (MISO)
f	the carrier frequency of the radio signal
g_k	receiver v_k shifts output signal Y_k with $g_k = \lvert g_k \rvert \cdot \mathrm{e}^{j \arg g_k}$
h	is the transfer function of the sent input X to the received output Y
h_i	transfer function of input X_i of sender u_i or height of a rectangular area
j	imaginary unit with property $j^2 = -1$
k	constants
K	in the modulation scheme in Chapter 5, each symbol is repeated K times
k_{phy}	conversion of output signal to electric field $Y \cdot k_{\mathrm{phy}} = E_v$
m, n	number of nodes/antennas (multiple senders or receivers, or in the network)
N_0	Additive white Gaussian noise (AWGN) power of the field E_v (no filtering)
o	an interfering node
P	power equivalent (without physical constant)
q	electrical charge
R	denotes the data rate (in bits per second)
s_i	sender u_i shifts input signal X_i with $s_i = \lvert s_i \rvert \cdot \mathrm{e}^{j \arg s_i}$
t	time, e.g. the modulation function $\varphi(t)$ is time dependent
u	a sender node, u_i the i-th multiple sender, u_x the x-coordinate
v	a receiver node, v_k the k-th multiple receiver, v_x the x-coordinate
w_k	additive white Gaussian noise (AWGN) in the output signal of receiver u_k
x, y, z	Cartesian coordinates (small letters)
X	the sender sends this input signal
X_i	for multiple input signals, sender u_i sends this input signal
Y	the receiver receives this output signal
Y_k	for multiple output signals, receiver v_k receives this output signal
α	signal attenuation $1/d^{\alpha}$ with path loss exponent α at sender's distance d
δ	delay
λ	wavelength
$\varphi_{\mathrm{am}}(t)$	digital data is modulated with Amplitude Shift Keying (ASK) at time t
$\varphi_{\mathrm{pm}}(t)$	digital data is modulated with Phase Shift Keying (PSK) at time t
$\varphi(t)$	digital data is modulated with ASK and PSK at time t
ω	the angular speed is $\omega = 2\pi f$ for frequency f
w_i	width of a rectangular area (in number of nodes)